FUNCTIONAL STUDIES ON

NERVE GROWTH FACTOR AND ITS

PRECURSOR FROM *NAJA SPUTATRIX*

DAWN KOH CHIN ING

NATIONAL UNIVERSITY OF SINGAPORE

2007

FUNCTIONAL STUDIES ON

NERVE GROWTH FACTOR AND ITS

PRECURSOR FROM *NAJA SPUTATRIX*

DAWN KOH CHIN ING

B.Sc. (Hons)

A THESIS SUBMITTED FOR THE DEGREE OF

DOCTOR OF PHILOSOPHY

DEPARTMENT OF BIOCHEMISTRY

NATIONAL UNIVERSITY OF SINGAPORE

2007

Acknowledgements

I would like to extend my heart-felt appreciation to my supervisor and mentor, Professor Kandiah Jeyaseelan. His mentorship, guidance, encouragement, understanding and support not only enabled me to complete this project successfully but also nurtured me to be a better researcher. My career as a researcher has just begun, thanks Prof for giving me the necessary and essential skills to start off this journey!

I am grateful to Dr. Arunmozhiarasi Armugam for training and guiding me. It is great to have someone to share and exchange ideas with. I value her patience, ideas, advice and motivation. In addition, I would like to thank her for showing me the joy, hard work and frustration of research. Her passion and zeal for science is an inspiration to me.

I would also like to thank the Head of Department of Biochemistry for giving me the opportunity to pursue my studies in the department and the National University of Singapore for providing a research scholarship throughout my course of study.

Special thanks to both past and present members of Prof Jay's lab, especially Charmain, Joyce and Siaw Ching for making this 'marathon' more enjoyable with their friendship. Apart from them, I would like to thank all my friends in NUS for their warmth, assistance, friendship and advice.

Most importantly, this thesis is dedicated to my family. They are my ardent supporters, without them, I would not have made it this far. Their constant encouragement and prayers have sustained me till this day. Thanks family for being all that you are!

Finally, I would like to thank my personal Lord, Jesus Christ, for leading me to this career as a researcher. *In his heart a man plans his course, but the Lord determines his steps (Proverbs 16: 9).*

Table of Contents

Chapter 1: Introduction

Chapter 2: Materials and Methods

Chapter 3: Sputa Nerve Growth Factor (Sputa NGF)

Chapter 4: The pro-domain of sputa NGF

Chapter 5: Effect of nPLA$_2$ on ischemia and its possible mechanism of action

Chapter 6: Discussion

Publications

1. Koh, DC-I, Armugam, A and Jeyaseelan, K. (2007). Cell death mediated by pro-domain of the precursor NGF involves sortilin and p75^{NTR} receptors. (Manuscript submitted).

2. Koh, DC-I, Armugam, A and Jeyaseelan, K. (2006). Snake venom components and their applications in biomedicine. *Cell Mol Life Sci.* **63:** 3030-3041.

3. Koh, DC-I, Armugam, A and Jeyaseelan, K. (2004). Sputa nerve growth factor forms a preferable substitute to mouse 7S-β nerve growth factor. *Biochem J.* **383:** 149-158.

4. Koh, DC-I, Nair, R.P., Armugam, A and Jeyaseelan, K. (2003). NGF from cobra venom, promotes the expression of the endogenous NGF in PC12 cells. *J Neurochem.* **87 (Suppl 1):** 175.

Conference papers

1. Koh, DC-I, Nair, R., Armugam, A. and Jeyaseelan, K. (2005) Sputa Nerve Growth Factor: A modulator of Aquaporins in hippocampal cells. *Gordon Research Conferences*: Cellular Osmoregulation: Sensors, Transducers and Regulators, Newport.

2. Koh, DC-I, Nair, R., Armugam, A. and Jeyaseelan, K. (2003) Global gene analysis of PC12 cells upon treatment with recombinant cobra nerve growth factor. 2nd Asia Pacific Conference and exhibition on anti-ageing medicine, Singapore.

3. Koh, DC-I, Nair, R., Armugam, A. and Jeyaseelan, K. (2003) NGF from cobra, promotes the expression of the endogenous NGF in PC12 cells. 19th biennial meeting of the International Society for Neurochemistry, Hong Kong.

4. Koh, DC-I, Nair, R., Armugam, A. and Jeyaseelan, K. (2002) Venom nerve growth factor as a modulator of aquaporins in the brain. 6th Asia Pacific Congress on Animal, Plant and Microbial Toxins of International Society on Toxicology in Australia and 1st Bilateral Symposium on Advances in Molecular Biotechnology and Biomedicine between the NUS and University of Sydney, Singapore.

Summary

Snake venom contains a toxic mixture of enzymes, low molecular weight polypeptides, glycoproteins and metal ions that is capable of causing local tissue damage as well as multiple system failure. However, nerve growth factor (NGF) activity was first discovered in snake venom and two sarcoma tissues. The nerve growth factor from *Naja sputatrix* has been purified by gel filtration followed by reverse-phase high performance liquid chromatography (RP-HPLC). The protein showed a very high ability to induce neurite formation in PC12 cells relative to the mouse nerve growth factor. Two cDNAs encoding isoforms of NGF have been cloned and an active recombinant nerve growth factor, sputa NGF has been produced in *E. coli* as a his-tagged fusion protein. Sputa NGF was found to be non-toxic in both *in vivo* and *in vitro* conditions. The induction of neurite outgrowth by this NGF has been found to involve the high affinity TrkA-p75^{NTR} complex of receptors. The pro-survival mechanism of p75^{NTR} was mediated by the activation of NFkB gene by a corresponding down regulation of IκB gene. Real-time PCR and protein profiling (SELDI-TOF) also confirmed that sputa NGF upregulates the expression of the endogenous NGF in PC12 cells. Preliminary microarray analysis has also shown that sputa NGF is capable of promoting additional beneficial effects such as the upregulation of arginine vasopresin receptor 1A, voltage-dependent T-type calcium channel, *etc*. Hence, sputa NGF forms a new and useful nerve growth factor.

In addition to the sputa NGF, the precursor [Pro (R/G) NGF] was shown to behave in a similar manner to the mature NGF when expressed in stably transfected CHO cells. It was capable of eliciting neurites, but to a lesser extent (2-fold) than the mature NGF. In addition, it was also found to involve the high affinity TrkA-p75^{NTR}

complex of receptors to cause neurite extension. The overall fate of the cell when exposed to pro (R/G) NGF is survival. Both mature NGF and pro (R/G) lead to cell survival upon treatment in both serum-starved and ischemic conditions. However, when exposed to an apoptotic agent (i.e staurosporine), only the mature NGF enabled cell survival. Apart from the property of the pro (R/G) NGF, the pro-domain was investigated. Both fluorescence microscopy experiments, as well as caspase-3 activity measurement indicated that pro-domain caused apoptosis and probably by the caspase pathway.

Both real-time studies and western blot analysis for the three surface receptors (TrkA, $p75^{NTR}$ and sortilin) indicated that with mature NGF, both TrkA and sortilin expression were upregulated, while $p75^{NTR}$ was downregulated. Though sortilin expression is relatively high, but in the presence of TrkA, $p75^{NTR}$ formed a high-affinity complex with TrkA, leaving minimal $p75^{NTR}$ to interact with the sortilin receptors. On the contrary, pro-domain had low expression levels of TrkA, while both $p75^{NTR}$ and sortilin were expressed in similar levels. The reduced expression of TrkA, allowed the interaction between $p75^{NTR}$ and sortilin, thereby activating the cell death pathway as observed in both caspase and DNA laddering studies. Hence, these functional studies indicated that the NGF-induced cell survival and death is far more complicated than previously appreciated. It depends on an intricate balance between precursor (ProNGF) and mature NGF, as well as the spatial and temporal expression of the three distinct receptors.

Another potentially useful component from *Naja sputatrix* venom is neutral phospholipase A2 (nPLA$_2$). Orgnotypic hippocampal cultures when exposed to ischemic conditions (oxygen-glucose deprivation) were protected when concurrently treated with PLA$_2$. Real-time PCR studies of related apoptotic genes showed that

anti-apoptotic genes (Bcl-2 and Bcl-$_{XL}$) were upregulated, while apoptotic genes (Bax) were downregulated with PLA$_2$. In addition, the mechanism of action of protection by PLA$_2$ was most likely via group I glutamate metabotrophic receptors, specifically mGluR1.

Abbreviations

Å	Angstrom
APS	Ammonium persulfate
AMPA	2-amino-3-hydroxy-5-methyl-4-isoxazole propionic acid
BSA	Bovine serum albumin
bp	Base pair (s)
CA	Cornus Ammonis
CD	Circular Dichroism
cDNA	Complementary DNA
CHO	Chinese Hamster Ovary
cRNA	Complementary RNA
CHPG	(R, S)-2-chloro-5-hydroxyphenylglycine
CP	7-hydroxyiminoclopropan[b]chromen-1a-carboxylic acid ethyl ester (CPCCOEt)
DMEM	Dulbecco's modified eagle's medium
DEPC	Diethyl pyrocarbonate
DHPG	(S)-3, 5-dihydroxy-phenylglycine
DMSO	Dimethyl sulphoxide
DNA	Deoxyribonucleic acid
DNase I	Deoxyribonuclease I
dsDNA	Double-stranded DNA
dNTPs	Deoxynucleoside triphophates
DTT	Dithiothreitol
E. coli	*Escherichia Coli*
EDTA	Ethylenediamine tetra-acetic acid

FBS	Fetal Bovine Serum
g	Gravitational force
g	Grams
h	Hour
HEPES	N-2-hydroxyethylpiperazine-N'-2-ethane-sulphonic acid
IgG	Immunoglobulin G
IPTG	Isopropyl-β-thiogalactopyranoside
KA	Kainic acid
kb	Kilobase(s)
kDa	Kilodalton(s)
kg	Kilograms
LDH	Lactate dehydrogenase
M	Molar
MES	2-(N-morpholino)ethanesulfonic acid
MPEP	6-methyl-2-(phenylethylnyl)-pyridine
μg	Microgram
μl	Microliter
μM	Micromolar
mg	Milligram
mGluR	Metabotrophic glutamate receptor
min	Minute
ml	Milliliter
mM	Millimolar
MOPS	Morpholinopropanesulphonic acid
mRNA	Messenger RNA

MTT	3-(4, 5-dimethylthiazole-2-yl) 2, 5-diphenyl tetrazolium bromide
NF-κB	Nuclear factor *kappa B*
NGF	Nerve growth factor
ng	Nanogram
NMDA	N-methyl-D-aspartate
NTX	Neurotoxin
OD	Optical Density (absorbance)
OGD	Oxygen-glucose deprivation
PAGE	Polyacrylamide gel electrophoresis
PBS	Phosphate buffered saline
PCR	Polymerase Chain Reacion
PI	Propidium Iodide
PLA_2	Phospholipase A2
PMSF	Phenylmethylsulfonyl fluoride
RNA	Ribonucleic acid
RNase	Ribonuclease
RP-HPLC	Reverse phase high performance liquid chromatography
rpm	Revolutions per minute
RT	Reverse transcription
s	Seconds
SAPE	Streptavidin phycoerythrin
SDS	Sodium dodecyl sulphate
SEM	Standard error of the mean
STS	Staurosporine
TEMED	N, N, N', N'-tetramethylethylenedi-amine

Tris	Hydroxymethyl aminomethane base
U	Units
V	Volts
X-Gal	5-bromo-4-chloro-indolylgalactoside

List of Tables

List of Figures

Chapter 1

Introduction

1.1   Nerve Growth Factor (NGF)

Nerve growth factor (NGF) is among the first growth factor to be identified and characterized (Cohen *et al*., 1954). Its name, NGF, is based on its ability to promote neuronal survival and neurite outgrowth of explanted sympathetic ganglia. NGF has been detected in various animals including snakes (Lipps, 1998; Guo *et al*., 1999; Kashima *et al*., 2002), human placental tissues (Goldstein, 1978) and bodily fluids (Lipps, 2000). Its activity was first detected from two sarcoma tissues and in snake venoms. However, the property of NGF was most extensively studied using NGF from the male mouse submandibular gland (mouse NGF; Kostiza and Meier, 1996). In the peripheral nervous system, NGF sensitive cells include neural crest deriviatives from sympathoadrenal origin: sympathetic neurons, para ganglia (carotid and abdominal paraganglia cells), chromaffin cells (normal and neoplastic, e.g. PC12 cells) and embryonic sensory neurons. While in the central nervous system, responsiveness to NGF is only restricted to cholinergic neurons from corpus striatum, basal forebrain and septum nucleus. Neurons in the basal forebrain project towards the hippocampus and cortex to obtain NGF. NGF is synthesized by the pyramidal cells of the hippocampal neurons of the dentate gyrus (Whittemore *et al*., 1986; Ayer-Lelievre *et al*., 1988) and transported retrogradely from the hippocampus to the cholinergic septal neurons (Schwab *et al*., 1979) that do not synthesize NGF (Korsching *et al*., 1985).

Since the discovery of NGF in 1954, more than 4000 papers have been published on its biochemical and biological activities. Fifty years of work have solved a few mysteries in this field, like the crystal structure of NGF (McDonald *et al*., 1991), its structural complex with its receptors (Wiesmann *et al*., 1999; He and Garcia, 2004), the paradoxical cell killing activities of one of the two NGF receptors (p75^{NTR}), as

well as the unexpected involvement of NGF and other members of the neurotrophin family in synaptic plasticity, learning and memory (Huang and Reichardt, 2001). Just when some thought that all is known, the roller coaster resumes, sparked from a study by Lee *et al.* (2001) that the precursor NGF (proNGF) is not just an innocent bystander.

1.1.1   Neurotrophin family

Nerve growth factor (NGF) belongs to the neurotrophin family. Its other members include brain-derived neurotrophic factor (BDNF), neurotrophin 3 (NT-3), neurotrophin 4/5 (NT-4/5) and neurotrophin 6 (NT-6). All neurotrophins share a 50% pair-wise sequence identity and function as growth factors that regulate the development, maintenance and survival of both central and peripheral nervous systems. Hence, this family has great potential as therapeutic targets for neurological disorders such as Alzheimer's disease, amyotrophic lateral sclerosis (ALS), peripheral neuropathy and spinal cord injury. Neurotrophins exist as noncovalently associated homodimers that are capable of promoting either neuronal cell survival or death, based on the context of their cellular environment (Lewin and Barde, 1996).

The pleiotrophic actions of neurotrophins are mediated by two structurally unrelated classes of receptors, the tropomyosin-related kinase (Trk) receptor tyrosine kinase (RTK) and the p75 neurotrophin receptor (p75^{NTR}), a member of the tumor necrosis factor (TNF) receptor superfamily. Trk has three members (TrkA-C) and the presence of p75^{NTR} helps to increase ligand selectivity to Trk receptors. Each neurotrophin is specific for different Trk receptors but all bind with same affinity to p75^{NTR}. For instance, BDNF, NT-3 and NT-4/5 are able to bind to TrkB receptor, but in the presence of p75^{NTR}, only BDNF caused a functional response (Bibel and

Barde, 1999). Similarly, both NT-3 and NGF are capable of binding to TrkA, but p75^NTR restricts the signaling of TrkA to NGF only (Benedetti *et al*., 1994).

1.1.2   Structure of NGF

Most of the study on NGF was done using the mouse NGF and it exists as homodimer. Each monomer is made up of 118 amino acids with six cysteines and three disulfide bridges. The sequence can be divided into three parts: (a) a N-terminal region that corresponds to the signal peptide, (b) a 'pro' domain part, whose function remains to be determined and (c) a carboxyl terminal that corresponds to the mature NGF. The primary structures of NGF (deduced from cDNA clones) are available for human, bovine, rat, chick and snake and comparison between them shows a high degree of homology among the different species (Whittemore *et al*., 1988). The sequence of the human NGF is shown in Fig. 1.1 (A). The three-dimensional structure of NGF was determined by X-ray crystallography and revealed a novel tertiary fold with two central pairs of anti-parallel β-stands that define the elongated shape of the molecule (McDonald *et al*., 1991; Fig. 1.1B). Each monomer is made up of β-stands (A-D) that are connected by a number of highly flexible hairpin loops (L1-L4). These loops are important for p75^NTR binding (L1, L3 and L4) and TrkA specificity (L2 and L4). The three disulphide bridges of the molecule are clustered with two disulphide bridges and help to connect residues forming a ring structure for the third disulphide bridge to form a 'cysteine' motif. This motif helps to stabilize the fold and locks the molecules in their conformation (McDonald and Hendrickson., 1993).

In the biologically active state, the two monomers are arranged in a parallel manner to form a tight homodimer, stabilized by hydrophobic interaction. In the case of

A
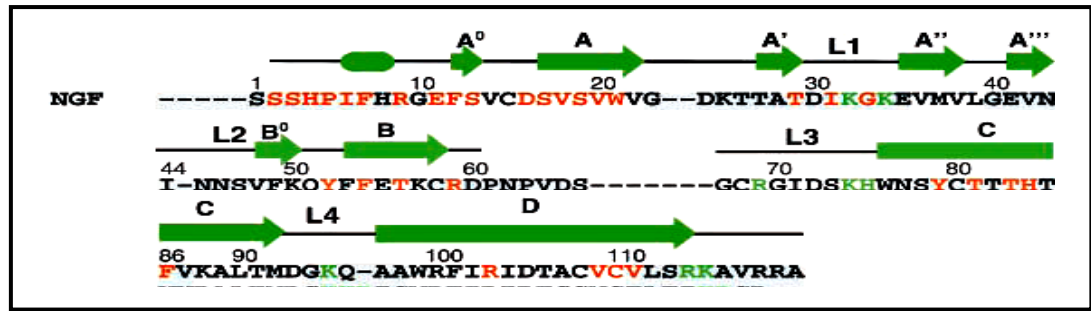
B
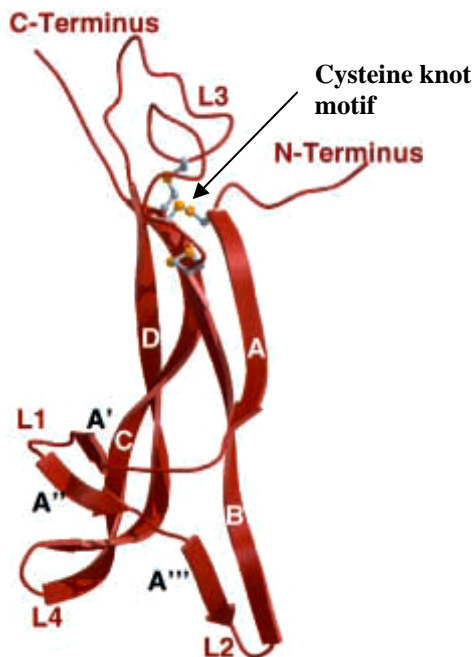
C
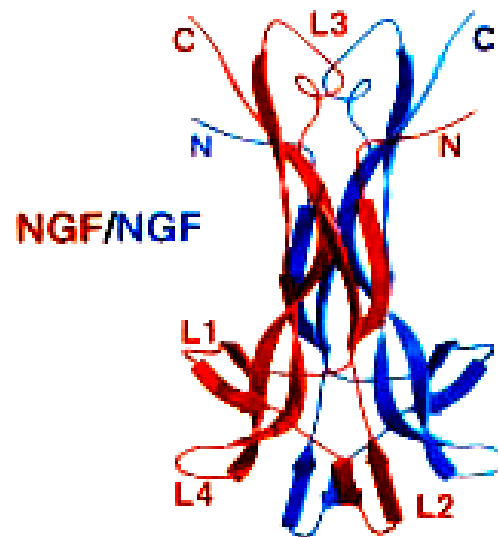
Fig. 1.1: Sequence and structure of NGF. **(A)** Secondary structure of NGF as indicated by Wiesmann *et al* (1999). NGF residues that are in contact with TrkA (domain 5) are indicated in red, while those for p75^{NTR} are in green. **(B)** Ribbon structure of NGF monomer (PDB code: 1BFT). The termini, loop region (L1-4) are indicated in red and cysteine-knot motif (*black arrow*) at the top of molecule is shown in grey and yellow. **(C)** Ribbon structures of NGF dimers (PDB code: 1BET) bound together in parallel fashion. The loops for receptor binding: p75^{NTR} (L1, L3 and L4) and TrkA (L2 and L4) are labeled (adapted from Wiesmann and de Vos, 2001).

NGF, it forms parallel dimers with both monomers assembled around a central twofold axis (Fig. 1.1C). The long axis of the dimer coincides with the twofold axis, giving NGF an overall dumbbell-like shape. The two central β-strands (AB and CD) from each of the monomers are packed against each other to form the 'handle' of the dumbbell. Residues from these four β-strands are responsible for the majority of the interactions that help to stabilize the dimer. The cysteine-knot motif, the N and C termini, and the third loop connecting strands B and C (L3) form one end of the dumbbell that face away from the membrane (Wiesmann *et al.*, 1999), while the other end containing the three hairpin loops (L1, L2, and L4), as well as four short β-strands arranged in two antiparallel β-sheets face the membrane.

1.1.3   Biosynthesis of NGF

The structure, biosynthesis and biological activity of NGF from the male mouse submandibular glands (mouse NGF) has been extensively studied. Mouse NGF is encoded by a single gene of more than 45 kilobases (Ullrich *et al.*, 1983), which consists of two separate promoters and four exons that are alternatively spliced to yield two major and two minor transcripts (Racke *et al.*, 1996). Translation from the two major alternatively spliced transcripts produce prepro species of 34 and 27 kDa, while removal of the signal sequence later in the endoplasmic reticulum (ER) by membrane-bound signal peptidase reduces the translation products to proNGF species of 32 and 25kDa respectively (Darling *et al*; 1983; Ullrich *et al*; 1983; Selby *et al.*, 1987; Edwards *et al.*, 1988b).

The first phase of glycosylation takes place in the ER and continues in the *trans-*Golgi network (TGN). ProNGF contains three potential glycosylation sites: two in

the prosegment and one in the mature segment. The function of N-glycosylation for pro- NGF is still unclear as both glycosylated (Suter *et al*; 1991) and unglycosylated proNGF (Chen *et al*., 1997; Fannestock *et al*., 2001) have been detected in tissues. ProNGF is cleaved within the TGN by furin or furin-like enzymes that act on the carboxyl terminal side of the multibasic sites (Hosaka *et al*., 1991) and later constitutively released (Dubois *et al*., 1995) as an active mature NGF. Recently, extracellullar cleavage of proNGF by both plasmin and matrix metalloprotease-7 (MMP-7) have also been reported (Lee *et al*., 2001). Plasmin cleavage of proNGF produces the mature form, whereas MMP-7 results in a 17kDa intermediate (Darling *et al*., 1983; Dicou, 1989). The roles of proNGF have been thought to be for proper folding of the mature NGF and sorting it to either constitutive or secretory pathway (Suter *et al*., 1991). However, the functions of the precursors and their intermediates are still poorly understood, while the role of proNGF is debated by two separate groups (Lee *et al*., 2001 and Fahnestock *et al*., 2004).

1.1.3.1 Debate on functionality of proNGF

Lee *et al* (2001) created a furin-resistant proNGF protein by changing the two conserved arginine residues to alanine. Nevertheless, it was susceptible to cleavage by extracellullar metalloproteases (MMP-7). Based on radioactive I^{125} binding studies, proNGF was found to bind to p75^{NTR} with greater affinity than mature NGF. Competition binding assays indicated that proNGF exhibited an equilibrium binding constant of 10^{-10} M for p75^{NTR} (five times more than mature NGF), while binding to TrkA receptors was less than mature NGF. The higher affinity binding of proNGF to p75^{NTR} resulted in enhanced p75^{NTR}-mediated apoptosis in a vascular smooth muscle cell line, while activation of TrkA, assessed by autophosphorylation and neurite

outgrowth in superior cervical ganglia (SCG) and PC12 cells were less for proNGF compared to mature NGF. The corresponding activation of p75^{NTR} with increased affinity of proNGF shed new light into proNGF being a potential agonist for p75^{NTR}-mediated apoptosis (Lee *et al.*, 2001).

A similar study by Fahnestock (2004) on proNGF resulted in a striking contrast to that of Lee *et al.* (2001). To determine the biological function of proNGF, the precursor-processing site was mutagenized and expressed as an unprocessed, cleavage-resistant proNGF protein in insect cells. Survival and neurite outgrowth assays on murine superior cervical ganglion neurons and PC12 cells indicated that proNGF exhibited similar neurotrophic activity to mature 2.5S NGF, but is approximately five-fold less active. ProNGF also binds to the high-affinity receptor, TrkA, as determined by binding studies but is less active in promoting phosphorylation to TrkA and its downstream pathway.

The cleavage-resistant proNGFs from the two separate groups are all mutated recombinant proteins. The different conclusions drawn by them showed that mutations made at different positions of the protein sequence may alter the property of the eventual proNGF molecule. However, for proNGF to be a true pathophysiological ligand for p75^{NTR}, it has to bind to p75^{NTR} and subsequently activate cell death *in vivo*. Harrington *et al.* (2004) reported that after brain injury, proNGF was induced and secreted in an active form capable of triggering apoptosis in culture. They also demonstrated that proNGF binds to p75^{NTR} *in vivo* and that the disruption of this binding rescued the injured adult corticospinal neurons. These data suggest that interference of proNGF and p75^{NTR} interaction may be a potential therapy for disorders involving neuronal loss. This study further strengthened the

observation made by Lee *et al.* (2001), that proNGF is apoptotic in nature both *in vitro* and *in vivo* conditions (Harrington *et al.*, 2004).

1.2 NGF receptors

The two receptors (TrkA and p75^{NTR}) are normally present in the same cell to modulate the response of neurons to NGF. The functions of these receptors vary from the sculpting of the developing nervous system to the regulation of the survival and regeneration of injured neurons. Surprisingly, TrkA receptors only activate positive signals (enhanced growth and survival) while p75^{NTR} activate both positive and negative signals. The signals generated by both receptors can either enhance or oppose each other, resulting in a paradoxical relationship (Kaplan and Miller, 2000).

1.2.1 Trk receptors

The neurotrophins bind to two receptors: Trk and p75^{NTR}. The Trk family is made up of three members (TrkA, B and C) in which neurotrophins bind directly and dimerize, resulting in the activation of the tyrosine kinases present in their cytoplasmic domains. However, each neurotrophin has specificity for different Trk receptors; NGF is the preferred ligand for TrkA, BDNF and NT-4 for TrkB and NT-3 for TrkC. Since the discovery of the three-dimensional structures for Trk receptors (Ultsch *et al.*, 1999) and complex between NGF and TrkA (Wiesmann *et al.*, 1999), the most important site for ligand binding on the Trk receptor is localized at the most proximal immunoglobulin (Ig) domain of each receptor. This structural information has provided information on the interaction between neurotrophins and their Trk receptors (Urfer *et al*, 1998).

1.2.1.1.   Structure of Trk A and NGF

The Trk family (TrkA, B and C) share the same structural architecture; with their extracellular portion made up of a cysteine-rich cluster (domain 1), three leucine-rich repeats (domain 2), a second cysteine-rich cluster (domain 3) and two immunoglobulin (Ig)-like domains (domains 4 and 5) (Schneider and Schweiger, 1991). The extracellular portion is linked by a single putative transmembrane helix to the intracellular tyrosine kinase domain. Though members of the Trk family only share a 50-55% sequence homology at extracellular regions (Lamballe *et al*., 1991), they share a conserved region (domain 5) that is common to all (Fig. 1.2A). This observation led to a suggestion that domain 5 could be an important ligand binding site. A number of studies focused on domains 4 and 5 of the Trk receptors, making use of truncated or chimeric versions of the receptors (Perez *et al*., 1995; MacDonald *et al*., 1996; Holden *et al*., 1997) and partial proteolytic digestion (Haniu *et al*., 1997). These studies from various groups confirmed that domain 5 was the neurotrophin binding site and their results were supported by the three-dimensional crystal structure of Ig domains on Trk (Ultsch *et al*., 1999).

The crystal structure of the Ig domain on Trk receptors (Ultsch *et al*., 1999) provided the first ever structural information on Trk receptors. The overall structure of Trk receptors (e.g. TrkA; Fig 1.2B) shows two β-sheets that are packed on top of each other in a β sandwich arrangement. Each of these sheets is made up of four strands, in one sheet (A, B, E and D) and the other (G, F, C and C'). In addition, three loops (AB, EF and CC') are located at the C-terminal pole of the domain, while another three loops (BC, DE and FG) at the opposite end. Two interesting observations were noted in this structure. Firstly, Ig-like domains are commonly found buried inside the β sandwich, but domain 5 (Ig-like domain) is located at the

A
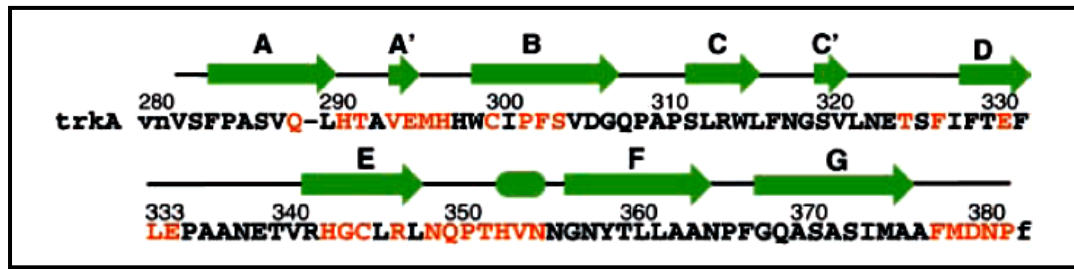
B
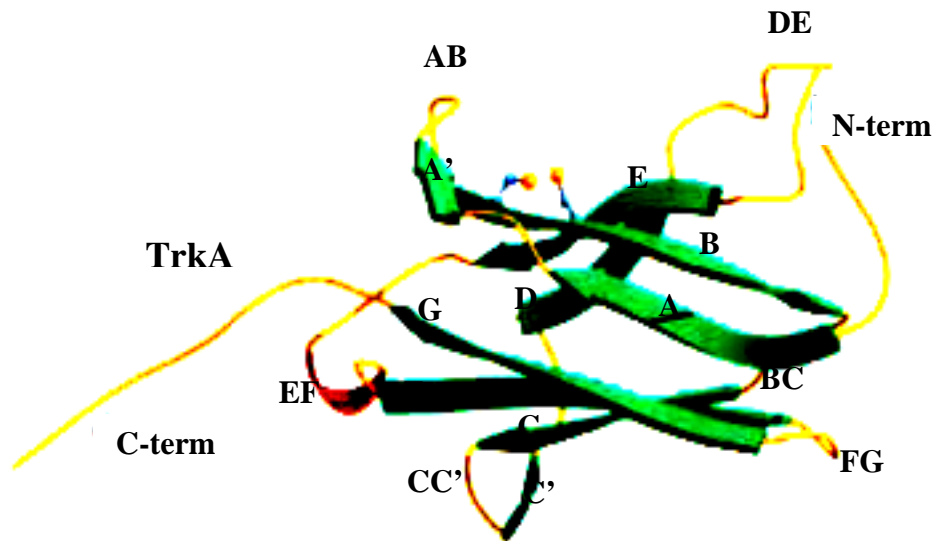
Fig. 1.2: Sequence and structure of domain 5 of TrkA receptors. (A) Secondary structure elements and numbering of domain 5 of the TrkA receptors based on Wiesmann *et al*., 1999. TrkA residues which are in contact with NGF and in the NGF-TrkA-d5 complex are indicated in red. **(B)** Ribbon structure of domain 5 of Trk A (PDB code: 1WWA). The β sandwich core of the molecules is made up of ABED and CC'FG and the exposed disulfide bridges connect strands B and E (adapted from Wiesmann and de Vos, 2001).

surface, making it easily accessible to form a solvent-exposed disulfide bridge with strands B and E. Secondly, this involves strand A. Strand A can be divided into two pieces: A and A' with A' at the GFCC' sheet. However, in Trk-d5, this A' strand continues to be associated with ABED via hydrogen bonds. These two regions have also been identified by alanine-scanning experiments to be involved in ligand binding for both TrkA and TrkC (Urfer *et al*., 1998).

The three-dimensional structure of the NGF-TrkA-d5 complex showed that the elongated, dumbbell-shaped NGF dimer is bound to 2 copies of domain 5 from TrkA via the central β sheet region (Fig. 1.3). This symmetric 2:2 stoichiometry helped established that observation that activation of Trk receptors by neurotrophin caused receptor dimerization (Wiesmann *et al*., 1999). Figure 1.3 shows the complex of NGF and Trk A (domain 5) structure with the orientation of the membrane surface at the bottom of the figure. Each of the symmetrical NGF-TrkA-d5 interface is buried about 2220Å^2 angstroms of the solvent-accessible surface. In each of these surfaces, two distinct patches are seen. The smaller patch ('specificity patch') consists of the N-terminus of NGF in contact with the surface of ABED sheet from TrkA-d5. This region is highly unique and responsible for the specificity of NGF to TrkA receptor. While the second patch ('conserved patch') is formed by residues from the central β-sheet of NGF and loops AB, C'D and EF of TrkA-d5. The sequence for this region is highly conserved among the neurotrophin family and is likely to be present in their respective complexes. The structural complex of NGF-TrkA-d5 also showed that residues important for p75^{NTR} binding are partially exposed; thereby supporting the notion that NGF can simultaneously bind to both TrkA and p75^{NTR} receptors (Wiesmann *et al*., 1999).
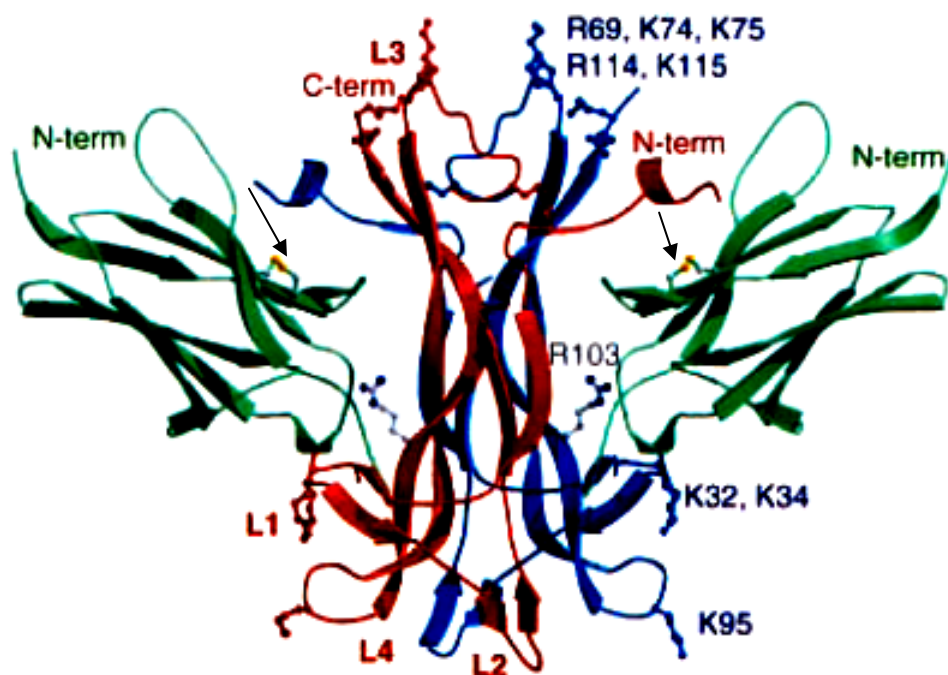
Fig. 1.3: Crystal structure of complex between NGF and domain 5 of TrkA (PDB access code: 1WWW). The two NGF monomers are represented in red and blue, while the two copies of TrkA-d5 are in green. Most of the residues (ball and stick representation) essential for p75^{NTR} binding are positively-charged and located in loops 1, 3 and 4 (L1, L3 and L4). The exposed disulfide bridge of TrkA-d5 that is in contact with the N-terminal helix of NGF is shown in green and yellow (indicated with *black arrows*). Most of the NGF residues shown are positively charged and for p75^{NTR} binding (adapted from Wiesmann and de Vos, 2001).

1.2.1.2   Trk receptor-mediated signaling mechanisms

Tyrosine-kinase mediated signaling by the Trk receptors lead to both survival and differentiation in all neuronal populations. In general, the expression of Trk receptor is sufficient to channel towards a neurotrophin-dependent survival and differentiation response (Allsopp *et al*., 1994; Barrett and Bartlett, 1994). Binding of neurotrophin to Trk receptors lead to both receptor dimerization and kinase activation. These receptors contain 10 conserved tyrosine residues in their cytoplasmic domains, of which three (Y670, Y674 and Y675) are present in the autoregulatory loop of the kinase domain that help regulate tyrosine kinase activity (Stephens *et al*., 1994; Inagaki *et al*., 1995). The remaining tyrosine residues once activated, promotes signaling by creating docking sites for adaptor proteins containing phosphotyrosine-binding (PTB) or src-homology-2 (SH-2) motifs (Pawson and Nash, 2000). These adaptor proteins couple Trk receptors to intracellular signaling cascades (Fig. 1.4) which includes the Ras/Erk (extracellular signal-regulated kinase) protein kinase pathway, phosphatidylinositol-3-kinase (PI-3K)/Akt pathway and phospholipase C (PLC)-γ1 (Reichardt and Fariñas, 1997; Kaplan and Miller, 2000). The major sites for endogenous phosphorylation are two tyrosine residues, Y490 and Y785 that are located away from the kinase activation domain. Most research groups focused on Y490 and Y785 as they interact with the adaptor proteins Shc and PLC-γ1 respectively.
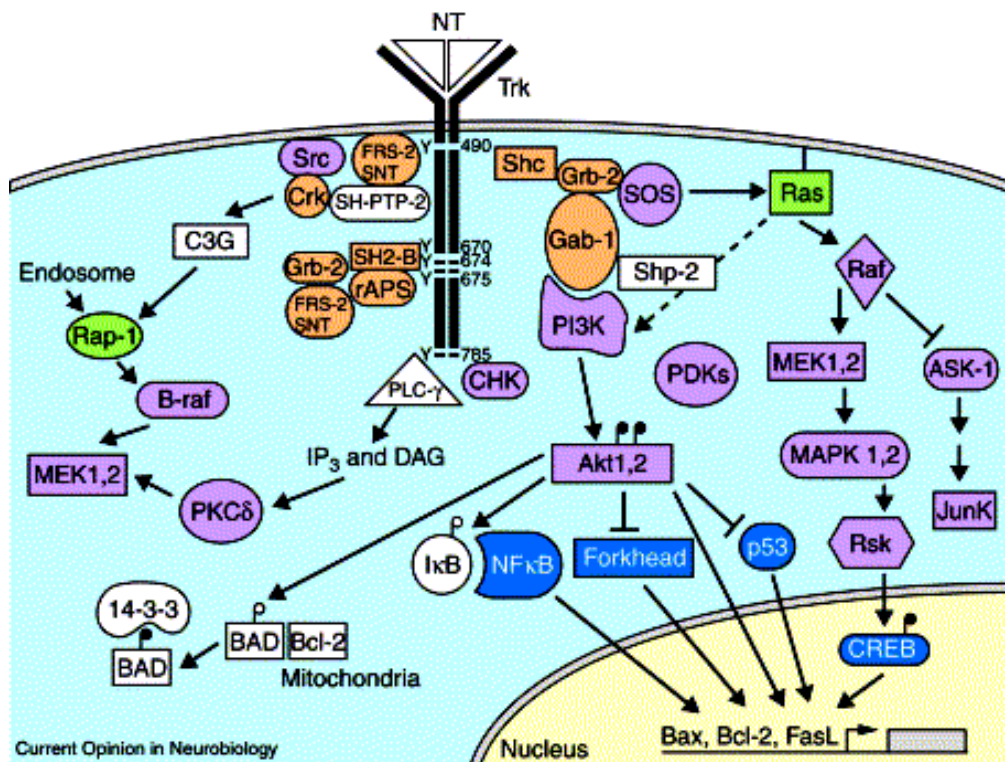
Fig. 1.4: Diagram of signal transduction pathway mediated by activated Trk receptors. The nomenclature for tyrosine residues of Trk receptors is based on the sequence of human TrkA. In the diagram, adaptor proteins are coloured orange, kinases in pink, small G proteins in green and transcription factors in blue. APS refers to adaptor molecule containing PH and SH2 domains; CHK, Csk homologue kinase; MEK, MAPK/ERK; P, serine/threonine (filled-phosphorylated); SNT, suc-1-associated neurotrophic factor target (Patapoutian and Reichardt, 2001).

Signaling through Ras

In most cases, Ras is responsible for 40-60% of the neurotrophin-dependent survival, but it does not act directly to promote survival. Instead, it acts by translating the neurotrophin-initiated signals into multiple signaling pathways. Ras activation is essential for the normal differentiation of PC12 cells and neurons. In addition, it also promotes survival of neurons via activation of either the PI3K/Akt pathway or the mitogen-activated protein kinase (MAPK)/ERK pathways. Transient versus prolonged activation of the MAP kinase pathway has been closely associated respectively, with a proliferation-inducing versus a differentiation-promoting response to neurotrophin application (Grewal *et al.*, 1999).

Neurotrophin signaling through Shc/Grb-2/SOS mediates transient activation of ERK pathway. Once Y490 is phosphorylated, it leads to a recruitment of the adaptor protein Shc via the Shc PTB domain (Stephens *et al.*, 1994). Subsequently, Shc is phosphorylated by Trk, resulting in further recruitment of a complex of adaptor protein Grb-2 and the Ras exchange factor son of Sevenless (SOS). SOS, in turn would activate Ras releasing a cascade of downstream events; like activation of PI-3K, c-raf/ERK and p38 MAP kinase/MAP-kinase-activated protein kinase 2 pathways (Xing *et al.*, 1996). The downstream targets of ERK kinases include the RSK kinases (ribosomal S6 kinase) and together with MAP-kinase-activated protein kinase 2, they phsophorylate CREB (cAMP-regulated enhancer binding protein) and other transcription factors (Xing *et al.*, 1998). These transcription factors in turn control the expression of many genes known to be regulated by NGF and other neurotrophins, e.g. CREB regulates genes important for the prolonged neurotrophin-dependent survival of neurons (Bonni *et al.*, 1999; Riccio *et al.*, 1999).

Several tyrosines on adaptor protein fibroblast growth receptor substrate (FRS-2) are phosphorylated by Trk which then function as binding sites for several additional proteins, including the adaptor protein Grb-2 and Crk, the protein phosphatase Src homology protein tyrosine phosphatase-2 (SH-PTP), the cyclin-dependent kinase substrate p13^{suc1} and Src. The binding of FRS-2 initiates a cascade of Crk, C3G, Rap-1 (small G-protein), B-ref respectively and eventually ERK signaling (York *et al.*, 1998 and 2000; Nosaka *et al.*, 1999). Activation of Erk is also facilitated by SH-PTP-2, which appears to inactivate an inhibitor, perhaps Ras-GAP or MAPK phosphatase (Wright *et al.*, 1997). FRS-2 also provides link to the Src family tyrosine kinases that are involved in receptor endocytosis as well as other cellular responses (Wilde *et al.*, 1999; Beattie *et al.*, 2000). In PC12 cells, the prolonged activation of ERK signaling and differentiation is dependent on the adaptor proteins attracted to phosphorylated Y490 on FRS-2, thereby activating distinct signaling pathway (York *et al.*, 1998; Meakin *et al.*, 1999).

Signaling through PI3K

The activation of the phosphatidylinositol-3-kinase (PI-3 kinase) is essential for the survival of many populations of neurons. Lipid products generated by PI3K will in turn, recruit many proteins containing the pleckstrin-homology domains to the membrane, including the Akt kinases and 3-phosphoinositide-dependent kinases (PDKs). Akt is activated at the membrane by PDK and it phosphorylates several proteins important in the control of cell survival (Datta *et al.*, 1999; Yuan and Yankner, 2000). These include BAD (Bcl-2/Bcl-x-associated death promoter), IκB, the forkhead transcription factor (FKHRL1), glycogen synthase kinase (GSK) 3-β and human caspase-9 (Brunet *et al.*, 1999).

BAD belongs to the Bcl-2 family and when unphosphorylated, promotes apoptosis by binding to Bcl-xL. The bcl-2 family is involved in pro- and anti-apoptosis signaling cascade. However, the phosphorylation of BAD by Akt/MAPKs results in its association with 14-3-3 proteins, preventing it from binding with Bcl-xL and subsequent apoptosis (Datta *et al.*, 1997). Another target of Akt is IκB (inhibitor of NF-κB) and the phosphorylation of IκB is often followed by its degradation and activation of NF-κB. Transcription activated by nuclear NF-κB has been shown to promote neuronal survival (Middleton *et al.*, 2000).

PI-3 kinase is activated by Ras. In most neurons, Ras-dependent activation of PI-3 kinase is the major pathway for neurotrophins to convey pro-survival signals (Vaillant *et al.*, 1999). PI-3 kinase and its downstream signaling can also be activated through adaptor proteins (Shc, Grb-2 and Gab-1) in a Ras-independent manner (Holgado-Madruga *et al.*, 1997). In some cells, but not PC12 cells, insulin receptor substrate (IRS)-1 has been phosphorylated in response to neurotrophins and in turn, able to recruit and activate PI-3 kinase (Yamada *et al.*, 1997).

Signaling through PLC-γ1

Phosphorylation of Y785 on TrkA recruits PLC-γ1 to be phosphorylated and activated. Once PLC-γ1 is activated, it hydrolyses phosphatidylinositides to generate diacylglycerol (DAG) and inositol 1, 4, 5 triphosphate (IP3). IP3 induces the release of calcium stores, causing an increase in cytoplasmic Ca^{2+} levels and activating many calcium-dependent pathways. It has been shown that in PC12 cells, NGF activates a DAG-regulated protein kinase, protein kinase C (PKC)-δ that is important for activation of the ERK cascade and neurite outgrowth (Corbit *et al.*,

1999). (PKC)-δ seems to act between Raf and MAPK/ERK in this signaling cascade.

1.2.2 P75 neurotrophin receptors (p75^{NTR})

P75^{NTR} belongs to the tumor necrosis factor family (TNF) receptor superfamily (TNFR). A family of cysteine-rich domain (CRD)-containing receptors. It is interesting that other members in the TNFR family bind trimeric ligands like TNF, while p75^{NTR} binds dimeric neurotrophins thus suggesting a different ligand-receptor recognition mechanism for p75^{NTR}. The binding of neurotrophins to p75^{NTR} result in two possible consequences. The first consequence is based on p75^{NTR}'s interaction with neurotrophin alone; while the second is a combined effect of both Trk and p75^{NTR}, in which p75^{NTR} confers ligand selectivity to Trk receptors for neurotrophin binding (Bothwell, 1995, Hempstead, 2002, Huang and Reichardt, 2003). Neurotrophin activation of p75^{NTR} without the involvement of Trk receptors has shown to induce neuronal apoptosis and modulate cell survival (Dechant and Barde, 2002; Huang and Reichardt, 2003; Rabizadeh and Bredesen, 2003). Both outcomes seem to be mediated by a wide selection of intracellular signaling molecules downstream of p75^{NTR} (e.g. nuclear factor κB (NF-κB), c-Jun N-terminal kinase (JNK)). A classically known "high affinity" complex is formed by both p75^{NTR} and with Trk receptors on neuronal cells (Hempstead *et al*., 1991; Bothwell, 1995). However, the molecular mechanisms of the cross talk are still unknown (Hempstead, 2002).

However, when p75^{NTR} is expressed in the same cell as Trk receptors, the survival signaling predominates with exposure to neurotrophin. This is due to the enhanced affinity of neurotrophins to their specific Trk receptor (one of the function of

p75^{NTR}) and activation of Akt pathway by Trk receptors that suppress the apoptotic signal initiated by p75^{NTR}. This 'Jekyll and Hyde' nature of p75^{NTR} is perplexing as this receptor sends out both apoptotic and pro-survival signals.

1.2.2.1   Structure of p75^{NTR} and NGF

The sequence of the extracellular region of p75^{NTR} (Fig. 1.5A) showed that it is made up of four cysteine-rich domains (CRDs) and has an elongated and kinked structure (Fig. 1.5B).The crystal structure of NGF in complex with the extracellular domain of p75^{NTR} reveals a 2: 1 (NGF/p75^{NTR}) stoichiometry (Fig. 1.5B; He and Gracia, 2004). Since unbound NGF (McDonald *et al.*, 1991) is a symmetric homodimer, both sides of the molecule have equal tendency to bind to p75^{NTR}. However, once one side of NGF has bound to p75^{NTR}, the second potential p75-binding site is altered by a conformational change caused by the p75^{NTR}-NGF interaction. In the absence of neurotrophin, p75^{NTR} exists as dimers on the cell surface (Grob *et al.*, 1985; Jing *et al.*, 1992).

Upon binding with homodimer NGF, p75^{NTR}'s overall structure is described as a roughly parallel configuration, in which the long axis of p75^{NTR} aligns with the 'seam' formed by the edge of the NGF dimerization interface (Fig. 1.5B). This complex is tethered together through two spatially separated binding epitopes, designated as "site I" and "site II". Site I is the site of interaction between the wider end of the NGF dimer and CRD 1 and 2 of p75^{NTR}. While site II is formed between the tapered end of the NGF dimer and CRD 3 and 4 domains of p75^{NTR}. The opposite face of the NGF dimer has identical sets of residues and designated as "pseudosites I and II". In addition, the binding sites for p75^{NTR} require contributions from the two NGF monomers.

A

B
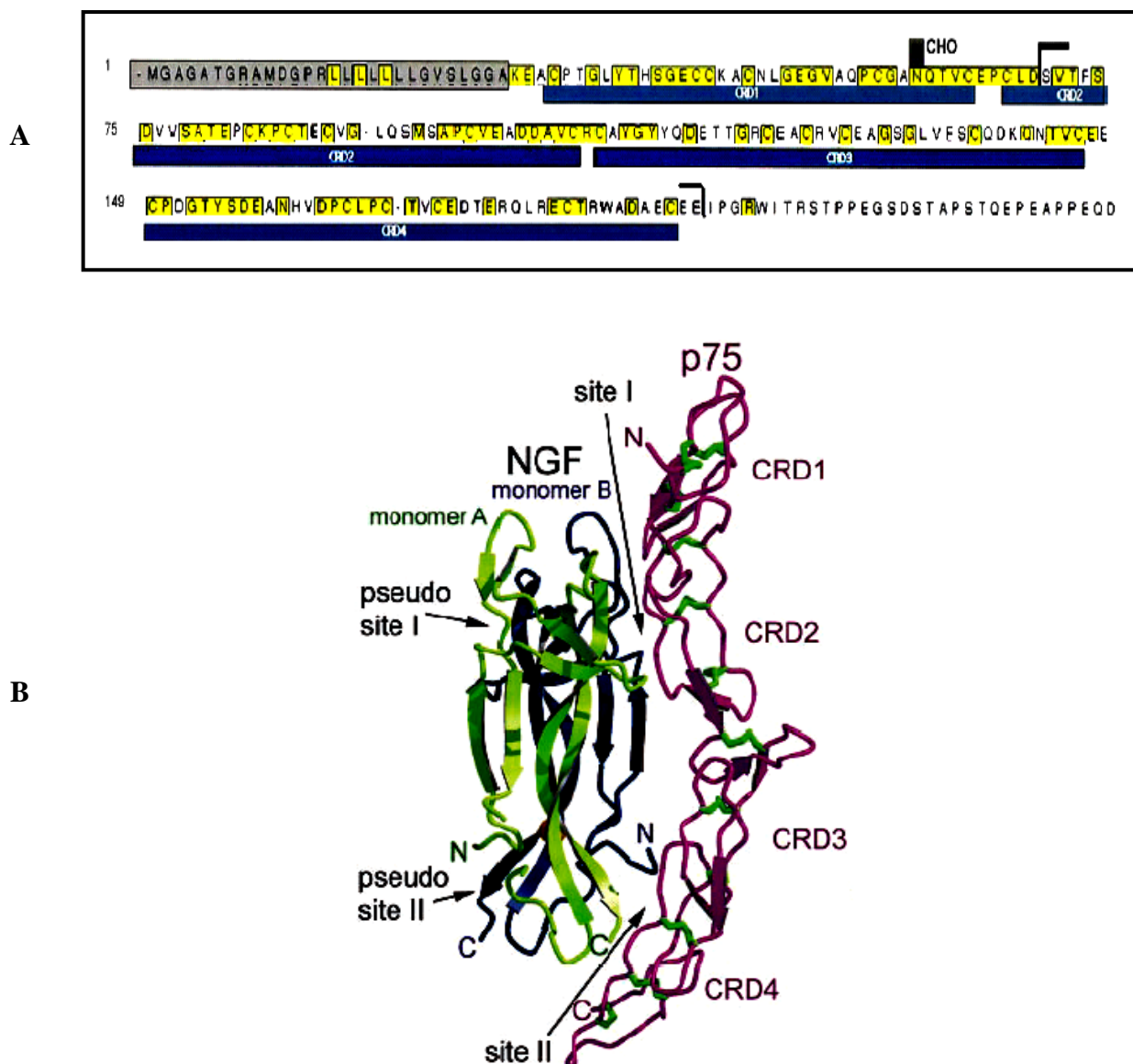
Fig. 1.5: Sequence and structure of p75^NTR. (A) Sequence of extracellular domain of p75^NTR as adapted from Roux and Barker (2002). The grey box represents the signal peptide of p75^NTR, while the blue bars indicate the extracellular cysteine-rich domains (denoted by CRD1-4). The extracellular N-linked glycosylation site is denoted by CHO. (B) Crystal structure of NGF with p75^NTR. P75^NTR binds along one side of the NGF homodimer. Backbone representation of NGF monomer A is coloured in green, while monomer B is blue and p75^NTR in purple. The green sticks on p75^NTR represent disulfide bonds (adapted from He and Garcia, 2004).

1.2.2.2   Functional roles of p75^{NTR}

P75^{NTR} is involved in a wide array of cellular responses including apoptosis, neurite outgrowth (Yamashita *et al*., 1999) and myelination (Cosgaya *et al*., 2002). Upon stimulation with neurotrophin, it can activate multiple downstream signals; including the small GTP binding protein Rac, transcription factors NF-κB and the stress-activated kinase JNK (Fig. 1.6). The two main pathways (apoptosis and pro-survival) activated by p75^{NTR} will be discussed in detail.

1.2.2.2.1.   P75^{NTR} receptor-mediated apoptotic signal

It is now established that in the absence of Trk signaling, neurotrophin binding to p75^{NTR} will activate apoptosis as seen in specific cell types (Roux and Barker, 2002). Several studies have shown that neurotrophin binding to p75^{NTR} had caused apoptosis, for instance in cultured Schwann cells (Syroid *et al*., 2000; Khursigara *et al*., 2001), oligodendrocytes (Casaccia-Bonnefil *et al*., 1996), motor neurons of embryonic spinal cord (Frade and Barde, 1999), hippocampal neurons (Friedman, 2000), neuroblastoma cells (Bunone *et al*., 1997) and smooth muscle cells (Wang *et al*., 2000). Various insults to the nervous system can result in a p75^{NTR}-dependent apoptotic program in motor neurons following lesions of the facial motor nerve (Ferri *et al*., 1998), hippocampal neurons after induction of seizures (Roux *et al*., 1999), Schwann cells after axotomy (Syroid *et al*., 2000), cortico-spinal neurons after axotomy (Giehl *et al*., 2001) and oligodendrocytes after spinal cord injury (Beattie *et al*., 2002). In addition, increased p75^{NTR} expression has been observed in patients with multiple sclerosis (Dowling *et al*., 1999) and Alzheimer's disease (Salehi *et al*., 2000), leading to a possibility that p75^{NTR} may be involved in these neurodegenerative diseases.
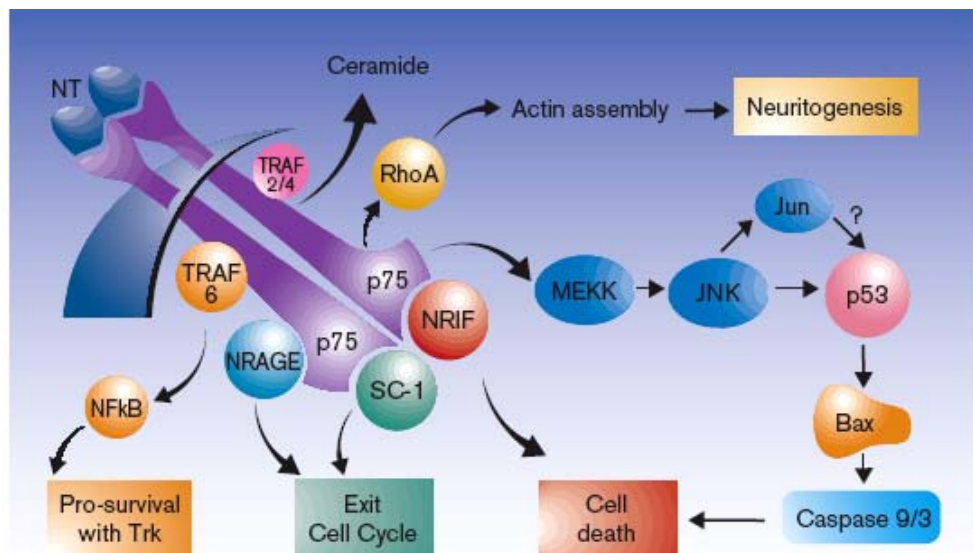
Current Opinion in Neurobiology

Fig. 1.6: p75^{NTR} signaling pathways. P75^{NTR} binds to a number of interacting proteins, including TRAF2, 4, and 6, NRAGE, SC-1, and RhoA, which play roles in cell survival, cell cycle regulation, and neurite outgrowth. It also increases ceramide levels and activates the JNK-p53-Bax cell death pathway (adapted from Kaplan and Miller, 2000).

However, the physiological actions of p75^{NTR} are not restricted to neural system, as recent *in vivo* and *in vitro* studies have found its involvement in non-neuronal tissues (i.e. vasculature; Wang *et al*., 2000).

The mechanism by which p75^{NTR}-mediated apoptosis is activated has not been fully solved, but stress-activated MAP kinase, c-jun N-terminal kinase, JNK has been shown to play an essential role (Yoon *et al*., 1998). The targets of JNK include the transcription factors c-jun, ATF-2 and p53. P75^{NTR}-mediated apoptosis is shown to be independent of c-jun (Palmada *et al*., 2002), while blocking p53 has shown to prevent the death signal (Aloyz *et al*., 1998). Unlike other members of the TNF receptor family where apoptosis activates caspase-8, p75^{NTR} does not. Only caspases (1, 3, 6 and 9) have been implicated in p75^{NTR}-mediated cell death (Gu *et al*., 1999; Agerman *et al*., 2000; Troy *et al*., 2002). However, the mechanism of caspase activation upon neurotrophin binding to p75^{NTR} and the role of JNK pathway remains to be determined.

1.2.2.2.2   P75^{NTR} receptor-mediated pro-survival signal

The function of neurotrophin binding to p75^{NTR} is to facilitate the pro-survival signals of the Trk receptors (Roux and Barker, 2002). In addition, it also has the ability to promote survival independent of Trk receptors. For example, neurotrophin binding to p75^{NTR} has been shown to block the death of neuroblastoma cell (Oh *et al*., 1993; Cortazzo *et al*., 1996), of sensory neurons from tropic factor deprivation (Longo *et al*., 1997) and hippocampal neurons after glutamate receptor activation (Bui *et al*., 2002). In addition, studies with p75^{NTR}-/- mice showed that this receptor is crucial for the survival of subplate neurons in the developing cortex (DeFreitas *et al*., 2001).

This finding that p75^{NTR} can initiate both opposing pathways (apoptosis and pro-survival) is not entirely shocking as other members of the TNF family can elicit both apoptotic and pro-survival signals. One of the best characterized anti-apoptotic signals generated is by the activation of the transcription factor, NF-κB (Karin and Lin, 2002). The activation of NF-κB after neurotrophin binding to p75^{NTR} functions as a pro-survival signal in both Schwannoma cell line (Gentry *et al*., 2000) and primary Schwann cells (Khursigara *et al*., 2001) that only express p75^{NTR}. Neurotrophin treatment also induced pro-survival signal via NF-κB in trigeminal (Hamanoue *et al*., 1999) and hippocampal neurons (Culmsee *et al*., 2002). However, in both PC12 cells (Taglialatela *et al*., 1997; Foehr *et al*., 2000; Wooten *et al*., 2001) and sympathetic neurons (Maggirwar *et al*., 1998) that coexpress both TrkA receptors and p75^{NTR}, it is uncertain which receptor is responsible for NGF-dependent induction of NF-κB that lead to overall cell survival.

Another possible pathway for the pro-survival signal of p75^{NTR} receptor is by the activation of the phosphatidyl inositol 3-kinase (PI3K)-Akt pathway (Roux *et al*., 2001; Bui *et al*., 2002). Akt pathway is able to prevent apoptosis through phosphorylation-dependent inactivation of caspase-9, pro-death domain Bad and members of the Forkhead family of transcription factors (del Peso *et al*., 1997; Cardone *et al*., 1998; Brunet *et al*., 1999). It was shown that hippocampal neurons were protected by the activation of p75^{NTR} after excitotoxic injury (Bui *et al*., 2002). Interestingly, activation of Akt also caused a corresponding activation of NF-κB (Beraud *et al*., 1999), leading to a possible link between the two signals.

1.2.3   Cross-talk between TrkA and p75^{NTR}

Most cells coexpress both Trk receptors and p75^{NTR}. Though these two receptors share no sequence similarity in either ligand-binding or cytoplasmic domains and each activates their own distinct neurotrophin-dependent signaling pathways, they collaborate to mediate the effects of neurotrophins. Individually, they interact with neurotrophins at similar affinity of about 10^{-9}M (Rodriguez-Tebar *et al.*, 1990, 1992; Kaplan *et al.*, 1991) which is much lower than the observed high-affinity NGF binding sites (Kd ~ 10^{-11}M) in PC12 cells and sensory neurons (Greene and Tischler, 1976; Sutter *et el.*, 1979; Rodriguez-Tebar *et al.*, 1990, 1992). The presence of both receptors also increased the association rate of NGF to TrkA by 25-fold (Mahadeo *et al.*, 1994). Hence, both receptors are required to form the high-affinity complex for neurotrophin binding (Hempstead *et al.*, 1991).

However, the precise molecular mechanisms that allow p75^{NTR} to enhance NGF binding to TrkA and increase TrkA responsiveness to NGF remain uncertain. So far, two hypotheses have been proposed. P75^{NTR} is proposed to either act as a co-receptor that presents NGF to TrkA in a favorable binding conformation or has an allosteric effect on Trk that confers high-affinity binding to the TrkA receptor irrespective of NGF binding to p75^{NTR} (Roux and Barker, 2002). The discovery of the complex structure of p75^{NTR} and NGF (He and Garcia, 2004) confirmed the high-affinity binding site functional studies. Despite a clash between the TrkA-d5 domain and p75^{NTR} CRD2-3 junction, homodimer NGF is capable of binding to both TrkA and p75^{NTR} simultaneously on opposite sides to form a trimolecular complex (Fig. 1.7). Furthermore, the p75^{NTR}-induced NGF conformational changes on the opposite side could be a mechanistic glimpse into the long-suspected allostery by
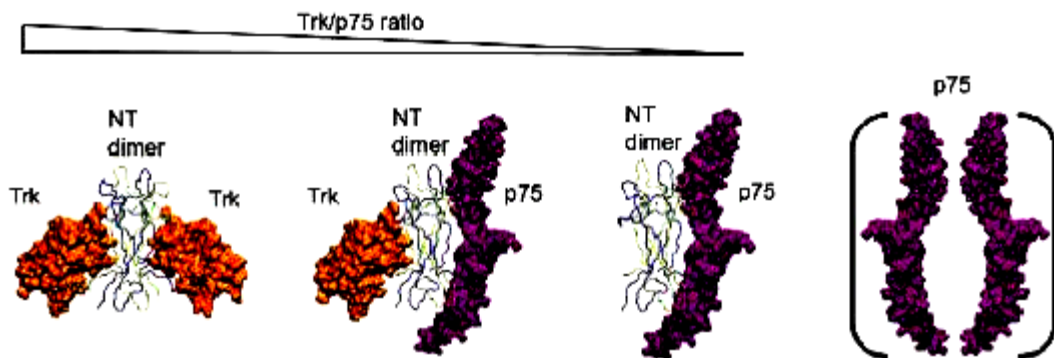
Fig. 1.7: Potential model of p75^NTR-Trk-neurotrophin trimolecular complex. Diagram of cell surface equilibrium between various neurotrophin, p75^NTR and TrkA receptor complexes and NGF is represented by tubes and receptors are represented as surfaces. From high to low TrkA/p75^NTR ratio, the complex could choose to be 2:2 NGF/TrkA, 1:2:1 TrkA/NGF/p75, 2:1 NGF/p75 and finally an unliganded p75 dimer (He and Garcia, 2004).

which p75^{NTR} modulates TrkA ligand affinity and specificity for NGF (He and Garcia, 2004).

Numerous studies have clearly shown that the presence of p75^{NTR} is capable of activating maximum Trk signaling (Roux and Barker, 2002); yet little is known about the influence of Trk on p75's downstream effect. Coactivation of both receptors (Trk and p75^{NTR}) has shown to block p75^{NTR} induced apoptosis (Yoon *et al.*, 1998) and is suggested to occur through Trk-dependent Ras activation, thereby blocking the pro-apoptotic p75^{NTR} activated kinase (JNK; Kaplan and Miller, 2000). Similarly, the Trk activation of PI3K and the subsequent activation of the pro-survival molecule Akt may be used to counteract pro-apoptotic signals from p75^{NTR} (Kim *et al.*, 2002). Another possible way whereby p75^{NTR} independent signaling could be modified by Trk activation is by recruitment of p75^{NTR} to the activated Trk complex. Adaptor molecules that connect the two receptors may alter the conformation of p75^{NTR} or change the stoichiometry of the receptor complex, thereby preventing signal molecules from binding and subsequent activation of pathways. Two such adaptor molecules have been identified.

The protein ankyrin repeat-rich membrane spanning (ARMS) was isolated from a yeast two-hybrid screen using the intracellular region of p7^{5NTR} as bait (Kong *et al.*, 2001). ARMS is a large protein (over 200-kDa), containing four potential transmembrane domains, N-terminal ankyrin repeats, a SAM domain and a potential PDZ binding domain at the extreme carboxyl terminus. Sensory neurons of the dorsal root ganglion (DRG) express ARMS into adulthood and in sympathetic neurons, it is also found to co-localize with both p75^{NTR} and Trk receptors and is tyrosine phosphorylated in response to Trk activation by neurotrophin. Gentry *et al* (2004) observed that a ternary complex is formed between Trk, p75, and ARMS,

leading to a speculation that ARMS may be the link signaling between p75^{NTR} and Trk, though functional effects of this connect remains to be determined.

A second adaptor protein, p62 may link both p75^{NTR} and Trk receptors indirectly. P62 has shown to bind and alter the localization of the atypical protein kinase C (aPKC) in response to NGF (Samuels *et al*., 2001). These aPKCs are unique as they do not require DAG or Ca^{2+} ions for activity and are thought to function upstream of NF-κB (Diaz-Meco *et al*., 1994). In PC12 cells, the endogenous p62 has been shown to bind to both TrkA and p75^{NTR} binding protein, TRAF6, to facilitate the activation of NF-κB by NGF (Wooten *et al*., 2001). The interaction of p62 with TrkA was also essential for TrkA internalization into endosomes (Geetha and Wooten, 2003), hence making this adaptor protein an important 'bridge' to facilitate synergistic signaling from the two receptors to promote survival and differentiation.

1.3 Therapeutic applications of NGF

Neurotrophins and their receptors are trophic factors known to play important roles in cutaneous tissues, nerve development and reconstruction after injury. Among the neurotrophins, the nerve growth factor (NGF) was one of the earliest used for clinical studies. NGF has been tested for potential therapeutic application in neuropathies of the central and peripheral nervous system and more recently in human corneal and cutaneous ulcers. This section will focus on the potential of NGF as a therapeutic agent in these three specific areas.

1.3.1 Neuropathies of the peripheral nervous system

Neurotrophin factors may play key roles in pathophysiological mechanisms of human neuropathies. NGF is trophic to small-diameter sensory fibers and regulates

nociception. The most common causes of human peripheral neuropathies world-wide are genetic neuropathy, leprous neuropathy, diabetes neuropathy and traumatic neuropathy and pain (Anand *et al.*, 1991, 1994, 1996; Anand, 1997).

1.3.1.1 *Genetic neuropathy*

The failure of trophic interaction between the target organ and its innervation may result in nerve dysfunction, degeneration and abnormal regeneration. In hereditary sensory and autonomic neuropathy type IV (HSAN IV) or congenital insensitivity to pain and anhidrosis (CIPA), mutations of the NGF receptor (TrkA) have been found (Indo *et al.*, 1996). CIPA is an autosomal recessive disorder that is characterized with failure to develop protective sensation which leads to non-painful injury and trophic mutilation, loss of sweating which result in fever and mental retardation. In this disorder, the three types of NGF-dependent neurons; sensory, sympathetic and cholinergic forebrain are affected. However, the mutations only cause a partial loss-in-function as larger sensory fibers and autonomic control of blood pressure are unaffected. Hence, recombinant human NGF could restore nociception in some patients.

1.3.1.2 *Leprous neuropathy*

Leprosy affects between 10-15 million people. Early reports stated that the nerve lesions present in both human and rodent leprosy occur in both unmyelinated fibers and Schwann cells (Shetty *et al.*, 1988). These lesions show hypoalgesia and hypopigmentation and hypohidrosis. The present treatment is with anti-bacterial drugs. However, the failure to regenerate nerves, especially nociceptor sprouting within the skin that aids trophic changes remains a major cause of disability. NGF

levels are decreased in skin and nerves of leprosy-affected human (Anand *et al.*, 1994). While sensory loss in leprosy skin is the consequence of invasions of *Mycobacterium leprae* of Schwann cells related to the unmyelinated fibers and early loss of cutaneous pain sensation (in the presence of nerve fibers and inflammation) is a characteristic of leprosy that remains unsolved. NGF is normally produced by basal keratinocytes and acts via Trk A receptor present on nociceptive nerve fibers to increase their sensitivity, especially during inflammation. A study that compared NGF and TrkA reactivity between normal and leprosy-affected patients (Facer *et al.*, 1998; 2000) showed a marked increase in TrkA staining in normal patients, suggesting that recombinant human NGF treatment may help restore pain sensation.

1.3.1.3   *Diabetic sensory polyneuropathy*

Sensory and autonomic polyneuropathy is a common form of neuropathy in diabetic patients and there is presently no specific and effective treatment for it. NGF immunostaining showed strong staining in the basal keratinocyte layer in control skin and decreased staining in diabetic skin. In early human diabetic neuropathy skin, both NGF levels and axon-reflex vasodilatation are decreased significantly (Anand *et al.*, 1996). Axon-reflex vasodilatation is a test of unmyelinated afferent fibers to stimulant, capsaicin. Intradermal application of capsaicin would induce flare and activate nociceptive fibers, leading to increased capillary flux (measured by laser Doppler; Anand, 1992). The reduced level of NGF in the target organ and decreased axonal transport may reduce the sensitivity to warm/heat pain. Since both the loss of nociception and axon-reflex vasodilatation caused foot ulceration (Parkhouse and Le Quesne, 1988), a major and serious complication in diabetic patients, treatment with NGF may cause relief.

Two sets of phase II clinical trials suggested that recombinant human NGF (rhNGF) administration was effective at ameliorating the symptoms associated with both diabetic polyneuropathy and HIV-related neuropathy (McArthur *et al.*, 2000). However, a large-scale phase III clinical trial (Apfel *et al.*, 2000) of 1019 patients randomized to receive either rhNGF or placebo for 48 weeks failed to confirm the earlier indications of efficacy. Among the explanations offered for the discrepancy between the two sets of trials were a robust placebo effect, inadequate dosage, different study populations, and changes to the formulation of rhNGF for the phase III trial. As a result, the pharmaceutical company, Genentech has decided not to proceed with further development of rhNGF (Apfel, 2002).

1.3.1.4 *Traumatic neuropathy and pain*

About less than 10% of patients with diabetic neuropathy would develop clinically significant persistent pain (Thomas and Tomlinson, 1993). In some patients, the pain is ironically controlled with treatment for diabetes, but mostly it is self-limiting. In injured nerve trunks, NGF levels are acutely reduced. However, neuropathic patients with chronic skin hyperalgesia showed marked increase in NGF levels. Hence, anti-NGF agents may provide relief to pain.

1.3.2 **Neuropathies of the central nervous system**

The ability of neurotrophins to prevent or reduce neuronal degeneration in animal models of neurodegenerative diseases has led to several clinical trials. However, one of the main obstacles is the mode of delivery. There must be sufficiently high doses of neurotrophin factors at the target regions of the brain to efficiently modify the

disease processes, but delivery has to be specific to targeted areas to minimize adverse effects.

Also, the entry of NGF protein to the brain is restricted by the blood-brain barrier and making it difficult to exert and assess its potential therapeutic effects. At present, several approaches have been developed to introduce NGF to the brain in a continuous manner such as continuous minipump (Williams *et al.*, 1986) microsphere carriers (Mahoney and Saltzman, 1999), polymeric implants (Powell *et al.*, 1990; Yamamoto *et al.*, 1992) and liposomes (Zou *et al.*, 1999). All these systems allowed a controlled NGF delivery to a localized area of the brain over a prolonged period of time.

1.3.2.1   Alzheimer's disease (AD)

AD is the most common neurodegenerative disorder affecting 4 million people in the United States alone. Its prevalence is set to increase in the next 25 years and effective therapies are urgently needed to prevent or slow down the progressive neuronal degeneration in AD. The hallmark features of this disease include neurofillary tangles and amyloid plaques. However, the mechanism leading to the widespread degeneration of synapses and neurons remain unanswered. One of the neuronal populations badly affected in AD is the cholinergic neurons of the basal forebrain (Whitehouse *et al.*, 1982; Perry *et al.*, 1997). The only drugs available target the cholinergic system by inhibiting acetylcholine degradation, to compensate for the loss of cholinergic neurons in AD.

Studies have shown NGF to be a potential therapeutic agent for AD. NGF is produced in the adult hippocampus and neocortex (Korsching *et al.*, 1985); infusing NGF to the ventricles prevented lesion-induced degeneration of cholinergic neurons

(Hefti, 1986) and reduced the atrophy of basal forebrain cholinergic neurons in aged rat brain (Fischer *et al*., 1987). Furthermore, NGF improved age-related impairments in learning and memory (Fischer *et al*., 1987). In these studies, NGF was delivered to the brain by intracerebroventricular infusions. This technique allowed NGF to reach the targeted cholinergic neurons in the basal forebrain, but was not specific enough; thereby causing adverse effects. Hence, a more spatially restrictive and targeted manner of NGF delivery was needed and *ex vivo* gene therapy was explored.

The recent phase I clinical trial on the therapeutic application of NGF in Alzheimer's disease (AD) used *ex vivo* NGF gene delivery method. Eight patients with mild AD were enrolled and had autologous fibroblasts that were genetically modified to express the human NGF implanted into their forebrains. The outcome was based on assessment of cognitive function, serial MRI scans and PET scans. These results showed improvement in the rate of cognitive decline and the group was warranted to continue the next phase of investigation that is still ongoing (Tusztnski *et al*., 2005).

1.3.3   Corneal and cutaneous ulcers

About 4% of the world's population suffers from burns and chronic skin ulcers. Cutaneous wound is known to elicit a series of typically cellular responses that include clotting, inflammatory infiltration, reepithelialization, the formation of granulation tissue (including new blood vessels), followed by tissue remodeling and wound contraction. Human corneal neurotrophic ulcer is an ocular disorder that is caused by a variety of endogenous and exogenous insults that may lead to eventual blindness. Enrollment of patients for the study was based on the corneal ulcer that is

unresponsive to conventional therapy. All patients (n=65) with corneal ulcer treated with NGF were completed healed. Hence, the recovery of corneal ulcers with NGF led to a suggestion that progressive corneal damage was a result of insufficient NGF levels (synthesis, release or utilization; Aloe, 2004). A recent study suggested that the mechanism of healing was by the modulation of functional activities of fibroblastic-keratocytes by NGF (Micera *et al.*, 2006).

Cutaneous ulcers can be caused by diseases (e.g. rheumatoid arthritis, systemic sclerosis and diabetes) and pressure (due to lack of mobility in old people). In both rheumatoid arthritis and systemic sclerosis, vasculitis is a common cutaneous disorder. It is characterized by skin inflammation, damage of peripheral blood vessels and local tissue necrosis (Dahn, 1998; Tuveri *et al.*, 2000). Patients with ulcers (n=4) were treated with NGF topically after showing no response to conventional treatment. The treatment with NGF showed progressive improvement and reaching complete recovery at eight weeks. A study by Tuveri *et al.* (2006) showed that NGF can promote healing of human corneal, cutaneous diabetic and pressure ulcers. Hence, there is great potential for NGF as a therapeutic agent in the treatment of corneal and cutaneous ulcers.

1.4   NGF from snakes

Snake venoms are one of the first sources from which NGF was isolated. Though NGF activity was observed in mouse sarcoma tissues, it was uncertain as whether the nerve growth promoting activity of mouse sarcoma tissues was due to proteins acting directly or indirectly via nucleic acid. Hence, Cohen and Levi-Montalcini (1956) used dried moccasin snake venom that possess phosphodiesterase activity, but free from nucleic acid contamination. To their surprise, they found that the crude

venom (*Agkistrodon piscivorus*) was approximately 3000-6000 times as active as crude tumor homogenate in promoting fibre outgrowth in spinal ganglia *in vitro*. NGF is present primarily in three families of venomous snakes – Viperidae, Crotalidae and Elapidae (Hogue-Angeletti and Bradshaw, 1979). Snake NGF, especially those from cobras have been reported to be superior in inducing neurite outgrowth in pheochromocytoma (PC12) cells when compared with NGFs from other snakes (Lipps, 1998). Server *et al.* (1976) mentioned that NGFs from cobra, *Naja naja* and mouse submandibular gland were able to elicit neurite outgrowth from chick embryonic dorsal root ganglion.

1.4.1 Venomous snakes

There are five families of venomous snakes, made up of colubrids (*Colubridae*), elapids (*Elapidae*), sea snakes (*Hydrophiidae*), true vipers (*Viperidae*) and pit vipers (*Crotalidae*). The largest family is the colubrids (1,500 species) that consists a few venomous members, whereas members in elapids (170 species), sea snakes (50 species), true vipers (40 species) and pit vipers (140 species) are all venomous (Edstrom, 1992). Snakes are equipped with venom apparatus (Fig. 1.8) to inflict serious bites in their victims to immobilize and ultimately kill them. The typical apparatus consists of a venom gland, venom duct and one or more fangs located on each side of the head. Venom is produced in paired modified salivary glands that are located superficially beneath the scales in the posterior part of the head and eyes. The gland is linked to the fangs by a duct and contraction of muscles around the gland compresses the gland, forcing the flow of the venom along the duct to the fang and is primed for an attack (Minton, 1990). Snake venoms consist of complex mixture of proteins, nucleotides and inorganic ions. The different peptides and
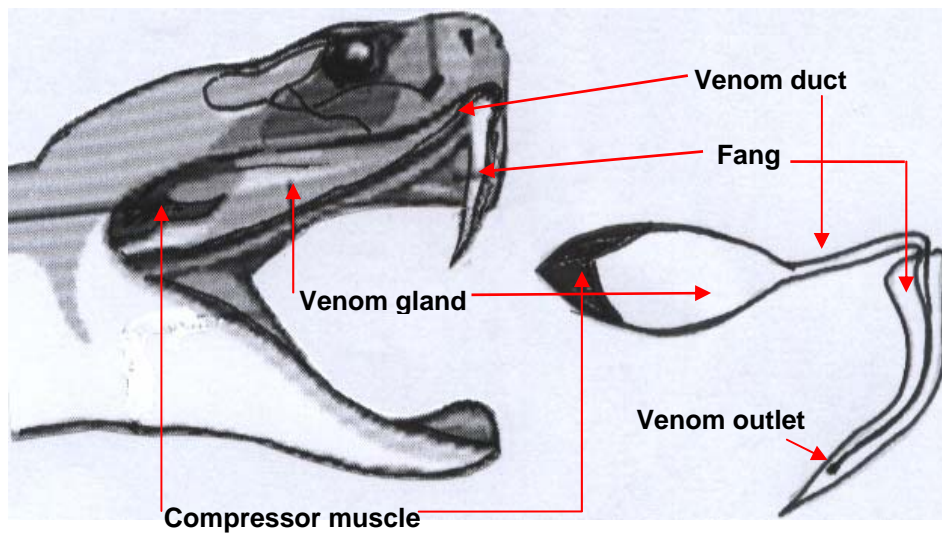
Fig. 1.8: Snake venom gland apparatus. It comprises of venom gland, venom duct and fang(s). The venom is produced in the venom gland (modified salivary gland) and linked to the fangs by the venom duct. Contraction of compressor muscles around the gland forces the venom from the duct to the fangs and the snake is primed for attack.

polypeptides present are responsible for the formidable array of toxic properties of the venom. At present, there are a total of 25 different enzymes identified in snake venoms alone, with the number varying with different species. The individual enzymes and their possible roles are stated in Table 1.1.

1.4.2   The Elapids

The elapids include the most poisonous and dangerous snakes in the world and are represented by 200 members. Its members include coral snakes, cobras, kraits, mambas and some of the Australian snakes. They are proteroglyphous snakes characterized by nonmovable, rather short fangs situated anteriorly in the upper jaw and connected to large venom glands. One of its members, the king cobra (*Ophiophagus Hannah*) is the largest of the venomous snakes reaching a length of 5 meters at maturity. It inhabits sparsely populated areas and is seldom in contact with humans. However, with its enormous size and strong venom, it is capable of killing a man in a few minutes. In addition, the black-necked spitting cobra (*Naja nigricollis*) and South Africa spitting cobra (*Hemachatus haemachatus*) are commonly found in Africa. They are characterized by the strange habit of spitting venom at the attacker, often targeting the eyes at great accuracy. The venom is discharged as two fine jets targeted at the enemy from a distance of 1.5 to 2.5 meters. Once the venom is in contact with the eyes, it causes serious lesions.

There is a very high proportion of venomous and dangerous snakes in Australia, mostly elapids. The strongly built Taipan (*Oxyuranus scutellatus*) has an average length of 2.5 meters and very long fangs that produce large amount of extremely potent venom a presynaptically acting neurotoxin (β-toxin) and various necrotic toxins. It caused many human deaths before its antivenom became available in 1955.

Enzymes found in most snake venoms	
Phospholipase A_2	Ribonuclease
L-amino acid oxidase	Adenosine triphosphatase
Phosphodiesterase	Hyaluronidase
5'-Nucleotidase	NAD-nucleosidase
Phosphomonoesterase	Acrylamidase
Deoxyribonuclease	Peptidase
Enzymes found in crotalid and/or viperid venoms	
Endopeptidase	Thrombin like enzymes
Arginine ester hydrolase	Factor X and/or V activator
Kininogenase	Metalloproteinases
Fibrinogenase	Serine proteinases
Heparinase	Fibrinogenase
Collagenase	Prothrombin activator
	Elastase
Enzymes found in elapid venoms	
Acetylcholinesterase	
Phospholipase B	
Glycerophosphatase	
Lactate dehydrogenase	

Table 1.1: Enzymes commonly found in snake venoms.

(Adapted from Edstrom, 1992)**.**

Another notorious Australian venomous snake is the Death Adder (*Acanthophis antarcticus*) that inhabits the bushland and looks like a viper with a broad head, thick neck and fat body, measuring to about 1m in length. It lures its prey by the twitching of its tail. However, it does not attack human unless provoked (Edstrom, 1992).

1.4.3 *Naja Sputatrix* and its venom

The *Naja sputatrix* (*N. sputatrix*) or the Malayan spitting cobra is found in Peninsular Malaysia, Singapore, Java, Bali, Lombok, Flores, Komodo and the Celebes Islands of Indonesia. It is capable of spitting venom up to 1.6m accurately, often targeting the eyes of aggressor. The venom causes pain and discomfort to the eyes or open wounds of the victim and needs to be washed out as soon as possible to prevent permanent damage (Tweedie, 1983; Gopalakrishnakone *et al.*, 1990). Apart from rainy seasons, in which it is most active, the *N. sputatrix* like most cobras is normally non-aggressive and will avoid contact with human beings. However, when cornered, it will give the warning display and bite only if the display is ignored by the intruder. However, the young cobras are very aggressive. The snake is found in a variety of habitats ranging from forested areas and grasslands to human habitations. Its preferred time for hunting and moving around are evenings and it feeds mainly on frogs, toads, small rodents and ants.

Envenomation by *N. sputatrix* results in local necrosis with systemic manifestations characteristic of myoneural curare-like (neurotoxic) and cardiovascular effects (Reid, 1964 and Viravan *et al.*, 1986). These effects are caused mainly by the toxic components present in *N. sputatrix* venom. The toxic component includes neurotoxins, phospholipase A_2 and cardiotoxin in a ratio of 3%, 18% and 60% by

weight of crude venom respectively (Tan, 1983), while the rest is made up of non-toxic components, one of which is the nerve growth factor (NGF). *N. sputatrix* venom contains three isoforms of both phospholipase A_2 enzymes (sputatrix PLA_2-1, PLA_2-2 and PLA_2-3; Tan and Armugam, 1989a, b) and cardiotoxins (sputa-cardiotoxins A, B and C; Tan, 1982) that have been successfully characterized. It was observed that during *N. sputatrix* envenomation, the victim suffers from local necrosis, hemolysis and cardiotoxicity. These effects are probably due to a synergistic action of cardiotoxin and phospholipase A_2 as reported by various groups (Tan and Arunmozhiarasi, 1990; Harvey, 1991; Fletcher and Jiang, 1993 and Ownby, 1993). In addition to the two toxins, *N. sputatrix* venom also contains two types of postsynaptic neurotoxins (NTXs), sputa-neurotoxin 1 and -2.

1.5   Aims of this project

This project attempts to study the effects of NGF from animal venom. **(1)** An initial screen will be carried out on venomous sources (e.g. snake, bees and scorpions) present in the laboratory to identify a source with the highest NGF activity and will be selected via PC12 cells bioassay. **(2)** A venom containing NGF with the highest activity will be selected and purified using gel filtration and reverse phase high performance liquid chromatography (RP-HPLC). **(3)** This protein will be characterized by N-terminal sequencing, mass spectrometry and will also be tested for its biological activity. **(4)** A cDNA encoding the NGF will be cloned from the RNA isolated from the venom gland, sequenced and the protein will be expressed as a recombinant NGF in both bacterial (*E. coli*) and mammalian (CHO) cells. The NGF protein expressed in   *E. coli* will be histidine-tagged (easy purification with nickel beads) and purified using denaturing (8M urea) conditions. It will later be

refolded into functional NGF protein for subsequent gene and protein expression studies in relation to mouse NGF. **(5)** The effects of recombinant NGF will be accessed at both the gene (real-time PCR and microarray) and protein (western blot and SELDI-TOF) levels.

(6) With the debate over the nature of proNGF being apoptotic or neurotrophic, cDNA constructs containing different segment of the NGF gene will be transfected into CHO cells for investigation. The Tet On/Off system will be used to regulate the expression of the proteins. These secretory proteins will be collected from the CHO media and introduced to PC12 cells to access their effects on both normal and ischemic cells. Their effects will be assessed by neurite outgrowth, cytotoxicity tests (LDH), changes in gene (real-time PCR) and protein (caspase assay) levels. **(7)** Another venom component -phospholipase A_2 was found to be neuroprotective by a fellow colleague (Cher, 2005), will be examined using the methods that have been developed during the course of this study.

Chapter 2

Materials and Methods

2.1 Materials

2.1.1 Bacteria and media

Escherichia coli DH5α and M15 strains were used to produce the recombinant sputa NGF. Long term storage of bacterial stocks was carried out in LB broth with 40% glycerol at -20°C. Media were supplemented with appropriate antibiotics to maintain bacteria containing plasmid DNA. All bacterial culture media were sterilized by autoclaving. Thermo-labile media supplements like antibiotics were subjected to filter-sterilization through 0.22µm filters and added to cooled (~50°C) sterilized media.

LB broth

Yeast extract	0.5% (w/v)
NaCl	1% (w/v)
Bacto-tryptone	1% (w/v)

Broth was adjusted to pH 7.0 with 1M NaOH prior to autoclaving.

LB-agar

Agar (Gibco) was added to a final concentration of 1.5% (w/v) to LB broth and mixed well before autoclaving. Approximately 25ml of cooled molten agar (55°C) was poured into each 90mm sterile petri dish. It was placed on levelled surface and allowed to set at room temperature. The LB-agar plates were stored inverted in plastic bags at 4°C. Prior to use, all plates were "dried" at 37°C for 1h.

SOC

Bacto-tryptone	2% (w/v)
Yeast extract	0.5% (w/v)
NaCl	0.05% (w/v)
KCl	2.5mM
MgCl$_2$	0.01mM

The pH was adjusted to 7.0 with 1M NaOH. The autoclaved media was cooled to 50°C and filter-sterilized glucose was added to a final concentration of 0.02mM.

2.1.2 Plasmids

Plasmids

Plasmids used in this study were pQE30 (Qiagen Company, U.S.A.), pcDNA4/TO/myc-His and pcDNA6/TR (Invitrogen Company, U.S.A.). pQE30 was used as vector to express recombinant sputa NGF as a histidine-tagged fusion protein. One major advantage of using this vector is that the histidine tag is conformation-independent. This feature makes it very easy to purify the fusion protein-of-interest even under denaturing conditions. The histidine tag is also small and poorly immunogenic. In addition, the uninduced expression level can be controlled by *lac* repressor, expressed by an endogenous pREP4 vector in M15 host strain.

Both the pcDNA4/TO/myc-HisA and pcDNA6/TR plasmids allowed a tetracycline-regulated expression of the gene of interest in mammalian host cell. In this study, the tetracycline (Tet) on/off system was used to decipher the role of the precursor sputa NGF protein (Chapter 4). Three mutated cDNA constructs containing the sputa NGF

gene were cloned individually into the pcDNA4/TO/myc-HisA and later co-transfected with pcDNA6/TR into CHO cells. The pcDNA4/TO/myc-HisA contains two tetracycline operator (TetO$_2$) sites within the human CMV promoter for the tetracycline-regulated gene expression (Yao *et al.*, 1998). The TetO$_2$ serves as binding sites for the 4 Tet repressor molecules (comprising of 2 Tet repressor homodimers) that confer tetracycline-responsiveness to the gene of interest (i.e., sputa NGF mutants). The Tet repressor is expressed from pcDNA6/TR. When these two vectors are co-transfected together, the gene expression can be induced by addition of tetracycline (1μg/ml).

Long term storage of plasmid DNA was carried out in TE buffer at -20°C. Plasmids used daily were stored in TE buffer at 4°C to minimize the deleterious effect of repeated freeze-thaw process.

TE buffer

Tris-HCl	10mM
EDTA	1mM

Buffer was sterilized by autoclaving and stored at room temperature.

2.1.2.1   Reagents for plasmid isolation

Solution 1: Resuspension buffer

Glucose	50mM
Tris-HCl (pH 8.0)	25mM
EDTA (pH 8.0)	10mM

Solution 1 without glucose was sterilized by autoclaving and filter-sterilized glucose was added later to the cooled sterile solution and stored at 4°C for routine use and at -20°C for extended storage.

Solution 2: Lysis buffer

NaOH	0.2M
SDS	1% (w/v)

Solution 2 was prepared fresh before use each time.

Solution 3: Precipitation buffer

Potassium acetate	3M
Glacial acetic acid	1.5% (w/v)

Solution 3 was stored at 4°C.

2.1.3   Antibiotics

Working concentration for ampicillin was 100mg/ml. For Tet-On induced eukaryotic gene expression, the final tetracycline concentration in the media was 1μg/ml. Both zeocin (Invitrogen, U.S.A.) and blasticidine (Invitrogen, U.S.A.) were used for selection and maintenance of stable clones. Working concentrations for pro-domain stable clones were zeocin (100μg/ml) and blasticidine (2.5μg/ml), while the others (mature NGF and pro (R/G) NGF) stable clones were maintained in zeocin (500μg/ml) and blasticidine (10μg/ml). The concentrated antibiotics stocks were aliquoted into small volumes and kept at -20°C.

Ampicillin (in water)	100mg/ml
Tetracycline (in absolute ethanol)	1mg/ml (kept in dark)
Zeocin	100mg/ml
Blastidicidine	10mg/ml

2.1.4   Cell lines and culture media

Both Pheochromocytoma (PC12) and Chinese hamster ovary (CHO) cells were obtained from the American Type Culture Collection (ATCC, U.S.A.) and cultured in complete Dulbecco's Modified Eagle's medium (DMEM). They were maintained in a 37°C incubator with 5% CO_2.

Saline

NaCl (0.9%, w/v) was diluted in sterile, deionized water and autoclaved. Once cooled, it was kept at room temperature

Complete DMEM (1L)

DMEM	17.4g
Fetal Bovine Serum (FBS)	10%
L-glutamine	0.4g
Sodium bicarbonate	1.74g
Penicillin-streptomycin (50U- 50μg/ml)	1%

Basal DMEM (1L)

DMEM	17.4g
L-glutamine	0.4g

Sodium bicarbonate	1.74g
Penicillin-streptomycin (50U- 50µg/ml)	1%

Freezing medium (100ml)

Basal DMEM	30ml
Fetal Bovine Serum (FBS)	70ml
Penicillin-streptomycin (50U- 50µg/ml)	1%

Powered medium was dissolved in deionized water and sterile-filtered with 0.22µm filter and stored in 4°C. Before use, medium was warmed up at the 37°C water bath. Cells were stocked with freezing medium and 10% sterile glycerol and kept in -80°C. Glucose-free basal DMEM for studies on oxygen-glucose deprivation (OGD) was purchased from Gibco-BRL (Paisley, U.K.).

2.1.5 Organotypic hippocampal cultures

Exactly 10-day-old Wistar rat pups were obtained from the Laboratory Animal Centre (National University of Singapore, Singapore). The actual date of birth of rats were noted and delivered to department on the 10th day. All animals were handled according to the guidelines (Howard-Jones, 1995) given by the council for International Organization of Medical Sciences (CIOMS) on animal experimentation (WHO, Geneva, Switzerland).

Minimal essential medium (MEM) with Earle's salt, but without glutamine was purchased from Cambrex and Hanks balanced salt solution (HBSS) from Gibco-BRL (Paisley, U.K.). Horse serum, D-glucose, L-glutamic acid and propidium

iodide were from Sigma Chemical Company Ltd (Poole, Dorset, U.K.) and MK-801 from ICN Biochemicals (Thames, Oxfordshire, U.K.). Six well plates were purchased from Nunc International (Hereford, U.K.), the microporous transmembrane biopore membrane was from Millipore Corp (Watford, Hertfordshire, U.K.) and the McIlwain tissue chopper from Mickle Laboratory Engineerging Co. Ltd (Guildford, Surrey, U.K.).

Anesthesia-Chloral hydrate

Chloral hydrate (3.5%, w/v) was dissolved in sterile, deionized water and used to cause euthanasia to the rats.

Dissection media

Dissection media was prepared by using MEM with 5mg/ml of glucose and kept in ice throughout the whole dissection procedure. The amount used for each rat pup's brain was approximately about 10ml. The media was prepared fresh on day of experiment.

Complete MEM

MEM	50%
HBSS	50%
Heat-inactivated horse serum	25%
D-Glucose	5mg/ml
Glutamine	2mM
Penicillin-streptomycin (50U- 50µg/ml)	1%

Basal MEM

MEM   75%

HBSS   50%

D-Glucose   5mg/ml

Glutamine   2mM

Penicillin-streptomycin   1%
(50U- 50µg/ml)

Propidium iodide (PI)

Propidium iodide was dissolved in deionized water to 1mg/ml and filter sterilized by

a 0.22µm filter and kept in aliquots at 4°C protected from light.

Source of glutamate agonists

Glutamate, KA, NMDA, and AMPA agonists were from Sigma Chemical Company

Ltd. Metabotrophic agonists and antagonists were purchased from Tocris Cookson

Inc.

2.1.6   *Naja sputatrix* venom

Lyophilized *N. sputatrix* crude venom was reconstituted in sterile saline and stored

at -20°C. Dilutions from the stock venom were all carried out using sterile saline

solution.

2.1.7   Buffers and solutions

Phosphate-buffered saline (1 X PBS)

NaCl   8g

KCl	0.2g
$Na_2HPO_4.7H_2O$	2.68g
KH_2PO_4	0.24g

The individual components were mixed together in 1L of sterile, deionized water and solution adjusted to pH 8.0.

TE buffer

Tris-HCl (pH 7.4)	10mM
EDTA (pH 8.0)	1mM

The buffer was sterilized by autoclaving and stored at room temperature.

2.1.8 Reagents for DNA and RNA isolation

Ethanol

Ethanol (75%, v/v) was diluted in sterile, deionized water.

2.1.8.1 Reagents for DNA gel electrophoresis

TBE running buffer (10X)

Tris base	0.9M
Boric acid	0.9M
EDTA	0.02M

Stock of TBE (10X) buffer was diluted 10-fold with deionized water to 1 X TBE.

DNA loading buffer (10X)

Ficoll 400	20% (w/v)
Bromophenol Blue	0.25% (w/v)
EDTA (pH 8.0)	0.1M

Ethidium bromide

Ethidium bromide was dissolved in deionized water to a concentration of 10mg/ml and stored at room temperature (25°C), protected from light. The final working concentration was 0.1µg/ml.

2.1.8.2 Reagents for the RNA gel electrophoresis

MOPS running buffer (10X)

MOPS (pH 7.0)	0.4M
Sodium acetate	0.1M
EDTA (pH 8.0)	10mM

DEPC-treated water

DEPC	0.2ml
Deionized water	100ml

In the fume hood, DEPC was added to the water and shook vigorously to mix. The solution was autoclaved to inactivate the DEPC and stored at room temperature.

Deionized formamide

Formamide (500ml) was stirred with 500mg of Dowex XG8 resin for 1h and filtered through Whatman No.1 paper. Deionized foramide was stored at room temperature and protected from light.

Formaldehyde

Formaldehyde (37%, v/v) was prepared and stored at room temperature and protected from light.

RNA sample buffer

Deionized formamide	10µl
37% formaldehyde	3.5µl
10X MOPS	2.0µl

RNA loading buffer

Glycerol	50% (v/v)
Bromophenol Blue	0.4% (w/v)
EDTA (pH8.0)	1mM

2.1.9   Reagents for real-time polymerase chain reaction (Real-time PCR)

Reverse transcription (RT) master mix

RT buffer (10X)	10µl
$MgCl_2$ (25mM)	110µl
dNTPs	100µl

(25mM of each dATP, dCTP, dGTP and dUTP)

Random hexamers (224µM)	25µl
RNase inhibitor (20 U/µl)	10µl
Reverse transcriptase (50U/µl)	12.5µl
DEPC-treated water	142.5µl

Solution was prepared for 50 reactions and stored at -20°C until use.

2.1.10   Reagents for oligonucleotide microarray

RLT buffer

RLT Buffer (Qiagen)	1ml
β-mercaptoethanol (14.3M)	10µl

This solution was prepared just prior to use. It is stable at room temperature for 1h.

2-(N-Morpholino) ethanesulfonic acid [MES] stock buffer (12X)

MES free acid monohydrate	1.2 M
MES sodium salt	0.89 M

The solution was made up to the desired volume with deionized water and sterilized by filtration through a 0.22µm filter. It was stored at 4°C and protected from light. The solution was discarded when it turned yellowish.

Fragmentation buffer (5X)

Tris-acetate (pH 8.1)	200mM
KCH$_3$COO	500mM

Mg (CH$_3$COO)$_2$ 150mM

The solution was made up to the desired volume with DEPC-treated water and sterilized by filtration through a 0.22µm filter. It was aliquoted into small volumes and stored a room temperature.

Hybridization buffer (2X)

12 X MES Stock buffer   0.1M

NaCl   1M

EDTA   0.02M

Tween-20   0.1%

The solution was made up to the desired volume with deionized water and filter sterilized by a 0.22µm filter. It was stored at 4°C and protected from light.

Non-stringent wash buffer (Wash buffer A)

NaCl   0.9M

NaH$_2$PO$_4$ 0.06M

EDTA   0.006M

Tween-20   0.01%

The solution was made up to the desired volume with deionized water and sterilized using a 0.22µm filter. It was stored in the dark at 4°C.

Stringent wash buffer (Wash buffer B)

12X MES Stock Buffer	0.1M
NaCl	0.1M
Tween-20	0.01% (v/v)

The solution was made up to the desired volume with deionized water and sterilized using a 0.22µm filter. It was stored in the dark at 4°C.

Stain buffer

12X MES stock buffer	0.1M
NaCl	0.1M
Tween-20	0.05% (v/v)

The solution was made up to the desired volume with deionized water and sterilized using a 0.22µm filter. It was stored in the dark at 4°C.

Goat IgG Stock

The antibody stock (10mg/ml) was resuspended in 5ml PBS and stored at 4°C.

2.1.11 Reagents for the isolation of proteins

Lysis buffer (SDS-PAGE)

NaCl	150mM
Tris-Cl (pH 7.6)	50mM
Triton X-100	1%
SDS	0.1%

EDTA	1mM
PMSF	1mM
NaF	50mM
Sodium pyrophosphate	10mM

When probing for phosphotyrosine, 0.1mM sodium orthovanadate was added to the lysis buffer.

Lysis buffer (SELDI-TOF)

Urea	50mM
Tris-HCl (pH 7.4)	8M
NaCl	0.4mM
Sucrose	0.25M
EDTA	1mM

2.1.12   Reagents for purification of histidine-tagged fusion proteins by denaturing conditions

Lysis buffer

Urea	8M
NaH_2PO_4	100mM
Tris-HCl	10mM

The solution was made up to the desired volume with deionized water and adjusted to an overall pH of 8.0.

Wash buffer

Urea	8M
NaH$_2$PO$_4$	100mM
Tris-HCl	10mM

The solution was made up to the desired volume with deionized water and adjusted to an overall pH of 6.3.

Elution buffer

Urea	8M
NaH$_2$PO$_4$	100mM
Tris-HCl	10mM

The solution was made up to the desired volume with deionized water and adjusted to an overall pH of 5.0.

Denaturing buffer

Urea	8M
Tris-HCl	50mM
EDTA (pH 8.0)	2mM
β-mercaptoethanol	50mM

The solution was made up to the desired volume with deionized water and overall pH adjusted to 8.0.

Nickel beads

The QIAexpress Ni-NTA protein purification system (Qiagen) is based on the selectivity of the Ni-NTA (nickel-nitriloacetic acid) resin for proteins containing an affinity tag of six consecutive histidine residues- the 6XHis tag. This system was used for the purification of histidine-tagged recombinant sputa NGF.

2.1.13   Reagents for Tris-tricine SDS-PAGE (Protein gel)

Gel buffer stock

Tris-HCl (pH 8.4)   3M

Cathode buffer (upper electrode buffer)

Tris base   0.1M

Tricine   0.1M

SDS (pH 8.25)   0.1%

Anode buffer (lower electrode buffer)

Tris-HCl (pH 8.9)   0.2M

SDS-PAGE loading buffer

Tris-HCl (pH 6.8)   50mM

Glycerol   12% (v/v)

SDS   4% (w/v)

2-mercaptoethanol   2%

Bromophenol Blue   0.2% (w/v)

Coomassie blue staining solution

Methanol	45% (v/v)
Deionized water	45% (v/v)
Glacial acetic acid	10% (v/v)
Coomassie Blue R-250	0.25% (w/v)

Destaining solution

Methanol	45% (v/v)
Deionized water	45% (v/v)
Glacial acetic acid	10% (v/v)

2.1.14   Reagents for Western blotting

Transfer buffer

Tris base	48mM
Glycine	39mM
Methanol	15% (v/v)

TBS buffer (10X)

Tris-HCl (pH 7.4)	500mM
NaCl	1.5M
KCl	300mM

TBST buffer

Stock of TBS (10X) buffer was diluted 10-fold with deionized water and Tween-20 added to a final concentration of 0.1%.

Blocking solution

Skim milk (1%, w/v) was diluted with TBST buffer and prepared prior to use.

2.1.15 Reagents for MTT cell viability assay

3-(4, 5-demethylthiazole-2-yl)-2, 5-diphenyl tetrazolium bromide (MTT, 0.5mg/ml) was prepared fresh, dissolved in basal DMEM (Section 2.1.4) and kept away from light.

2.1.16 Kit for apoptotic, necrotic and healthy cells assay

The 3-dye (FITC-Annexin V, Ethidium homodimer III and Hoechst 33342) kit was purchased from Biotium, Inc (CA, U.S.A.) and carried out based on the manufacturer's protocol.

2.1.17 Cytotoxicity assay (LDH)

Release of the cytoplasmic enzyme lactate dehydrogenase into the culture medium was used as a measure of cytotoxicity. The enzyme released was determined using a lactate dehydrogenase detection kit (Roche Molecular Biochemicals).

2.1.18 Reagents for caspase-3 activity assay

Cell lysis buffer

HEPES (pH 7.4)	10mM
EDTA	2mM
CHAPS	0.1%
DTT	5mM
PMSF	1mM

Aprotinin	10μg/ml
Pepstatin A	10μg/ml
Leupeptin	20μg/ml

Reaction buffer (2X)

HEPES	10mM
EDTA	2mM
KCl	10mM
$MgCl_2$	1.5mM
PMSF	1mM
Aprotinin	10μg/ml
Pepstatin A	10μg/ml
Leupeptin	20μg/ml

Protease inhibitors (PMSF, aprotinin, pepstatin A and leupeptin) were added to the buffers prior to use.

2.2   Methods

2.2.1   Electrophoresis

2.2.1.1   DNA gel electrophoresis

The principle of DNA gel electrophoresis is to separate different sizes of DNA molecules. This method can be used for separation, identification and purification of DNA fragments. The percentage of agarose in the gel used is dependent on the sizes of DNA fragments to be separated, higher percentage agarose gels are used for separation of low molecular weight DNA molecules and vice versa. In routine gel electrophoresis, gels were made with 0.7 to 1.5% (w/v) electrophoresis grade agarose melted in 50ml of 1 X TBE buffer (Section 2.1.8.1) containing 0.1μg/ml of ethidium bromide. The molten agarose was cooled to 60°C and poured into a horizontal gel-casting tray. An appropriate "comb" was inserted immediately to the molten agarose to cast the wells (for loading DNA samples later) and left to set for 30min. Once the gel had set, the "comb" was removed and the gel together with its tray was submerged in the electrophoresis tank containing 0.5 X TBE buffer (Section 2.1.8.1) and DNA samples premixed with the appropriate amount of 10 X loading buffer was loaded into the wells. Electrophoresis was normally carried out at 5V/cm field strength together with a known ladder and migration of DNA fragments were visualized under UV light. The DNA fragment-of-interest was later excised from the agarose gel and purified by Qiagen gel-extraction kit.

2.2.1.1.1   DNA extraction from agarose gels

The QIAquick Gel Extraction kit (Qiagen) was used for the extraction and purification of DNA fragments electrophoresed on 1 X TBE (Section 2.1.8.1) agarose gel. The DNA fragment-of-interest was excised from the gel under UV with

a clean, sharp scalpel. The size of the excised gel was minimized as much as possible by trimming the excess gel. The gel slice was weighed and 3 volumes of buffer QG (Qiagen) was added to 1 volume of gel for DNA fragments of 100bp to 4kb. After the gel has completely dissolved, one volume of isopropanol was added to increase the yield of DNA fragments <500bp and >4kb. The sample was later applied into QIAquick spin column (attached to a collection tube) and centrifuged at 10,000 x g for 1min. The flow-through in the collection tube was discarded. Column was later washed once with 0.75ml of buffer PE (Qiagen), followed by centrifugation at 10,000 x g for 1min and flow-through discarded. The spin column was then placed into a clean 1.5ml microfuge and the bound DNA was eluted by addition of either 50µl of 10mM Tris-HCl (pH 8.5) or TE buffer to the center of the spin column matrix and centrifuge at 10,000 x g for 1min. The eluted DNA is suitable for most downstream applications such as restriction digestion, labeling, ligation, PCR and sequencing.

2.2.1.2 RNA gel electrophoresis

Ribonucleic acids were separated by electrophoresis in agarose gels containing formaldehyde. This is necessary to determine the integrity of the RNA isolated. Electrophoresis grade agarose (1% w/v) was melted in 43.5ml of sterile, deionised water and cooled to 60°C in a water bath, once cooled 5ml of 10 X MOPS (Section 2.1.8.2) running buffer, 0.7ml of formaldehyde and 1µl of 10mg/ml ethidium bromide (Section 2.1.8.1) were added. The molten agarose was poured into a horizontal gel-casting tray and an appropriate 'comb' inserted immediately to create wells for sample loading. Once the gel is set, the 'comb' was removed and the gel submerged into the electrophoresis tank containing 1 X MOPS running buffer on its

tray. RNA samples were prepared as described as in section 2.1.8.2 and incubated for 10min at 65°C in a water bath prior to loading. Migration of the bands was visualized using a UV illuminator.

2.2.2 Enzymatic reactions

2.2.2.1 Restriction endonuclease digestion of DNA

Restriction of DNA is normally carried out in a total volume of 20µl using appropriate buffers as recommended by the enzyme manufacturers. A typical digestion mixture is made up of:

DNA in TE or water	2µg
Restriction enzyme buffer (10X)	2µl
Restriction enzyme (5-10U/µg of DNA)	1µl
Sterile water	Top up to 20µl

2.2.2.2 Ligation

Ligation reactions were carried out with a vector: insert molar ratio of approximately 1:3 to increase the ligation efficiency and reduce the occurrence of multiple inserts. In general, 100ng of the appropriate plasmid vector was used in a 20µl reaction mixture [7mM Tris-HCl (pH 7.5), 7mM β-mercaptoethanol and 0.5mM ATP.T4 DNA ligase (1-2 Weiss unit)]. The resultant mixture was incubated at 16°C overnight.

2.2.3 **Purification of nerve growth factor and phospholipase A$_2$ from**

crude venom

Phospholipase A2 (PLA$_2$) was purified from *Naja sputatrix* crude venom using

Sephadex G-100 gel filtration chromatography (Amersham Biosciences, England)

followed by reversed phase high performance liquid chromatography (RP-HPLC;

Akta Explorer, Amersham Pharmacia; Armugam *et al.*, 1997). Purified fractions

were quantitated using Bradford assay (Section 2.2.8.2). Nerve growth factor (NGF)

was purified in a similar manner. Freeze-dried *Naja sputatrix* crude venom (50mg)

was reconstituted in 1ml of water and subjected to gel filtration followed by RP-

HPLC (Vision systems; Applied Biosystems, Foster City, C.A., U.S.A.) using a

Sephasil C18 column. Individual fractions were tested for neurite outgrowth on

PC12 cells and fractions showing neurite outgrowth were used for further studies.

2.2.4 **Methods for DNA cloning**

2.2.4.1 **Isolation of total cellular RNA from snake**

An adult snake (*N. sputatrix*) from the Singapore Zoological Gardens (Singapore)

was kept undisturbed and later milked. Venom was collected, freeze-dried and

stored at -20°C. Venom glands from the same snake were frozen in liquid nitrogen

immediately after euthanasia and stored at -85°C. Total RNA was isolated from the

venom glands in a single step using the Trizol® reagent (Invitrogen, Carlsbad, CA.

U.S.A.) according to the manufacturer's instructions. Briefly, the excised snake

tissues (100mg) were first homogenized in 1ml Trizol® reagent. The contents were

vortexed and allowed to stand at room temperature for 10min. Mixture was

centrifuged at 14,000rpm for 10min at 4°C. The aqueous phase was transferred into

fresh tubes, in which 200µl of chloroform was added and subsequently vortexed for

15sec. The mixture was further centrifuged at 12,000rpm for 10min at 4°C. Resultant pellet was washed with 100µl of 75% ice-cold ethanol. The supernatant was discarded and the pellet was dried at 37°C for 10min. The RNA was fully dissolved in 25µl of DEPC-treated water by heating in a 60°C water bath for 10min. The concentration of each RNA preparation was determined by measuring absorbance at the wavelength of 260nm and integrity checked by RNA gel electrophoresis (Section 2.2.1.2).

2.2.4.2   Reverse Transcription Polymerase Chain Reaction (RT-PCR)

Oligonucleotide primers synthesized by Oswel DNA services (Southampton, U.K.) were based on the sequences at the 5' and 3' untranslated regions of cDNA encoding NGF in *Agkistrodon halys* Pallas and the sense and antisense primers were: 5'-ctg gtg cat acg cta atg tcc atg-3' and 5'-aat cta gaa taa ttt aca gg(ct) tg(at) ggt a-3' respectively (Guo *et al*., 1999). Total RNA (3µg) was reverse transcribed using 10 units of MuMLV reverse transcriptase, 40ng of antisense primer, 2µl of reverse transcription buffer [100mM Tris-HCl (pH 8.4); 250mM KCl; 12.5mM $MgCl_2$ and 0.5mg/ml BSA] in a total volume of 10µl at 42°C for 1h. All the reverse transcribed products (10µl) were used for the polymerase chain reaction (PCR). PCR was carried out for 30 cycles with each cycle consisting of a denaturing step (94°C for 1min), an annealing step (50°C for 1min) and an elongation step (72°C for 2min) followed by a final extension step (72°C for 10min), using a Perkin Elmer Cetus thermal cycler (Model 480). The reaction mixture contained 250µmol each of dNTPs, 10µmol of sense and antisense primers each in a final 50µl reaction buffer [50mM KCl, 10mM Tris-HCl (pH 8.3), 1.5mM $MgCl_2$ and 0.1mg/ml gelatin] and 1 unit of *Taq* DNA polymerase (Armugam *et al*., 1997).

2.2.4.3   Cloning

The PCR products were cloned into pT7Blue (R) vector (Novagen, Madison, WI. USA) using the procedures described by the supplier. This vector has been specifically designed for cloning of PCR products. It has a single 3' dT residue at each end of the insert site into which DNA when amplified by Taq polymerase would leave single 3' dA overhangs, which could be ligated. A typical 10µl ligation mixture consists of:

TA vector	50ng
Purified PCR products	70ng
Ligase buffer (10x)	1µl
T4 DNA ligase (400U/µl)	0.5µl

Reactions were carried out at 16°C for overnight, prior to transformation.

2.2.4.4   Transformation

Competent cells from the -70°C were thawed on ice. The ligation mixture (10µl) was added into competent cells (DH5α; 100µl) and mixed gently. The reaction mixture was kept on ice for 30min. Cells were subjected to heat-shock at 42°C for 90s, transferred to a 10ml culture tube and 200µl SOC was added. The cells were incubated at 37°C for 1h before plating on LB-ampicillin (50µg/ml) agar plate supplemented with IPTG and X-Gal according to Sambrook *et al.* (1989) for growth at 37°C for 18h.

2.2.4.5   Plasmid DNA isolation

Plasmid DNA from bacterial culture was prepared by alkaline lysis method of Birnboim and Doly (1979). A 1.5ml overnight bacterial culture in L-broth containing ampicillin was centrifuged at 10,000 x g for 20s and the supernatant discarded. The pellet was resuspended in 100μl of cold solution I (Section 2.1.2.1) by vortexing and left at room temperature for 5min. 200μl of freshly prepared solution II (Section 2.1.2.1) was added to the supernatant and mixed by inversion or tapping and left on ice for 5min. Cold solution III (150μl; section 2.1.2.1) was added and the nucleic acid pelleted by centrifugation at 10,000 x g for 10min. The supernatant was transferred into a new tube. Plasmid DNA was precipitated by adding an equal volume of isopropanol and left at room temperature for 30min, followed by centrifugation at 10, 000 x g for 15min. The pellet was washed twice in 70% ethanol; vacuum dried and dissolved in 50μl TE buffer (Section 2.1.7) containing DNAase-free pancreatic RNase A at 20μg/ml. The recombinant plasmids from the transformants were subjected to Sanger dideoxy DNA sequencing.

2.2.4.6   Sanger Dideoxy DNA sequencing

Cloned DNA fragments were sequenced using the cycle-sequencing technique and the sequencing was carried out in an automated DNA sequencer (Model 3100; Applied Biosystems) using M13/pUC forward and reverse primers. The cycle sequencing method is a combination of traditional Sanger-Dideoxy sequencing chemistry (Sanger *et al*., 1977) and PCR technology.

2.2.4.6.1   Sequencing reaction

The sequencing reaction is essentially polymerase chain reaction (PCR) which uses

the ABI PRISM™ Dye Terminator cycle sequencing kit (ABI), appropriate primer

and a good quality, double-stranded DNA template. Apart from the *Taq* DNA

polymerase and the deoxynucleotides, the sequencing premix also contains

fluorescence-tagged dideoxynucleotides, which would emit different fluorescence,

based on which dideoxynucleotide, when hit by the laser. Reactions were carried out

in a volume of 20µl and comprised of:

Double stranded template DNA	500ng
Premix solution	8µl
Primer (M13/pUC; 6.4ρmol)	4µl
Sterile water	Top up to 20µl

Prior to the thermal cycling, the reaction mixture was overlaid with 50µl mineral oil

to reduce evaporation. The following PCR profile was carried out for 25 cycles:

96°C (DNA denaturation)	30sec
50°C (Primer annealing)	15sec
60°C (Primer extension)	4min

2.2.4.6.2   Purification of sequencing products

The cycle-sequencing products need to be cleaned and concentrated prior to

sequencing. The volume of the sequencing reaction was top up to 100µl by addition

of sterile water and the sequencing products were ethanol precipitated. Equal

volume of phenol was added and vortexed at low speed. After brief centrifugation to separate the phases, the upper aqueous layer was transferred to a fresh 1.5ml tube. Equal volume of chloroform was added, vortexed briefly and centrifuged to separate the phases. The upper phase was transferred to a fresh tube and 1/10 volumes of 3M sodium acetate (pH 4.5), 2 volumes of ice-cold 95% ethanol and 20µg glycogen were added. The resultant pellet was washed in 100µl of ice-cold 80% ethanol and centrifuged at 10,000 x g for 5min. The pellet was vacuum dried and stored in dark at -20°C until use.

2.2.5   Expression and purification of recombinant sputa NGF protein from *E. coli.*

The cDNA-encoding NGF was amplified using the sense and anti-sense primers, 5'-cctggatccgaagatcatcctgtg-3' and 5'-ctcaagctttcagtttccagtt-3', respectively and subcloned into pQE-30 expression vector (Qiagen, Chatsworth, CA, U.S.A.) between *Bam*HI and *Hind*III sites. The resultant recombinant protein has histidine residues tagged at its N-terminal, allowing easy purification by nickel beads. *E coli*, DH5α was used as host strain for the expression of his-tagged recombinant sputa NGF proteins. 20ml of overnight bacterial culture was used to inoculate into 1L of LB media supplemented with ampicillin (100mg/L). Once the optical density of the LB media reached 0.5-0.6 OD measured at 600nm, the recombinant protein production was induced by addition of 1mM IPTG (final concentration).

After 3h of induction, cells were harvested by centrifugation. The cell pellet was resuspended in lysis buffer (Section 2.1.12) and disrupted by sonication 6 X 10s with 10s pauses at 200-300W. The lysate was kept on ice at all times. The lysate was centrifuged at 10,000 x g at 4°C for 20-30min. The supernatant was collected, kept

on ice and incubated with nickel beads (with rotation) for 30min at ice-cold condition. For his-tagged fusion protein, the clarified protein supernatant (together with beads) was loaded into an empty column. The non-specific proteins were removed by wash buffer (pH 6.3; Section 2.1.12) and fusion proteins were eluted using elution buffer (pH 5.0; Section 2.1.12). Purified proteins were checked on SDS-PAGE gels and concentration determined by Bradford assay (Section 2.2.8.2).

2.2.5.1 Refolding of recombinant sputa NGF

Purified proteins from various batches were pooled together and urea was removed by overnight dialysis with 1 X PBS (pH 8.0; Section 2.1.7). Protein was concentrated by speed-vac and then fully denatured by dilution with 5 volumes of denaturing buffer (Section 2.1.12) and incubated for two hours at room temperature. *In vitro* renaturation of unfolded proteins was performed overnight at room temperature (25°C) by dialysis in the following buffer: 1 X PBS (pH 8.0) containing 4mM GSH and 2mM GSSG. Protein concentration was determined by Bradford assay (Section 2.2.8.2) and its activity by bioassay using PC12 cells.

2.2.5.2 Circular dichroism (CD)

The CD spectra for both native and recombinant sputa NGF were recorded on a Jasco spectropolarimeter, model J715, equipped with an interfaced personal computer. The instrument was regularly calibrated with ammonium *d*-10-camphorsulphonate. The results were expressed as mean residue ellipticity, $[\theta]$, which is defined as $[\theta] = \theta/60lc$, where θ is the observed ellipticity in degrees, c is the concentration in *d*mol/L, *l* is the length of the light path in cm and constant 60 is the number of amino acid residues in the protein. All the CD spectra were measured

with the appropriate concentrations using 0.1cm path-length cells. Data was collected and averaged from at least five recordings to be considered acceptable.

2.2.6 Expression of recombinant sputa NGF protein from mammalian CHO cells

Oligonucleotide primers were synthesized by Oswel DNA services (Southampton, U.K.) based on the sputa NGF cDNA sequence. The cDNA encoding mature NGF, pro (R/G) NGF and pro-domain were amplified by PCR using gene specific primers that contained restriction sites for *KpnI* and *XhoI* (Fig. 2.1). The positive clones were then restricted with enzymes (*KpnI* and *XhoI*) and subcloned into pcDNA4 that was restricted with the respective endonuclease. Reactions were carried out at 16°C for overnight.

2.2.6.1 DNA transfection

CHO cells were maintained in complete DMEM (Section 2.1.4) and the Tet on/off system was used. The ratio of 6: 1 for TR: TO respectively was used for all transfection experiments. Prior to transfection, 2 x 10^5 of CHO cells were seeded in a T25 flask. After 16-18h, two solutions were prepared in sterile 2ml tubes for transfection. Solution 'A' contained 3μg of total DNA mixed with 300μl OPTI-MEM (Gibco) and solution 'B' contained 18μl of lipofectamine (Invitrogen) mixed with 300μl OPTI-MEM. Solution 'B' was added to Solution 'A'' and the mixture was tapped gently every 10min for a total of 45min (to allow DNA-liposome complexes to form) at room temperature. Meanwhile, the CHO cells were rinsed once with sterile saline (Section 2.1.4) and 2ml of basal DMEM (Section 2.1.4) was

```
GCTCTGGTGCATACGCTAATGTCCATGCTGTGCTACACTCTGATTATAGCATTTCTGATT - 60
 A   L   V   H   T   L   M   S   M   L   C   Y   T   L   I   I   A   F   L   I
GGCATATGGGCAGTACCAAAGTCTGAAGATAATGCCCCTCTGGGCTCCCTGCAACGTCT - 120
 G   I   W   A   V   P   K   S   E   D   N   A   P   L   G   S   P   A   T   S
GACCTTTCCGACACCAGCTGTGCTCAAACTCACGAGGGTCTGAAAACATCTCGAAACACA - 180
 D   L   S   D   T   S   C   A   Q   T   H   E   G   L   K   T   S   R   N   T
GATCAGCGCCATCCAGCTCCTAGAAGTCAGAGGATCAAGCAATTTGGATCAGCATCAAAC - 240
 D   Q   R   H   P   A   P   R   S   Q   R   I   K   Q   F   G   S   A   S   N
ATCATTGTGGATCCCAAGCTTTTTCAGAAGAGGCGGTTCCAGTCGCCTCGTGTTCTGTTC - 300
 I   I   V   D   P   K   L   F   Q   K   R   R   F   Q   S   P   R   V   L   F
AGCACTCAGCCCCCACCATTGTCAAGAGATGAGCAAAGTGTGGAGTTCCTGGACAATGAA - 360
 S   T   Q   P   P   P   L   S   R   D   E   Q   S   V   E   F   L   D   N   E
GACGCTCTTAACAGGAATATCCGGGCCAAACGTGAAACTCATCCTGTGCATAACCGAGGG - 420
 D   A   L   N   R   N   I   R   A   K   R   E   T   H   P   V   H   N   R   G
GAATATTCTGTGTGTGACAGTATCAGTGTCTGGGTTGCCAACAAAACCACAGCAACGGAC - 480
 E   Y   S   V   C   D   S   I   S   V   W   V   A   N   K   T   T   A   T   D
ATCAAAGGCAAACCGGTGACTGTGATGGTAGATGTAAATCTTAATAACCATGTCTACAAG - 540
 I   K   G   K   P   V   T   V   M   V   D   V   N   L   N   N   H   V   Y   K
CAGTACTTTTTTGAAACCAAGTGCAGAAATCCAAATCCAGTACCAAGTGGGTGCAGGGGC - 600
 Q   Y   F   F   E   T   K   C   R   N   P   N   P   V   P   S   G   C   R   G
ATTGATTCCAGGCATTGGAATTCTTATTGCACGACAACACACATTTGTCAAGGCATTA - 660
 I   D   S   R   H   W   N   S   Y   C   T   T   T   H   T   F   V   K   A   L
ACCATGGAAGGCAATCGGGCATCCTGGCGCTTCATTCGGATTGACACTGCCTGTGTGTGC - 720
 T   M   E   G   N   R   A   S   W   R   F   I   R   I   D   T   A   C   V   C
GTAATCAGTAGAAAAACTGAGAACTTCTGATGGACCATTGATTGCTCCAATACTCACTT - 781
 V   I   S   R   K   T   E   N   F   *
```

Fig 2.1: Gene-specific primers for NGF mutants. 2 sets of primers were used and highlighted in blue and grey. All forward primers had Kpn1 site at the 5' end, while reverse primers had Xho1 site at the 3' end. The signal peptide and mutated furin residue site are indicated in blue and red respectively.

added to each T25 flask. For each transfection 1ml of basal DMEM was added to the DNA-liposome mixture to rinse and added gently to the rinsed cells. The cells were incubated for 5h at 37°C in CO_2 incubator. After 5h, the media was removed and replaced with complete DMEM (Section 2.1.4).

2.2.6.2   Generation of stable NGF clones

The Tet on/off system allowed the gene of interest to be regulated by tetracycline. The two plasmids (pcDNA4/TO/myc-His; TO and pcDNA6/TR; TR) were co-transfected into CHO cells and allowed to recover in complete DMEM overnight. The following day, the transfected cells were subjected to dual selection with selective medium [complete DMEM containing both blasticidine (TR) and zeocin (TO; 500μg/ml) antibiotics]. For the cells to survive in the selective media, only successfully transfected cells, which contained both TR and TO plasmids were resistant to the antibiotics selection. The selective media was changed every 3-4 days until cell foci were identified. The resistant cells were transferred to 24-well plates and grown to confluence and only surviving clones were selected for quantification by real-time PCR (Section 2.2.7.2.1). After 6 weeks of selection and purification, the stably transfected CHO cells were expanded and established as a cell line.

2.2.6.3   Quantitation of plasmid copy number in stable CHO
transfectants

Total DNA from the cells was isolated and gene-specific primers to mature NGF (NGF) and pro-domain (Table. 2.1) were used to quantitate the plasmid copy number by SYBR green real-time PCR (section 2.2.7.2.1). A standardization assay

Genes of interest	Sense primer	Antisense primer
Bax	5'-actcccccccgagaggtctt-3'	5'-cccagttgaagttgccatca-3'
Bcl-2	5'-tgggatgcctttgtggaacta-3'	5'-gacagccaggagaaatcaaacag-3'
Bcl-$_{XL}$	5'-gaaaggccaggagcgtttc-3'	5'-agcagaactacaccagccacagt-3'
β-actin	5'-agggaaatcgtgcgtgaca-3'	5'- gccatctcctgctcgaagtc-3'
IκB	5'-gctgcccgagagtgcggat-3'	5'-cagtcatcgtagggcaactcatc-3'
Homer	5'-caggacgctttccgcagtaa-3'	5'-cccgcaattctgttagttcaat-3'
Pro-domain	5'-agttccagtcgcctcgtgtt-3'	5'-ccacactttcctcatctcttgaca-3'
Sortilin	5'-ttacagcatctcccagaagctaa-3'	5'-atgcccacggcattgg-3'
TrkA	5'-catggagaacccacagtacttcag-3'	5'-ctagctcccacttgagaatgatgtc-3'
NGF	5'-catggtacaatccctttcaac-3'	5'-ccaacccacacactgacactg-3'
NF-κB	5'-gaagagtcctttcaatggaccaa-3'	5'-tcgggaaggcacagcaata-3'
P75^{NTR}	5'-gtggtcgtgggccttgtg-3'	5'-gcgccttgtttattttgtttgc-3'

Table 2.1: Primer sequences for real-time PCR.

with known amount of DNA was used to determine amount of DNA in the clones. A C_T (cycle threshold) value of 2.0 was found to be equivalent to 150ng of DNA. Hence, a C_T of 2.0 was used to select clones for all three different constructs.

2.2.6.4 Induction of expressed proteins in cell culture media

One day prior to induction, the stable transfected CHO cells were reseeded into T75 flasks (2.8 x 10^6 cells) and grown in selective medium (complete DMEM with zeocin and blasticidin). The following day, the medium was changed to induction medium (basal DMEM with tetracycline; 1μg/ml) and left for 16-18h. The medium was collected and depleted of cells by centrifugation and introduced into PC12 cells for functional studies.

2.2.7 Gene expression studies

2.2.7.1 Isolation of total cellular RNA from PC12 cells and hippocampal tissue slices

Total RNA from both PC12 cells and hippocampal tissues were extracted by a single-step method using Trizol® reagent (Invitrogen, Carlsbad, CA. U.S.A) according to the manufacturer's instructions. Briefly, the samples were homogenized in 1ml of Trizol® reagent per well from 6-well plate and vortexed. Saturated chloroform (0.5ml per 1ml of Trizol® reagent) was added to the homogenates and the samples were shaken vigorously for 15s and allowed to stand at room temperature for 2-3min. The mixture was centrifuged at 13,000rpm for 15min and the aqueous phase transferred to fresh tubes, in which Rnase-free Dnase I was added and the samples were incubated in 37°C water bath for 20min. Total RNA was precipitated with 500μl of isopropanol at -80°C for 20min and centrifuged at

13,000rpm for 15min. Resultant pellet was washed with 75% ice-cold ethanol. The supernatant was discarded and the pellet was dried at 37°C for 20min. The RNA was dissolved in DEPC-treated water by heating in a 60°C water bath for 10min. The concentration of each RNA preparation was determined by measuring absorbance at the wavelength of 260nm and integrity checked by RNA gel.

2.2.7.2   Quantitative real-time polymerase chain reaction (real-time PCR)

The introduction of real-time PCR technology has significantly improved and simplified the quantitation of nucleic acids (Klein, 2002). The unique feature of this technology lies in the real time monitoring of the amplification process using fluorescent techniques (Heid *et al.*, 1996) such that PCR products are detected as they accumulate. The information obtained can be used to quantitate the initial amounts of template molecules (mRNA) with high precision over a wide range of concentrations. The major advantages of real-time PCR in relation to other similar techniques are attributed to its wide dynamic range, significantly higher reliability and increased accuracy of detection relative to end-point determinations (Wilhelm and Pingoud, 2003).

2.2.7.2.1   Principles of real-time PCR

Quantitative real-time PCR systems are based on a set of primers and/or probes that accounts for its high specificity. Fluorescence signals that are proportional to the amount of PCR product can be generated by fluorescent dyes that are specific for double-stranded DNA (dsDNA) or by sequence-specific fluorescent oligonucleotide probes.

SYBR® green I is the most frequent dye used in real-time PCR and it largely binds to sequence independent to the minor groove of dsDNA (Morrison *et al.*, 1998). The binding affinity of SYBR® green I is more than 100-times higher than that of ethidium bromide and the fluorescence of the bound dye is more than 1000-fold greater than that of free dye, making it suitable for monitoring product accumulation during PCR. Assays using SYBR® green I detection must be carefully optimized to reduce the quantification of non-specific products. Changes in the expression of various genes due to venom components were quantitated using a kinetic PCR protocol which monitors transcript amplication in real-time. In this project, the SYBR® green assay was used and described below:

Gene-specific PCR primers were designed using the PrimerExpress 2.0 (Applied Biosystems, U.S.A) software according to their corresponding mRNA sequences. The primers were designed to yield amplicons of less than 100bp and synthesized by Alpha-DNA (Montreal, Quebec, Canada). Ribosomal RNA (18S) was used as an internal calibrator. The primer sequences are listed in Table 2.1. A two-step RT (reverse-transcription)-PCR was used. Reverse transcription of total RNA was first carried out to generate cDNA strands. The reaction was set up as follows:

Reverse transcription master mix   12 µl
(Section 2.1.9)
Total RNA (100ng/µl)   3µl

The reverse transcription reaction was carried out at 25°C for 10min, 37°C for 60min followed by 95°C for 5min. The resultant cDNAs were subjected to PCR amplifications.

The following reaction was set up for the **SYBR® green assay**:

SYBR® green mastermix	25µl
Forward primer (gene of interest)	100nM
Reverse primer (gene of interest)	100nM
cDNA	15µl
Sterile, deionized water	Top up to a final volume of 75µl

The amplification was performed at 50°C for 2min and 95°C for 10min followed by 40 cycles at 94°C for 15s and 60°C for 1min per cycle. All reactions were carried out in triplicate using the ABI Prism 7000 SDS (Applied Biosystems, U.S.A).

2.2.7.3 Oligonucleotide microarray

A microarray can be imagined as a minature gene hybridization or detection assay with cDNAs or oligonucleotides as probes. All procedures were carried out according to the protocols described in the GeneChip™ expression analysis technical manual (Affymetrix, Santa Clara, CA).

2.2.7.3.1 Principles of microarray

The production of arrays begins with the selection of probes to be used and is typically selected from databases like GenBank, dbEST and Unigene (Duggan *et al*., 1999). Complementary DNA arrays are produced by spotting PCR products (approximately 0.6-2.4 kb) representing specific genes onto a matrix, which can either be glass or a membrane. The printing is carried out by a robot and the DNA is cross-linked to the matrix by ultraviolet irradiation. The state of bound DNA is ill-defined and can be deposited as double-stranded, intra-strand cross-linked to some

extent and even have multiple constraining contacts with the matrix along its length. Hence, oligonucleotides make better hybridization probes and such arrays are typically manufactured by a process known as photolithography (Lipshutz *et al.*, 1999). In this case, the nucleotides (25-80 bases in length) are deposited on a glass substrate or 'chip'. Both platforms are extremely high throughput and sequences representing whole genomes have been deposited on the matrix or chip.

Each element on an array contains a DNA sequence from one gene and is used to measure the expression of its corresponding mRNA in a cell or tissue sample. Messenger RNA from control and experimental samples are used to synthesize fluorescently-labeled cDNA or cRNA probes, which are then hybridized to the microarray. Frequently, total RNA pools are labeled (rather than mRNA) to maximize the amount of message that can be obtained from a single sample. The fluorescent signal from the hybridized probes is measured by a laser scanner capable of detecting emission from a variety of dyes. To normalize the results, the intensity signals from the control and experimental samples can be compared to deduce the expression of a particular gene, whether it has been upregulated, downregulated, unchanged or even absent (Barett and Kawasaki, 2003). The sensitivity of the assay is very high, with reports of microarrays being able to detect one mRNA per cell. In most cases, the gene identification obtained from an array is validated by other methods such as northern blot analysis (Bustin, 2000), competitive reverse transcription PCR (Vanden Heuvel *et al.*, 1993) or real-time PCR (Schulze and Downward, 2001).

2.2.7.3.2 cDNA probe preparation

Total RNA clean-up

The RNA clean-up was done using the RNeasy mini kit (Qiagen, Germany) and both RLT and RPE buffers were included in the kit. Total RNA were isolated from control and treated (mouse or sputa NGF) PC12 cells and cleaned up using RNeasy spin columns (Qiagen, Germany) before cDNA synthesis. The final volume of total RNA was made up to 100µl with sterile, deionized water. RLT buffer (section 2.1.10; 350µl) was added into the RNA and transferred into a spin column. The sample was subsequently centrifuged for 2min and the eluant collected and reloaded into the spin column and a further centrifuged for 2min. The resulting eluant was discarded and 500µl of RPE buffer was added to wash the RNA. The sample was centrifuged for 2min and eluant discarded. The column was air-dried until the β-mercaptoethanol had evaporated. RNase-free water (15-30µl) was added into the column, followed by centrifugation for 2-3min to elute the RNA. The clean RNA was quantitated spectrophotometrically at 260nm.

First strand cDNA synthesis

To synthesis the first strand cDNA , the T7-(dT) primer was allowed to hybridize to the poly(A) tails of the mRNA molecules in a reaction that was set up as follows:

Total RNA	5µg
T7-d (T) 24 primer (100ρmole/µl)	1µl
DEPC water	Top up to a final volume of 20µl

The reaction mixture was incubated at 70°C for 10min after which the sample was pulsed and put on ice. Subsequently, following reagents were added to the reaction mixture and incubated at 37°C for 2min.

5X first strand cDNA buffer	4µl
DTT (100mM)	2µl
dNTP mix (10mM)	1µl

SuperScript II reverse transcriptase (1µl) was added to initiate the synthesis and the sample was incubated at 37°C for 1h. The reaction mix was terminated on ice.

Second strand cDNA synthesis

Synthesis of the second cDNA strand was carried out immediately after the first strand synthesis. The following were added to the first stand cDNAs:

5X second strand reaction buffer	30µl
dNTP mix (10mM)	3µl
E. coli DNA ligase (10U/µl)	1µl
E. coli DNA polymerase I (10U/µl)	4µl
E. coli RNase H (2U/µl)	1µl
DEPC water	91µl

The reaction mixture was incubated at 16°C for 2h in a cooled water bath after thorough mixing. This was followed by addition of 2µl (10U) of T4 DNA

polymerase and incubation at 16°C for an additional 5min. The reaction was terminated by addition of 10µl of 0.5M EDTA.

2.2.7.3.3   Clean-up of double stranded cDNA

The synthesized cDNA was cleaned up in two-step procedure. In the first step, phase lock gel (PLG: Qiagen, Germany)-phenol/chloroform extraction was carried out to remove unwanted proteins, followed by ethanol precipitation to recover the cDNA. The PLG formed an inert, sealed barrier between the aqueous and organic phases of phenol-chloroform extractions. The solid barrier allowed more complete recovery of the sample (aqueous phase) and minimized interface contamination of the sample. A standard phenol/chloroform extraction can be performed as an alterative to the PLG procedure. The PLG tube was spun briefly for 12,000 x g for 20-30sec. Phenol-chloroform: isoamyl alcohol (162µl) in a 25:24:1 ratio saturated with 10mM Tris-HCl (pH 8.0) was added to the final cDNA synthesis preparation. The contents were vortexed briefly and the entire cDNA-phenol/chloroform mixture was added to the PLG tube. This suspension was centrifuged at 12,000 x g for 2min. The upper aqueous phase was transferred to a fresh tube. In the proceeding step, 2.5 volumes of absolute ethanol were added to the sample and vortexed. The mixture was centrifuged at 12,000 x g for 20min. The supernatant was removed and pellet washed with 0.5ml of ice-cold 80% ethanol. The pellet was washed twice and later air-dried. Finally, the pellet was resuspended in 12µl of RNase-free water.

2.2.7.3.4   Synthesis of biotin-labeled cRNA

This procedure is important for the production of large amounts of hybridizable biotin-labeled RNA targets by *in vitro* transcription from bacteriophage T7 RNA

polymerase promoter. By using T7 RNA polymerase and biotin-labeled nucleotides, large amounts of single-stranded non-radioactive RNA molecules can be produced within a short incubation period. RNA-DNA hybrids have a higher melting temperature than corresponding DNA-DNA hybrids, therefore single stranded RNA targets offer higher target avidity and greater sensitivity than DNA probes. The *in vitro* transcription reaction (Bioarray, Enzo Diagnostics Inc, U.S.A) was set up as follows:

Template cDNA	1μg
Reaction buffer (10X)	4μl
Biotin labeled ribonucleotides (10X)	4μl
DTT (10X)	4μl
RNase inhibitor mix (10X)	4μl
T7 RNA polymerase (20X)	2μl
Sterile, deionized water	Top up to a final volume of 40μl

The reaction mixture was incubated in 37°C water bath for 4-5h with tapping every 40min. The cRNA was stored at -20°C.

2.2.7.3.5   Clean-up and quantification of *in vitro* transcription (IVT) products

The IVT clean-up reaction is essential to remove unincorporated NTPs and was carried out as described as in the section above (Section 2.2.7.3.4). The eluted cRNA was quantitated using the spectrophotometer. Since total cellular RNA was the starting material, adjusted cRNA yield was calculated to reflect carryover of

unlabeled total RNA. Using an estimated 100% carryover, the following formula was used to determine the adjusted cRNA yield.

Adjusted cRNA yield = RNA_m- (total RNA_i) (y)

RNA_m = amount of cRNA measured after IVT (µg)

Total RNA_i = starting amount of RNA (µg)

Y = Fraction of cDNA reaction used in IVT

The minimum concentration of purified cRNA that was required was 0.6µg/µl.

2.2.7.3.6 Fragmentation of cRNA for target preparation

The adjusted amount of cRNA was fragmentated and the reaction was set up as follows:

Clean cRNA	20µg
5 X Fragmentation buffer (Section 2.1.10)	8µl
RNase-free water	Top up to a final volume of 40µl

The final concentration of RNA in the fragmentation mixture ranges from 0.5µg/µl to 2µg/µl and full-length cRNA was broken down into 35-200 base fragments by metal-induced hydrolysis. The fragmentation mixture was incubated at 94°C for 35min and the reaction was terminated in ice. The undiluted, fragmented sample RNA was kept at -20°C.

2.2.7.3.7 Eukaryotic target hybridization

The hybridization cocktail for a single probe array-hybridization was prepared as follows:

Fragmented cRNA	15µg
Control oligonucleotide B (3nM)	25µl
Eukaryotic hybridization controls (20X)	15µl
Herring sperm DNA (10 mg/ml)	3µl
Acetylated BSA (50 mg/ml)	3µl
Hybridization buffer (2X; Section 2.1.10)	150µl
Sterile deionised water	Top up to a final volume of 300µl

The frozen stock of 20 X GeneChip® Eukaryotic hybridization control cocktail (Affymetrix) was heated at 65°C for 5min to completely resuspend the cRNA before storing in aliquots. It contains the genes *bioB, bioC, bioD* and *cre* which code for prokaryotic enzymes. These enzymes serve as hybridization controls when mixed with the labeled eukaryotic cRNA samples. These controls were spiked into the samples to monitor the efficiency of target preparation, hybridization, washing and staining. The probe array was equilibrated to room temperature immediately before use. The hybridization cocktail was heated to 99°C for 5 min in a heat block while the probe array was filled with 80µl or 200µl (for test and whole-genome chips respectively. Test chips were first run to ascertain the quality of the prepared cRNA before they are hybridized on the whole-genome chip) of 1 X hybridization buffer and incubated at 45°C for 10min with rotation. The hybridization cocktail was

transferred to a 45°C heat block and incubated for 5min. The cocktail was centrifuged at 13,000 x g for 5min to precipitate any insoluble material from the hybridization mixture. The buffer solution was removed from the probe array cartridge and filled with 80µl or 200µl of hybridization cocktail supernatant. The probe array was placed in a rotisserie box in a 45°C oven and rotated at 60rpm for 16h.

2.2.7.3.8   Washing, staining and scanning

After 16h, the hybridization cocktail was removed from the probe array and stored at -70°C. The probe array was filled with 80µl or 200µl of Buffer A (Section 2.1.10). An antibody amplification wash and stain procedure was employed. Streptavidin phycoerythrin (SAPE) staining reagent was prepared and stored in the dark at 4°C. The stain buffer was prepared for each probe array as follows:

2X MES Stain buffer (Section 2.1.10)	600µl
Acetylated BSA (50 mg/ml)	48µl
SAPE (1 mg/ml)	12µl
Sterile, deionised water	540µl

The stain solution was mixed well and divided into two aliquots of 600µl each to be used for first and third staining steps respectively. An antibody mixture for the second phase of staining was prepared as follows:

2X MES stain buffer	300µl
Acetylated BSA (50 mg/ml)	24µl

Normal goat IgG (10 mg/ml)   6µl

Biotinylated antibody (0.5 mg/ml)   3.6µl

Sterile, deionized water   266.4µl

The fluidics protocols, 'Micro1v1' and 'EukGE WS2v4' (Affymetrix® Microarray Suite 5.0, USA) were selected to wash and stain the test and whole-genome chips, respectively, using the GeneChip® Fluidics Station 400. At the end of the fluidics protocols, the probe arrays were scanned and the resulting image was stored as a .dat file.

2.2.7.3.9 Microarray data analysis

In the initial phase of analysis, a grid was automatically placed over the .dat file demarcating each probe cell. One of the probe array library files, the .cif file, was used by Microarray Suite 5.0 to determine the appropriate grid size to be used. The alignment of the grid was confirmed by zooming in on each of the four corners and on the centre of the image. If the grid was not aligned properly, the alignment was adjusted by placing the cursor on an outside edge or corner of the grid. The cursor image was changed to a small double-headed arrow and the grid was adjusted. The software then analyzed the hybridization intensity from the GeneChip® expression probe arrays where the data from each array were scaled to an average intensity of 800. The gene expression levels from treated and control samples were compared using an expression comparison analysis that calculated a set of comparison metrics. Some of the metrics which were used by a decision matrix to determine a Difference Call for each transcript; Increased (I), Decrease (D), Marginally Increased (MI), Marginally Decreased (MD) or No Change (NC). Only the 'I' and 'D' transcript

levels calls were taken into consideration for further analyses in all microarray experiments.

2.2.7.4   Applications of gene expression studies

As the numbers of uncharacterized open reading frames are identified in different organisms by various genome sequencing projects, an important question arises as to whether the expression pattern of a gene can be used to predict the functional role of its protein and its involvement in physiology or pathogenesis of certain diseases. An increasingly common approach involved using the gene expression behaviour observed over multiple experiments to first cluster the genes into groups, followed by assignment of tentative roles to unknown genes in a biological process, based on the same clustering group as known genes (Lockhart and Winzeler, 2000). The basic assumption underlying this approach is that genes with similar expression behaviours are likely to be related functionally. The validity of this method has been demonstrated for many genes in *Saccharomyces cerevisiae* (Eisen *et al*., 1998 and Chu *et al*., 1998). Changes in normal cellular physiology and the corresponding changes in gene expression are also important to help decipher and define the relationships between the genes and related pathways (Marton *et al*., 1998 and Winzeler *et al*., 1999). However, it should be noted that not all cellular events are reflected in the mRNA level. In addition, gene expression data can be used to identify new *cis*-regulatory elements and transcriptional units, given the strong correlations between the specific sequence motifs in promoter regions and gene expression patterns (Wolfsberg, 1999).

Apart from being an important tool in basic research and target discovery, gene expression analysis has other specific applications. In areas such as *biomarker*

determination- to find genes that correlate with and presage disease progression, *pharmacology*- to determine differences in gene expression in tissues exposed to various doses of drug compounds, *toxicogenomics*- to find gene expression patterns in a model tissue or organism exposed to toxin compounds and their use as early predictors of adverse effects in humans, *target selectivity*- to define a compound by the gene expression pattern it elicits in a target tissue and compare it with other compounds based on the pattern, *prognostic tests*- to find a set of genes that is able to accurately differentiate one disease from the rest and *disease subclass determination*-to find multiple subcategories of tumors in a single clinical diagnosis (Butte, 2002).

In particular, gene expression studies have been extremely useful in dissecting the molecular mechanism underlying cancer behaviour (Morcellin *et al*., 2003; Weeraratna *et al*., 2004). For instance, the molecular profiling of cutaneous melanoma allowed for the identification of a more motile group of tumours histopathologically indistinguishable from their less aggressive counterparts (Bittner *et al*., 2000). Real-time PCR has also been used to detect and quantitate tumor cells during cancer remission, circulating T cells after anti-cancer therapy and DNA copy-number to determine the extent of genomic imbalance that underlies most malignancies (Morcellin *et al*., 2003).

2.2.8 Protein analysis

2.2.8.1 Protein Isolation from cells

Total protein was isolated from cells with lysis buffer (Section 2.1.11), vortexed and left in ice for further 15min. The insoluble material was removed by centrifugation

at 10,000 rpm for 10min at 4°C. Supernatant containing the protein and was

quantitated by Bradford method (Section 2.2.8.2).

2.2.8.2   Protein determination using the Bradford method

Bradford's reagent (Bio-Rad Laboratories, U.S.A) was diluted 5-fold with deionized

water and 1ml of diluted reagent was added to each protein sample. Absorbance at

the wavelength of 595nm was measured after incubation at room temperature for

10min. Bovine serum albumin (2-10µg) was used as standards.

2.2.8.3   Tris-tricine SDS-PAGE

Tris-tricine SDS-PAGE was carried out according to the method of Schagger and

von Jagow (1987). Preparation of 10ml and 5ml solutions of 12% resolving and 5%

stacking gels respectively was carried out as follows:

Stock solution	Resolving gel (ml)	Stacking gel (ml)
Acrylamide, 40%	3.0	0.625
Gel buffer (Section 2.1.13)	3.33	1.25
10% SDS	0.1	0.05
Glycerol	1.1	-
Deionized water	2.4	2.85

TEMED (10µl) and 10% (w/v) ammonium persulfate (100µl) were added to the

solutions which were quickly mixed and added to a gel caster. The resolving gel was

allowed to set before the stacking gel mixture was added. The gel was fixed to the

vertical electrophoresis unit which was filled with the upper and lower electrode

buffers (Section 2.1.13). Protein samples (70μg) were mixed with an equal volume of SDS-PAGE loading buffer (Section 2.1.13) and boiled for 10min. Electrophoresis was carried out at 120V until the dye ran out into the buffer. To confirm equivalent loading of samples, separate sets of gel were run simultaneously and stained with Coomassie Brilliant Blue followed by destaining (Section 2.1.13).

2.2.8.4   Western blotting

The SDS-PAGE gel (Section 2.2.8.3) was soaked twice in transfer buffer (Section 2.1.14) for 15min each time. Nitrocellulose membrane was cut to cover the gel sufficiently and was also soaked in transfer buffer for 30min, together with the scotchbrite and 2 sheets of 3MM paper. They were assembled in the following order: scotchbrite, 3MM paper, gel, nitrocellulose membrane, 3MM paper and scotchbrite. When the nitrocellulose membrane was placed on the gel, air bubbles were rolled out with a glass tube. The blotting assembly was then secured in the transfer apparatus that was half-filled with pre-cooled (-20°C) transfer buffer and electro-transfer was carried out at 110V for 1h.

At the end of blotting, the apparatus was disassembled and the nitrocellulose membrane was blocked for 1h with shaking, in blocking solution (Section 2.1.14). This is followed by incubation overnight at 4°C with either monoclonal anti-phosphotyrosine (AG10; Upstate Biological, Lake Placid, N.Y., U.S.A.) or polyclonal anti-TrkA or anti-p75^{NTR} (Advanced Targeting Systems, San Diego, CA, U.S.A.) or anti-sortilin (BD Biosciences, Franklin Lakes, N.J., U.S.A.) at 1μg/ml or monoclonal anti-β-actin (Sigma Chemicals, St Louis, MO, U.S.A.) at a dilution of 1:2500. Anti-β-actin was used as a reference for quantification. All antibodies were diluted in 0.5% blocking solution. After three washes of 10min each in TBST

(Section 2.1.14), membranes were incubated for 1h at room temperature with either horseradish peroxidase-conjugated goat anti-rabbit (polyclonal) or rabbit anti-mouse (monoclonal) at a dilution of 1:50,000 in 0.5% blocking solution, washed twice for 10min each in TBST and visualized via enhanced chemiluminescence (Supersignal; Pierce, U.S.A) with suitable exposure times (Kodak-MS film). Films of western blots were scanned (Acer SWZ3300U) and labeling intensities of bands were quantitated using AIS software (Synoptics Imaging Systems).

2.2.8.5   Principles of protein profiling by surface-enhanced laser-desorption- ionization time- of-flight (SELDI-TOF)

The arrays are 10mm wide and 80mm in length and have either 8 or 16 spot surfaces. After the sample preparation, a few microlitres of sample (total proteins) are bound onto the chemically treated surface of the chip by incubating the sample over a short period of time. The surfaces of the arrays have different specific properties, classical and specialized affinity capture surfaces. Classical surfaces include normal phase for general binding; hydrophobic surfaces for reversed-phase capture; cation- and anion- exchange surfaces and immobilized metal affinity capture (IMAC) for metal-binding proteins. Specialized affinity capture surfaces allow specific protein of interest to be covalent immobilized on pre-activated surface arrays, enabling customized experiments to investigate antibody-antigen, DNA-protein, receptor-ligand and other molecular interactions.

Proteins or other analytes are retained on the surface of the ProteinChip Array by means of specific surface chemistries of by bimolecular covalently bound to the array. The specific capture of the subset of proteins in the sample occurs through simple chemical interactions or protein-protein interactions. After binding, the array

is washed thoroughly to remove any impurities and unbound proteins. An Energy Absorbing Molecule (EAM) solution is applied to the sample retained on the chip surface and is important to mediate the ionization of the sample. It could be 1±-cyano-4-hydroxycinnaminic acid (CHCA) which generates matrix ions less than 800 Daltons (Da) or sinnapinic acid (SPA) which generates higher mass to charge ratio ions, typically less than 2000 Da. The EAM (e.g SPA) was applied to the chip surface in a saturated solution of 10% acetonitrile and 1% trifluoacetic acid and allowed to dry, thereby leaving a crude crystal forms that included both the protein (or other analyte of interest) and a large molar excess of EAM molecules. Protein chip was placed into the ProteinChip reader for mass spectrometric analysis.

The ProteinChip reader has a laser that is directed to the chip surface, causing the desorbed proteins to be launched as charge ions by the addition of (usually) one proton. The vacuum chamber has an acceleration region and a free flight region known as the drift tube and ions leaving the source are accelerated to the same energy to the drift tube by a voltage of 20kV applied across the surface of the chip. The time-of-flight (TOF) for each ion is analyzed to determine the mass to charge ratio (m/z) and due to the different velocities exhibited by various masses, they arrive at the detector at different times. The accuracy of the ProteinChip reader at measuring the molecular mass is aided by regular calibration using samples of known molecular weight and can be done either by adding known proteins to the chip containing the sample (internal calibration) or running the standards through the machine on separate chip (external calibration). The computer programme attached to the analyzer then measures the time-of-flight and gives a mass to charge ratio. All procedures were carried out according to the protocols described in the Ciphergen ProteinChip® System users guide (Palo Alto, C.A., U.S.A.).

2.2.8.5.1   Sample preparation for SELDI-TOF

Treatment with NGF (mouse or sputa) caused neurite outgrowth in PC12 cells. Cells were rinsed with sterile saline (Section 2.1.4) and scraped by the rubber policeman and resuspended in 50µl of chilled lysis buffer (Section 2.1.11). They were vortexed and incubated on ice for 15min. The supernatant was collected and total protein quantitated using Bradford assay (Section 2.2.8.2).

2.2.8.5.2   SELDI-TOF

Prior to total proteins fractionation on Ciphergen hydrophobic reverse-phase chip (H4 Protein Chip™), each spot on the protein chip was outlined with a hydrophobic pen and allowed to air dry. The spots were pre-treated with 5µl of acetonitrile (20% acetonitrile diluted with 1 X PBS; Section 2.1.7). Acetonitrile was removed and replaced with 5µg of total protein (suspended in 20% acetonitrile). The spots have to remain moist even during the sample exchange. The chip was incubated in a humidity chamber for about 90min. 2µl of standard was loaded followed by washing with 5µl of binding buffer (20% acetonitrile) five times. Chip was left to air dry. To mediate the ionization of the sample, 0.5µl of saturated sinapinic acid was added to each spot. Upon activation, the chip is ready for analysis using the SELDI-TOF MS (Protein Biology System II) from Ciphergen (Palo Alto, CA, U.S.A.).

2.2.8.5.3   SELDI-TOF analysis

Public databases were used to help identity a protein of interest using the mass values of its internally calibrated peptides. To increase the chances of protein identification, only the masses of peptides derived from the protein of interest were entered and the database used in this study was from:

Expasy- http://www.expasy.ch/tools/peptident.html.

2.2.8.5.4 Applications of SELDI-TOF

The field of proteomics is rapidly progressing and development of new technologies in the last decade has greatly enhanced the knowledge in this field. Yet, developing a comprehensive library of the human proteome is still considered a more daunting task than the human genome project. The rising need for new methods to identify disease biomarkers is underscored by the survival rate of patients diagnosed at the early stages of cancer. SELDI-TOF is a novel approach to biomarker discovery by a combination of both chromatography and mass spectrometry techniques. One of the main features is its ability to provide a rapid protein expression profile from a variety of both biological and clinical sample. It has been used for biomarker identification, as well as for the study of protein-protein and protein-DNA interactions. The flexibility of SELDI-TOF has allowed it to be used in projects ranging from the identification of potential diagnostic markers for cancers (e.g. prostate, bladder, breast and ovarian) and Alzheimer's disease, to the study of biomolecular interactions and even the characterization of post-translational modifications (Issaq *et al.*, 2002).

2.2.9   Biochemical assays

2.2.9.1   Detection of DNA fragmentation

PC12 cells were seeded at a density of 5 x 10^5/well of 6-well plates and incubated at 37°C overnight at 37°C and serum-starved for 16-18h prior to treatment. They were treated with either condition media from CHO cells (mature NGF or pro (R/G) NGF or pro-domain) or STS for 16-18h at 37°C. Genomic DNA was isolated using

DNAzol$^®$ Reagent (GibcoBRL, Life Technologies, USA), which is a novel guanidine-detergent lysing solution that permits the selective precipitation of DNA from the cell lysate. The medium was first discarded and cells were washed twice with saline (Section 2.1.4). DNAzol$^®$ reagent (500µl) was added to each well and the cells were completely lysed by gently pipetting the lysate. Cell debris was removed by centrifugating the lysate at 10,000 x g for 10min, after which the supernatant was retained and 0.5ml of absolute ethanol per 1ml of DNAzol$^®$ used, was added. The samples were mixed by inversion and incubated at room temperature for 2 min. Genomic DNA was precipitated by centrifugation at 4,000 x g for 2 min at room temperature. The supernatant was discarded and the pellet was washed twice with 75% ice-cold ethanol. The DNA pellet was dried at 37°C, dissolved in sterile, deionized water and quantitated spectrophotometrically at a wavelength of 260nm before electrophoresis. Cleaved DNA typically appears as a "ladder" consisting of non-random, oligonucleosomal fragment lengths when electrophoresed. The DNA gel was set and ran according to section 2.2.1.1.

2.2.9.2 MTT cell viability test

This is basically a colorimetric assay that measures the reduction of MTT into an insoluble formazan product by the activity of mitochondrial enzymes in viable cells. 2 X 10^5 PC12 cells were seeded in 24-well plates and incubated overnight at 37°C in complete DMEM (Section 2.1.4). The next day, cells were exposed to either normal or ischemic condition known as oxygen-glucose deprivation (OGD). During OGD, cells were deprived of oxygen and glucose and incubated in a 95%N_2/O_2 chamber. The cells were allowed to recover in glucose-containing basal DMEM (Section 2.1.4) in 95%CO_2/O_2 conditions for 24h prior to MTT test. The media was also

collected for LDH assay. Before the MTT assay, cells were washed twice with sterile saline (Section 2.1.4) and MTT solution (300µl/well of 24-well plate; Section 2.1.15) was added. The cells were incubated at 37°C for 60min. Subsequently, the MTT-containing medium was removed and the resulting crystals of formazan were dissolved in 200µl of DMSO. Complete dissolution of crystals was achieved by shaking the plates gently at room temperature for 10min. 100µl of dissolved crystal solution was transferred to 96-well plate for reading and scanning. Blanks were set up in wells that did not contain cells. Absorbance at a wavelength of 550nm was measured using a multi-plate scanning spectrophotometer (Model 680 Microplate Reader).

2.2.9.3   LDH (lactate dehydrogenase) cytotoxicity test

The cytotoxicity detection kit is a fast and simple colorimetric alternative to quantitate cytotoxicity/cytolysis based on measurement of LDH activity released from damaged cells. LDH is a stable cytoplasmic enzyme present in all cells and rapidly released into the cell culture supernatant upon damage to the plasma membrane. Cell culture media was collected and centrifuged for 10min at maximum speed to remove all cells. The supernatant was collected and 100µl was added to each well of 96-well plate. Each treatment was done in triplicates. Meanwhile, the reaction mixture (catalyst and dye solution) was prepared according to the manufacturer's instructions and kept on ice. 100µl of reaction mixture was added to each well and mixed. Total lactate dehydrogenase activity was determined by lysing cells in 2% Triton X-100 in basal DMEM and measuring the total amount of lactate dehydrogenase in the medium. Absorbance at a wavelength of 550nm was measured using a multi-plate scanning spectrophotometer (Model 680 Microplate Reader) in a

kinetic assay for 30min. Absorbance values were expressed as a percentage of total cellular lactate dehydrogenase in the cell lysate relative to Triton.

2.2.9.4   Assay for the determination of caspase-3 activity

A hallmark feature of apoptosis is the fragmentation of genome and cleavage or degradation of several cellular proteins. Members of the caspase family of proteases have been found to be crucial mediators of the biochemical events associated with apoptosis. In particular, the activation of caspase-3 was shown to be important for the initiation of apoptosis. Cells were scraped by the rubber policeman and resuspended in 50µl of chilled lysis buffer (Section 2.1.18) and incubated on ice for 10min. Protein concentration of the lysates were determined by Bradford method (Section 2.2.8.2) and 40µl of the 2 X reaction buffer (Section 2.1.18) followed by 4µl of 1mM DEVD-[7-amino-4-trifluoromethyl-coumarin] (ALEXIS Biochemicals, U.S.A), were added to an equal volume of each sample. The lysates were incubated at 37°C for 30min and caspase activity was determined by measuring the relative fluorescence units (RFU) at a wavelength of 505nm following excitation at 400nm using a spectrofluorimeter (SpectraMax GeminiEM, Molecular Devices).

2.2.9.5   Annexin V / Ethidium homodimer III / Hoechst nuclear staining

A quantification kit (Biotium, U.S.A.) that enabled the differentiation of apoptotic, necrotic and healthy cells was used. The two major processes of cell death are apoptosis and necrosis. The morphological assessment of cell death was carried out using Ethidium homodimer III/Annexin V/Hoechst 33342 dyes on the basis of cell membrane permeability and chromatin condensation. Apoptotic cells typically have intact membranes and condensed, fragmented chromatin whilst necrotic cells have

disrupted cell membranes and enlarged nuclei. At the onset of apoptosis, phosphotidylserince (PS) which is normally found in the integral part of the plasma membrane becomes translocated to the extracellular face. The human anticoagulant, annexin V, is a 35kDa Ca^{2+}-dependent phospholipid protein with high affinity for PS. Annexin-V is labeled with fluorescein (FITC) and able to stain cells green by binding to PS exposed on the outer leaflet.

Necrosis normally results from a severe cellular insult. Both internal organelle and plasma membrane integrity are lost, resulting in spilling of cytosolic and organellar contents into the surrounding environment. Ethidium homodimer III (EtD-III) is a highly positively charged nucleic acid probe, which is impermeable to live cells or apoptotic cells, but stains necrotic cells with red fluorescence. While Hoechst 33342 is a cell membrane-permeable, minor groove-binding DNA stain that emits bright blue fluorescence upon binding to DNA and used to stain the nuclei of living cells. In apoptotic cells, the condensation of DNA can be detected using Hoechst 33342.

Cells were seeded, treated and rinsed with sterile saline (Section 2.1.4) on 24-well plates prior to staining. They were later incubated with dye solution (200µl per well) for 15min at room temperature. The dye solution was made up of 5µl of FITC-Annexin V, 1µl of Ethidium Homodimer III and 5µl of Hoechst 33342 per 100µl of 1 X binding buffer. The stained cells were protected from light till visualized by fluorescence microscopy (DM IRB, Leica).

2.2.10   Organotypic hippocampal culture

2.2.10.1   Obtaining hippocampal slices from rats

Organotypic hippocampal slice cultures were prepared according to the method by Stoppini *et al.* (Stoppini *et al.*, 1991). For these experiments exactly 10-day-old

Wistar rats were anesthetized and subsequently decapitated. The skin over the top of the skull was cut with a scalpel in a longitudinal cut from the nose to the neck. This was pulled back to expose the skull, which was then cut horizontally with scissors. The top part of the brain was removed using a blunt-end forceps and quickly transferred to ice-cold dissection media (Section 2.1.5). The anterior cortex was removed and the remaining cortex was pulled back, exposing the hippocampal formation. The hippocampus was freed at its temporal and septal ends, and the remaining white matter removed. The hippocampus was transferred to a 50ml petri dish, containing dissection media.

The pair of hippocampi (per rat) were placed on the stage of a McIlwain tissue chopper and cut perpendicular to the long axis to give transverse slices. A thickness of 350μm was used; if slices were thinner, they are more difficult to plate out onto the membranes. The slices are then returned to in $4^{o}C$ dissection media and separated using a paddle Pasteur pipette (Alpha Laboratories, U.K.). This allowed tissue debris and potentially toxic substances, such as excitatory amino acids to diffuse away. The slices were placed onto culture plate inserts (Millicell with pore size of 0.4μm), consisting of a microporous transmembrane bio pore membrane. Each membrane had 4 hippocampal slices, each from a separate rat. The membrane was placed in 6-well plates that contained 1ml of complete MEM (Section 2.1.5; Gahwiler *et al*., 1997). The slices were exposed to both oxygen and nutrients as the membrane was at the surface of the media. All hippocampal slices were checked under microscope for complete CA1-3 structure (Fig. 2.2).
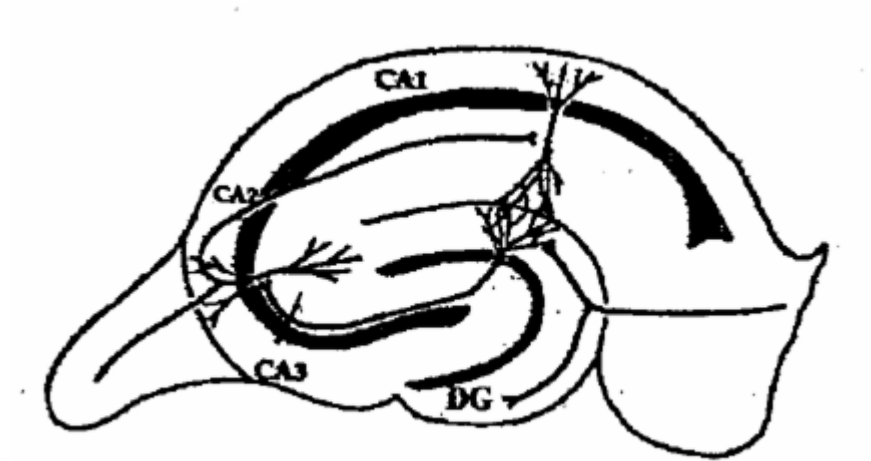
Fig. 2.2: Structure of CA1-3 region of hippocampal slice obtained for cultures.

CA1: Cornus Ammonis 1, CA3: Cornus Ammonis 3, DG: Dentate Gyrus (adapted

from Lahtinen *et al.*, 2001).

2.2.10.2 Maintenance of hippocampal slices

The slices favoured were those from the septal half, as these contained the dentate gyrus with an angular apex. These restricted the loss of the CA1 during glutamate experiments. The organotypic hippocampal cultures were maintained in $95\%O_2/5\%CO_2$ at 37°C incubator. The media, complete MEM (Section 2.1.5) was changed every 3 or 4 days, replacing 1ml with a fresh 1ml of medium. Diffusion of medium through the membrane is sufficient to ensure survival. However the volume of 1ml is crucial, as more than this can cause the cultures to drown. These cultures were allowed to cultivate *in vitro* for 14 days. At the end of this period the hippocampal slices had stabilised and thinned out, to about 150μm, (due in part to a general spreading of the tissue and to death of neurons at the cut surface of the slice). The various subgroups of neurons in each of these slices can be identified by this stage allowing pharmacological studies to be performed (Gahwiler, 1984 and Stoppini *et al*., 1991).

2.2.10.3 Procedure for analysing cell damage

To analyse cell death, the fluorescent exclusion dye propidium iodide (PI; 5μg/ml) named due to its inability to enter healthy intact cells, was used. Plasma membrane integrity, which is lost in necrotic but not apoptotic cells, was probed by the exclusion dye propidium iodide. The PI enters the cells and upon binding to the DNA becomes concentrated in the nucleus rendering it highly fluorescent. PI fluorescence was detected using a confocal laser scanning microscope equipped with an argon laser. A simultaneous transmission image was collected on a second channel and used to identify cell subfields within each culture. Images were saved as 'TIFF' files and subsequently analysed using the Image Pro Plus analysis software.

Cell death was quantified using the following method. The areas of the CA1-3 subfields were determined from the transmission image, on which they were clearly identifiable. Using an interactive drawing tool, the CA1-3 region was divided into two polygons: 1) CA1 and 2) CA2-3 regions of each culture were outlined as areas of interests (AOIs). The same two polygons were kept for all analysis, thereby maintaining a constant AOI. The area of each cell field expressing PI fluorescence above the background level was counted using the 'density mean' function present in the software. This function counts two-dimensional arrays of pixels of the AOI outlined. Results were expressed as percentage survival in relation to the treatment with maximum damage in each case.

Statistical Analysis

The results are expressed as mean + SEM., *n* indicating the number of slices. In the statistical comparison, analysis of variance (ANOVA) was used to evaluate the overall difference between the groups. The differences between each treatment group versus insult (e.g. OGD, glutamate, etc.) were analyzed using the unpaired Student's *t*-test.

2.3   **Chemicals and reagents**

Standard analytical grade laboratory chemicals for the preparation of general reagents obtained from Merck, Damstadt, Germany and BDH, Poole, U.K. Molecular biology work was carried out using molecular biology grade chemicals. Sources of specialty reagents used were mentioned in the text while others were obtained from:

Alpha DNA, U.S.A.
Random hexamers

Amersham International plc, U.K.
E coli DNA polymerase I (Klenow fragment)
T4 polynucleotide kinase
DNA restriction enzymes
Nitrocellulose membrane

Applied biosystems, U.S.A.
Reagents for reverse transcription and real-time PCR

Boehringer Mannheim, Germany
Deoxyribonucleotides (dATP, dCTP, dGTP, dTTP and dUTP)
Taq DNA polymerase

Biorad, Hercules, C.A., U.S.A.
40% Acrylamide solution (29:1)
TEMED
Tricine

BRL
Urea

Gibco-BRL, Gaitherssburg, M.D., U.S.A.
Agar
Agarose
Fetal Bovine Serum (FBS)
Guanidine HCl
OPTI-MEM medium

Invitrogen, Life Technologies, U.S.A.
Acetylated BSA
Reagents for oligonucleotide microarray cDNA synthesis

J.T. Baker Inc., U.S.A.
Glycine

Kodak Eastman, U.S.A.
X-ray film (X-Omat AR)

Merck
DMSO
Formaldehyde

Molecular Probes Inc., U.S.A.
R-Phycoerythrin Streptavidin (SAPE)

New England Biolabs, Beverly, M.A., U.S.A.
T4 DNA ligase

Pharmacia, U.S.A.
Bromophenol blue
RNAse-free DNAase I
Sephadex G-100

Promega
M-MLV reverse transcriptase

Promega Corporation U.S.A.
Herring sperm DNA

Sigma Chemicals Co., St Louis, MO, U.S.A.

2-mercaptoethanol	IPTG
APS	L-glutamine
Ampicillin	MES free acid monohydrate
Aprotinin	MES sodium salt
BSA	Penicillin-streptomycin
CHAPS	Pepstatin A
DEPC	PMSF
DMEM basal medium	Sodium acetate
DTT	SDS
Ethidium bromide	Tris-base
Glutathione (reduced form)	Triton X-100
HEPES	Tween-20

Sigma-Aldrich, U.S.A.
Goat IgG
Goat anti-streptavidin antibody
MTT

Chapter 3

Sputa nerve growth factor

(sputa NGF)

3.1   Introduction

Since the discovery of nerve growth factor (NGF) activity in snake venoms by Cohen and Levi-Montalcini (1956), snake venoms have been considered rich sources of NGF (Kostiza and Meier, 1996). Snake NGFs are found mainly in venoms of the *Elapidae*, *Viperidae*, and *Crotalidae* families (Lipps, 1998). However, the neuronal influence of snake venom NGFs as well as other non-mammalian NGFs on the developing nervous system and on the maintenance of the neurons is completely unclear. In fact, it has not been demonstrated whether NGF is of any importance for the reptile nervous system or not (Kostiza and Meier, 1996).

The yield of NGF from *Naja naja atra* snake was calculated to be in the range of 0.2%-0.5% (w/w; Kostiza *et al.*, 1995), while that of mouse 7S NGF from submandibular gland homogenate was found in a range of 0.002%-0.0025% (w/w; Longo *et al.*, 1989). Despite snake venom being the first source of NGF, the physical and biochemical properties of NGF were deduced from the NGF of male mouse submandibular gland (mouse NGF; Lipps, 1998). The amino acid homology between NGF from snakes and rodents is about 60%. Snake NGFs, particularly those from cobras were reported to be superior in inducing neurite outgrowth on PC12 cells as compared to NGFs derived from other types of snakes (Lipps, 1998). In addition, Server *et al* (1976) reported that NGFs from cobra (*Naja naja*) and mouse submandibular glands were able to elicit neurite outgrowth from chick embryonic dorsal root ganglion.

However, the biological effects elicited by NGF are best studied using the pheochromocytoma cell line (PC12). PC12 cells express both TrkA and $p75^{NTR}$ receptors and in response to NGF will differentiate into cells, resembling sympathetic neurons, making it an ideal tool to study the intracellular and

biochemical events following NGF binding to surface receptors (Kaplan and Miller, 1997). NGF is required for the survival of the differentiated cells. Both $p75^{NTR}$ and TrkA receptors act synergistically to mediate the trophic effects of NGF. Co-expression of $p75^{NTR}$ has also been found to enhance the biological response of cells expressing TrkA (Culmsee *et al*., 2002). Interestingly, the TrkA receptor activates positive signals such as increased survival and growth, while the $p75^{NTR}$ receptor is known to activate both positive and negative signals. Complexes of $p75^{NTR}$ with TrkA are found to enhance the neurotrophin binding affinity and TrkA-associated signaling pathway (Casaccia-Bonnefil *et al*., 1999). In addition, neuroprotection by NGF and activation of NF-κB (a pro-survival transcription factor) have shown to be dependent on the expression of $p75^{NTR}$ in PC12 cells (Bui *et al*., 2002).

This chapter describes the cloning and sequencing of two new cDNAs encoding NGF from the venom glands of a Malayan spitting cobra- *Naja sputatrix*. In addition, I expressed one of the cDNAs as a histidine-tagged fusion protein in *E coli*. and investigated its downstream pathways in relation to mouse 7S-NGF.

3.2   Methods of NGF purification from snake venoms

Snake venom NGF was found to be made up of a homodimeric complex of β-subunits, which share comparable biological activities with NGF of other species (Siigur *et al*., 1992). The similarity of its activity and sequence with other known NGFs (McDonald *et al*., 1991; Alkin and Bradshaw, 1993) led to the suggestion that purification methods should be similar to those of mouse NGF (Longo *et al*., 1989). Some of the purification methods for purifying NGF from snake venoms include; centrifugation, dialysis, lyophilization, ionophoresis, HPLC chromatography, monoclonal antibodies chromatography, gel filtration, ion (cation/anion) exchange

chromatography, starch gel electrophoresis, preparative gel electrophoresis and RP-HPLC chromatography (Angeletti, 1970; Mohamed *et al.*, 1970; Siigur *et al.*, 1987; Smith *et al.*, 1992). Following the purification method used to obtain NGF from the venom of Chinese cobra, *Naja Naja Atra* (Kostiza *et al.*, 1995), this study made use of a two-step purification method, involving gel filtration followed by RP-HPLC to obtain pure NGF from crude venoms.

3.2.1 Gel filtration

Gel filtration is a technique that separates proteins in a mixture according to their molecular weights. The first stage of crude venom purification was performed on Biogel 100. The elution profile of the protein mixture was monitored by measuring the absorbance of the resultant fractions at a wavelength of 280nm. Two major peaks were obtained from the chromatogram and were designated P1 and P2 (Fig. 3.1A). The first peak, P1 consisted of high molecular weight proteins (14-50kDa) while the P2 contained the low molecular weight proteins (4-10kDa). Each fraction (100ng/ml) was tested for its ability to promote neurite growth in PC12 cells (Table 3.1). The corresponding fraction was also subjected to SDS-PAGE analysis to verify their homogeneity and to determine the molecular mass.

3.2.2 RP-HPLC

Hydrophobic chromatography involved the interaction of non-polar regions of a protein with the non-polar surface of the binding matrix. In RP-HPLC, the stationary phase is hydrophobic (non-polar) while the mobile phase is polar. This will result in the retention of the hydrophobic components of the crude venom within the
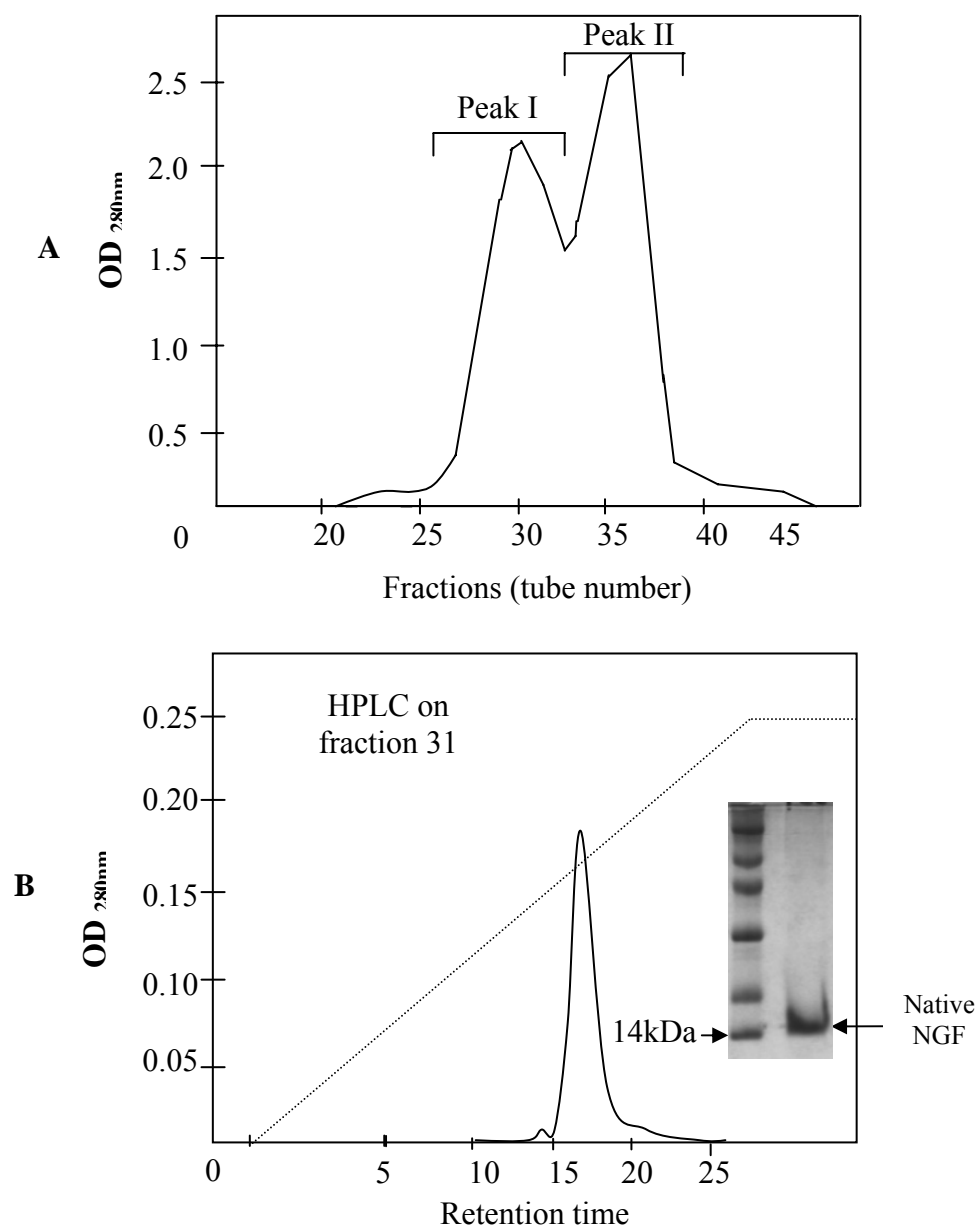
Fig. 3.1: Purification of native NGF from venom of *Naja sputatrix*. (A) Gel-filtration chromatography of crude venom. **(B)** Reversed phase HPLC chromatography of active fraction obtained from gel filtration. Inset shows the protein (native sputa NGF fraction) analyzed by SDS-PAGE.

stationary phase while the hydrophilic constituents would flow through. The hydrophobic components are subsequently eluted.

In the final stages of purification, the fraction showing the highest neurite outgrowth was purified further by RP-HPLC (Fig. 3.1B). It was loaded onto a C18 (Nucleosil) reverse phase-HPLC column and the elution profiles were monitored by measuring the absorbance of the resultant peak at a wavelength of 280nm. One homogenous protein peak was obtained and it showed neurite outgrowth at 1ng/ml (Table 3.1). This active protein was 14kDa in size (Fig. 3.1B insert). The N-terminal amino acid sequence of this protein was found to be -ETHPVHNRGEYSV- and the protein was found to be non-lethal up to 1μg/g in mouse.

3.3   Screening of NGF activity from venom fractions using PC12 cells

PC12 cells have been used as the prime dopaminergic cellular tool in molecular neuroscience for investigating NGF mechanism of action (Vaudry *et al.*, 2002) and in *in vitro* cell death studies. It is the most established bioassay to detect NGF activity from fractions and thus normally used for screening fractions from chromatographic procedures (Greene and Rukenstein, 1989). PC12 bioassay was proven to be sensitive enough to detect NGF even in highly diluted venom fractions at concentrations where cytotoxic contaminations of the pre-purified fractions were ineffective (Kostiza *et al.*, 1995). Venoms from several Elapids, *Naja sputatrix, Bungarus candidus, Pseudonaja textilis*, *Austrelaps superbus* as well as venoms from Chinese and Indian scorpions (*Buthus martensi Karsch, Mesobuthus tumulus*) and honey bee (*Apis mellifera)* were tested for neurite outgrowth in PC12 cells. β-Nerve Growth Factor (7Sβ-NGF) from the mouse submaxillary gland was used as a positive control. Cell processes with length equivalent to one or more diameters of a

Sample	Neurite outgrowth
Mouse NGF (positive control; 100ng/ml)	+++
Bungarus candidus (250ng/ml)	++
Naja sputatrix (250ng/ml)	++++
Austrelaps superbus (250ng/ml)	++
Pseudonaja textilis (250ng/ml)	+++
Chinese scorpion (250ng/ml)	++
Indian scorpion (250ng/ml)	+
Bee venom (250ng/ml)	++
Biogel P10 gel fractions of *N. sputatrix* (Fig. 3.1A)	
Fraction 27	++
Fraction 28	+++
Fraction 29	++
Fraction 30	+++
Fraction 31 (1ng/ml)	+++++
Fraction 33	++
Fraction 34	Lysis
Fraction 35	Lysis
Fraction 36	Lysis
HPLC fractions (Fig. 3.1B)	
Fraction 3	-
Fraction 4	-
Fraction 5	+
Fraction 6	++
Fraction 7	+++++
Fraction 8 (1ng/ml)	++++++
Fraction 9	+++
Fraction 10	+
Denatured and refolded recombinant nerve growth factor (NGF)	
Denatured recombinant NGF (100ng/ml)	++
Refolded recombinant NGF (100ng/ml)	++++

Table 3.1: Neurite outgrowth in PC12 cells. Protein concentrations at 100ng/ml were used unless otherwise stated. '+++' denotes number of neurites observed in positive control (mouse NGF), while '++++' denotes 50% increase in the number of neurites observed as compared to mouse NGF.

cell body were counted as neurites and at least 100 cells were analyzed for each condition from each of the three independent experiments (Koike *et al*., 2006). The highest neurite outgrowth was observed for *N. sputatrix* crude venom at 250ng/ml. Mouse NGF (7S) showed a comparable activity at 100ng/ml (Table 3.1). *N. sputatrix* was selected to be the snake with venom having the highest NGF activity and a recombinant protein was to be synthesized.

3.4   cDNA cloning of the nerve growth factor from *N. sputatrix*

Once *Naja sputatarix* was identified as the snake containing the highest amount of NGF activity, total RNA was extracted from its venom gland, reversed transcribed and amplified using gene specific primers. A 700bp fragment of PCR products was obtained. The cDNA was subcloned and 30 positive clones were sequenced. All clones showed the presence of cDNA encoding nerve growth factor. The cDNA encoded for a 22 amino acid signal peptide, a 112 amino acid pro-domain and a mature NGF protein consisting of 117 amino acid residues. Analysis of the sequences indicated the presence of two isoforms (nsNGFI and II) of venom nerve growth factor (Fig. 3.2).

3.5   Expression of NGF in *E. coli*

In this study, two new cDNAs encoding the NGF in the venom glands of a spitting cobra, *Naja sputatrix* were cloned and sequenced. Due to its higher homology to the mammalian homolog, nsNGFI was selected for the expression as a recombinant protein in *E. coli* and termed "sputa NGF". The cDNA encoding the mature protein of nsNGFI was subcloned into pQE30 expression vector in-frame with the $(His)_6$-tag at the N-terminal region of the recombinant protein. The expression fusion protein

```
bmngf      MSMLCYTLIIAFLIGIWAAPKSEDNVPLGSPAKSDFSDTNCAQTHEGLKTSRNTDQHHPT
nsngfI     MSMLCYTLIIAFLIGIWAVPKSEDNAPLGSPATSDLSDTSCAQTHEGLKTSRNTDQRHPA
agpngf     MSMLCYTLIIAFLIGVWAAPKSEDNVPLGSPATSDLSDTSCAKTHEALKTSRNTDQHYPA
mousengf   MSMLFYTLITAFLIGVQAEPYTDSNVPEGDSVPEAHWTKLQHSLDTALRRARSAPTAPIA
humNGF     MSMLFYTLITAFLIGIQAEPHSESNVPAGHTIPQVHWTKLQHSLDTALRRARSAPAAAIA
           ****·****·*****··*·*····*·*·*·············*····*
            ++++++++++·+·····················++····++····+

nsngfII    PQKAEDQELRTAANIIVDPKLFQKRQFQSPRVLFSTQPPLLSRDEESVEFLDNEDS-LNR
bmngf      PKKSEDQELGSAANIIVDPKLFQKRRFQSPRVLFSTQPPPLSRDEQSVKFLDTEDT-LNR
nsngfI     PRSQRIKQFGSASNIIVDPKLFQKRRFQSPRVLFSTQPPPLSRDEQSVEFLDNEDA-LNR
agpngf     PKKAEDQEFGSAANIIVDPKLFQKRRFQSPRVLFSTQPPPLSRDEQ---SVDNVNS-LNR
mousengf   AR-----VTGQTRNITVDPRLFKKRRLHSPRVLFSTQPPPTSSDTLDLDFQAHGTIPFNR
humNGF     AR-----VAGQTRNITVDPRLFKKRRLRSPRVLFSTQPPREAADTQDLDFEVGGAAPFNR
                      **·***·**·**····**********·*·············**

                ·+·+·+····++·····+·+··++·········++····++····+·+

nsngfII    NIRAKRED-HPVHNLGEHSVCDSVSAWVT-KTTATDIKGNTVTVMENVNLDNKVYKQYFF
bmngf      NIWANNEN-HPVHNQGEHSVCDSISVWVTNKTKATDIKGNTVTVMVDVNLNNEVYKQYFF
nsngfI     NIRAKRET-HPVHNRGEYSVCDSISVWVANKTTATDIKGKPVTVMVDVNLNNHVYKQYFF
agpngf     NIRAKRED-HPVHNRGEYSVCDSVSVWVGNKTTATDIRGNLVTVMVDVNLNNNVYKQYFF
mousengf   THRSKRSSTHPVFHMGEFSVCDSVSVWVGDKTTATDIKGKEVTVLAEVNINNSVFRQYFF
humNGF     THRSKRSSSHPIFHRGEFSVCDSVSVWVGDKTTATDIKGKEVMVLGEVNINNSVFKQYFF
           ^^······**·····**·····**·*****·*·**···**·****·*··*·*····**·*·****

             +··········+····+····+···········++···········++

nsngfII    ETKCKNPNPVPSGCRGIDSSHWNSYCTETDTFIKALTMEGNQASWRFIRIDTACVCVITK
bmngf      ETKCRNPNPVPSGCRGIDSRHWNSYCTTTDTFVKALTMEGNRASWRFIRIDTACVCVISR
nsngfI     ETKCRNPNPVPSGCRGIDSRHWNSYCTTTHTFVKALTMEGNRASWRFIRIDTACVCVISR
agpngf     ETKCRNPNPVPTTCGGIDARHWNSYCTTTHTFVKALTMEDNQASWRFIRIDTACVCVISR
mousengf   ETKCRASNPVESGCRGIDSKHWNSYCTTTHTFVKALTTDEKQAAWRFIRIDTACVCVLSR
humNGF     ETKCRDPNPVDSGCRGIDSKHWNSYCTTTHTFVKALTMDGKQAAWRFIRIDTACVCVLSR
           ****···***····*·***··*******·*·**·****······*·*************

             +·+

nsngfII    KTGNN--
bmngf      KTENFPP
nsngfI     KTENF--
agpngf     KNENFG-
mousengf   KATRRG-
humNGF     KAVRRA-
           *
```

Fig. 3.2: Comparison of amino acid sequences of various NGF. Sputa nsngf I&II refer to the two isoforms of NGF from *Naja sputatrix*; bmNGF is from *Bungarus multicinctus* (S56212); agpngf is from *Agkistrodon halys pallas* (Guo *et al.,* 1999); mousengf (K01759) and human ngf (humNGF, X52599). The pro NGF region is underlined and the mature peptides are in bold letters. Identical amino acids are shown by (*) and the proteolytic cleavage site (KR) for the mature peptide is indicated by ^ ^. The variant residues between nsngf I and II are shown by (+).

was induced with 1mM of IPTG for 3h at 37°C and several clones were selected for a preliminary analysis of the induction efficiency. The expressed fusion protein was analyzed on 12% SDS-PAGE (Fig. 3.3, lanes 2 and 3).

3.6 Production of recombinant sputa NGF

Expression of recombinant NGF was carried out as mentioned in section 2.2.5. The eluted histidine-tagged protein from the Ni-NTA column were subjected to SDS-PAGE analysis (Fig. 3.3, lane 4) and a protein of about 20kDa was obtained, which constitute the mass of sputa NGF plus the $(His)_6$-tag. Sputa NGF protein was denatured fully (to expose all the cysteine residues) in 8M urea and β-mercaptoethanol and later subjected to *in vitro* refolding in the presence of oxidized and reduced glutathione (Fig. 3.3, lane 5). The yield of properly refolded protein is about 3mg/L. However, both denatured and refolded recombinant NGFs varied in their potency to induce neurite outgrowth on PC12 cells (Table 3.1). The CD spectrum of the refolded protein was found to correlate well with that of the native NGF protein (Fig. 3.4).

3.7 Biological activity of recombinant sputa NGF

Apart from its expression, recombinant sputa NGF was tested for its biological activity by incubation with PC12 cells, with mouse NGF as a reference. Neurite outgrowth was observed after an overnight incubation with either mouse NGF or recombinant sputa NGF (Fig. 3.5). A quantification of neurite outgrowth in the presence of native *Naja sputatrix* NGF has also been found to induce neurite outgrowth in PC12 cells in a dose-dependent manner, but at a relatively lower protein concentration (1-10ng/ml; Fig 3.6A). Likewise, a similar quantification of
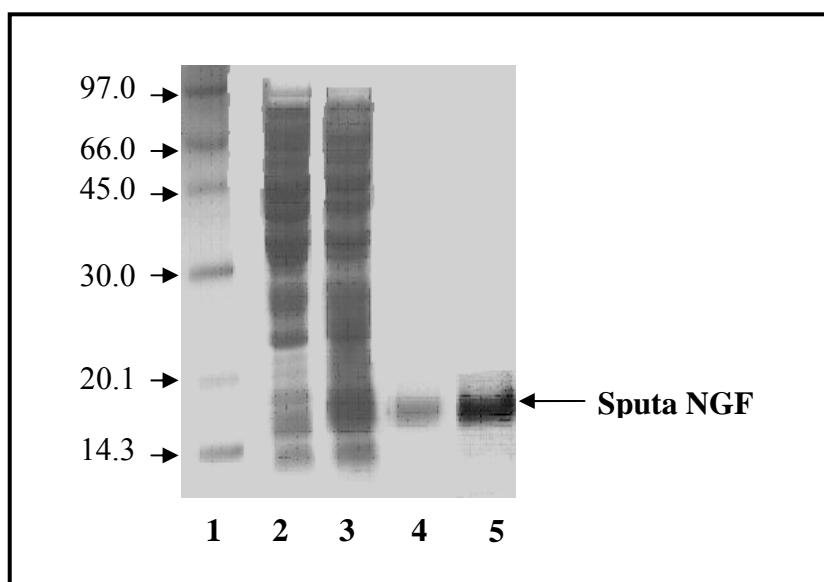
Fig. 3.3: Expression, purification and folding of recombinant NGF (sputa NGF). SDS PAGE analysis of sputa NGF protein: lane 1 represents protein molecular mass standards with sizes indicated in kilodaltons (kDa); lane 2 refers to *E. coli* cell lysate before induction; lane 3; *E. coli* cell lysate (inclusion bodies) after 3h induction with 1mM of IPTG; lane 4 refers to purified sputa NGF after affinity chromatography with Ni-NTA column and lane 5; refolded sputa NGF after dialysis.
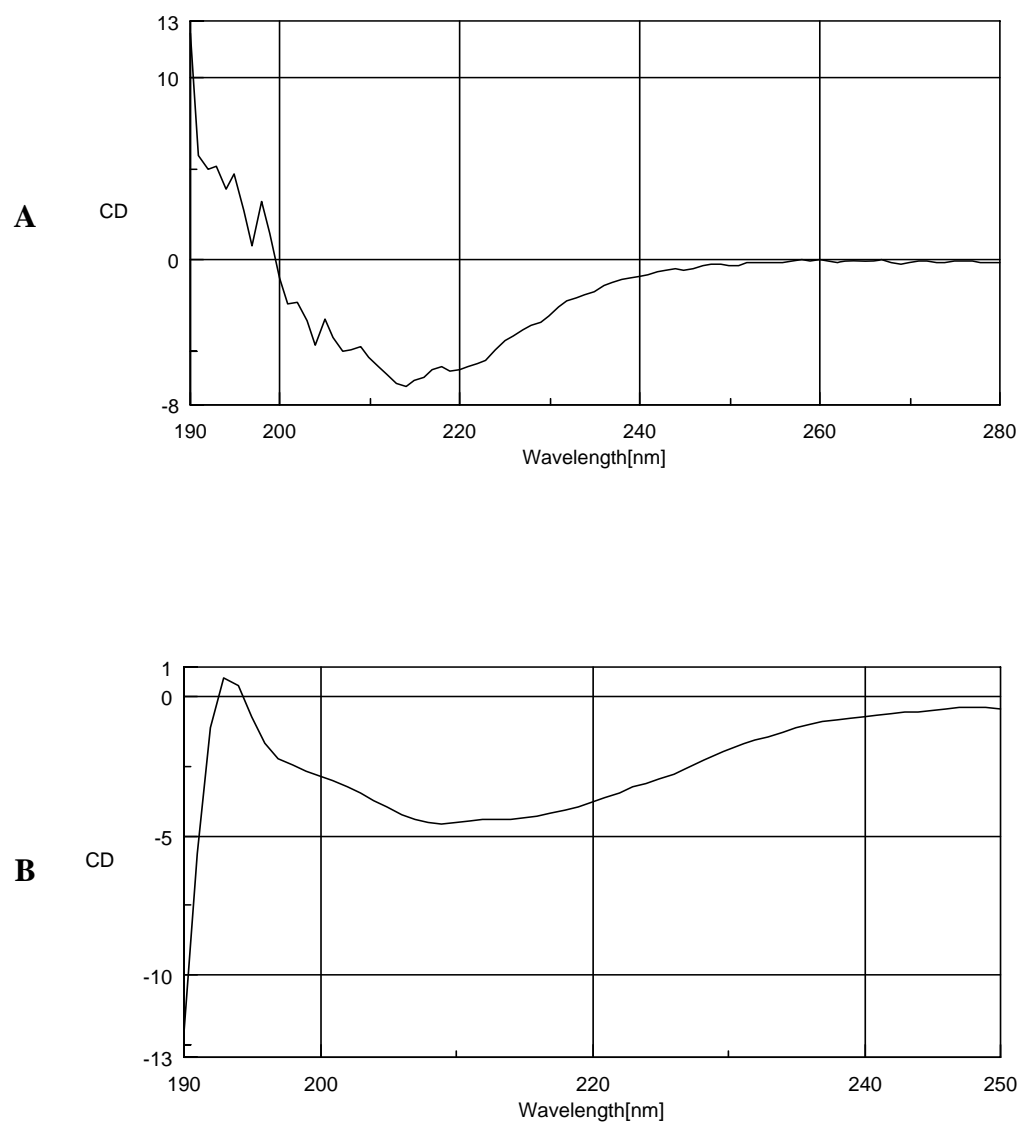
Fig. 3.4: Circular dichroism (CD) spectrum of NGF. **(A)** Spectrum of refolded protein and **(B)** spectrum of native *Naja sputatrix* NGF protein.
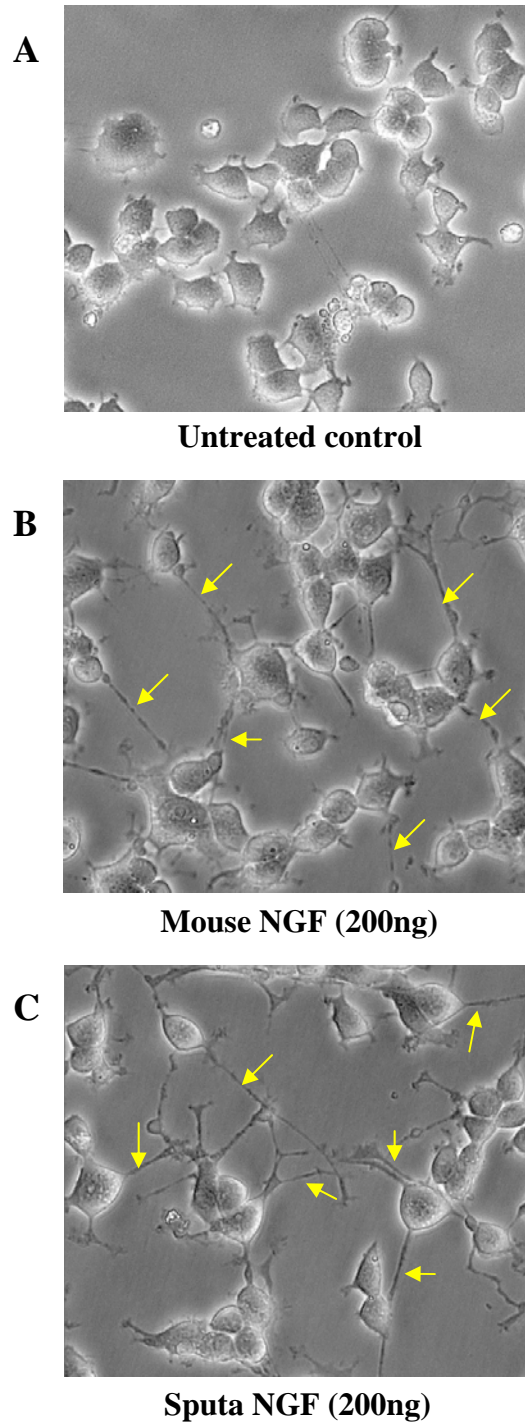
Fig. 3.5: Neurite extension after treatment with mouse and sputa NGF. PC12 cells at 1×10^6 were plated and grown overnight. Following day, cells were treated with either mouse or sputa NGF, at 200ng/ml for 16-18h. Untreated control PC12 cells do not have any neurites **(A),** while neurite extensions were observed upon treatment with mouse NGF **(B)** and sputa NGF **(C)** at 200ng/ml.
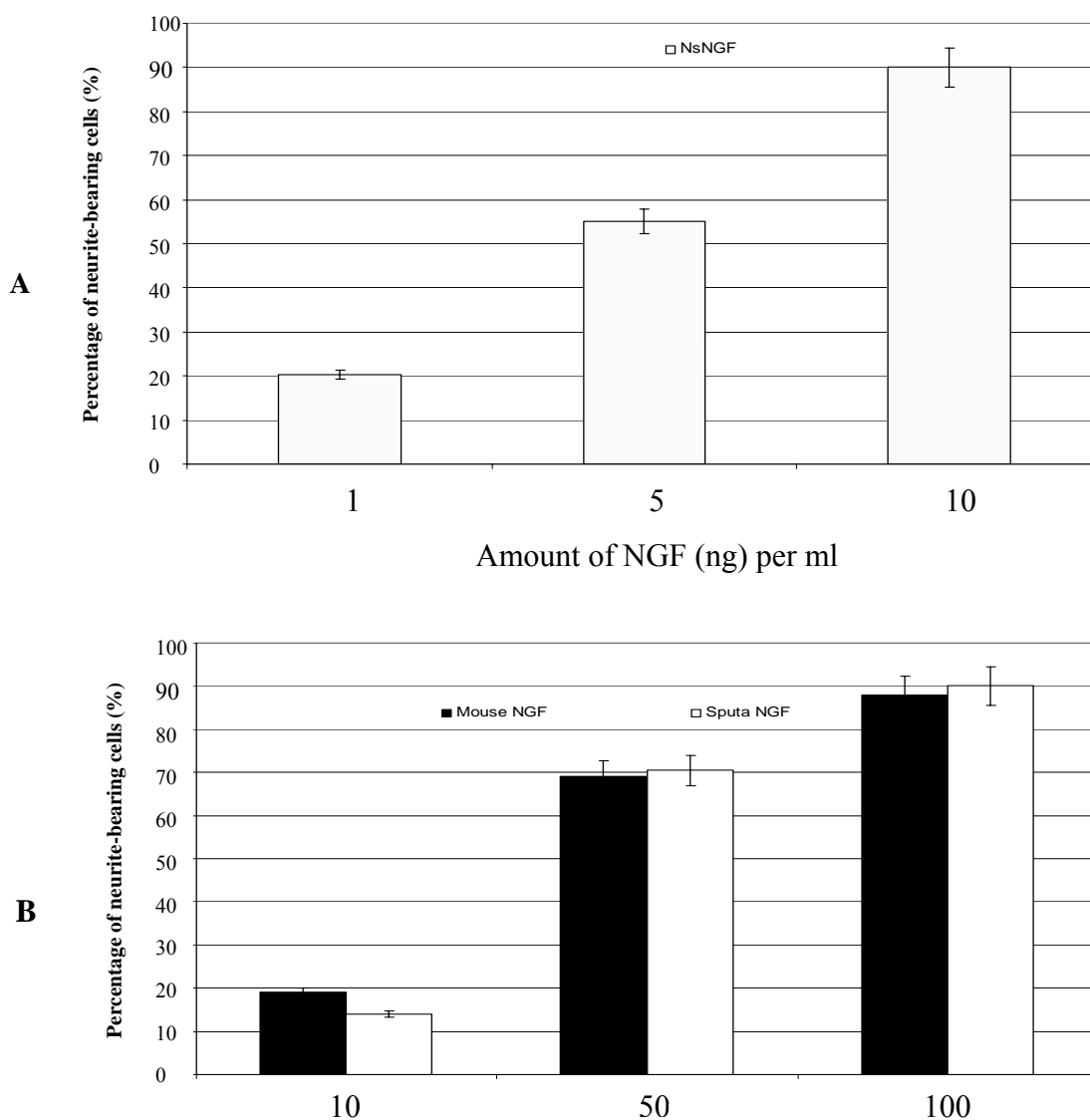
Fig. 3.6: Percentage of neurite-bearing cells. PC12 cells were treated with **(A)** native sputa NGF in a dose-dependent manner and the percentage of neurite-bearing cells were tabulated. **(B)** A similar dose-dependent experiment was carried out using mouse NGF (filled boxes) and recombinant sputa NGF (empty boxes).

neurite outgrowth was done for mouse and recombinant sputa NGF, by counting the number of neurite-bearing cells expressed in percentage, both for (i) dose-dependent manner (Fig. 3.6B) and (ii) time-dependent manner (Fig. 3.7). The results showed that the recombinant sputa NGF exhibited a comparable activity with that of mouse NGF at 200ng/ml and the optimum time for neurite extension is between 16-18 hours. The optimized time (16-18h) and dose (200ng/ml) of sputa NGF treatment were used for subsequent experiments.

3.8 Activation of TrkA receptors

PC12 cells contain both NGF receptors (TrkA and $p75^{NTR}$) and were used to analyze receptor activation. Western blot analysis of the PC12 cells treated separately with the mouse and sputa NGF for 15 minutes showed that the sputa NGF increased the production of the precursor $gp110^{trkA}$ receptors compared to the mouse NGF. However, the mature $gp140^{trkA}$ receptor was found in equal amounts for both treatments (Fig. 3.8A and B).

3.9 Real-time PCR analysis after NGF treatment

To detect the regulation of genes upon treatment with NGF, PC12 cells were treated with either mouse NGF or sputa NGF (200ng/ml) for 16-18h. Neurites were observed with treatment and total RNA was extracted. The regulation of genes was assessed by real-time PCR. In addition to receptor genes (TrkA and $p75^{NTR}$), the expression patterns of endogenous NGF, NFκB and IκB were accessed. The expression of IκB (inhibitor of NFκB gene) was found to be negatively regulated, while an interesting elevated expression of the endogenous NGF gene was noted only upon treatment with the sputa NGF (Fig. 3.9). NGF treatment in PC12 cells and
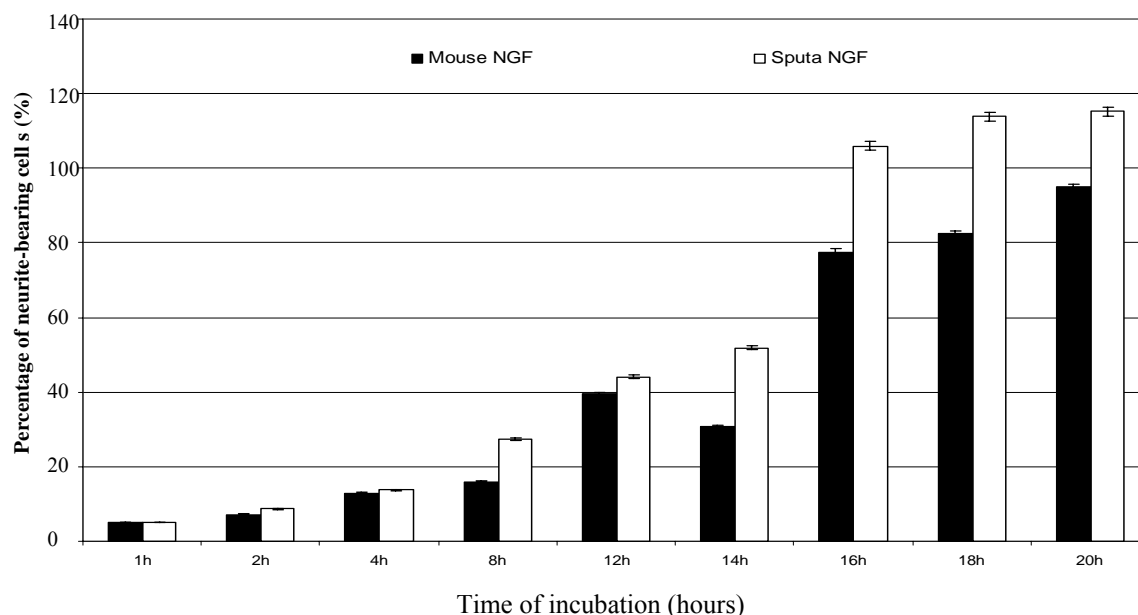
Fig. 3.7: Time dependent manner of neurite-bearing cells. PC12 cells were incubated for various time intervals indicated at 200ng/ml with either mouse NGF (filled boxes) or recombinant sputa NGF (empty boxes) and the number of neurites was counted the following day. The percentage of neurites were tabulated against time, by 16-18 hours, maximum number of neurites were obtained. This timing was used for the rest of the study.
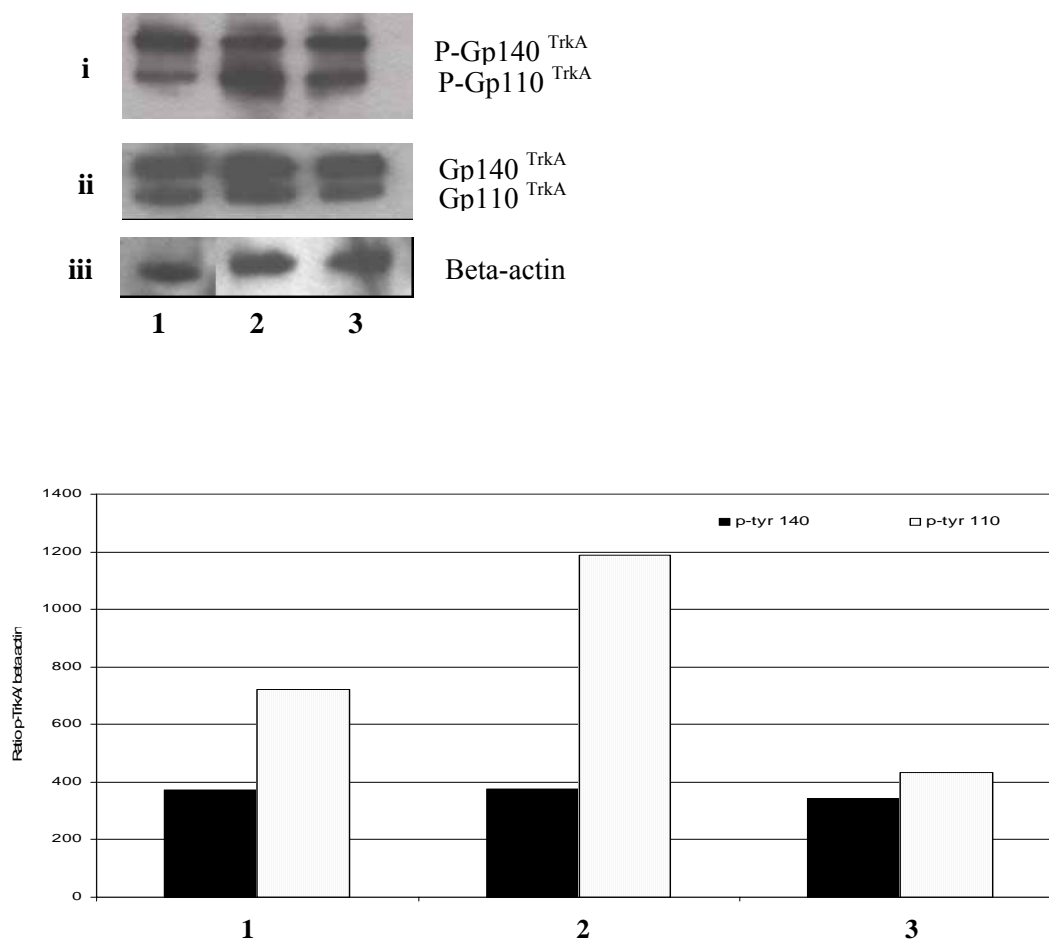
Fig. 3.8: Activation of TrkA receptor determined by western blot. (A) Cells were treated for 15min and total protein extracted. Equal amounts of protein was separated on a 7.5% SDS-PAGE and subsequently blotted onto nitrocellulose membrane. (i) Phosphorylated TrkA receptors (gp110 and gp140) were detected using monoclonal anti-phosphotyrosine antibody. The same membrane was stripped and probed with (ii) anti-TrkA and (iii) anti-beta-actin antibodies. **(B)** Densitometry analysis shows the ratios of the phsophorylated TrkA and beta actin (internal control) levels and lane 1: mouse NGF-treated cells; lane 2: sputa NGF-treated cells and lane 3: untreated control cells.
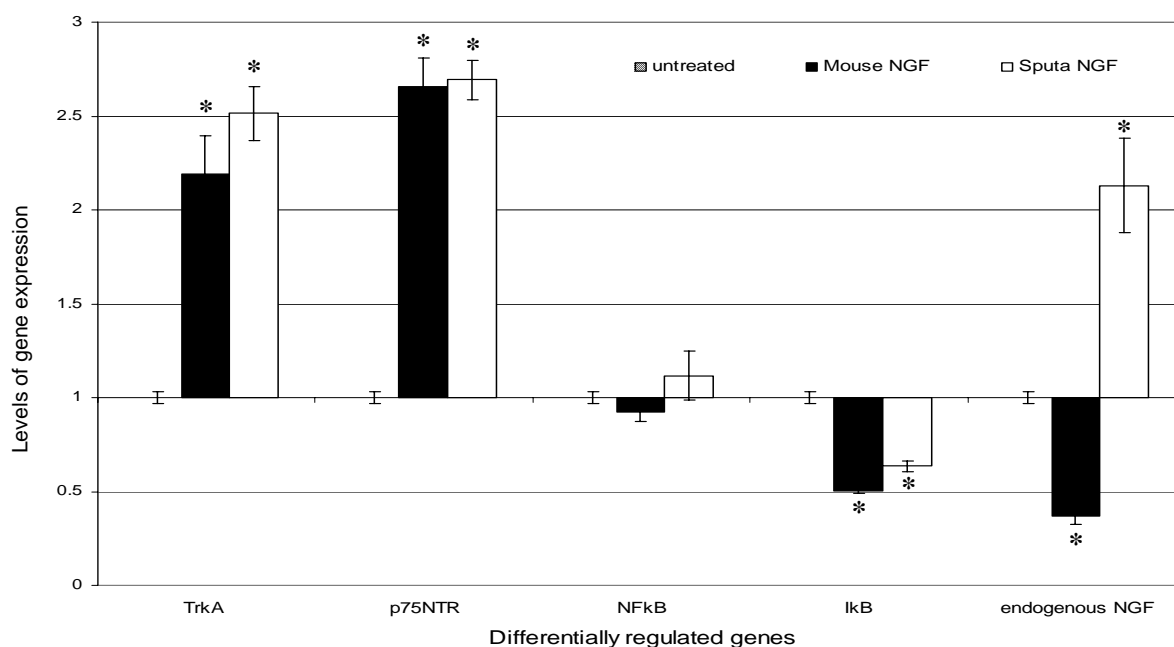
Fig. 3.9: Quantitative real-time PCR gene analysis using SYBR Green assay.
Total RNA from treated (mouse and sputa NGF) and untreated PC12 cells was used
to study the expression of 5 genes, TrkA, p75^{NTR}, NF-κB, IκB and endogenous
NGF. Values are expressed as ± SEM, experiments performed in triplicates and *: p-
value < 0.01 by unpaired Student's *t*-test.

sympathetic neurons are known to induce pro-survival signal via NF-κB (Taglialatela *et al*., 1997; Maggirwar *et al*., 1998; Foehr *et al*., 2000; Wooten *et al*., 2001). In addition, several studies have shown neurotrophin factors, including NGF, constitute an important class of endogenous modulators of excitotoxicity (Mattson *et al*., 1993). Hence, an up-regulation of NFκB and endogenous NGF genes by sputa NGF treatment may have potential neuroprotective roles.

3.10   Protein profiling (SELDI-TOF) analysis

Proteins regulated upon treatment of NGF (sputa or mouse) treatment were detected by protein chip (SELDI-TOF) and mouse NGF was used as a reference. Protein profiling results identified 5 proteins that showed significant changes upon NGF treatment (Fig. 3.10). The analysis showed changes in expression of both growth-related (NGF precursor and neurogranin) and an apoptotic protein (BAD). Cells treated with sputa NGF (Fig. 3.10A) showed a decrease (~6-fold) in an 8kDa protein and an increase (~2-fold) in an 11.4kDa protein. Cells treated with mouse NGF (Fig. 3.10B) showed a down regulation (~10-fold) of a 13.9 kDa protein. Comparison between sputa NGF and mouse NGF treatments (Fig. 3.10C) showed that sputa NGF caused an increase in the growth-associated proteins like A-kinase anchoring protein (11.4 kDa) and the endogenous NGF precursor (13.9 kDa) as compared to pro-apoptotic protein (BAD). Expression of protein at 8kDa (possibly neurogranin) was greatly decreased (~5-fold), whereas proteins at 22.3kDa (BAD) and 67.2kDa (SHP-1) showed a marginal up and down regulation respectively (Fig. 3.10C).
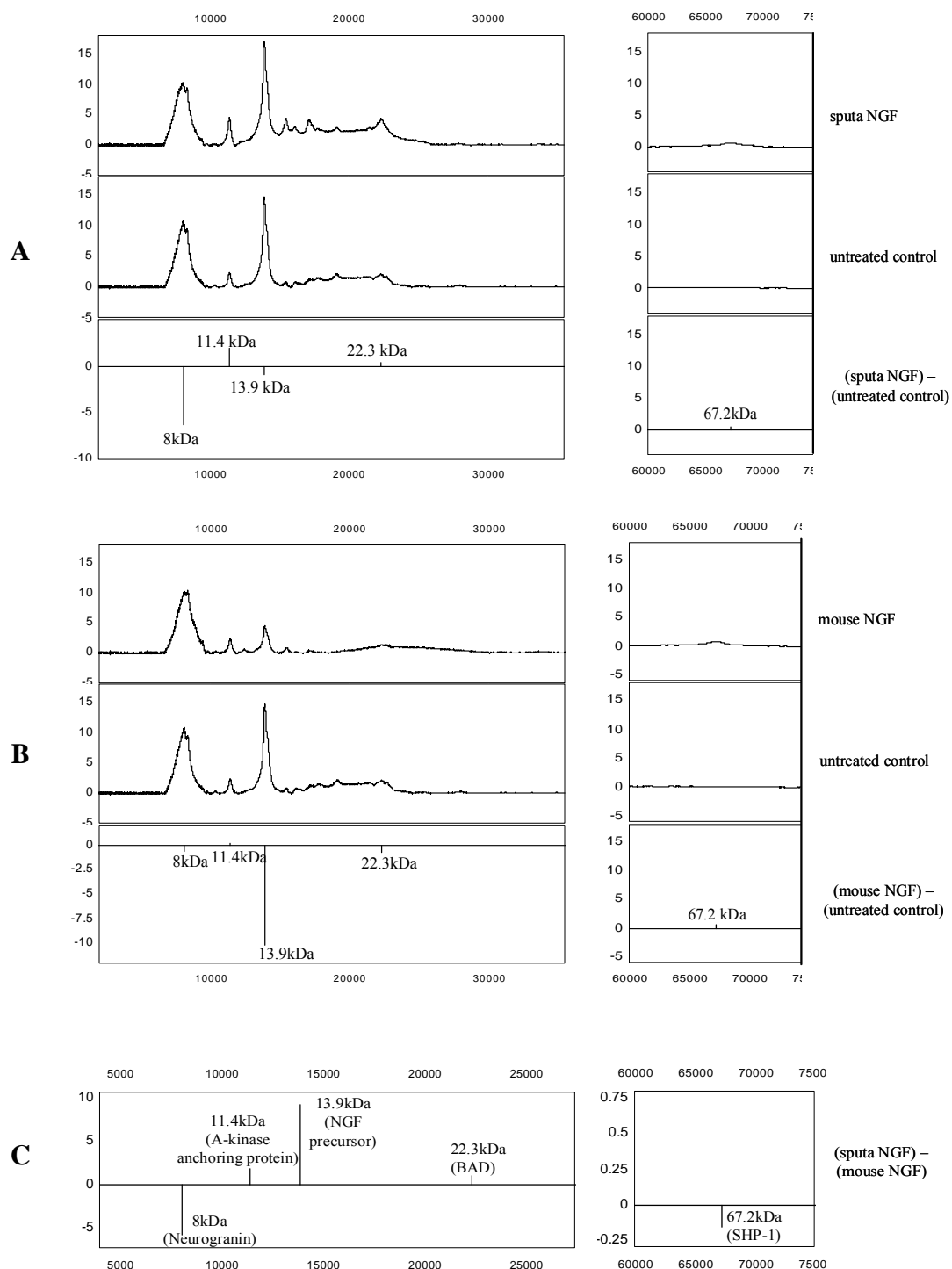
Fig. 3.10: Protein profiling analysis. Total protein extracts from cells treated with either mouse NGF or sputa NGF for 16-18 hours were used. **(A)** Protein profiles obtained from cells treated with sputa NGF versus untreated control. **(B)** Protein profiles obtained from cells treated with mouse NGF versus untreated control. **(C)** Protein profiles obtained for sputa NGF versus mouse NGF.

3.11   Microarray analysis of NGF treated PC12 cells

The global gene expression upon treatment with both NGFs was studied using oligoprobe microarrays. The genes whose expression is altered by 2-fold or more were taken as significant (Li *et al.*, 2004) from about 730 genes examined in our study. These probe sets were subjected to self-organizing map (Data Mining Tool; Affymetrix, USA) clustering and were grouped according to their expression patterns. The genes were also further assigned to categories according to their biological functions. Some of them are shown in Table 3.2. The majority of these genes were found to be involved in the cell cycle and growth pathways.

Category of genes	Description	mouse NGF (fold-change)	sputa NGF (fold-change)
Cell cycle	growth arrest and DNA-damage-inducible 45 alpha	3.63	3.18
	proliferating cell nuclear antigen	-2.07	-1.74
	ret proto-oncogene	2.87	2.91
	ret proto-oncogene	4.06	4.41
	cyclin-dependent kinase inhibitor 1A	4.99	4.26
	growth associated protein 43	2.27	2.10
Apoptosis	apoptotic death agonist BID	3.36	2.85
	Bcl-2-like-1	2.22	1.77

Category of genes	Description	mouse NGF (fold-change)	sputa NGF (fold-change)
Eicosanoid synthesis	**prostaglandins-endoperoxide synthase 1**	**4.59**	**2.36**
	interleukin 12 p35 subunit	**6.19**	**4.72**

Category of genes	Description	mouse NGF (fold-change)	sputa NGF (fold-change)
Transcription factors	core promoter element binding protein	2.53	1.57
	fos-like antigen 1	**8.57**	**3.51**
	nuclear transcriptional factor-Y-beta	2.01	1.14
	ISL1 transcriptional factor, LIM/ homeodomain 1	2.75	1.74
	global ischemia induced protein GIIG15B	-2.38	-2.07
	DNA polymerase beta	2.20	1.88
	GATA binding protein 4	1.39	2.17
	myelin transcription factor 1-like	-2.20	-1.33
	signal transducer and activator of transcription 3	2.04	1.66
	activating transcription factor 3	**2.2**	**-1.54**
	early growth response 1	**15.14**	**12.91**
Translational factors	eukaryotic initiation factor-5	2.03	1.60
	eukaryotic initiation factor-2B, subunit 3	2.04	1.82

Category of genes	Description	mouse NGF (fold-change)	sputa NGF (fold-change)
Others	meprin 1 alpha	2.55	2.10
	cathepsin E	**11.08**	**8.22**
	mast cell protease 7	**88.65**	**71.51**
	plysia ras-related homolog A2	2.69	2.33
	small GTP-binding protein rab5	2.20	1.79
	GTP cyclohydrolase 1	3.20	2.10
	phospholipase D	2.41	2.55
	kinesin family member 1B	1.45	2.01
	procollagen, type XII, alpha 1	2.30	1.41
	integrin beta 1	2.31	2.39
	insulin receptor substrate 1	2.06	1.27
	double cortin and calcium/calmodulin-dependent protein kinase-like 1	2.69	1.84
	gap junction membrane channel protein beta 5	2.79	2.04
	Jun-B oncogene	2.28	2.39
	opiod receptor-like	2.13	2.73
	arginine vasopressin receptor 1A	**5.43**	**20.25**

purinergic receptor P2X, ligand-gated ion channel 2	**-2.91**	**-1.59**
purinergic receptor P2X, G-protein coupled 2	2.06	2.11
adenosine monophosphate deaminase 3	2.48	1.85
myelin basic protein	1.04	2.35
prolactin receptor	2.17	1.54
serum-inducible kinase	**7.26**	**3.12**
syntaxin	2.71	1.45
dynamin 1	-2.07	-1.39
guanosine diphosphate dissociation inhibitor 3	2.17	2.39
annexin 5	3.03	2.77
neural receptor protein-tyrosine kinase	9.19	3.16
moesin	2.97	2.48
vesicle-associated membrane protein, associated protein B and C	1.71	2.10
ADP-ribosylation-like 4	2.71	2.28
solute carrier family 1, member 3	**6.28**	**4.99**
solute carrier family 9, member 4	-1.44	2.23
syndecan 1	2.95	2.39
myosin IXA	2.22	1.99
potassium inwardly rectifying channel, subfamily J, member 6	2.20	1.95
protein kinase, cAMP dependent regulatory, type I, alpha	2.53	2.08
coated vesicle membrane protein	2.00	1.89
regulator of G-protein signaling protein 2	2.25	1.38
cold inducible RNA-binding protein	1.97	2.30
microtubule-associated protein 1b	2.31	1.29
acid phosphatase 5	2.01	1.91
profilin II	2.38	2.06
glutamate receptor, ionotrophic, NMDA2C	-2.50	-1.91
lysosomal membrane glycoprotein 2	-1.97	-2.20
nerve growth factor receptor-associated protein	-2.03	-1.55

Calcium-related pathway		
very low density lipoprotein receptor	2.16	1.83
very low density lipoprotein receptor	2.57	2.00
very low density lipoprotein receptor	2.22	2.10
calcium binding protein p22	3.66	2.19
S-100 related protein, clone 42C	3.36	2.71
S-100 related protein A4	2.06	1.95
cadherin	-3.14	-2.33
calcium channel, voltage-dependent, T-type, alpha II subunit	**5.54**	**7.21**
protein phosphatase 3, regulatory subunit B, alpha isoform, type 1	2.23	1.78

Table 3.2: Classification of genes obtained from microarray. Genes were grouped based on their biological functions. Notable changes in gene expression were highlighted in **BOLD** text.

Chapter 4

The pro-domain of sputa NGF

4.1   Introduction

NGF belongs to the neurotrophin family and is synthesized as immature precursors that are proteolytically cleaved intracellularly by furin and other proconvertases, to release mature ligands. The function of the NGF precursor was initially thought to be for protein folding and regulation of neurotrophin secretion (Suter, 1991 and Rattenholl *et al.*, 2001). However, the function of the NGF precursor was recently challenged by two independent groups. Fahnestock *et al.* (2001) proved it to be neurotrophic, while Lee *et al.* (2001) proved it to be apoptotic (2001). The debate from the two groups was elaborated in detail in section 1.1.3.1. This chapter attempts to investigate the function of the pro-domain of sputa NGF protein using PC12 cells.

4.2   Analysis of sequence by bioinformatics tools

The sequence of NGF from *Naja sputatrix* (nsNGFI; chapter 3) was compared to the other two mammalian counterparts (mouse and human NGFs) using bioinformatics tools. NsNGFI showed about 70% homology to the mammalian NGFs at the mature protein region and hence was chosen for expression in *E. coli* as a recombinant protein. The entire sequence containing both the pro-domain and mature regions were compared between the three NGFs. NetNES 1.1 analyses (Fig. 4.1A) revealed that nsNGF I had one site for nuclear export signal (NES) whereas the mammalian NGFs had none. In addition, other post-translational modifications were compared. Potential amino acid residues that could be phosphorylated include serine, threonine and tyrosine. NetPhos 2.0 server predicted that nsNGFI and human NGF had 9 serine and 4 threonine residues, whereas mouse NGF had 11 serine, 7 threonine and 1 tyrosine residues as possible phosporylation sites (Fig. 4.1B). Mammalian NGFs
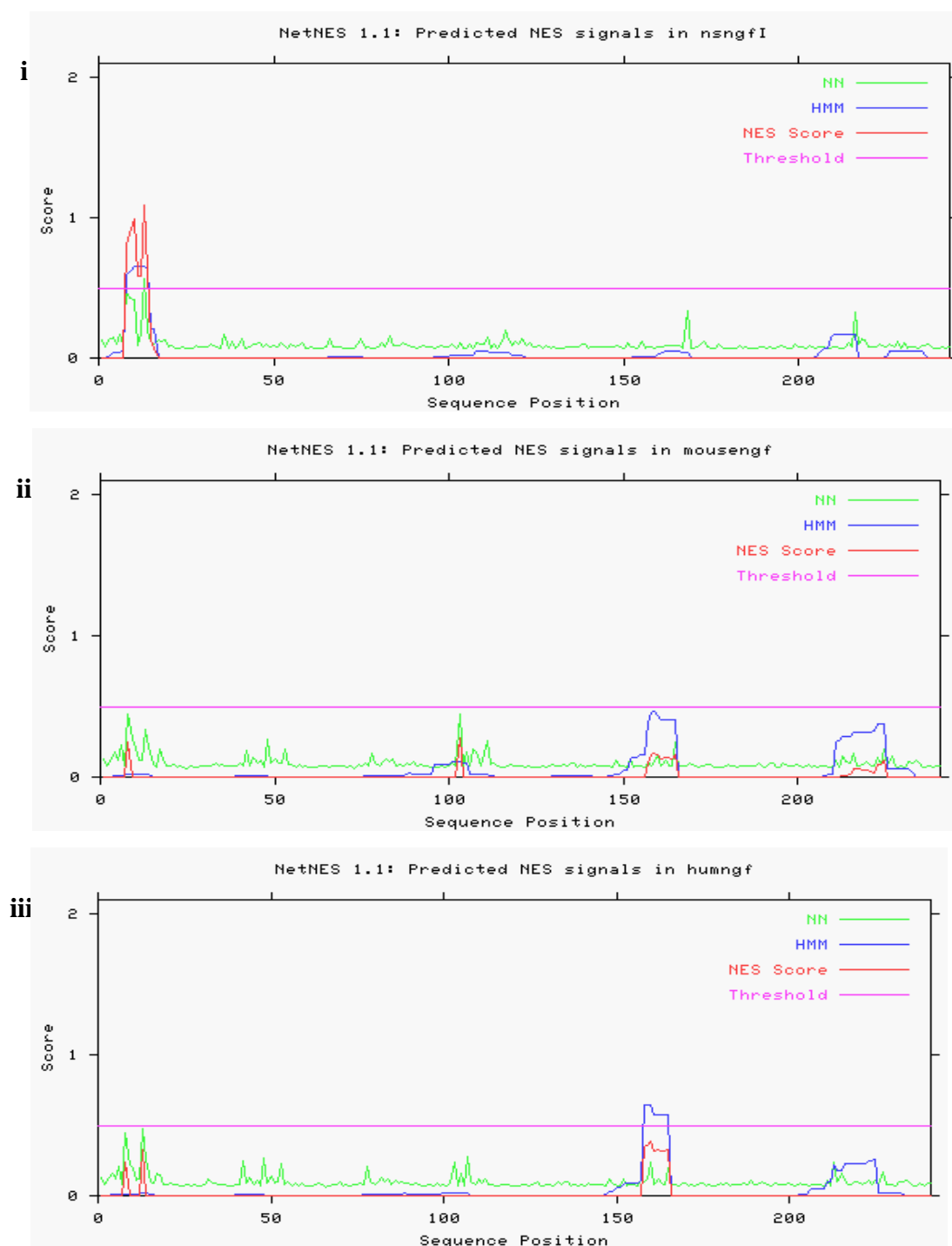
Fig. 4.1A: Prediction of potential leucine-rich nuclear export signal (NES) by NESbase version 1.0 database. It was used to predict potential NES sites from protein sequences. There is one predicted site for NES in **(i)** *Naja sputatrix* NGF (Nsngf I) and none for **(ii)** mouse NGF and **(iii)** human NGF (humngf).
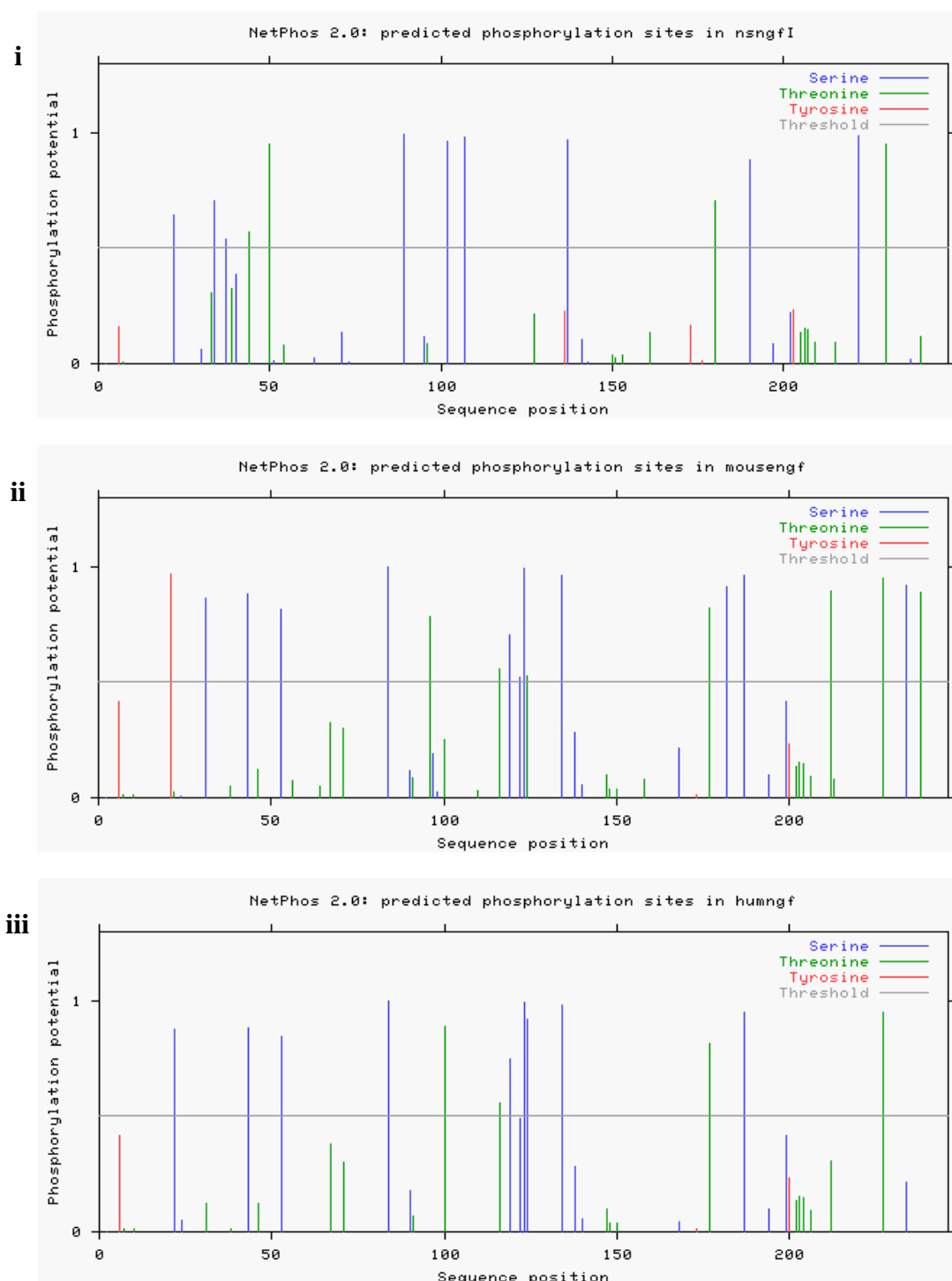
Fig. 4.1B: Prediction of potential phosphorylation sites by NetPhos 2.0 server. It was used to predict potential serine, threonine and tyrosine phosphorylation sites from NGF protein sequences. The server predicted that **(i)** *Naja sputatrix* NGF (nsngfI) has 9 serine and 4 threonine residues, **(ii)** mouse NGF has 11 serine, 7 threonine and 1 thyrosine residues while **(iii)** human NGF (humngf) has 9 serine and 4 threonine residues.

had 2 possible N-glycosylation sites (Fig. 4.1C), while nsNGFI had none. In addition, there were 3 possible O-glycosylation sites (Fig. 4.1D) for both mouse NGF and nsNGFI, and none for human NGF. The precursor NGF is usually cleaved at the -1 and -2 sites by furin to become a mature NGF (Heymach *et al*., 1996). Hence it is of interest to determine the number of possible furin-cleavage sites. NsNGFI has only one furin-cleavage site, whereas the mammalian NGFs have two possible sites (Fig. 4.1E). To study the effect of proNGF, the furin-cleavage site for nsNGFI was mutated to impair intracellular proteolysis. A combination of all the possible post-translational modifications is shown in Fig. 4.1F, hence there may be variation in function of proNGF from *Naja sputatrix* as compared to mouse NGF, as there are differences in their post-translational modifications.

4.3 Plasmid construction

Three constructs were created to carry out the study of the pro-domain of sputa NGF and are represented in Fig. 4.2A. In the subsequent experiments, the following terms will be used to describe the different mutants of sputa NGF: **mature NGF** (sequence of full-length sputa NGF with pro-domain and the signal peptide); **pro (R/G) NGF** (sequence of full-length NGF with a mutation at the furin cleavage site with pro-domain and signal peptide) and **pro-domain** (sequence of pro-domain with the signal peptide).

The mature NGF and its corresponding constructs were amplified by PCR from a full-length sputa NGF cDNA sequence. The primers used to amplify these fragments contained restriction sites for *KpnI and XhoI*. The positive clones were then restricted with enzymes (*KpnI* and *XhoI*) and subcloned into pcDNA4 (Fig. 4.2B). The pro(R/G) NGF was created by a cytosine-to-guanine mutation in the sputa NGF
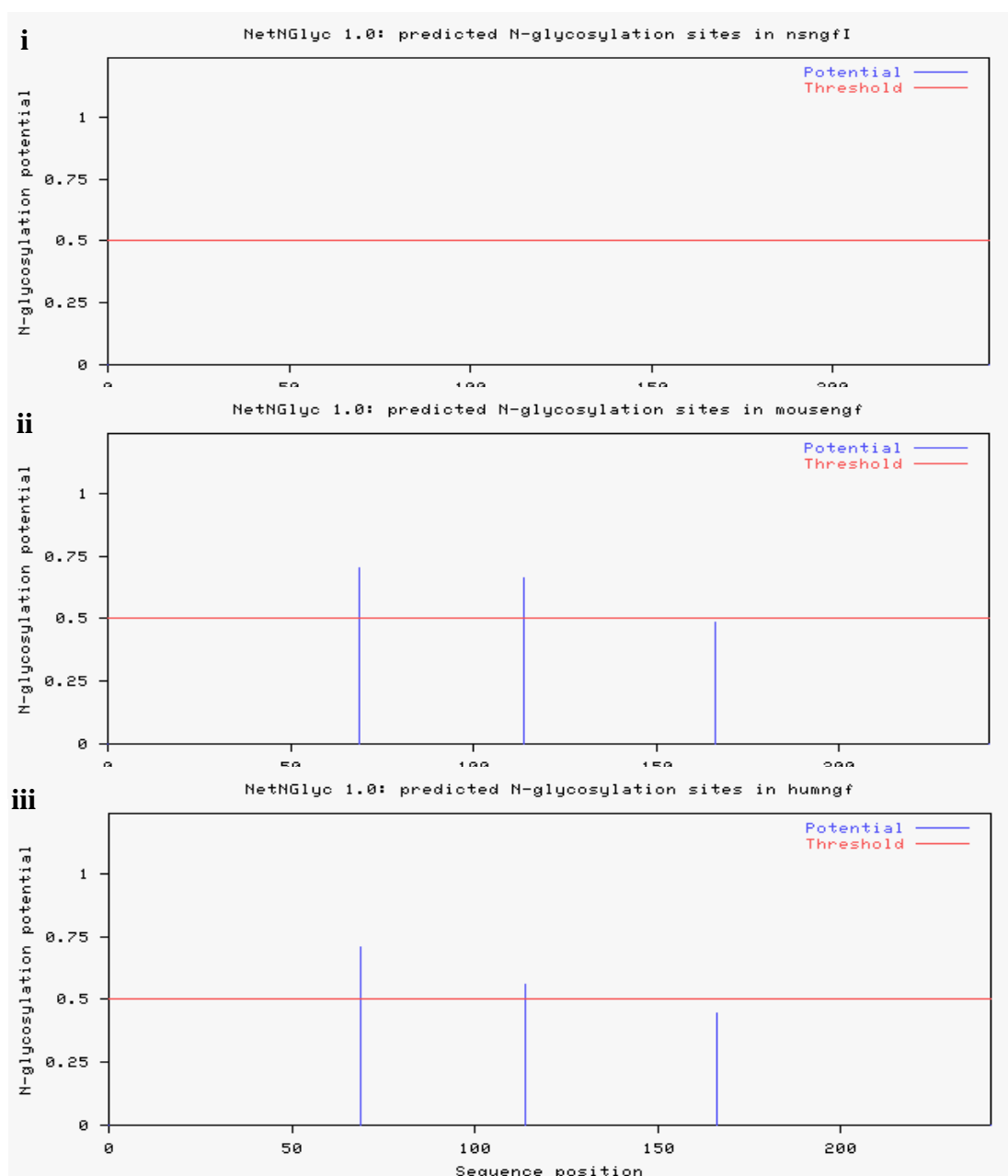
Fig. 4.1C: Prediction of potential N-glycosylation sites by NetNglyc 1.0 server. It was used to predict N-glycosylation sites in human proteins using artificial neural networks that examine the sequence context of Asn-Xaa-Ser/Thr sequences. Result showed that **(i)** *Naja sputatrix* NGF (nsngfI) has none; while both **(ii)** mouse NGF and **(iii)** human NGF (humngf) have two sites.

i

NetOGlyc 3.1: predicted O-glycosylation sites in nsngfI

ii

NetOGlyc 3.1: predicted O-glycosylation sites in mousengf

iii

NetOGlyc 3.1: predicted O-glycosylation sites in humngf
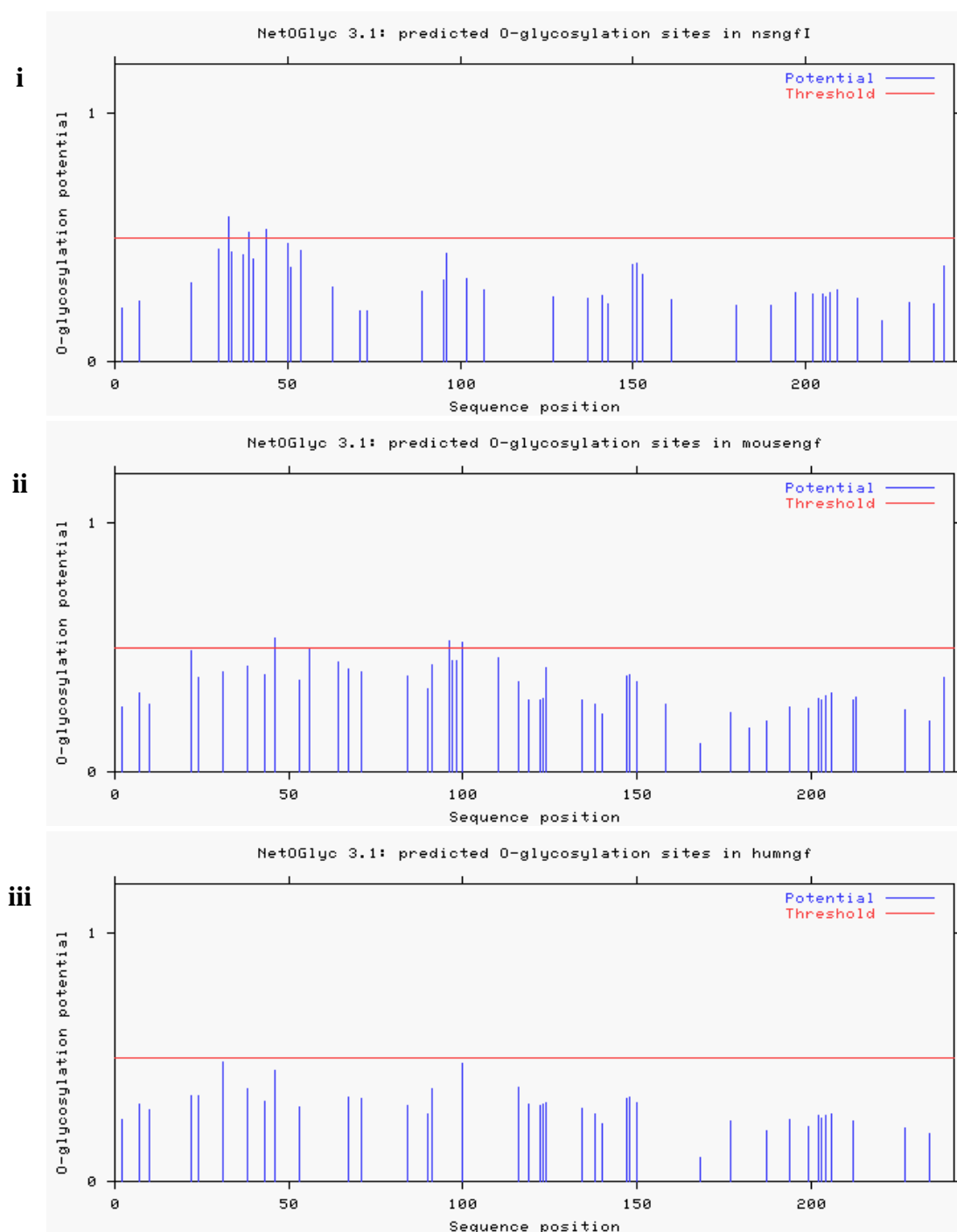
Fig. 4.1D: Prediction of potential O-glycosylation sites by NetOglyc 3.1 server. Its prediction is based on neural network predictions of mucin type GalNAc O-glycosylation sites in mammalian proteins. Results showed that **(i)** *Naja sputatrix* NGF (nsngfI) and **(ii)** mouse NGF have three, while **(iii)** human NGF (humngf) has none.

i

ii

iii
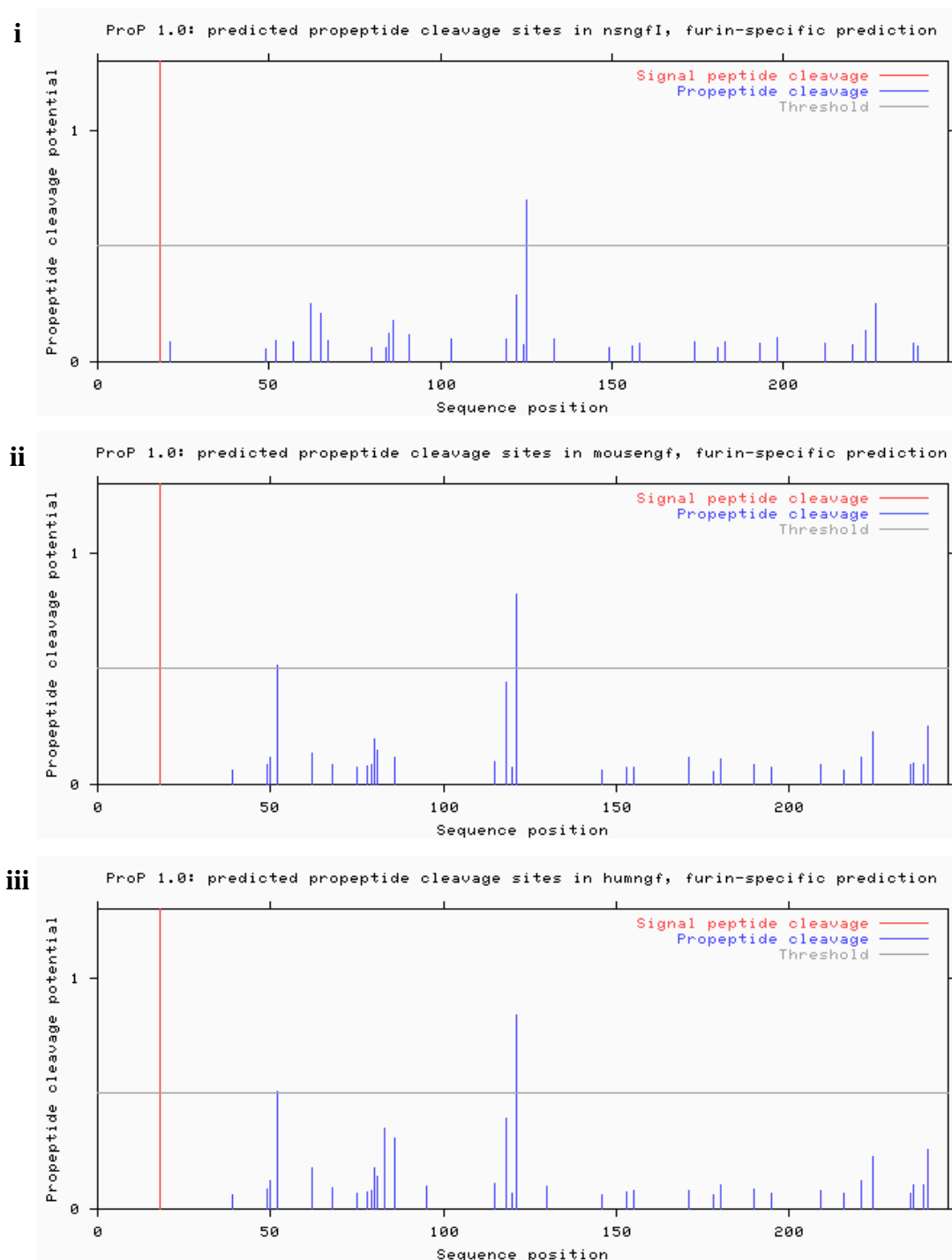
Fig. 4.1E: Prediction of potential furin-cleavage sites by ProP 1.0 server. It predicts arginine and lysine propeptide cleavage sites in eukaryotic protein sequences using an ensemble of neural networks and furin-specific is set as the default. Results showed that the propeptide for **(i)** *Naja sputatrix* NGF (nsngfI) is cleaved at one site while both **(ii)** mouse NGF and **(iii)** human NGF (humngf) are cleaved at two sites.

```
nsngfI      MSMLCYTLIIAFLIGIWAVPKSEDNAPLGSPATSDLSDTSCAQTHEGLKTSRNTDQRHPA
mousengf    MSMLFYTLITAFLIGVQAEPYTDSNVPEGDSVPEAHWTKLQHSLDTALRRARSAPTAPIA
humngf      MSMLFYTLITAFLIGIQAEPHSESNVPAGHTIPQVHWTKLQHSLDTALRRARSAPAAAIA
            **** **** *****: * * ::.*.* *  .   .    . . .*: :*.:    :

nsngfI      PRSQRIKQFGSASNIIVDPKLFQKRRFQSPRVLFSTQPPPLSRDEQSVEFLDNEDA-LNR
mousengf    AR-----VTGQTRNITVDPRLFKKRRLHSPRVLFSTQPPPTSSDTLDLDFQAHGTIPFNR
humngf      AR-----VAGQTRNITVDPRLFKKRRLRSPRVLFSTQPPREAADTQDLDFEVGGAAPFNR
            .:         : ** ***:**:**::**********  : *              :**

nsngfI      NIRAKRET-HPVHNRGEYSVCDSISVWVANKTTATDIKGKPVTVMVDVNLNNHVYKQYFF
mousengf    THRSKRSSTHPVFHMGEFSVCDSVSVWVGDKTTATDIKGKEVTVLAEVNINNSVFRQYFF
humngf      THRSKRSSSHPIFHRGEFSVCDSVSVWVGDKTTATDIKGKEVMVLGEVNINNSVFKQYFF
            .  ::..  **:.: **.*****:*.** ** .****:*: * *: :**::* *::****

nsngfI      ETKCRNPNPVPSGCRGIDSRHWNSYCTTTHTFVKALTMEGNRASWRFIRIDTACVCVISR
mousengf    ETKCRASNPVESGCRGIDSKHWNSYCTTTHTFVKALTTDEKQAAWRFIRIDTACVCVLSR
humngf      ETKCRDPNPVDSGCRGIDSKHWNSYCTTTHTFVKALTMDGKQAAWRFIRIDTACVCVLSR
            ****: .*** : * ***: ******* *.**:**** : ::*:**************:::

nsngfI      KTENF--
mousengf    KATRRG-
humngf      KAVRRA-
            *   .
```

predicted N-glycosylation site
predicted O-glycosylation site
digestion/furin cleavage site
signal peptide

Fig. 4.1F: Clustal alignment of NGFs. NGF protein sequences from *Naja Sputatrix* (nsngfI), mouse NGF (mousengf) and human (humngf) were compared by multiple sequence alignment with the ClustalW program (Thompson *et al*. 1994). The signal peptide region is coloured in green, furin-cleavage sites in red, N-glycosylation in blue and O-glycosylation in purple. The pro-domain region is underlined and the mature peptides are in bold letters. Identical amino acids are shown by (*) and the proteolytic cleavage site (KR) for the mature peptide is indicated in red.

i)

ii)

```
GCTCTGGTGCATACGCTAATGTCCATGCTGTGCTACACTCTGATTATAGCATTTCTGATT - 60
  A   L   V   H   T   L   M   S   M   L   C   Y   T   L   I   I   A   F   L   I
GGCATATGGGCAGTACCAAAGTCTGAAGATAATGCCCCTCTGGGCTCCCCTGCAACGTCT - 120
  G   I   W   A   V   P   K   S   E   D   N   A   P   L   G   S   P   A   T   S
GACCTTTCCGACACCAGCTGTGCTCAAACTCACGAGGGTCTGAAAACATCTCGAAACACA - 180
  D   L   S   D   T   S   C   A   Q   T   H   E   G   L   K   T   S   R   N   T
GATCAGCGCCATCCAGCTCCTAGAAGTCAGAGGATCAAGCAATTTGGATCAGCATCAAAC - 240
  D   Q   R   H   P   A   P   R   S   Q   R   I   K   Q   F   G   S   A   S   N
ATCATTGTGGATCCCAAGCTTTTTCAGAAGAGGCGGTTCCAGTCGCCTCGTGTTCTGTTC - 300
  I   I   V   D   P   K   L   F   Q   K   R   R   F   Q   S   P   R   V   L   F
AGCACTCAGCCCCCACCATTGTCAAGAGATGAGCAAAGTGTGGAGTTCCTGGACAATGAA - 360
  S   T   Q   P   P   P   L   S   R   D   E   Q   S   V   E   F   L   D   N   E
GACGCTCTTAACAGGAATATCCGGGCCAAACGTGAAACTCATCCTGTGCATAACCGAGGG - 420
  D   A   L   N   R   N   I   R   A   K   R   E   T   H   P   V   H   N   R   G
GAATATTCTGTGTGTGACAGTATCAGTGTCTGGGTTGCCAACAAAACCACAGCAACGGAC - 480
  E   Y   S   V   C   D   S   I   S   V   W   V   A   N   K   T   T   A   T   D
ATCAAAGGCAAACCGGTGACTGTGATGGTAGATGTAAATCTTAATAACCATGTCTACAAG - 540
  I   K   G   K   P   V   T   V   M   V   D   V   N   L   N   N   H   V   Y   K
CAGTACTTTTTTGAAACCAAGTGCAGAAATCCAAATCCAGTACCAAGTGGGTGCAGGGGC - 600
  Q   Y   F   F   E   T   K   C   R   N   P   N   P   V   P   S   G   C   R   G
ATTGATTCCAGGCATTGGAATTCTTATTGCACGACAACACACACATTTGTCAAGGCATTA - 660
  I   D   S   R   H   W   N   S   Y   C   T   T   T   H   T   F   V   K   A   L
ACCATGGAAGGCAATCGGGCATCCTGGCGCTTCATTCGGATTGACACTGCCTGTGTGTGC - 720
  T   M   E   G   N   R   A   S   W   R   F   I   R   I   D   T   A   C   V   C
GTAATCAGTAGAAAAACTGAGAACTTCTGATGGACCATTGATTGCTCCAATACTCACTT - 781
  V   I   S   R   K   T   E   N   F   *
```

Fig. 4.2A: Plasmid construction. (i) The signal peptide, pro-domain and active NGF segment are represented by "sp", "pro" and "NGF" respectively. NGF cDNAs are denoted as: **(1) Pro-domain** refers to the sequence from the signal peptide to the pro-domain. **(2) Pro (R/G) NGF** refers to the sequence of full-length NGF with the furin cleavage site mutated from R to G, thereby restricting the release of mature NGF sequence from the pro-domain. **(3) Mature NGF** refers to the sequence of the full length NGF including the furin cleavage site. The three cDNAs were cloned into pcDNA4 plasmids. **(ii)** Deduced amino acids sequence of NsNGFI. The signal peptide region is highlighted in yellow, 'pro' region in green, the furin cleavage site in blue and the remaining sequence refers to the mature NGF
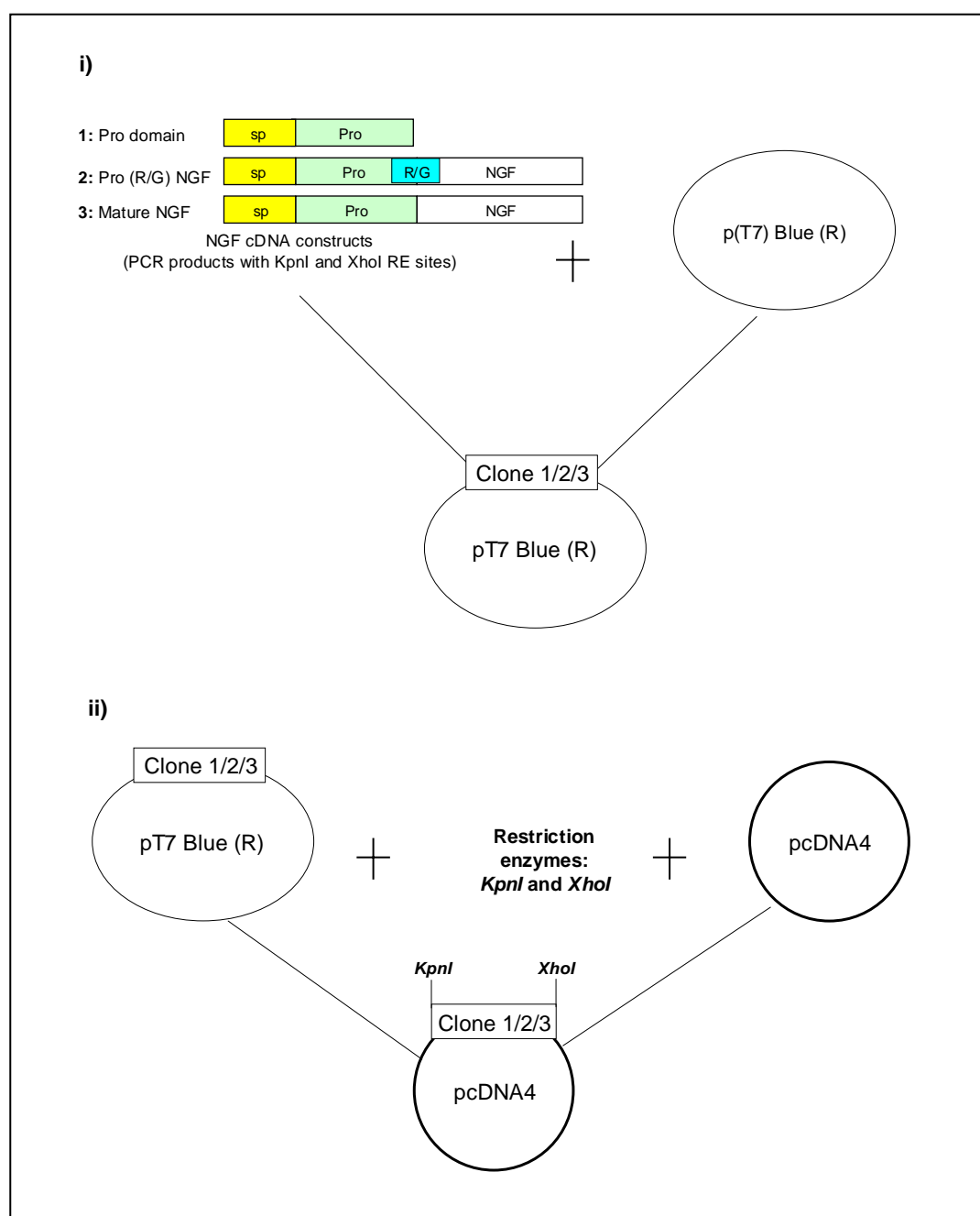
Fig. 4.2B: pcDNA4 constructs. **(i)** The PCR products were cloned into pT7 Blue (R) vector. The three constructs (1-3) were individually cloned into the vector. **(ii)** Each of the constructs (1-3) were restricted by *KpnI* and *XhoI* and individually inserted into expression vector, pcDNA.

incorporated by site-directed mutagenesis of pcDNA-NGF. The mutation was verified by loss of restriction enzyme site and sequencing of both strands.

4.3.1 Tet on/off system in CHO cells

The pcDNA4/TO/myc-His vector contains two tetracycline operator 2 (TetO$_2$) binding sites with the human CMV promoter for the tetracycline-regulated expression of the target gene of interest (Yao *et al*., 1998). The TetO$_2$ sequences serve as binding sites for 4 Tet repressor molecules (comprising two Tet repressor homodimers) and confer tetracycline-reponsiveness to NGF genes. The Tet repressor is expressed from the pcDNA6/TR (Fig. 4.2Cii) plasmid. In the absence of tetracycline, the expression of cloned gene is repressed by the binding of Tet repressor homodimers to the TetO$_2$ sequences. Addition of tetracycline to the cells will remove the Tet repressor homodimer from the CMV/TetO$_2$ promoter in the pcDNA4/TO/myc-His (Fig. 4.2Ci) and allows high level of expression of the NGF genes. As gene regulation can be stringently regulated by the Tet repressor, this system was also used for the investigation of other cytotoxic proteins in eukaryotic cells (Massie *et al*., 1998; Nakagawa *et al*., 1999; Pollock *et al*., 2000).

The three cDNAs recombinant pcDNA4/TO/myc-His-A tetracycline inducible vector constructs containing the mature NGF, pro (R/G) NGF and pro-domain sequences were transfected separately into CHO cells via lipofectamine™ reagent. The pcDNA6/TR plasmid was also transfected.

4.3.2 Generation of stable cell line that is tetracycline-regulated

CHO cells that have successfully incorporated both TO (zeocin-resistant) and TR (blasticidin-resistant) plasmids are able to survive in dual-selective medium. The

i)
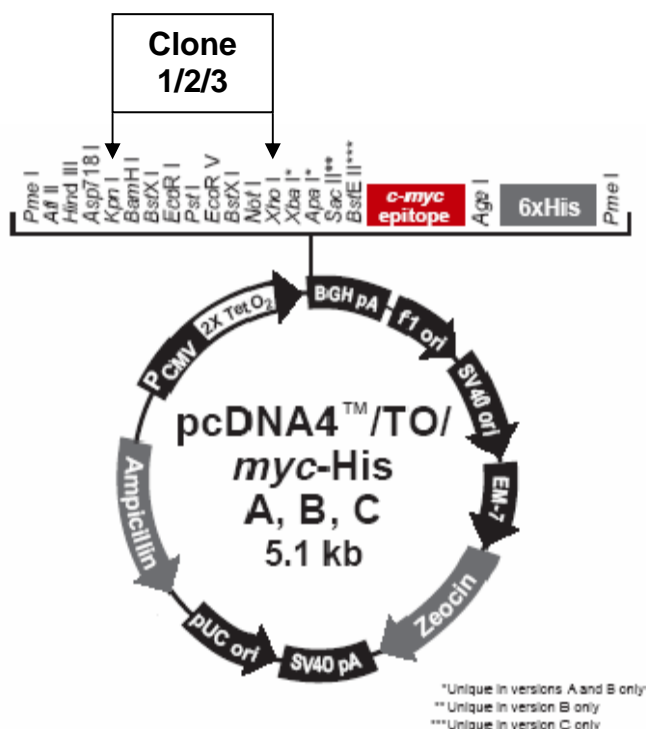
CMV promoter: bases 232-958
Tetracycline operator 2 (2X TetO$_2$)
sequences: bases 820-859
CMV Forward priming site: bases 769-789
Multiple cloning site: bases 968-1089
c-myc epitope: bases 1073-1102
Polyhistidine (6XHis) tag: bases 1118-1135
BGH reverse priming site : bases 1158-1175
BGH polyadenylation sequence : bases 1164-1388
f1 origin : bases 1434-1862
SV40 promoter and origin: bases 2824-2954
pUC origin : bases 3337-4010 (complementary strand)
bla promoter: bases 5016-5114 (complementary strand)
Ampicillin (*bla*) resistance gene: bases 4155-5015 (complementary strand)

ii)
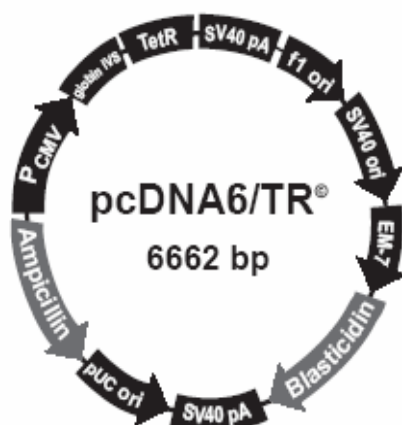
CMV promoter: bases 232-819
Rabbit β-globin intron II (IVS): bases 1028-1600
TetR gene : ases 1684-2340
SV40 early polyadenylation sequence : bases 2346-2477
F1 origin : bases : 2897-3325
SV40 promoter and origin : bases 3335-2675
EM-7 promoter: bases 3715-3781
Blasticidin resistance gene: bases 3782-4180
SV40 early polyadenylation sequence: bases 4338-4468
pUC origin: bases 4851-5521
bla promoter: bases 6521-6625 (complementary strand)
Ampicillin (*bla*) resisitance gene: bases 5666-6526 (complementary strand)

Fig. 4.2C: Plasmids used for Tet on/off system and its detailed description (adapted from Invitrogen Inc, U.S.A). **(i)** The cloning site used in this study for constructs (1-3) is indicated on the Tet-on plasmid: pcDNA4/TO/*myc*-His A. **(ii)** The Tet-off plasmid: pcDNA6/TR.

selective medium was made up of complete DMEM with antibiotics (zeocin; 500µg/ml and blasticidin; 10µg/ml) and used to select for the dual-resistant cells. The medium was changed every 3-4 days until all untransfected control cells were eliminated. About one week after transfection of CHO cells with NGF expression vector and dual selection by antibiotics (blasticidin and zeocin), cells were serially diluted in the zeocin-blasticidine complete DMEM and the remaining surviving cells were reseeded into 96-well plates (~ 1 cell per well). A total of 67 clones for each mature NGF and pro (R/G) NGF, as well as 19 clones for pro-domain were obtained. All the clones were subjected to real-time PCR for quantitation of the plasmid copy number.

4.3.3 Selection of clones with equal copy number

Real-time PCR using specific primers (Table 2.1) to the sputa mature NGF and pro-domain sequences were used to access the plasmid copy number in each clone. The DNA from each clone was isolated and used for real-time PCR by SYBR Green assay. The clones were selected based on their C_T (cycle threshold) values, the lower the C_T, the higher is the copy number. Hence, C_T of 2.0 was selected to normalize the amount of all the three different constructs. Fig. 4.3A shows the results from the 67 clones containing the mature NGF cDNA. Based on the C_T of 2.0, two clones (F1 and F6) were chosen. Fig. 4.3B shows the results obtained from the 67 clones containing the pro(R/G) NGF cDNA. Among these, M36 and M38 were chosen as representatives. Similarly, for pro-domain, of the 19 clones, S2 and S7 were selected with their C_T values closed to 2.0 (Fig. 4.3C). From the standardization assay carried out using known amount of DNA, a C_T value of 2.0 was found to be equivalent to 150ng of DNA.
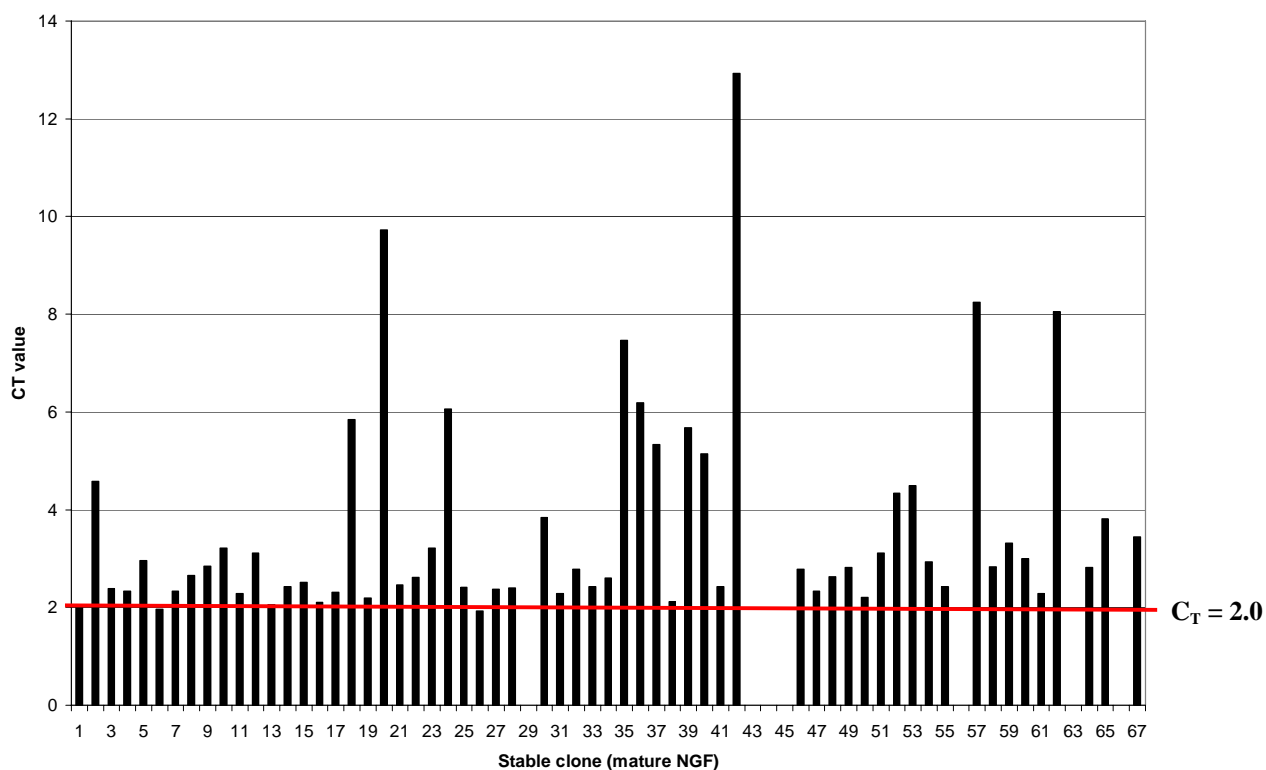
Fig. 4.3A: Quantitation of plasmid copy number by real-time PCR of mature NGF. Real-time PCR using the SYBR Green assay and primers specific for mature NGF was used to quantitate the amount of plasmid. The larger the C_T value, the lesser the copy number of plasmid. The C_T value of 2.0 (red line) was taken to select clones for comparison with the other two constructs. For mature NGF, the clones F1 and F6 were selected for further studies.
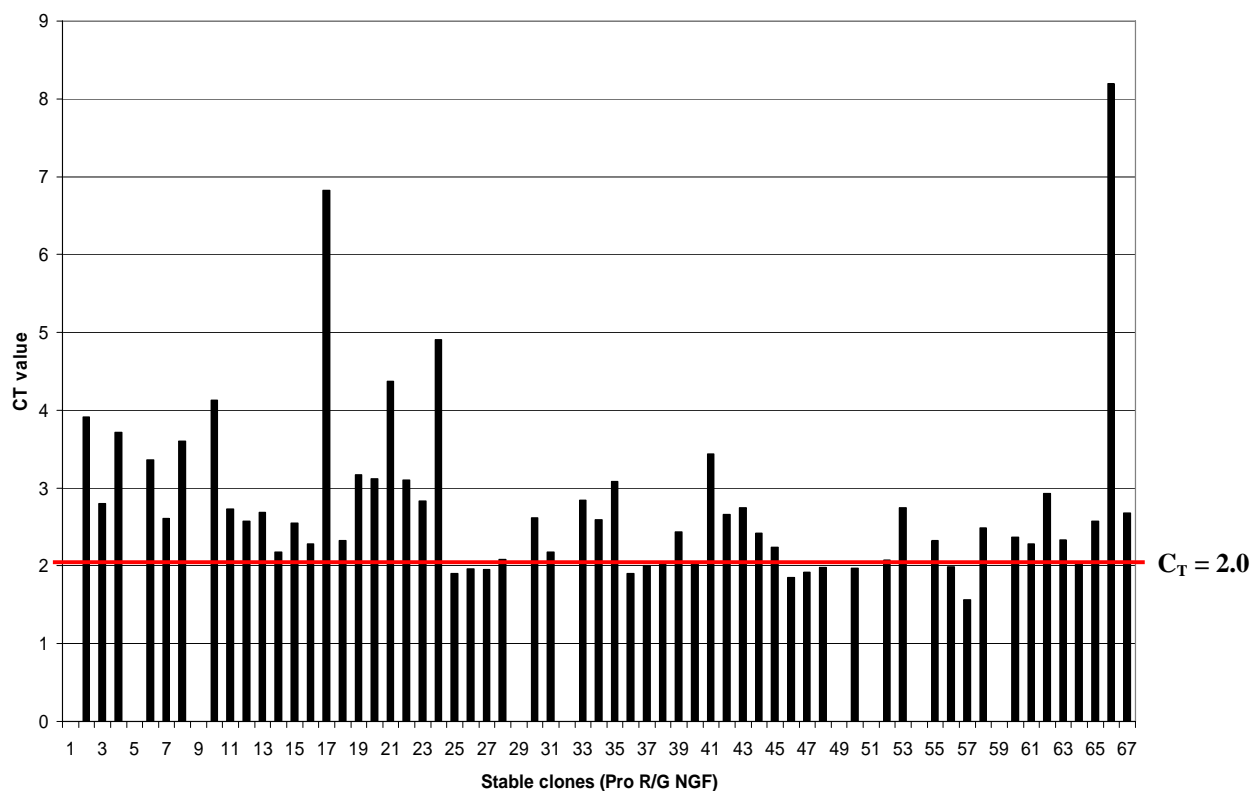
Fig. 4.3B: Quantitation of plasmid copy number by real-time PCR of Pro(R/G) NGF. Pro (R/G) NGF has both pro-domain and mature NGF, so primers specific for mature NGF was used to quantitate the amount of plasmid via real-time PCR (SYBR Green assay). The larger the C_T value, the lesser the copy number of plasmid. The C_T value of 2.0 (red line) was taken to select clones for comparison with the other two constructs. For pro (R/G) NGF, the clones M36 and M38 were selected for further studies.
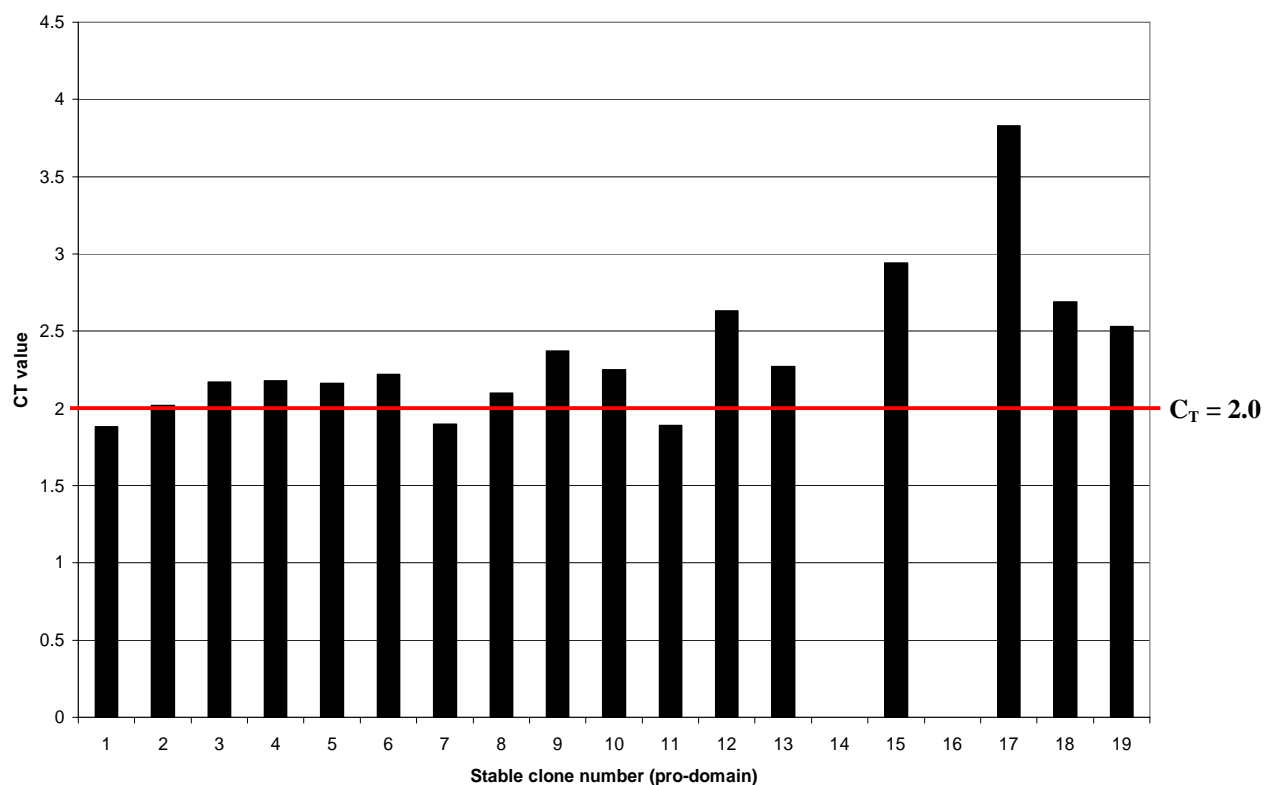
Fig. 4.3C: Quantitation of plasmid copy number by real-time PCR of pro-domain. Primers specific for pro-domain were used to quantitate the amount of plasmid via real-time PCR (SYBR Green assay). The larger the C_T value, the lesser the copy number of plasmid. The C_T value of 2.0 (red line) was taken to select clones for comparison with the other two constructs. For pro-domain, the clones S2 and S7 were selected for further studies.

4.3.4 Expression of recombinant proteins from stable transfectants

Stable clones for the three constructs were selected based on the same plasmid copy number as determined by real-time PCR. Two clones from each construct were chosen; mature NGF (F1 and F6), pro (R/G) NGF (M36 and M38) and pro-domain (S2 and S7). The stable clones were grown in complete DMEM with antibiotics (zeocin; 500µg/ml and blasticidine; 10µg/ml) and protein expression was induced in serum-free DMEM using 1µg/ml tetracycline for 16-18h. The media were collected separately and depleted of cells by centrifugation. In subsequent experiments, the same conditions were used to obtain conditioned CHO media containing either mature NGF, pro (R/G) NGF or pro-domain.

4.4 Neurite outgrowth activity of sputa NGF proteins on PC12 cells

The neurite outgrowth bioassay was done on PC12 cells to determine the different levels of NGF activity between the three constructs. PC12 cells were seeded at a density of 1 X 10^5 cells/well in 24-well plates with 0.5ml of complete DMEM per well. The cells were then subjected to serum starvation for 24 hours prior to treatment with conditioned CHO media containing either mature NGF or pro (R/G) NGF or pro-domain for further 16-18h. Neurite outgrowth (percentage of cells with neurites > 2 x cell's diameter in a representative visual field) was observed in PC12 cells after 16-18 hours incubation. Among these three constructs, only conditioned CHO media expressing mature NGF and pro (R/G) NGF proteins were able to elicit neurites in PC12 cells that were similar to those in exogenous treatments of sputa NGF. However, the extent of neurites was more for the mature NGF compared to the pro (R/G) NGF. The control conditioned media (untransfected CHO cells) did not support any neurite outgrowth, thereby showing that the neurite outgrowth from

the mature NGF and pro (R/G) NGF treatment were due to the presence of recombinant protein overexpressed by CHO stable clones, rather than the conditioned media from CHO cells (Fig. 4.4).

4.4.1 Competitive antibody inhibition

To show the presence of the expressed protein from CHO cells, 2×10^4 PC12 cells were seeded on 96-well plate and treated concurrently with conditioned media from CHO cells containing either mature NGF or pro (R/G) NGF, together with antibodies specific for either sputa NGF (anti-NsNGF) or pro-domain (anti-pro). Cells were incubated for 16-18h at 37°C and observation of the neurite outgrowth was made the next day. In Fig. 4.5A, neurites (representative of neurites indicated with yellow arrows) were observed for treatments with mature and pro (R/G) NGF.

An anti-proNGF antibody, termed as anti-pro in this study, was purchased from Chemicon, Millipore (U.S.A). This antibody was derived from the pro domain of NGF and shown to be proNGF specific and not to deplete the mature NGF (Beattie *et al*., 2002). The other antibody (called anti-NsNGF) was synthesized by directing against a peptide corresponding to the mature domain of the NGF (VMENVNLDNKVYKQKC) in rabbits. The synthesis and production of the polyclonal anti-NsNGF was done by Abgent, Inc (U.S.A.). Treatment with either anti-pro or anti-NsNGF antibodies blocked neurite outgrowth for pro (R/G) NGF, while only anti-NsNGF antibody blocked the neurite outgrowth for mature NGF. Hence, the anti-NsNGF antibody was efficient in blocking neurite outgrowth for both mature and pro (R/G) treatments and anti-pro for pro (R/G) NGF.

Total RNAs from samples treated concurrently with either anti-NsNGF or anti-pro antibodies were isolated and the gene expressions of three genes (TrkA, p75^{NTR} and
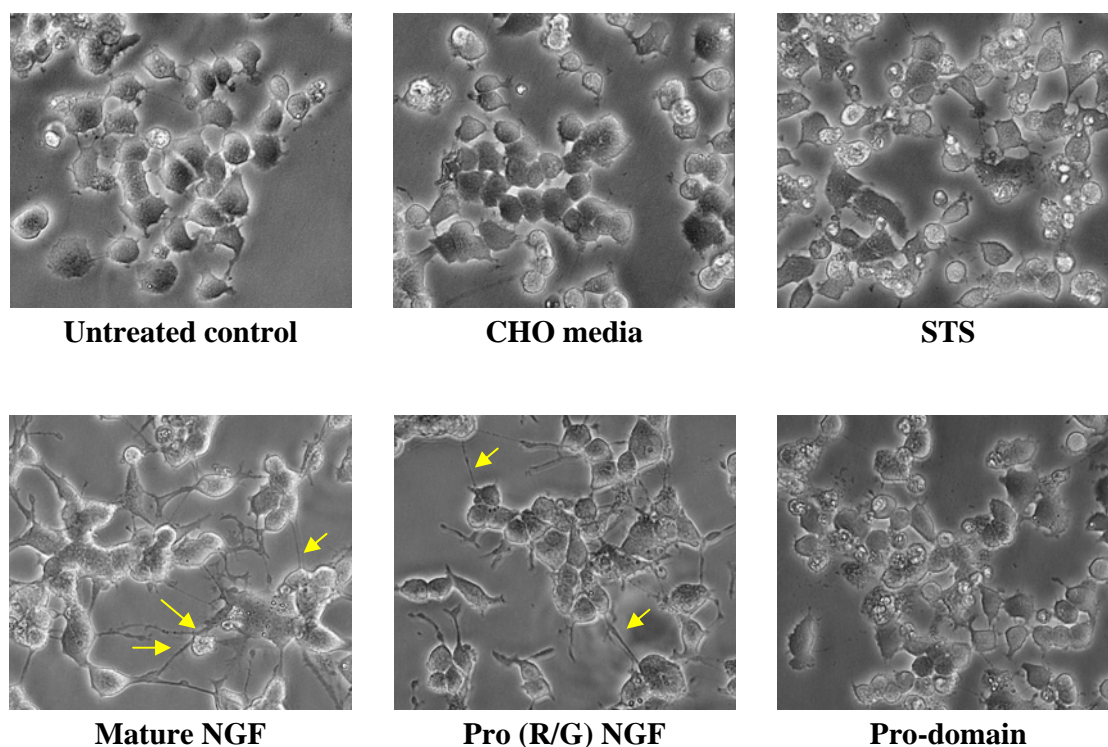
Fig. 4.4: Neurite outgrowth of PC12 cells after incubation with conditioned media from CHO media. All treatments were carried out in serum-free media and incubated for 16-18h. PC12 cells were treated with conditioned CHO media containing mature NGF, pro (R/G) NGF and pro-domain, as well as CHO media alone. PC12 cells were incubated with CHO media alone and no neurites were observed, similar to untreated control. Staurosporine (0.5µM) was used as a marker for apoptosis. Under normal light microscope, treatment with mature NGF and pro (R/G) NGF treatments resulted in neurites formation, while there were more neurites (*yellow arrows*) in mature NGF compared to pro (R/G) NGF. In pro-domain treatment, there were no neurites and cells do not look healthy. Photomicrographs are shown in x200 magnification and representative of 3 independent experiments, performed in triplicates.
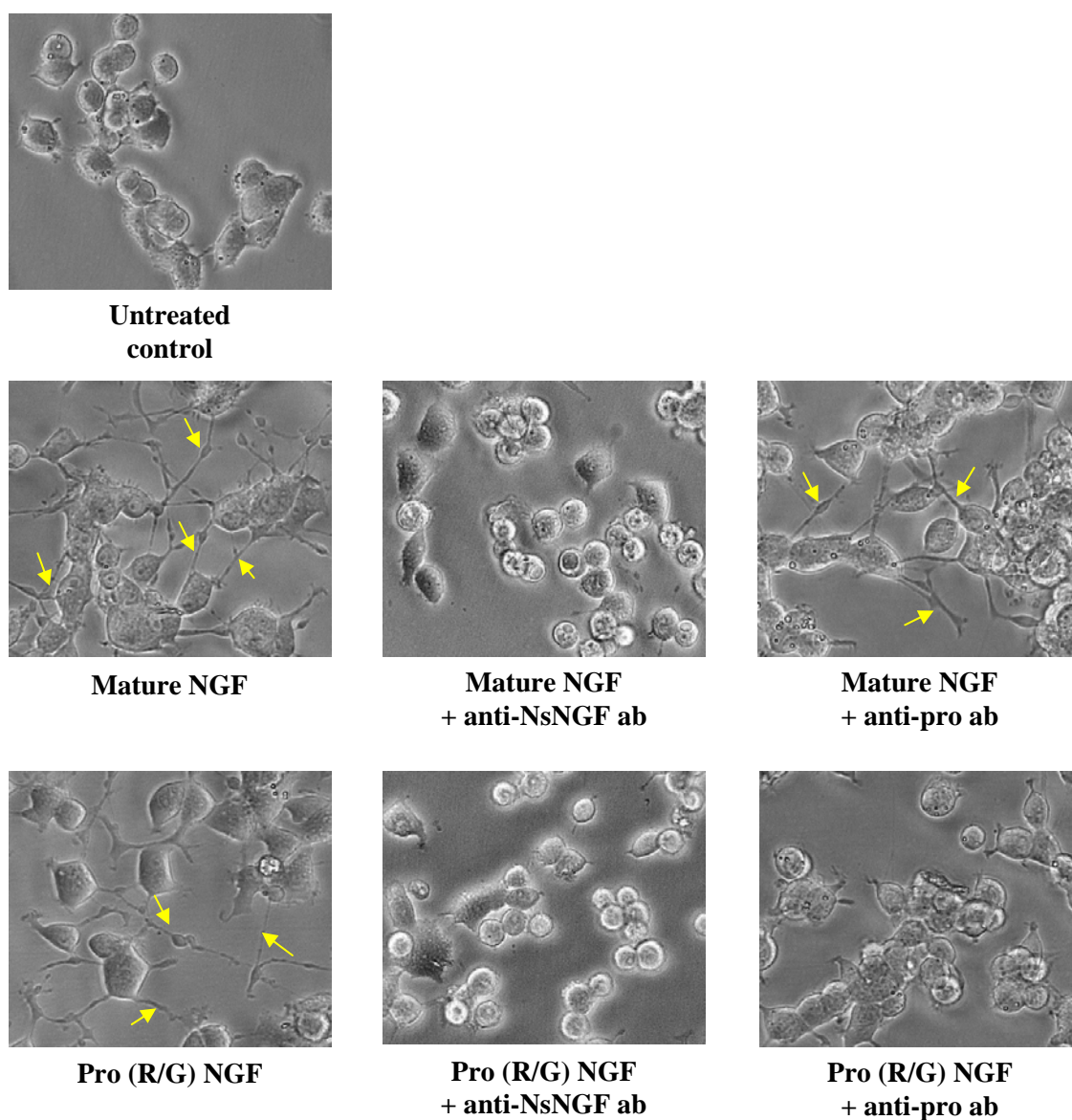
Fig. 4.5A: Competitive antibody inhibition on neurite outgrowth of PC12 cells. PC12 cells were seeded on 96-well plate and exposed to CHO media containing mature NGF (F1 and F6) and pro (R/G) NGF (M36 and M38), together with the anti-NsNGF(~43ug) and anti-pro (1µl/100µl of media) antibodies for 16-18h. Neurites (indicated by *yellow arrows*) were observed the following day. Photomicrographs were obtained at x200 magnification and are representative of 3 independent experiments, performed in triplicate.

sortilin) were quantitated by real-time PCR (Fig. 4.5B). Inhibition by anti-NsNGF antibodies (Fig. 4.5Bi), caused mature NGF's effect on TrkA and p75^{NTR} to be greatly reduced, whereas, pro (R/G) NGF caused an increased in expression for both receptors. Similarly, inhibition by anti-pro antibodies for both pro (R/G) NGF and pro-domain led to an increase in TrkA, p75^{NTR} and sortilin expression (Fig. 4.5Bii). The drastic change in gene expression for these three genes (TrkA, p75^{NTR} and sortilin) by both anti-NsNGF and anti-pro antibodies treatments is possibly due to the efficient blocking of mature NGF, pro (R/G) NGF and pro-domain action.

4.4.2 Analysis of cell death by fluorescence microscopy

PC12 cells treated with conditioned media from CHO cells (mature NGF, pro (R/G) NGF and pro domain) for 16-18h were later stained with three dyes (Annexin V, Ethidium Homodimer III and Hoechst 33342) and staurosporine (STS) at 0.5µM was used as positive marker for apoptosis. One major event in the course of apoptosis is the shift of phosphatidylserine (PS) from the inner to the outer leaflet of the cell membrane. PS externalization can be examined by staining cells green with the FITC-conjugated Annexin V, a protein that binds to PS with high affinity (Thiagarajan and Tait, 1990). Ethidium homodimer III is impermeable to both healthy and apoptotic cells, but will stain necrotic cells with red fluorescence, while Hoechst 33342 will show the condensation of nuclei, a hallmark of apoptosis. Under normal light microscope, cells grown in complete DMEM showed minimal death, however, with basal DMEM (media used for induction of stable CHO cells), there is a basal level of cell death. Treatment with mature NGF and pro (R/G) NGF showed a sharp reduction in cells stained with the Annexin V (green) and Ethidium Homodimer III (red) as compared to the untreated control in serum-free medium.
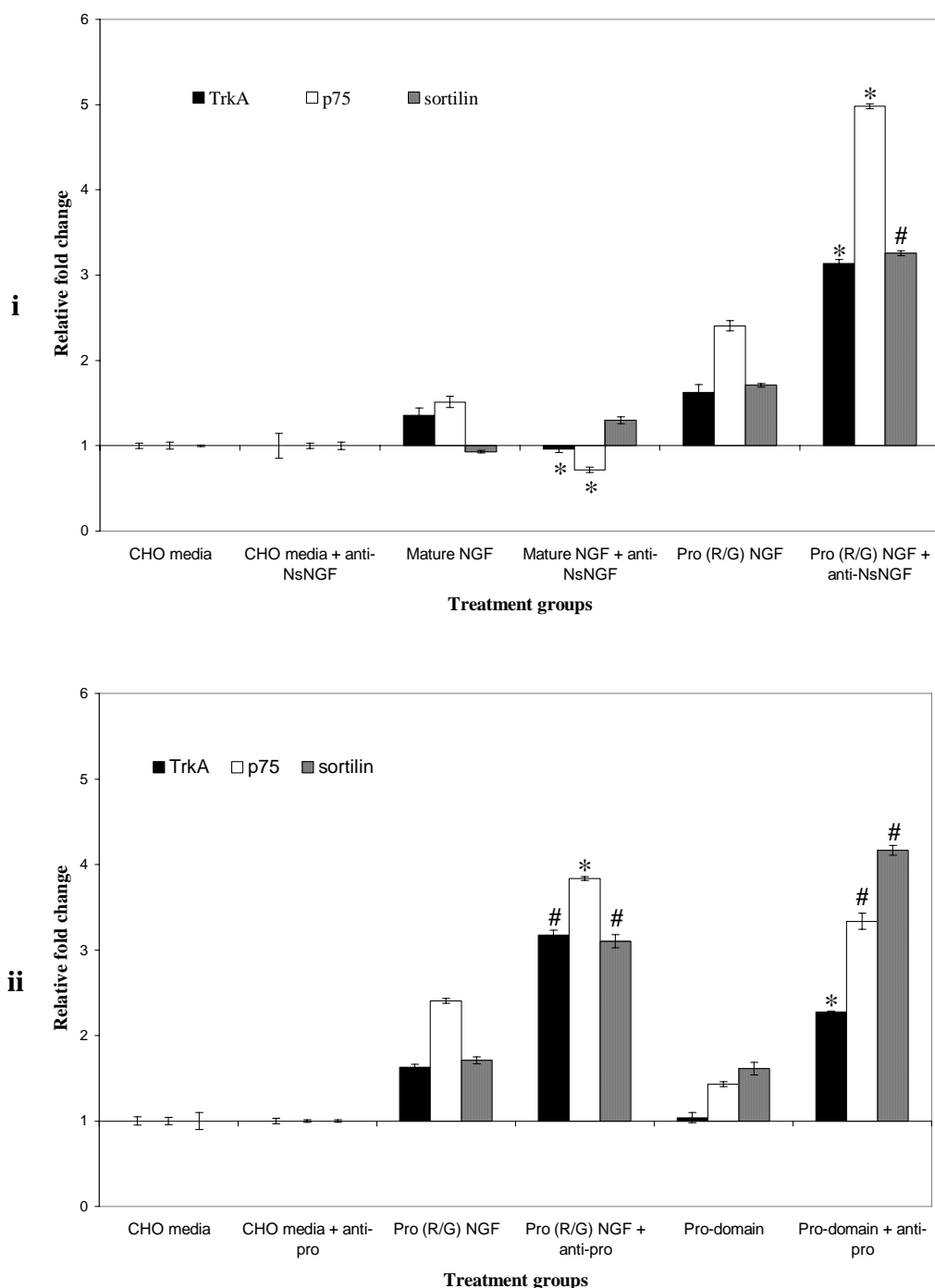
Fig. 4.5B: Quantitative gene analysis using SYBR Green assay. PC12 cells were incubated with **(i)** anti-NsNGF (~43ug) or **(ii)** anti-pro (1µl/100µl of media) antibodies concurrently with conditioned CHO media containing mature NGF, pro (R/G) NGF and pro-domain for 16-18h. Antibodies were added in excess. RNAs from the treated and untreated samples were isolated and used to study the expression of receptor genes: TrkA, p75^{NTR} and sortilin. Values are expressed as ± SEM and *: p-value <0.01 and #: p-value < 0.05 by unpaired Student's *t*-test. The experiments were performed in triplicates.

The treatment with pro-domain showed increased in cell death, with more cells stained green and red (Fig. 4.6A). Cells were also stained with Hoechst 33342 to detect DNA condensation upon apoptosis. With Hoechst staining, both pro-domain and staurosporine treated cells were visibly fragmented and condensed (Fig. 4.6B), leading to a possibility that pro-domain caused cell death by apoptosis.

4.4.3 Assessment of cell death by lactate dehydrogenase (LDH) and caspase assay

LDH assay is based on the measurement of LDH activity released from damaged cells. It is a stable cytoplasmic enzyme present in all cells and rapidly released into cell culture media upon damage to the plasma membrane. It can be used as a measure of cell cytotoxicity. Likewise, caspases are activated by death receptors at the cell surface or by cytochrome c, which leaks into the mitochondria. The cleaved caspase substrates are themselves mediators that activate downstream events in apoptosis. As caspases play a very important role in the apoptotic process, a fluorogenic cleavage assay was used to determine the activity of the specific caspase, caspase-3, after PC12 cells were treated.

In Fig. 4.7Ai, LDH assay showed that PC12 cells treated with conditioned media from CHO cells, in particular, those containing the mature NGF (F1 and F6) and pro (R/G) NGF (M36 and M38) were significantly reduced as compared to control. Conditioned media from CHO cells alone had no significant increase; hence the reduction is solely due to the overexpressed NGF proteins. Pro-domain (S2 and S7) treatment caused a significant increase in both LDH and caspase activities as compared to control (Fig. 4.7A).
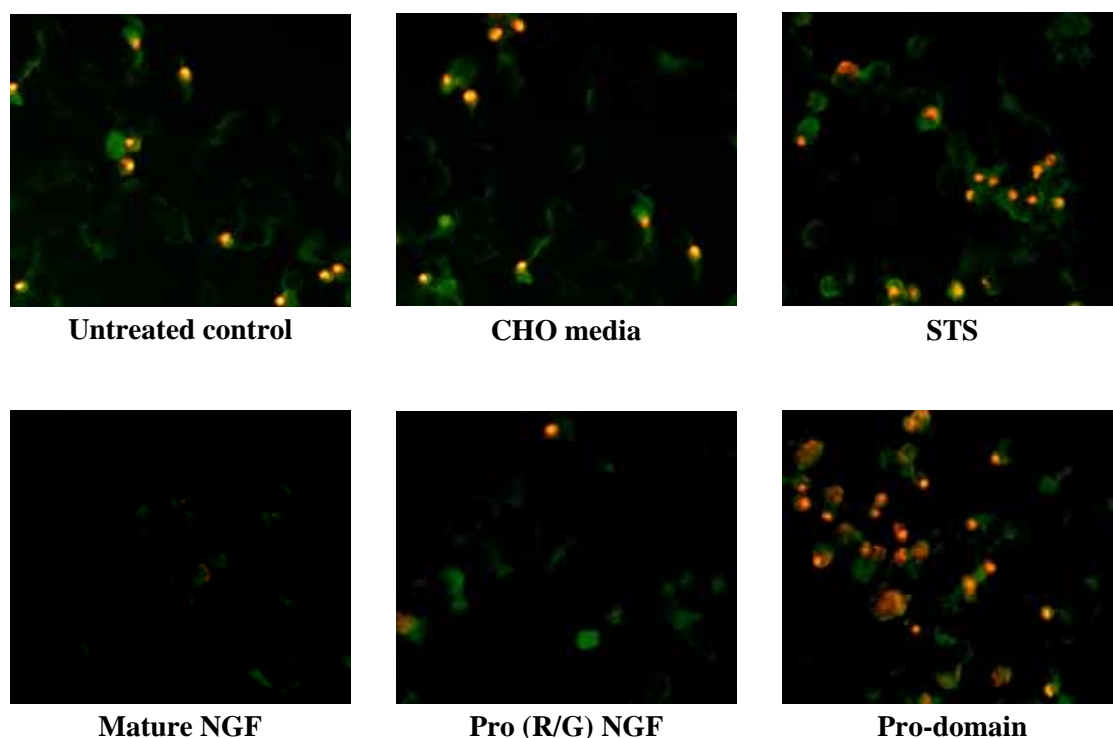
Fig. 4.6A: Annexin V/ Ethidium Homodimer III staining of PC12 cells after incubation with conditioned media from CHO media. After treatment, the PC12 cells were stained with 3 dyes: FITC-conjugated Annexin V (green) and Ethidium Homodimer III (red), and Hoechst 33342 (blue). Results when viewed using green filter. Cells were stained with green and red dyes and staurosporine (0.5μM) was used as a marker for apoptosis. Cells positive for green fluorescence only are apoptotic whilst those that are positive for both green and red are necrotic. Mature NGF and pro (R/G) NGF are able to protect from basal necrosis of the serum-starved PC12 cells when compared to untreated control. Pro-domain and staurosporine-treated cells have both apoptotic and necrotic cells. Photomicrographs are shown in x200 magnification and representative of 3 independent experiments, performed in triplicates.
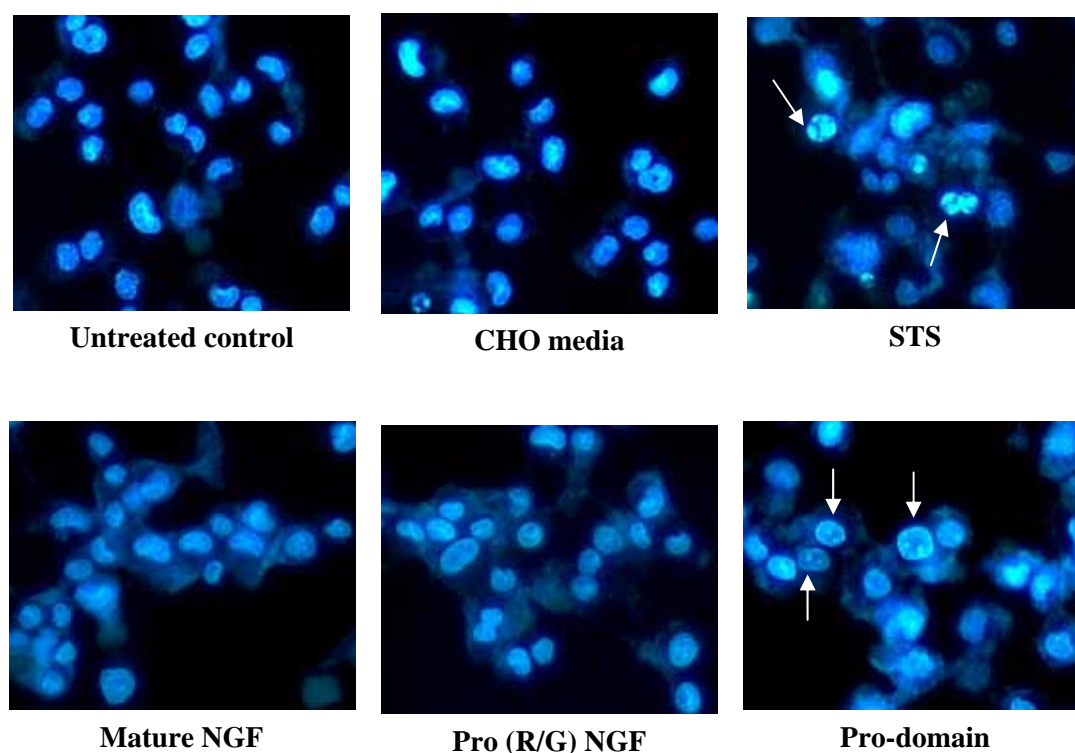
Fig. 4.6B: Hoechst 33342 staining of PC12 cells after incubation with conditioned media from CHO media. After treatment, the PC12 cells were stained with 3 dyes: FITC-conjugated Annexin V (green) and Ethidium Homodimer III (red), and Hoechst 33342 (blue). Results obtained when viewed under blue filter showed no DNA fragmentation for all treatments except for staurosporine (0.5µM) and pro-domain. In these two treatments, the chromatins of the apoptotic cells are visibly fragmented and condensed (white arrows). Photomicrographs are shown in x400 magnification and representative of 3 independent experiments, performed in triplicates.
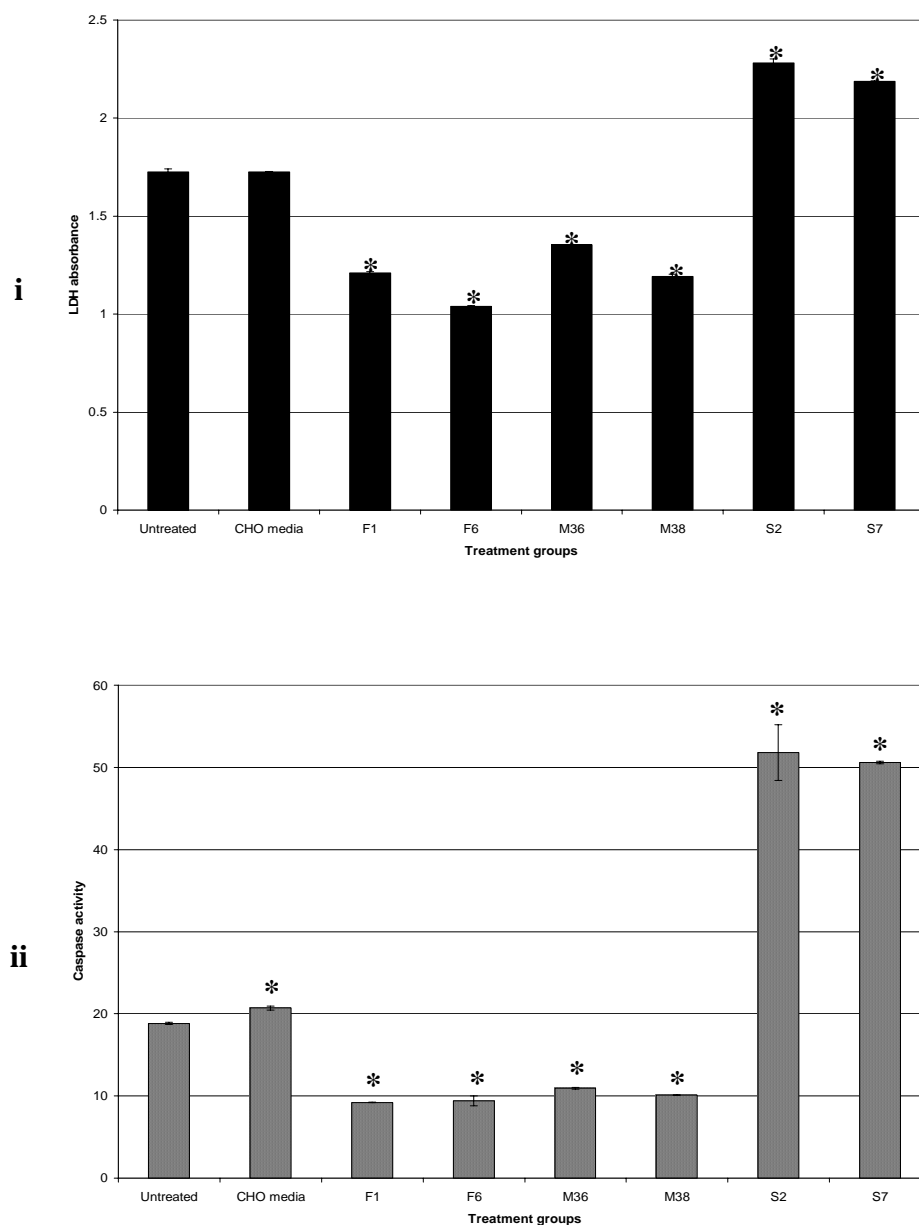
Fig. 4.7A: Determination of cell death using (i) LDH assay and (ii) caspase assay. PC12 cells were assessed for cell death via two assays after treatment (16-18h) with conditioned media from CHO stable transfectants (mature NGF, pro (R/G) NGF and pro-domain). Mature NGF represented by F1 and F6; pro R/G NGF represented by M36 and M38 and pro-domain by S2 and S7. **(i)** LDH assay showed that both mature NGF and pro (R/G) NGF have significantly lower death as compared to pro-domain. ANOVA was done in relation to untreated control and *: p-value < 0.01. **(ii)** Caspase assay showed that both mature NGF and pro (R/G) NGF have significantly lower caspase activity as compared to pro-domain. ANOVA was done in relation to untreated control and *: p-value < 0.01.

In addition, the decrease in caspase activity for both mature NGF (F1 and F6) and pro NGF (R/G) NGF were observed to be 2-fold lower than the control, while that of pro-domain (S2 and S7) was higher than the control (Fig. 4.7Aii). Based on the results obtained from LDH, caspase assay and Hoechst staining (fluorescent microscopy), pro-domain was shown to cause cell death via apoptosis.

4.4.4 Detection of oligonucleosomal DNA fragmentation

In addition to the previous experiments, one of the hallmarks of apoptosis is the internucleosomal cleavage of DNA (Wyllie, 1980). PC12 cells were treated with conditioned media from CHO containing either mature NGF (F1 and F6) or pro (R/G) NGF (M36 and M38) or pro-domain (S2 and S7) for 16-18h and DNA extracted for determination of the occurrence of DNA fragmentation. Cells treated with staurosporine (0.5µM and 1µM) for 16-18h were used as positive controls. Oligonucleosomal fragmentation was observed in cells treated with pro-domain (S2 and S7) and STS (0.5µM and 1µM). In addition, cells treated with CHO media alone had a slight amount of fragmentation, most probably due to the serum-free media. On the contrary, no DNA fragmentation was observed in mature NGF (F1 and F6) and pro (R/G) NGF (M36 and M38; Fig. 4.7B). Hence, pro-domain caused DNA fragmentation by apoptosis; while both mature NGF and pro (R/G) protected the cells from the slight apoptosis due to the serum-free medium.

4.4.5 Inhibition by caspase-3-specific inhibitor

Since pro-domain caused cell death by apoptosis, it was of interest to determine whether it was mediated by caspase. PC12 cells were pretreated with 100µM of DEVD-CHO (caspase-3-specific inhibitor) for 2h (Margarita *et al.*, 1998). This was
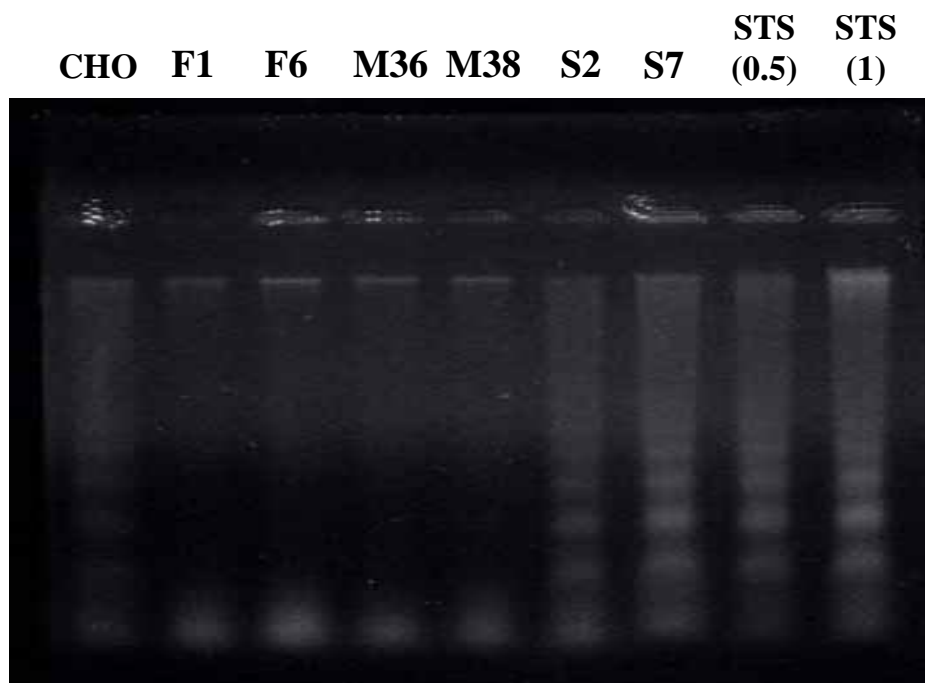
Fig. 4.7B: Treatment with CHO media containing mature NGF/pro (R/G) NGF/ pro-domain or STS treatment. PC12 cells were seeded in 6-well plates and exposed to CHO media containing mature NGF (F1 and F6) or pro (R/G) NGF (M36 and M38) or pro-domain (S2 or S7) or STS (0.5µM or 1µM) at 37°C for 16-18h. The control was cells in CHO media alone. DNA was isolated from the cells and electrophoresed on a 1% agarose gel. The DNA from S2, S7 and STS (0.5µM and 1µM) displayed a 'ladder' of short fragments, indicating that internucleosomal cleavage had taken place. There is a less intense 'ladder' in the CHO media, possibly due to it being in serum-free media. In contrast, cells treated with F1, F6, M36 and M38 appeared as a 'smear' with no visible fragmentation. Results are representative of 3 independent experiments, performed in duplicate.

followed by treatment with conditioned media from CHO containing pro-domain (S2 and S7) and staurosporine (0.5μM) as a positive control. Fig. 4.7Ci showed that there was a significant decrease in LDH activity when incubated with inhibitor prior to treatment with both pro-domains and staurosporine (0.5μM). However, the reduction varied between pro-domains and staurosporine. Concurrent treatment with staurosporine and inhibitor had a 19% reduction of caspase activity, while S2 and S7 had 10.3% and 14.7% reduction respectively. Similarly, the same trend was observed for caspase assay (Fig. 4.7Cii). The percentage of caspase-related death was inhibited by 64.2% for staurosporine, while S2 and S7 had 26% and 36.4% respectively. Hence, pro-domain caused apoptosis via caspase-mediated cell death.

4.4.6 Real-time PCR analysis

PC12 cells were treated with CHO conditioned media containing mature NGF, pro (R/G) NGF and pro-domain for 16-18h. The total RNA was extracted and gene expression pattern of four genes (TrkA, p75^{NTR}, sortilin and bcl-2) were quantitated by real-time PCR (Fig. 4.8A). Neurotrophin precursors (e.g. NGF and BDNF) are known to induce neuronal apoptosis via activation of a receptor complex of p75^{NTR} and sortilin (Kaplan and Miller, 2004). Hence, apart from the NGF receptors (TrkA and p75^{NTR}), sortilin and bcl-2 (pro-survival gene) were also investigated. TrkA and p75^{NTR} were upregulated upon treatment with both mature and pro (R/G) NGFs, while downregulated with pro-domain and staurosporine treatments. Bcl-2, was only upregulated for both pro-domain and staurosporine treatment. Hence, these two treatments may have caused cell death, leading to a compensatory mechanism for the cell to survive. Sortilin gene was downregulated in all treatments and all results were normalized to the 18S gene (internal control).
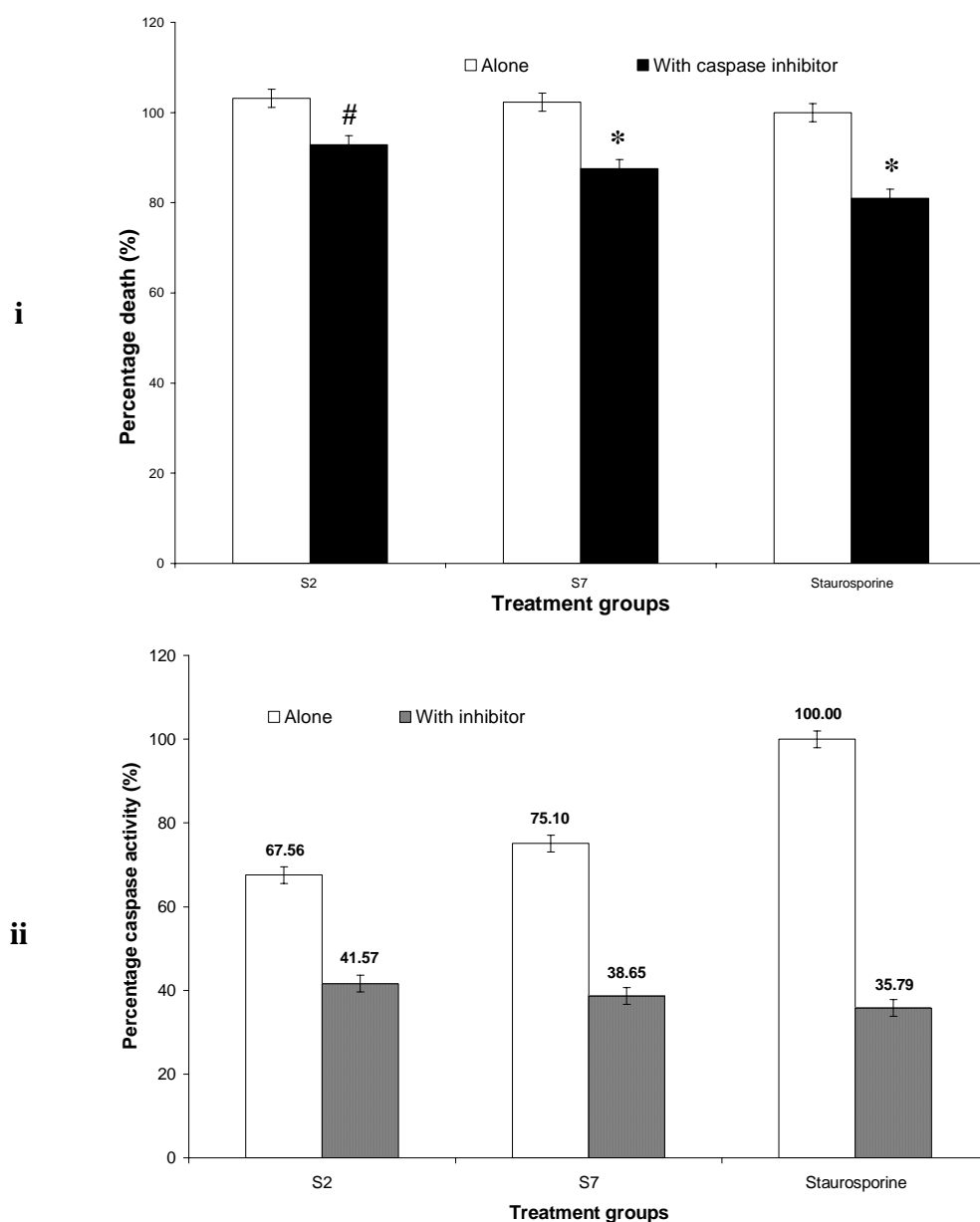
Fig. 4.7C: Inhibition by caspase-specific inhibitor (DEVD-CHO). PC12 cells were pretreated with caspase3-specific inhibitor (DEVD-CHO) at 100μM for 2 hours prior to treatment with conditioned CHO media from pro-domain (S2 and S7) for 16-18h, staurosporine (0.5μM) was used as a positive control. The values are expressed as a percentage to staurosporine-treated ± SEM and data points are means of 3 independent experiments, performed in triplicates. **(i) LDH assay** showed both pro-domain (S2 and S7) are decreased when treated concurrently with DEVD-CHO with #: $p < 0.05$ and *: $p < 0.01$ by unpaired Student's *t*-test. **(ii) Caspase assay** showed a greater decrease than LDH in death due to pro-domain (S2 and S7) on PC12 cells when treated concurrently with DEVD-CHO. P-value in relation to without inhibitor is less than 0.01 for all by unpaired Student's *t*-test.
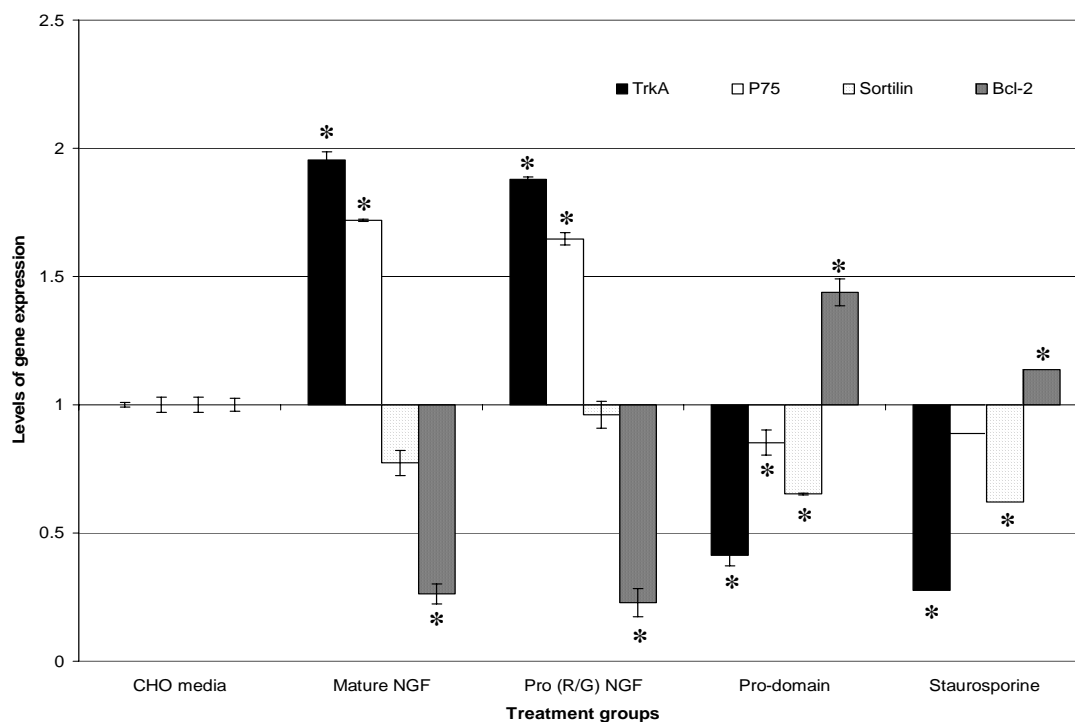
Fig. 4.8A: Quantitative real-time PCR analysis via SYBR Green assay. The RNA from the treated PC12 cells was used to study the expression of four genes: TrkA, p75[NTR], Sortilin and Bcl-2. PC12 cells were treated with either conditioned media from CHO cells (mature NGF, pro (R/G) NGF and pro-domain) individually or staurosporine (0.5µM) for 16-18h. Values are expressed as ± SEM, experiments performed in triplicates and * p<0.01 by unpaired Student's *t*-test.

4.4.7 Western blot analysis of NGF receptor proteins

Western blot analysis of PC12 cells treated individually with CHO conditioned media containing mature NGF, pro (R/G) NGF or pro-domain for 15min showed TrkA to be highly phosphorylated with mature NGF, followed by pro (R/G) NGF and pro-domain (Fig. 4.8B). Recombinant sputa NGF (200ng/ml) was used as a positive control. Hence, both mature and pro (R/G) NGFs caused an activation of TrkA receptors in a similar manner as sputa NGF, with an increased production of the mature gp140^{trkA} receptors. Apart from this, western blot analysis was done on PC12 cells treated individually with CHO conditioned media containing mature NGF, pro (R/G) NGF or pro-domain for 16-18h.

Treatment with mature NGF caused a greater increase in both mature (gp140^{trkA}) and precursor (gp110^{trkA}) TrkA, when compared to pro (R/G) NGF (Fig. 4.8C). However, mature NGF treatment caused a lesser increase in p75^{NTR} expression when compared to pro (R/G) NGF treatment. Treatment with pro-domain caused an increase in p75^{NTR} protein and minimal level of TrkA (gp110 and gp140). The presence of TrkA will activate the pro-survival pathway and together with p75^{NTR} form the high-affinity complex with NGF (Roux and Barker, 2002). However, once it is absent or minimal, the apoptotic pathway of p75^{NTR} will predominate, as observed in pro-domain treatment. Sortilin expression is relatively the same across the three treatments (mature NGF, pro (R/G) NGF and pro-domain). Beta-actin was used an internal control to show equal loading of samples (Fig. 4.8C). In addition, the same trend was observed and confirmed by real-time PCR (Fig. 4.8A).
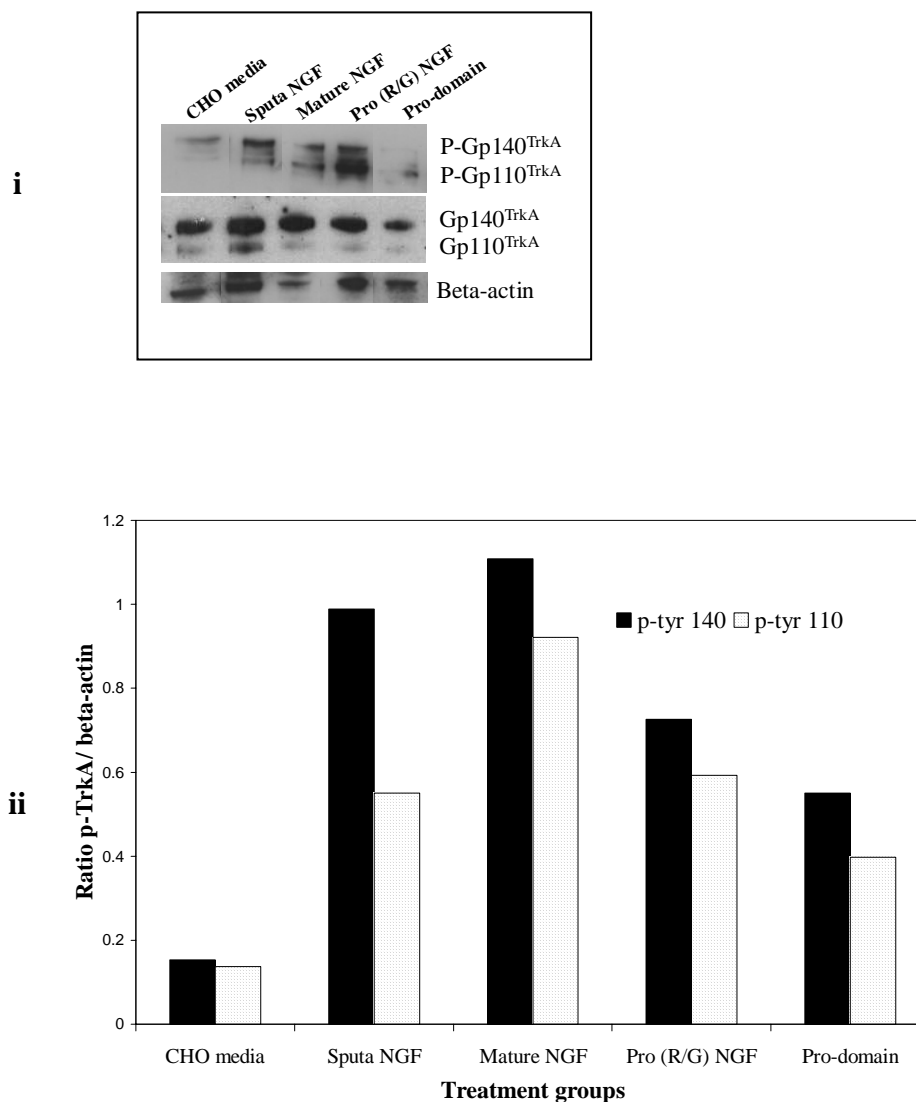
Fig. 4.8B: Activation of TrkA receptor as determined by western blot analysis.
PC12 cells were treated with conditioned CHO media containing mature NGF, pro
(R/G) NGF and pro-domain, as well as a positive control: sputa NGF (200ng/ml) for
15min and the total protein extracted. Equal amount of protein from each treatment
was separated on a 10% SDS/PAGE gel and subsequently blotted onto nitrocellulose
membrane. **(i)** Phosphorylated TrkA (gp140 and gp110) were detected using
monoclonal anti-phosphotyrosine antibody. The same membrane was stripped and
probed with anti-TrkA and anti-beta-actin antibodies. **(ii)** Ratios of the
phosphorylated TrkA and beta-actin were measured by densitometry.

i

ii
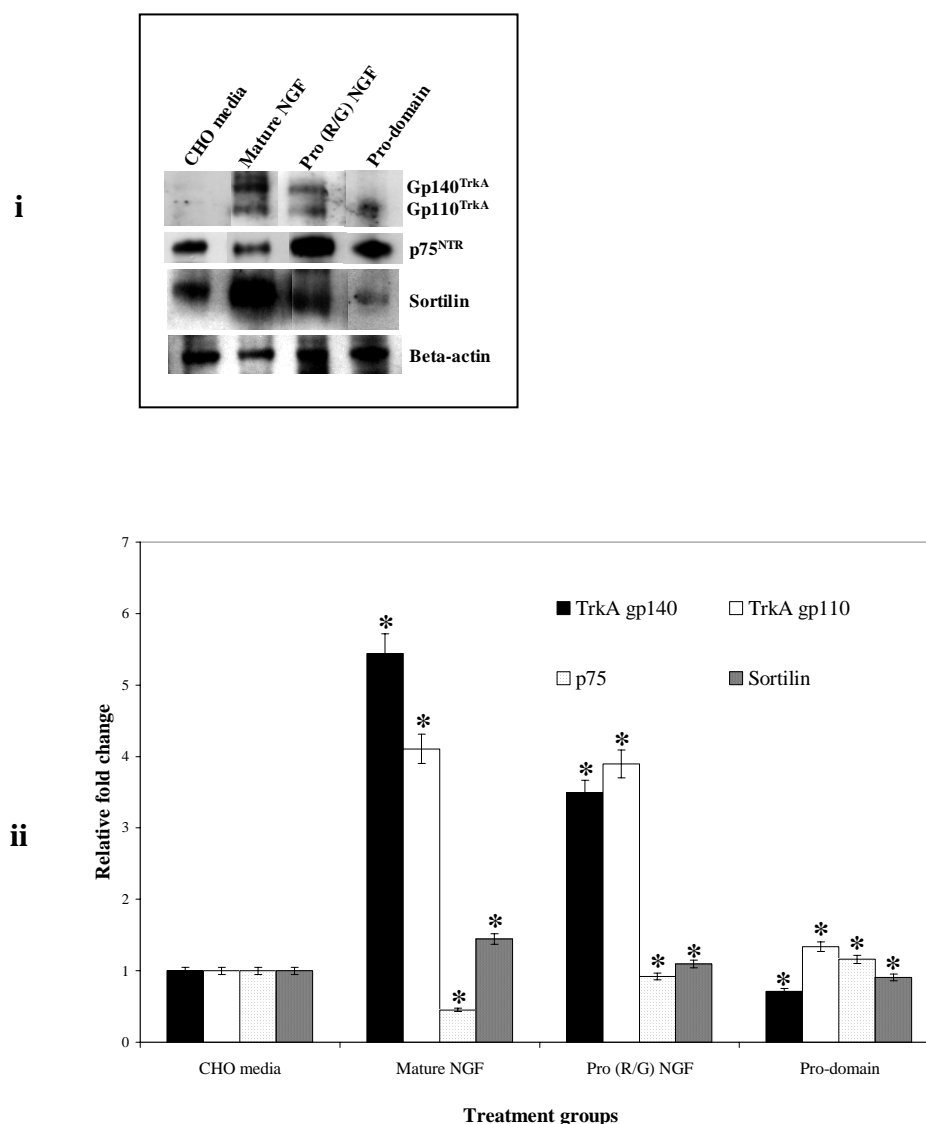
Fig. 4.8C: Receptor protein expressions after treatment with conditioned CHO media containing mature NGF, pro (R/G) NGF and pro-domain. PC12 cells were treated for 16-18h and the total protein extracted. Equal amount of protein were separated on a 10% SDS/PAGE gel and subsequently blotted onto nitrocellulose membrane. **(i)** Membrane was probed with anti-TrkA, anti-p75 and beta-actin antibodies. It was later stripped and probed with anti-sortilin antibodies as it is about 100kDa, similar to TrkA (110kDa). Beta-actin was used to as a internal control. **(ii)** Relative fold change in protein expression compared to cell treated with CHO media alone were measured by by densitometry. Western blot analysis showed that pro-domain caused a significant reduction in TrkA (gp110 and 140). Values are expressed as $\pm$ SEM and *: p-value < 0.01 by unpaired Student's *t*-test.

4.4.8 Specific inhibition of receptor proteins by antibodies

PC12 cells were incubated with antibodies specific to TrkA, p75^{NTR} and sortilin separately for 4h at 4°C prior to treatment with condition CHO media containing mature NGF or pro (R/G) NGF or pro-domain for a further 16-18h at 37°C. Concentration of antibodies for TrkA and p75^{NTR} was 2µg/ml, while that for sortilin was 1µg/ml. The following day, the number of neurites was counted and both MTT and LDH assays performed. Under normal conditions, only mature NGF and pro (R/G) NGF would produce neurites and pro (R/G) NGF produced 2-fold less than mature NGF (Fig. 4.9A). In addition, inhibition by both TrkA and p75^{NTR} antibodies reduced the number of neurites drastically for both mature and pro (R/G) NGFs treatments. A combination of antibodies to both p75^{NTR} and sortilin also caused a reduction in the number of neurites (Fig. 4.9A). Inhibition of sortilin receptors alone has no effect on neurite outgrowth for both mature and pro (R/G) NGFs treatments. MTT viability assay was used to determine the effect of both mature and pro (R/G) NGFs (pro-survival) with antibodies, while LDH assay for pro-domain (apoptotic).

LDH assay showed that concurrent treatment with all the three antibodies (anti-TrkA, p75^{NTR} and sortlin) and pro-domain led to a decrease in the cytotoxic effect (Fig. 4.9B). MTT assay showed that inhibition by anti-TrkA did not cause any significant change for all treatments; however, anti-p75^{NTR} caused a reduction in cell viability in both mature and pro (R/G) NGFs treatments (Fig. 4.9C).

4.5 Oxygen-glucose deprivation (OGD) of PC12 cells

Ischemic stroke causes a significant amount of cell damage resulting from an insufficient supply of glucose and oxygen to brain tissue (Lipton, 1999). PC12 cells have been extensively used as an *in vitro* system to study the mechanisms of
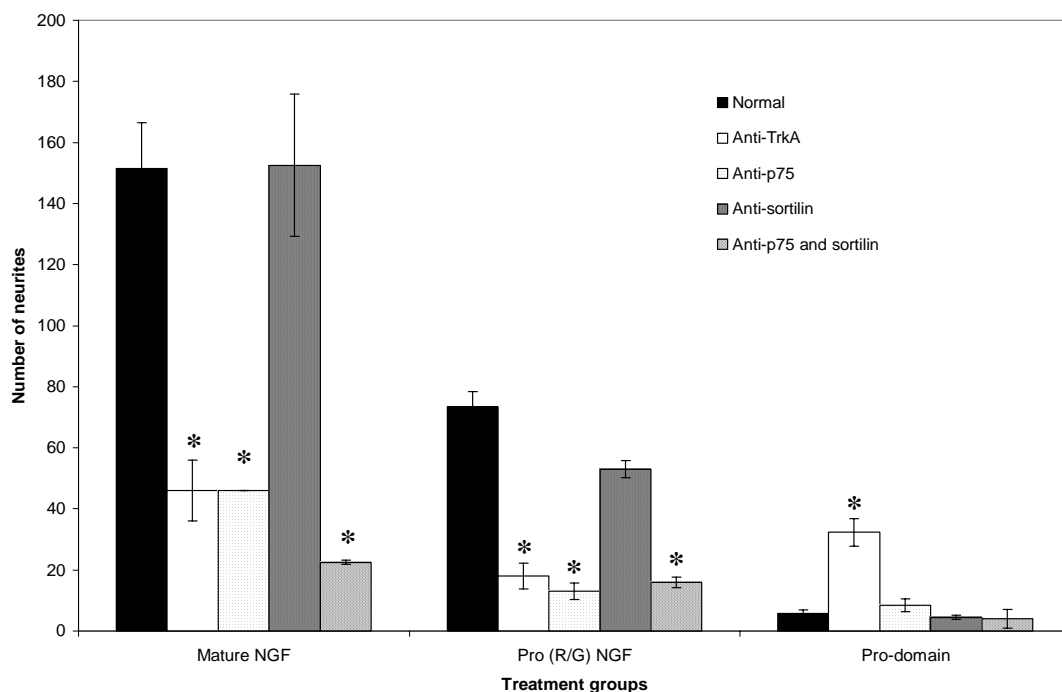
Fig. 4.9A: Inhibition of receptors by specific antibodies and its effect on neurite outgrowth. PC 12 cells were incubated with anti-TrkA (2µg/ml), anti-p75^{NTR} (2µg/ml) and anti-sortilin (1µg/ml) antibodies separately for 4h at 4°C. Antibodies were used in excess. In addition, a combination of anti-p75^{NTR} and anti-sortilin was used. This was followed by incubation with conditioned CHO media containing mature NGF, pro (R/G) NGF and pro-domain for 24h at 37°C. Both mature and pro (R/G) NGFs have their number of neurites significantly reduced upon addition of antibodies specific to p75^{NTR} and TrkA. ANOVA was done in relation to the untreated control and *: p-value < 0.01.
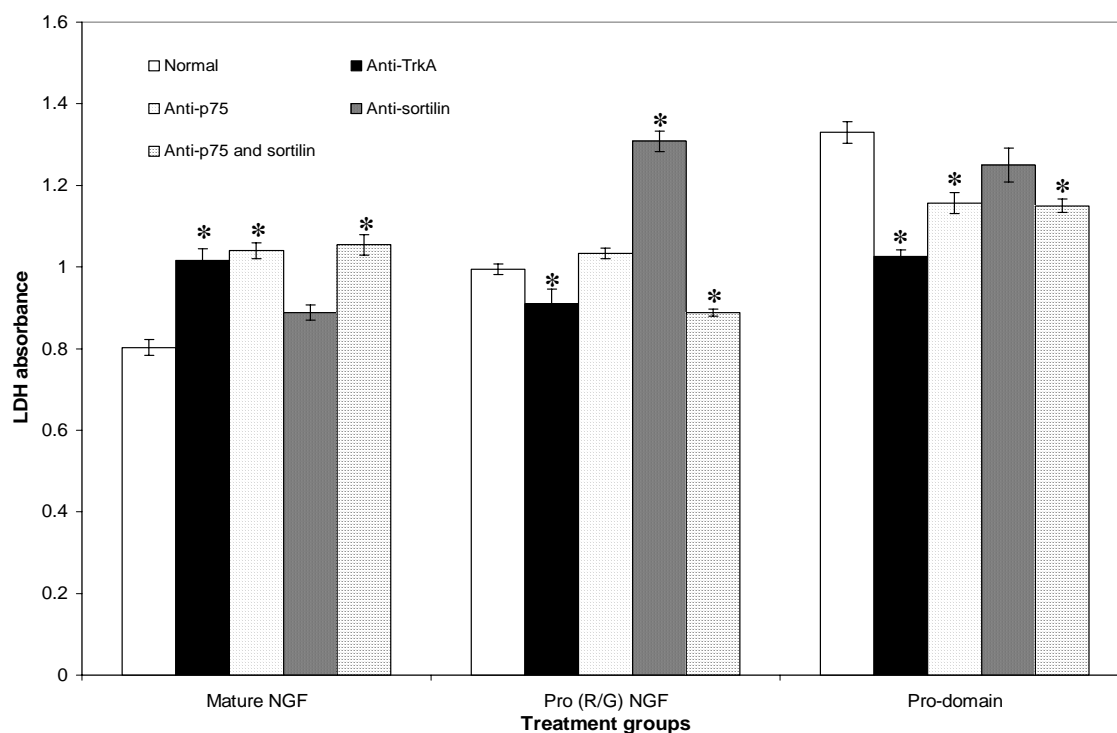
Fig. 4.9B: Inhibition of receptors by specific antibodies and its effect on cell death by LDH assay. PC 12 cells were incubated with anti-TrkA (2µg/ml), anti-p75[NTR] (2µg/ml) and anti-sortilin (1µg/ml) antibodies separately for 4h at 4°C. Antibodies were used in excess. In addition, a combination of anti-p75[NTR] and anti-sortilin was used. This was followed by incubation with conditioned CHO media containing mature NGF, pro (R/G) NGF and pro-domain for 24h at 37°C. Results are representative of triplicate experiments and expressed as LDH absorbance . ANOVA was done in relation to the untreated control and *: p-value < 0.01.
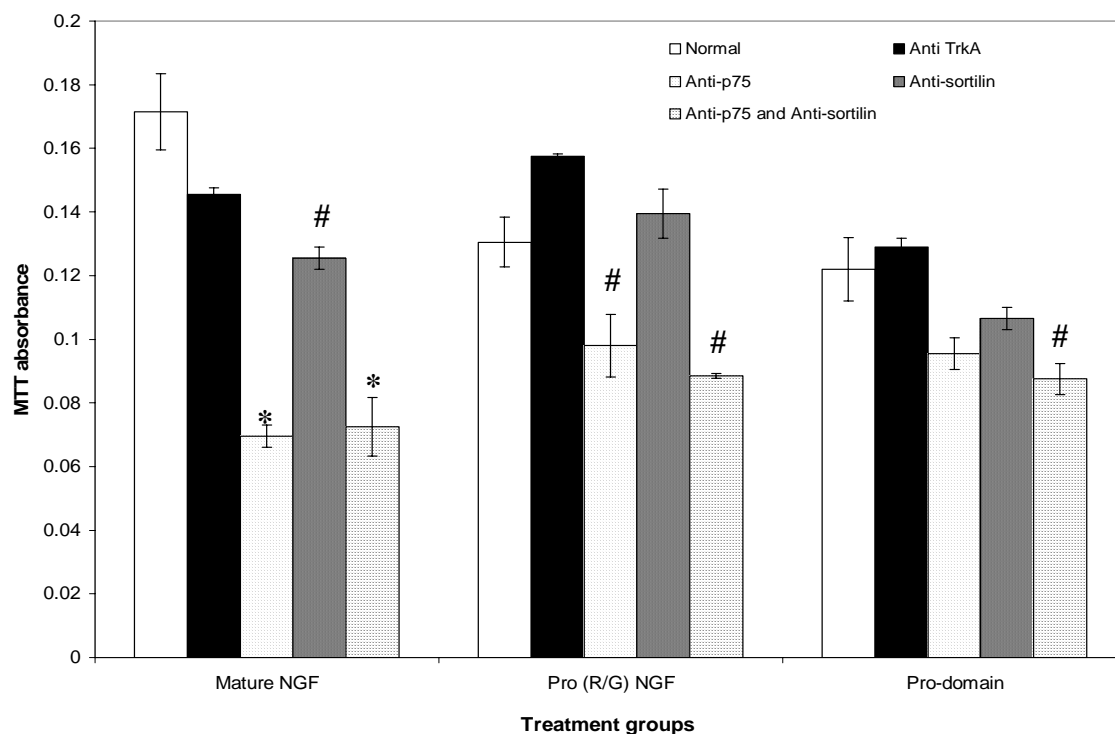
Fig. 4.9C: Inhibition of receptors by specific antibodies and its effect on cell death by MTT viability assay. PC 12 cells were incubated with anti-TrkA (2µg/ml), anti-p75[NTR] (2µg/ml) and anti-sortilin (1µg/ml) separately for 4h at 4°C. Antibodies were used in excess. In addition, a combination of anti-p75[NTR] and anti-sortilin was used. This was followed by incubation with conditioned CHO media containing mature NGF, pro (R/G) NGF and pro-domain for 24h at 37°C. Results are representative of triplicate experiments and expressed as MTT absorbance . ANOVA was done in relation to the untreated control and *: p-value < 0.01 and #: p-value < 0.05.

neuronal cell death after ischemic insult to develop potential neuroprotective agents (Abu-Raya *et al*., 1993). In addition, they have also been employed to study the mechanisms of neuronal survival after ischemic conditions (Abu-Raya *et al*., 1999; Tabakman *et al*., 2002). Hence, PC12 cells were used as an *in vitro* model of ischemia to decipher the effects of the mature NGF or pro (R/G) NGF or pro-domain.

The whole procedure of the oxygen-glucose deprivation experiment is illustrated in Figure 4.10Ai. Prior to induction of OGD, PC12 cells were seeded at a density of 2 x 10^5 cells/well of 24-well plate with complete DMEM. For the induction of OGD, cells were washed twice with freshly nitrogen-saturated, serum-free DMEM without glucose (0.3ml) and placed in the anaerobic chamber. The serum free DMEM without glucose was saturated with nitrogen by bubbling nitrogen gas into the media for 30min at 37°C. The plates were later placed in the 95% N_2/5% CO_2 chamber, the chamber was flushed for 10min at a flow-rate of 3L/min. A constant flow of nitrogen was maintained throughout the experiment. Sister plates containing serum-free DMEM with glucose were placed in 95% O_2/5%CO_2 incubator. After OGD treatment, media was changed to serum-free DMEM for a further 24 hours for reperfusion and MTT assay.

MTT assay is based on the ability of viable cells to reduce MTT (C, N-diphenyl-N'4-5-dimethyl thiazol-2-yl tetrazolium bromide) to insoluble colored formazan crystals, which can be detected spectrophotometrically. PC12 cells were exposed to various time interval of OGD and cell viability was determined by MTT assay (Fig. 4.10Aii). A time-dependent experiment was used to determine the length of OGD treatment and 5 hours was selected, based on its ability to kill 50% of the cells.

i
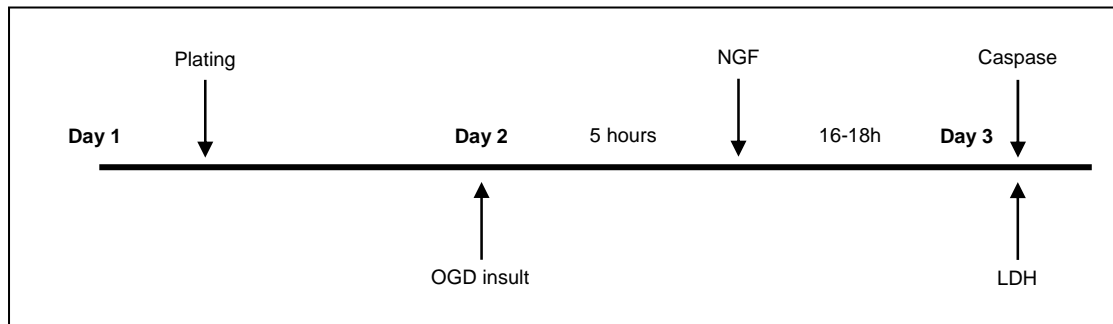
ii
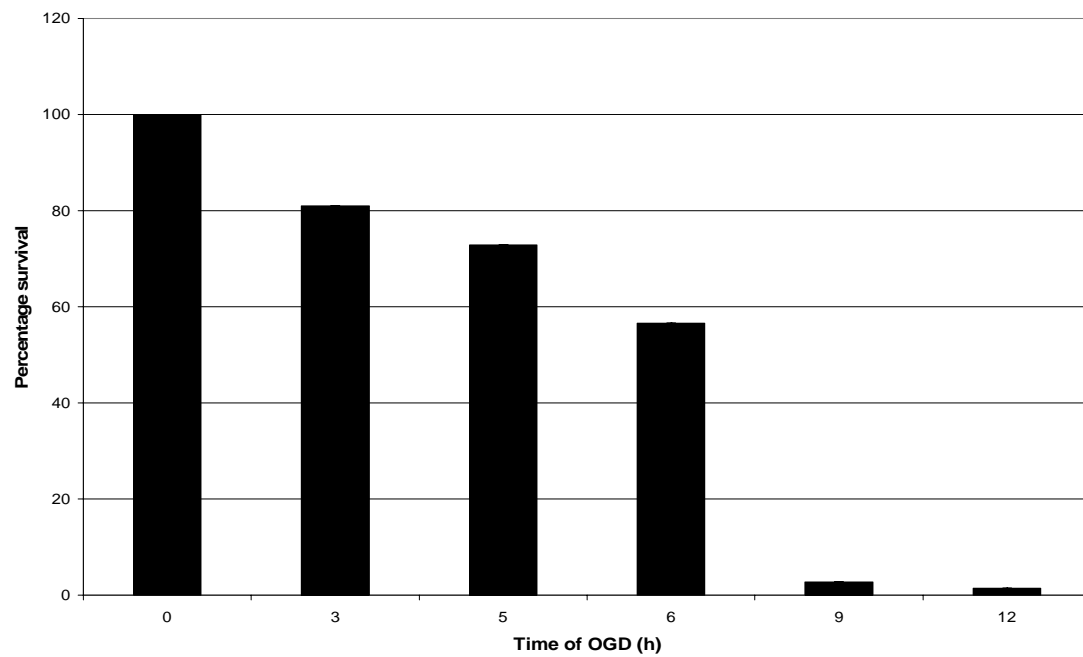
Fig. 4.10A: Oxygen-glucose deprivation (OGD) experiment. (i) Time scale for (OGD) experiment. **(ii)** Time-dependent of OGD exposure for PC12 cells. Cell viability was determined by MTT assay.

4.5.1 Classification of the mode of cell death

Before the investigation in the role of mature NGF, pro (R/G) NGF and pro-domain, it is important to clearly define the hallmark features between the two types of cell death- apoptosis and necrosis. Apoptosis was originally described as a progress that serves to eliminate damaged cells in a multi-cellular organism without affecting neighbouring cells by inflammatory reactions, i.e., without the release of intracellular material from the dying cells into the extracellular space (Saunders, 1966). This can be achieved by maintaining the integrity of the cell membrane while packaging the dying cells into smaller bodies and triggering the phagocytic activity of the neighbouring cells. On the other hand, necrosis is characterized by the loss of membrane integrity and spillage of enzymes and cellular debris that initiate an inflammatory reaction. This is an early event that may be accompanied by features characteristic of apoptosis, such as DNA fragmentation. However, the final goal of avoiding detrimental effects on neighbouring tissue or cells is not achieved by necrosis (Dartsch *et al*., 2002).

Therefore, two points are crucial for the distinction between apoptosis and necrosis. Firstly, apoptosis is characterized by the occurrence of DNA fragmentation, nuclear changes or other hallmarks with concomitant maintenance of membrane integrity. Secondly, it involves the exposure of phosphatidylserine which acts as the signal for phagocytic elimination of the apoptotic bodies. All these morphological changes take place downstream to caspases and caspase activation is also a pre-requisite. On the contrary, necrosis is cell death characterized by the early loss of membrane integrity which may or may not show traits like DNA fragmentation or caspase activation. This is important and has to be well-defined since phagocytes are

obviously absent in standard cell culture experiments and even apoptotic cells will eventually lose their membrane integrity.

4.5.2   Cell morphology with OGD and CHO conditioned media

After PC12 cells were exposed to OGD, they were treated with conditioned CHO media containing either mature NGF, or pro (R/G) NGF or pro-domain. Both mature NGF and pro (R/G) NGF were still capable of forming neurites, with a larger percentage for mature NGF treatment (Fig. 4.10Bi). The cells were later stained with three dyes: Annexin V (green), Ethidium Homodimer III (red) and Hoechst 33342 (blue). In Fig. 4.10Bii, cells treated with both mature and pro (R/G) NGFs had a reduction in the number of cells stained green and red (both apoptotic and necrosis). The number of green-stained cells was in this decreasing order: pro-domain > pro (R/G) NGF > mature NGF. When stained with Hoechst (blue; Fig. 4.10Biii), there was no significant change in DNA condensation for all treatments, apart for treatment with pro-domain with DNA condensation.

4.5.3   Assessment of cell death by lactate dehydrogenase (LDH) and caspase assay for cells exposed to OGD

In Fig. 4.10Ci, LDH assay showed a decrease in cell death for both mature NGF (F1 and F6) and pro (R/G) NGF (M36 and M38), while no significant change for pro-domain (S2 and S7). However, when assayed for caspase activity (Fig. 4.10Cii), both mature and pro (R/G) NGF were reduced significantly, while pro-domain increased in caspase activity. Hence, both mature and pro (R/G) NGF were able to protect, while pro-domain enhanced the damage of PC12 cells after OGD exposure.

i

Normal	**OGD alone**	**OGD + CHO media**
OGD + mature NGF	**OGD + pro (R/G) NGF**	**OGD + pro-domain**
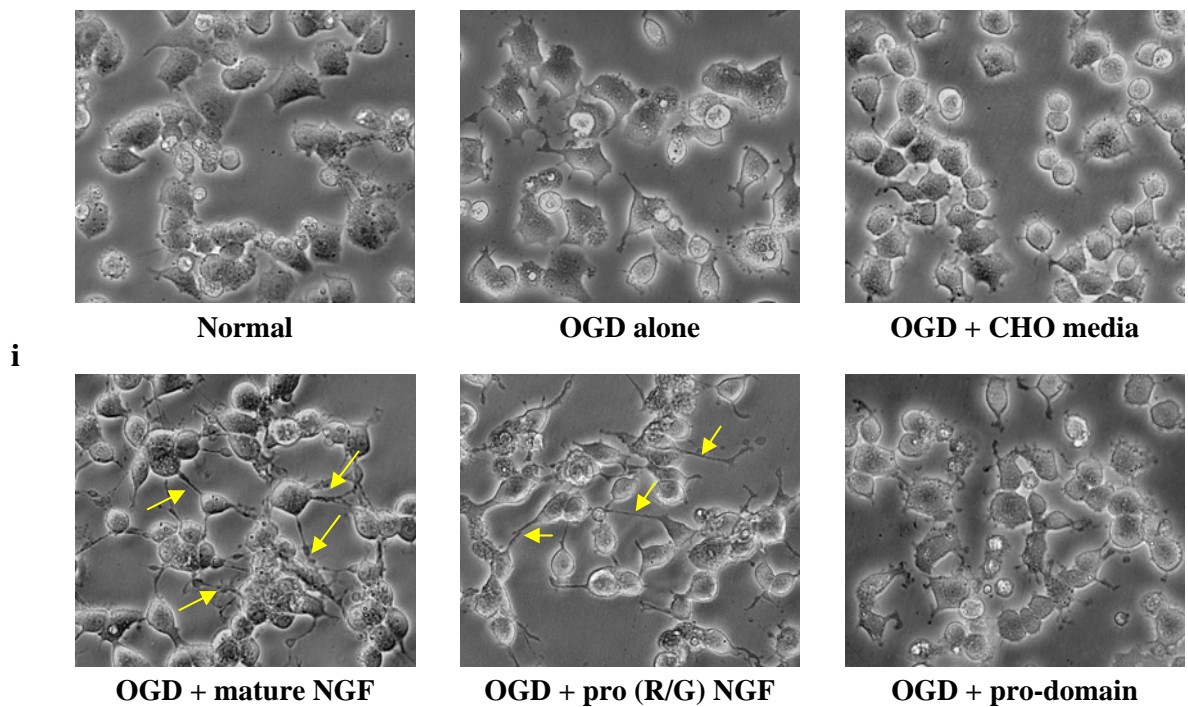
Fig. 4.10Bi: Cell morphology of PC12 cells exposed to OGD and post-treated with conditioned CHO media with NGF proteins. After exposure to OGD, PC12 cells were treated with conditioned CHO media containing mature NGF, pro (R/G) NGF and pro-domain for 16-18h. Neurites were observed for the mature and pro (R/G) NGF treatments and the cells appeared to be healthy, while treatment with the pro-domain resulted in more rounded dead cells as compared to OGD alone. Photomicrographs were obtained at x200 magnification and are representative of 3 independent experiments, performed in triplicate.

Normal   **OGD alone**   **OGD + CHO media**

ii

OGD + mature NGF   **OGD + pro (R/G) NGF**   **OGD + pro-domain**
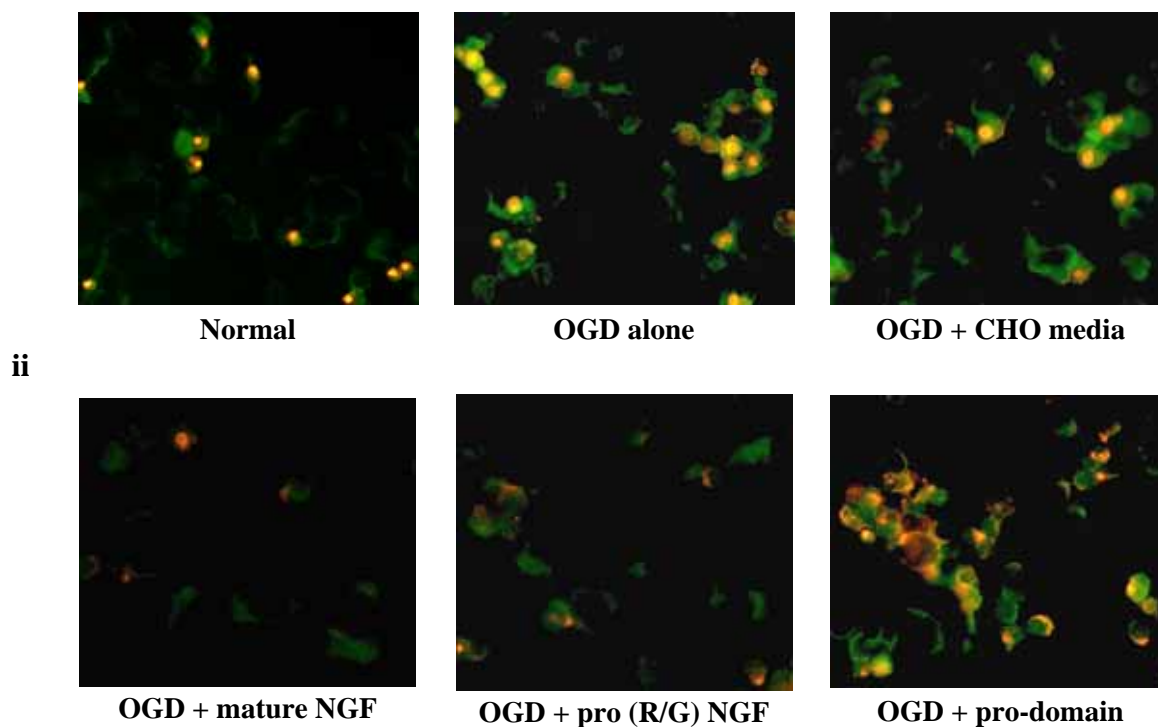
Fig. 4.10Bii: Annexin V/ Ethidium Homodimer III staining of PC12 cells exposed to OGD and post-treated with conditioned CHO media with NGF proteins. After treatment, the PC12 cells were stained with 3 dyes: FITC-conjugated Annexin V (green) and Ethidium Homodimer III (red), and Hoechst 33342 (blue) and viewed using green filter. The extent of cell damage was in this order: mature NGF < pro (R/G) NGF < pro-domain. Both mature and pro (R/G) NGFs were able to rescue the cells from the ischemic (OGD) treatment. Photomicrographs were obtained at x200 magnification and are representative of 3 independent experiments, performed in triplicate.
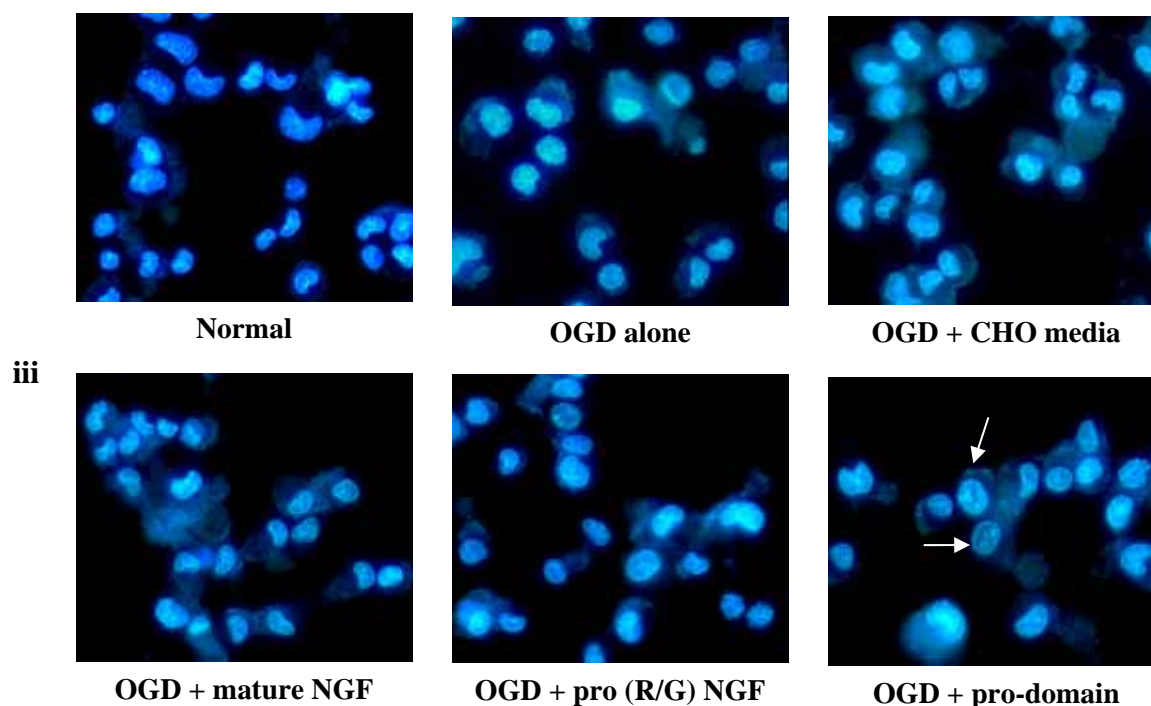
Fig. 4.10Biii: Hoechst 33342 staining of PC12 cells after exposure to OGD and post-treated with conditioned CHO media with NGF proteins. After treatment, the PC12 cells were stained with 3 dyes: FITC-conjugated Annexin V (green) and Ethidium Homodimer III (red), and Hoechst 33342 (blue) and viewed using the blue filter. With Hoeshst 33342 staining, the chromatins of the apoptotic cells with pro-domain are visibly fragmented and condensed (arrows). Nuclei of cells treated with mature and pro (R/G) NGFs look normal. Photomicrographs were obtained at x400 magnification and are representative of 3 independent experiments, performed in triplicate.
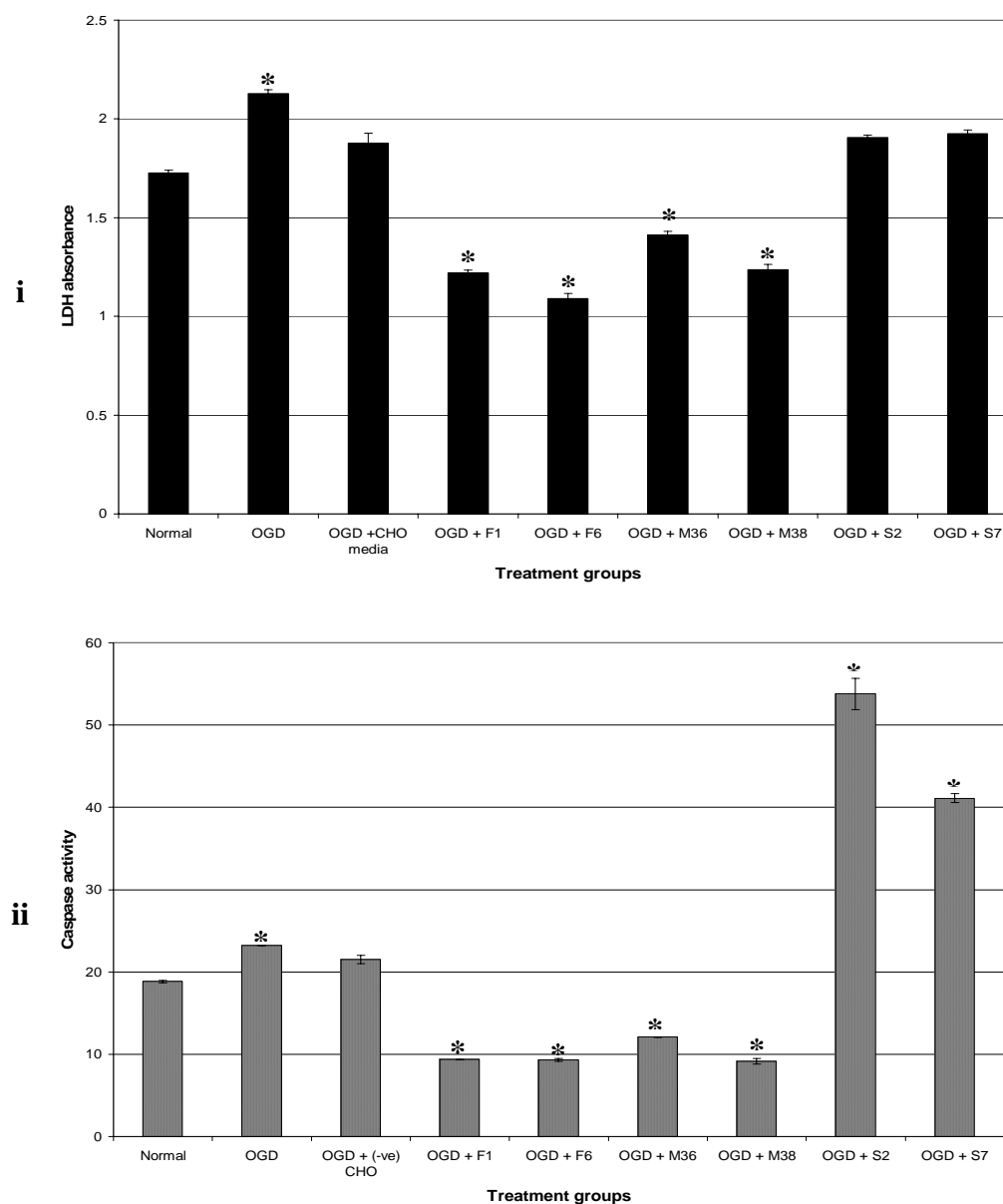
Fig. 4.10C: Determination of cell death of OGD-exposed PC12 cells. Two assays were used: **(i)** LDH assay and **(ii)** caspase assay. PC12 cells were assessed for cell death after exposure to OGD and post-treatment (16-18h) with conditioned CHO media containing mature NGF (F1 and F6), pro (R/G) NGF (M36 and M38) and pro-domain (S2 and S7). **(i)** LDH assay showed that both mature NGF and pro (R/G) NGF have significantly lower death as compared to pro-domain. ANOVA was done in relation to untreated control and *, p-value < 0.01. **(ii)** Caspase assay showed that both mature NGF and pro (R/G) NGF have significantly lower caspase activity as compared to pro-domain. ANOVA was done in relation to untreated control and *, p-value < 0.01.

4.5.4 Real-time PCR analysis for cells exposed to OGD

After OGD exposure, PC12 cells were treated with CHO conditioned media containing mature NGF, pro (R/G) NGF and pro-domain for 16-18h. The total RNA was extracted and used to check for genes regulated upon treatment. The eight genes were TrkA, p75^{NTR}, sortilin, NF-κB, IκB, Bcl-2, Bcl-$_{XL}$ and Bax (Fig. 4.10D). By studying the regulation of these genes by real-time PCR, the possible pathway activated by mature NGF, pro (R/G) NGF and pro-domain can be determined. NGF receptors (Trk A and p75) are highly expressed with mature NGF treatment and decreased with pro (R/G) NGF and pro-domain. Sortilin expression is only increased by pro-domain treatment, possibly activating the apoptotic pathway. This is supported by upregulation in both NFκB and IκB expression, NFκB is a transcription factor important for cell survival. However, the high increased in IκB levels may indicate the cell's compensatory mechanism to survival. This is supported by the regulation of pro-survival genes (Bcl-2 and Bcl-$_{XL}$), they are increased in pro-domain, but decreased for both mature and pro (R/G) NGF. While, the apoptotic Bax is decreased only with pro-domain treatment.

4.6 Staurosporine-induced apoptosis on PC12 cells

The protein kinase C inhibitor staurosporine is widely used to induce apoptosis in neuronal and nonneuronal cells (Krohn *et al*., 1998, 1999). In comparison with other insults like the exposure to glutamate or ischemia-like conditions where both types of cell death, apoptosis and necrosis, could be observed (Cheung *et al*., 1998), staurosporine selectively induces apoptosis including the activation of caspases, the release of cytochrome c from the mitochondria into the cytosol and the activation of endonucleases (Krohn *et al.*, 1998, 1999). Hence, PC12 cells were exposed to
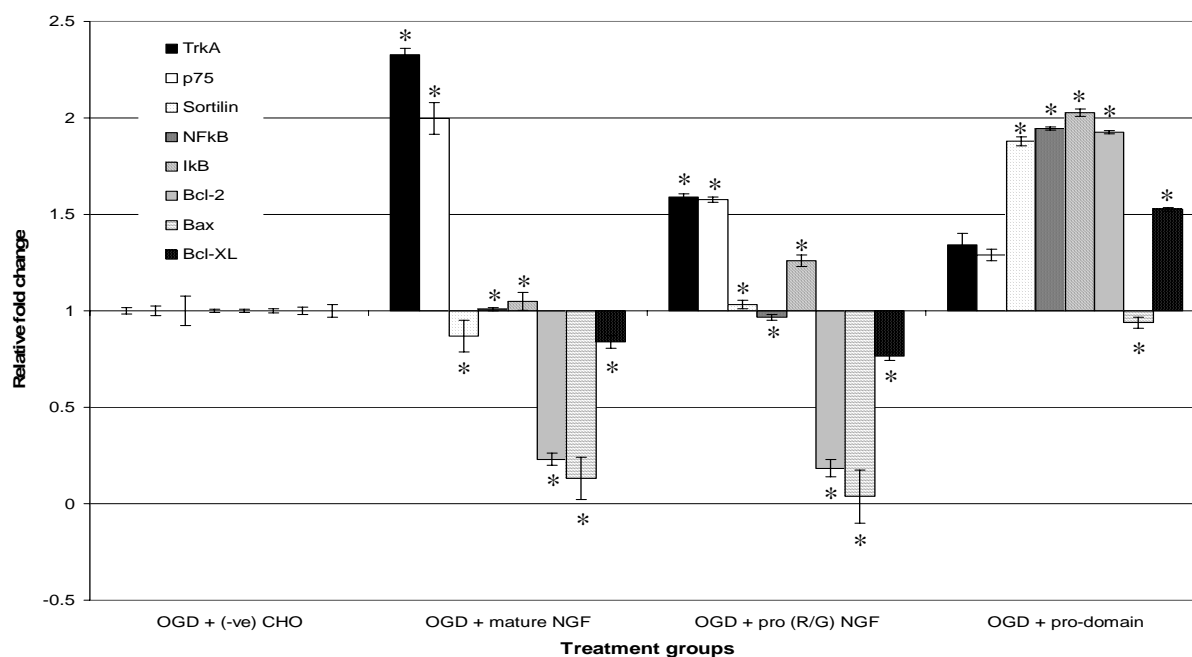
Fig. 4.10D: Quantitative real-time PCR (SYBR green) analysis of PC12 cells exposed to OGD. Total RNA from the treated PC12 cells was used to study the expression of eight genes: TrkA, p75^{NTR}, sortilin, NFκB, IκB, Bcl-2, Bax and Bcl-XL. PC12 cells were treated with conditioned CHO media containing mature NGF (F1 and F6), pro (R/G) NGF (M36 and M38) and pro-domain (S2 and S7) individually for 16-18h. Values are expressed as $\pm$ SEM, experiments performed in triplicates and * p < 0.01 by unpaired Student's *t*-test.

staurosporine-induced apoptosis and accessed whether the NGF proteins [mature NGF, pro (R/G) NGF and pro-domain] could reduce apoptosis.

4.6.1 Cell morphology with staurosporine

PC12 cells were treated with 0.5µM of staurosporine (STS) concurrently with CHO media containing mature NGF (F1 and F6), pro (R/G) NGF (M36 and M38) and pro-domain (S2 and S7). More neurites were seen which appeared longer, upon treatment with mature NGF, it seems like the cells were not affected with the STS in the media. Pro (R/G) NGF had a fewer neurites, but cells still appeared healthy. However, treatment with pro-domain increased the amount of rounded, dead cells as compared to STS alone. Hence, only mature NGF and pro (R/G) NGF was able to rescue the cells from staurosporine-induced apoptosis (Fig. 4.11Ai).

The treated PC12 cells were later stained with three dyes (Annexin V, Ethidium Homodimer III and Hoechst 33342). In Fig. 4.11Aii, the cells were viewed for Annexin V (green) and Ethidium Homodimer III (red) labeling, when merged together, the nucleus appeared orange. When treated with STS alone, the number of apoptotic cells (green) was comparable to with CHO media, indicating that the conditioned media was neutral. However, when cells were exposed to treatment with mature NGF, the number of cells stained green (apoptotic) was greatly reduced. The number of green-stained cells was in this order: STS = pro-domain > pro (R/G) NGF > mature NGF. Hence, only mature NGF was able to protect the cells from STS.

In Fig. 4.11Aiii, cells were viewed for Hoechst 33342 (blue) labeling. Treatment with STS resulted in a condensation of the DNA in the nuclei, as indicated by white arrows. The magnitude of DNA condensation was in this order: STS = pro-domain >

i
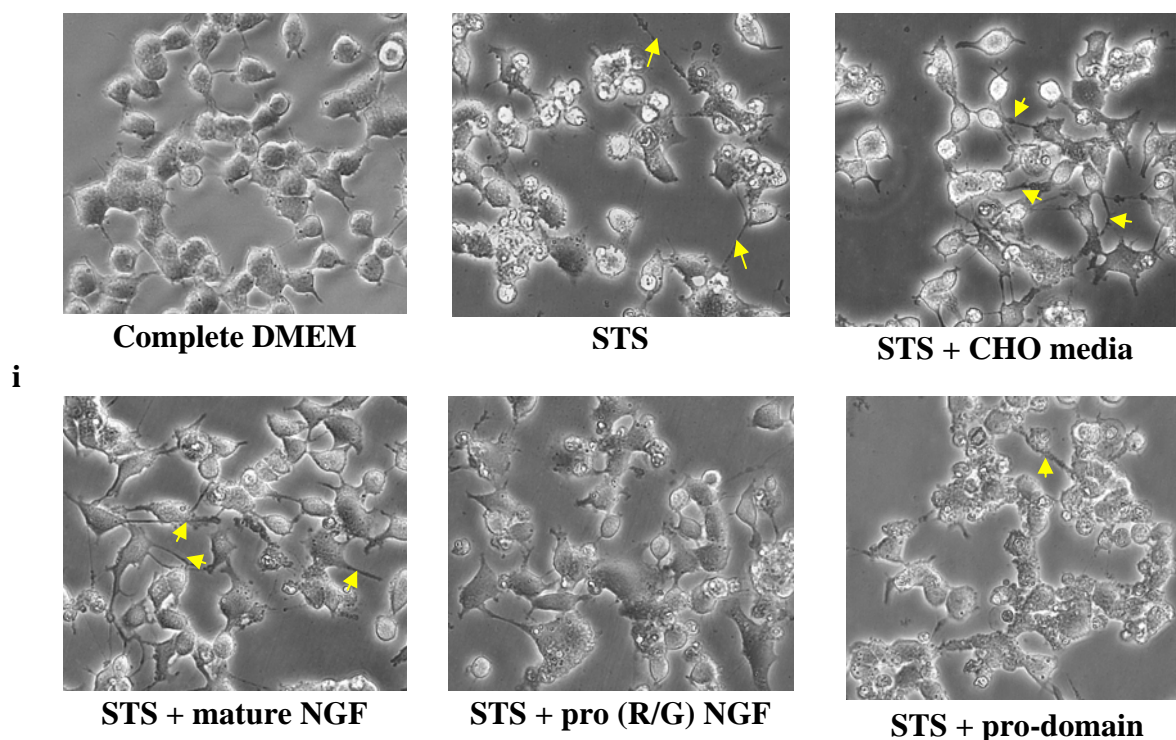
Fig. 4.11Ai: Cell morphology of staurosporine (STS)-induced apoptosis on PC12 cells when treated concurrently with conditioned CHO media with overexpressed NGF proteins. PC12 cells were treated concurrently with STS (0.5µM) and conditioned CHO media containing mature NGF, pro (R/G) NGF and pro-domain for 16-18h. Staurosporine treatment caused neurites and hence no comparison will be made to the quantity of neurites. Treatment with mature and pro (R/G) NGFs, the cells looked healthy, while treatment with the pro-domain resulted in more rounded dead cells as compared to STS alone. Photomicrographs were obtained at x200 magnification and are representative of 3 independent experiments, performed in triplicate.

ii

Complete DMEM   **STS**   **STS + CHO media**

STS + mature NGF   **STS + pro (R/G) NGF**   **STS + pro-domain**
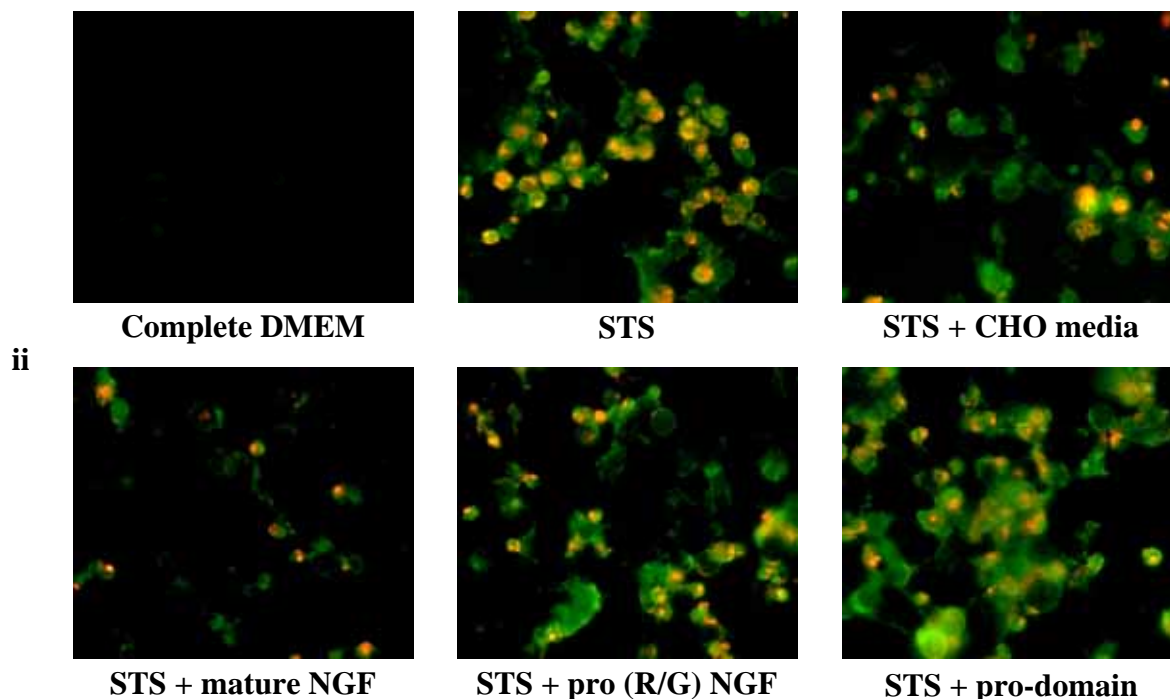
Fig. 4.11Aii: Annexin V/ Ethidium Homodimer III staining of PC12 cells treated concurrently with staurosporine (STS) and conditioned CHO media with NGF proteins. After treatment, the PC12 cells were stained with 3 dyes: FITC-conjugated Annexin V (green) and Ethidium Homodimer III (red), and Hoechst 33342 (blue) and viewed using green filter. Staining with Annexin V and Ethidium Homodimer III showed the extent of cell damage to be of this order: mature NGF < pro (R/G) NGF < pro-domain. Only mature NGF was able to rescue the cells from the toxic staurosporine treatment. Photomicrographs were obtained at x200 magnification and are representative of 3 independent experiments, performed in triplicate.

| Complete DMEM | STS | STS + CHO media |

iii

| STS + mature NGF | STS + pro (R/G) NGF | STS + pro-domain |
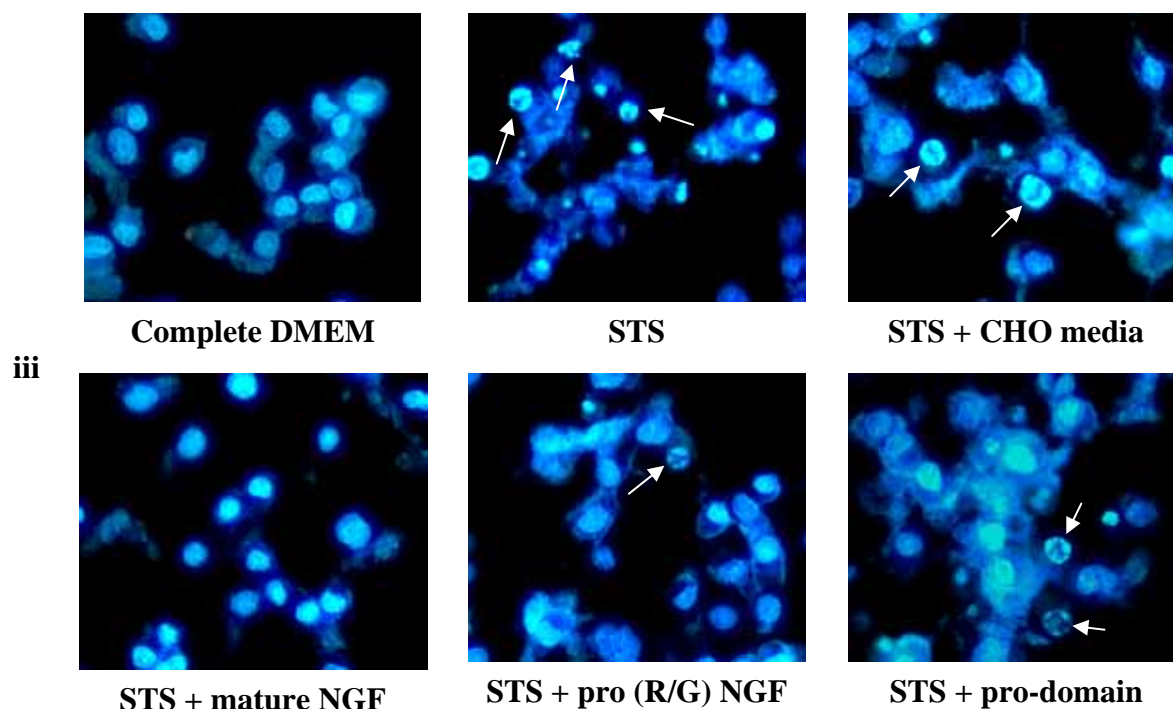
Fig. 4.11Aiii: Hoechst 33342 staining of PC12 cells treated concurrently with staurosporine (STS) and conditioned CHO media with NGF proteins. After treatment, the PC12 cells were stained with 3 dyes: FITC-conjugated Annexin V (green) and Ethidium Homodimer III (red), and Hoechst 33342 (blue) and viewed using blue filter. With Hoeshst 33342 staining, the chromatins of the apoptotic cells are visibly fragmented and condensed (arrows). Control cell nuclei look healthy. Photomicrographs were obtained at x400 magnification and are representative of 3 independent experiments, performed in triplicate.

pro (R/G) NGF > mature NGF. Similarly, only mature NGF was able to protect the cells from STS.

4.6.2   Assessment of cell death by lactate dehydrogenase (LDH) assay

PC12 cells were treated concurrently with staurosporine (STS; 0.5µM) and the CHO conditioned media containing mature NGF (F1 and F6), pro (R/G) NGF (M36 and M38) and pro-domain (S2 and S7) for 16-18h. The media was collected, deprived of cells by centrifugation and assayed for LDH activity. The LDH activity was significantly decreased for mature NGF (F1 and F6) and increased for pro-domain (S7; Fig. 4.11B). This result corresponded to the cell morphology observed by three-dye staining in the section above (section 4.6.1), the mature NGF (F1 and F6) protected against staurosporine-induced death, while pro-domain (S2 and S7) enhanced the damage.
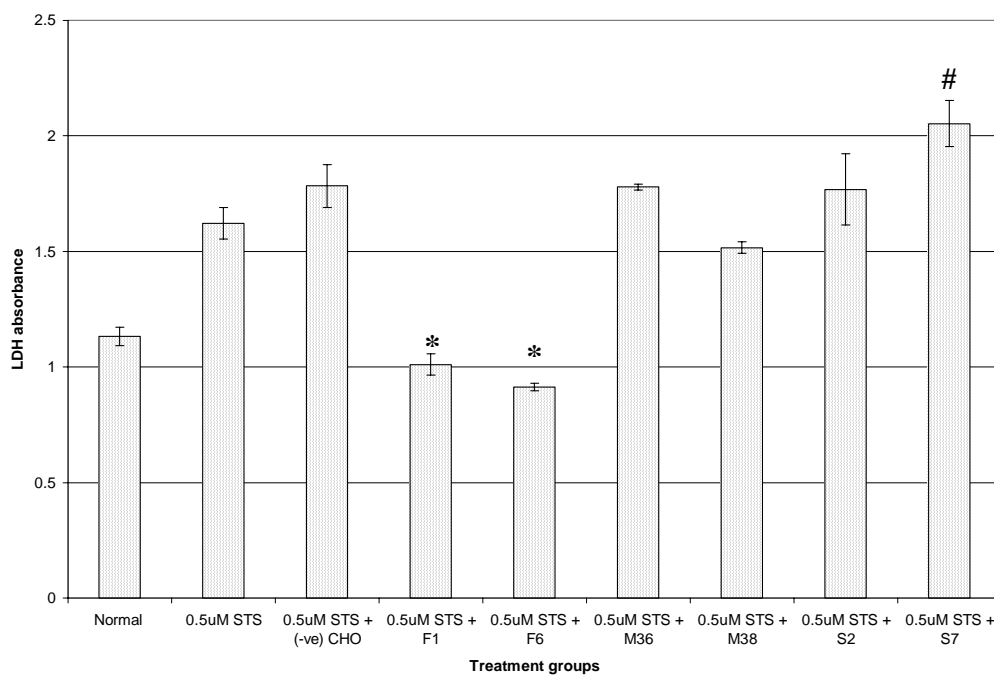
Fig. 4.11B: Determination of cell death using LDH assay. PC12 cells were treated concurrently with staurosporine (0.5μM) and CHO conditioned media containing mature NGF (F1 and F6), pro (R/G) NGF (M36 and M38) and pro-domain (S2 and S7) for 16-18h. Media was collected and assayed for LDH activity. ANOVA was done in relation to staurosporine (0.5μM) and *: p-value < 0.01 and #: p-value < 0.05. Only F1, F6 and S7 showed significant changes in LDH activity.

Chapter 5

Effect of nPLA$_2$ on ischemia and

its possible mechanism of action

5.1   Introduction

Phospholipase A2 (PLA$_2$) constitutes a superfamily of enzymes that catalyze the hydrolysis of the phospholipids *sn*-2 ester bond, thereby generating a free fatty acid and lysophospholipid. Snake venoms are rich sources of PLA$_2$ enzymes and often contain a large number of isozymes. There are currently several hundred snake venom PLA$_2$ enzymes that have been purified and characterized. They share similar catalytic function and properties of hydrolyzing phospholipids. However, in contrast to mammalian PLA$_2$ enzymes, most snake venoms are toxic and induce a wide spectrum of pharmacological effects by interfering with the normal physiological processes. Among these pharmacological effects, only neurotoxic, myotoxic and anticoagulant have been well-studied (Kini, 1997).

Stroke is the third cause of death in Europe and North America after heart disease and cancer and non-fatal strokes are the commonest cause of disability. Brain ischemia occurs when the supply of glucose and oxygen to the brain is disrupted. Glutamate excitotoxicity plays a critical role in brain ischemia, which in turn, causes depolarization of neurons and the release of large amount of glutamate. Approximately about 3-4 minutes after an ischemic attack, the concentration of glutamate increases by up to 10 to 100-fold (Choi, 1992; Nagasawa and Kogure, 1989). This is followed by a rise in intracellular calcium, which initiates a whole cascade of biochemical changes that eventually leads to cell necrosis and apoptosis. These in turn, lead to later consequences including cerebral edema and inflammation (Choi, 1988), which can further enhance the damages.

Reperfusion itself can cause damage by the production of free radicals and other reactive species when the oxygenation is restored. The secondary injury usually takes a few hours to develop and this window of time has the potential for

therapeutic intervention. Neuroprotective treatments have been investigated through the use of compounds that (a) reduce the intracellular accumulation of calcium (Choi, 1992; Kristian and Siesjo., 1998), (b) inhibit free radical formation (Zhao *et al*., 1994), and (c) activate neurotrophic factors such as nerve growth factor (NGF; Hsu *et al*., 1993) and brain-derived neurotrophic factor (BDNF; Schabitz, *et al*., 1997). However, all these drugs used presently for stroke therapy are not convincingly successful and hence there is a need for new therapeutic strategies.

Many aspects of ischemic neurodegeneration have been demonstrated in animal models; however, they represent a complex environment to dissect the cellular and molecular mechanisms involved in ischaemic neurodegeneration. Although cell culture systems are further from *in vivo* situation, they represent a more defined microenvironment. Most studies have used mixed neuronal and glial cultures to investigate the effects of oxygen and/or glucose deprivation (Goldberg *et al*., 1987; Rothman, 1988; Monyer *et al*., 1989; Swanson and Choi, 1993), but the regional organization and neuronal connectivity are lost in most mixed cultures. On the contrary, these are substantially retained in organotypic hippocampal cultures (Gahwiler, 1984; Stoppini *et al*., 1991). In addition, organotypic hippocampal cultures retain a similar glutamate receptor population as those found in adult animals (Bahr *et al*., 1995).

The study of the agonist properties of glutamate is further complicated by the brain's high affinity, high capacity transport system for glutamate. In brief, direct injection of glutamate into the brain is not toxic (Mcbean and Roberts, 1985). This problem can be overcome by using *in vitro* systems, including brain slices (i.e. organotypic hippocampal culture) and cultures, in which higher concentrations of glutamate can be maintained and the effect of the transport can be overcome. Glutamate receptors

that mediate these injuries (e.g. cerebral ischemia, head trauma and prolonged seizures) are divided into a number of types based on their selectivity to different agonists. As the endogenous ligand, glutamate activates all these receptors, including the NMDA receptor family, the AMPA/kainate receptor family and the metabotrophic (mGluR) receptor family (Vornov *et al*., 1995).

Since glutamate-mediated mechanisms play an integral role in the generation of ischemic damage, organotypic hippocampal cultures were used to investigate the effect of PLA_2 on ischemia and its possible mechanism of action. This study will be divided into three main sections, effect of $nPLA_2$ (a neutral phospholipase A2 from *Naja sputatrix*) on organotypic hippocampal cultures when exposed to 1) ischemic conditions (i.e. oxygen-glucose deprivation; OGD); 2) glutamate (pretreatment, concurrent and post-treatment) and 3) specific glutamate receptor agonists (i.e., NMDA, KA, AMPA and mGluRs).

5.2 Effect of NGF and PLA_2 on PC12 cells exposed to OGD conditions

Two components (NGF and PLA_2) from the venom of *Naja sputatrix* were tested for their ability to protect against ischemic conditions using PC12 cells and organotypic hippocampal culture models. PC12 cells were post-treated with either NGF (mouse and sputa) at 200ng/ml or PLA_2 (1µg/ml or 2µg/ml) for 16-18h after subjecting to hypoxia (lower oxygen) conditions. Both sputa NGF (200ng/ml) and PLA_2 (1µg/ml and 2µg/ml) caused an increase in cell survival (Fig. 5.1A). Similarly, PC12 cells when subjected to ischemic conditions (OGD) for 1.5h and both sputa NGF (200ng/ml) and PLA_2 (2µg/ml) protected the cells as seen by MTT assay (Fig. 5.1B). Concurrent treatment with NGF (mouse and sputa) and PLA_2 (1µg/ml and
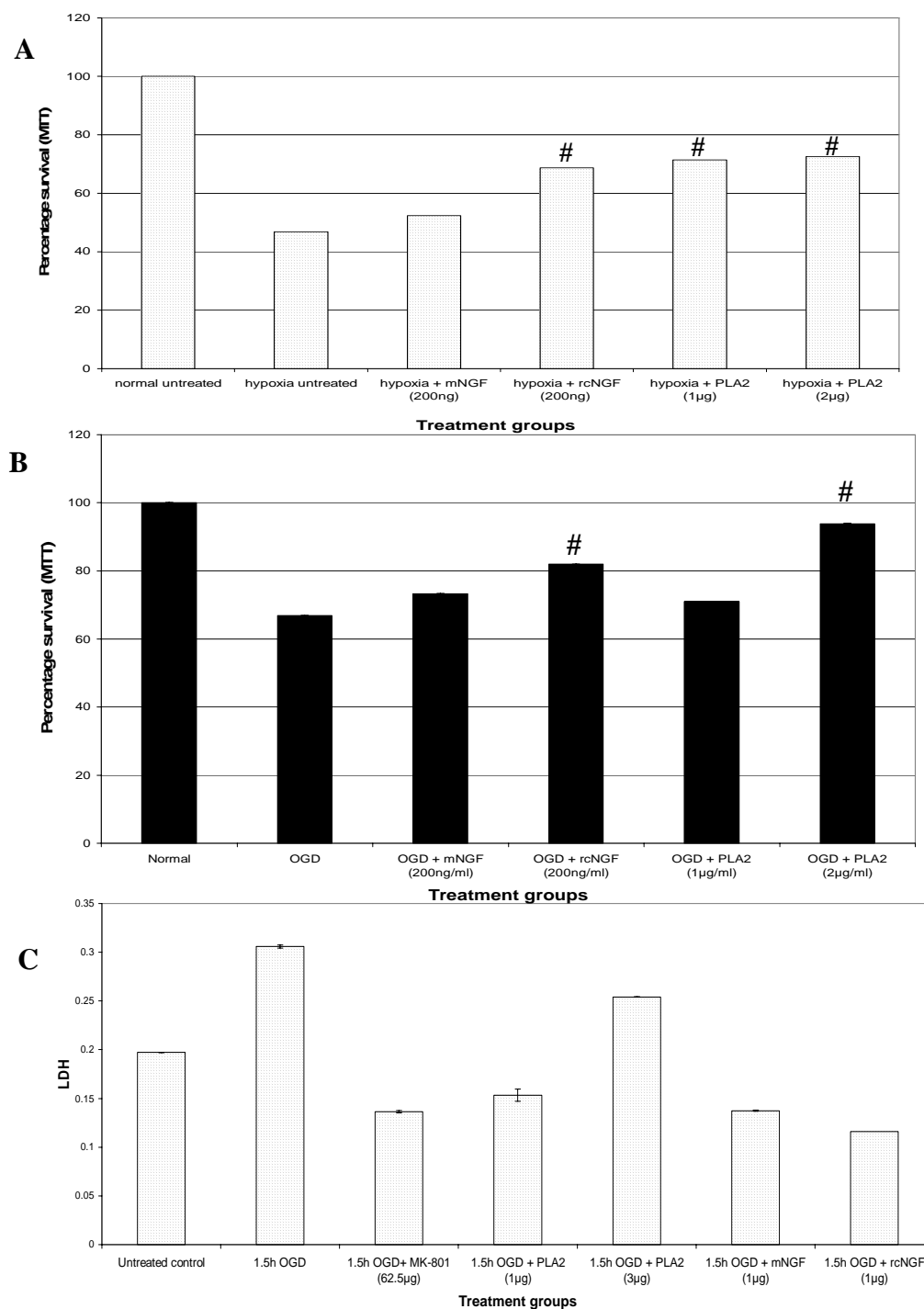
Fig. 5.1: Effect of PC12 cells and organotypic hippocampal cultures with NGF and PLA₂. PC12 cells were exposed to (**A**) hypoxia and (**B**) OGD conditions and post-treated with mouse NGF and sputa NGF (200ng/ml) and PLA₂ (1μg/ml and 2μg/ml). MTT assay showed that sputa NGF and PLA₂ caused increase in survival for hypoxia and OGD condition. (**C**) LDH assay on media from organotypic hippocampal cells. LDH activity is reduced for both PLA₂ and sputa NGF (200ng/ml) treatments. Values obtained are expressed as ± SEM. #: p-value < 0.05 and *: p-value < 0.01 by unpaired Student's *t*-test.

2µg/ml) on organotypic hippocampal cultures exposed to OGD showed a decrease in LDH activity (Fig. 5.1C). Hence, both sputa NGF (200ng/ml) and PLA$_2$ (1 and 2µg) have shown to protect the cells from both hypoxia and OGD.

5.3   Oxygen-glucose deprivation- a model for ischemia

Fourteen-day old organotypic hippocampal cultures were placed in serum-free media for 16h prior to OGD treatment. Before initiation of treatment, cultures were placed in basal MEM (Section 2.1.5) containing 5µg/ml PI for 3hours and imaged. Any cultures in which PI fluorescence was detected at this time were excluded from further study. Simulated ischemia (combined hypoxia and hypoglycemia) was induced by placing the cultures in basal MEM (devoid of glucose) containing 5µg/ml PI which had previously been saturated with 95%N$_2$/5%CO$_2$. The culture was then placed in an air-tight chamber equipped with inlet and outlet valves and 95%N$_2$/5%CO$_2$ and was flushed with 95%N$_2$/5%CO$_2$ for 10min to ensure maximal removal of oxygen. The chamber was maintained at 37°C throughout the whole experiment.

After OGD treatment, cultures were returned to glucose-containing basal MEM and placed in cell culture incubator for further 24h. All cultures were imaged 24h later. Regional patterns of neuronal injury in the organotypic cultures were observed by performing all experiments in the presence of propidium iodide, a polar, fluorescent dye that does not stain cells with normal membrane integrity. However, once the membrane is injured, the dye enters the cells and binds to nucleic acids and accumulates, rendering the cell brightly fluorescent (Vornov *et al*., 1994).

In the initial experiments, the time-dependent curve for OGD incubation was established using cytotoxicity assay- lactate dehydrogenase assay (LDH). 3 plates of

culture were placed in the chamber for varied time interval (from 1h to 3h) and the medium was collected and assayed for LDH activity. Fig. 5.2 showed that 1h OGD treatment caused 27.1% death, while 2h OGD treatment caused about 98% death. Hence, about 1.5h OGD would cause approximately 50-60% death and this timing was used to access the effect of PLA_2 on OGD-treated cultures.

5.4   Effect of PLA_2 on cultures exposed to OGD

For subsequent experiments, PLA_2 will be referred as: 0.5µg/ml = 0.38µM; 1µg/ml = 0.75µM and 2µg/ml = 1.5µM. The results of the concurrent treatment of PLA_2 (0.75µM and 1.5µM) and OGD showed that PLA_2 (0.75µM) was able to rescue both CA1 and CA3 from OGD damage to about 58% and 94%, respectively (Fig. 5.3). However, PLA_2 (1.5µM) was better at rescuing the hippocampal cultures from OGD damage. Its protection was ~95% and similar to the MK801 (antagonist for NMDA receptor). Hence, this dose of PLA_2 (1.5µM) was used for subsequent experiments. Treatments with PLA_2 (0.75µM and 1.5µM) and MK801 (0.19mM) only were non-toxic to the cultures.

5.5   Real-time quantitation of gene expression

The expression of four genes (Homer, Bcl-2, $Bcl-_{XL}$ and Bax) was quantitated by real-time PCR to elucidate the possible mechanism of action of PLA_2's neuroprotection against the OGD damage (Fig. 5.4). Specific primers were used for the SYBR green assay. The relative expression of each gene in cultures treated with either PLA_2 (0.75µM or 1.5µM) or MK801 (0.19mM) was obtained after normalizing against an internal control (18S ribosomal RNA) and a calibrator, in this case, culture exposed to OGD only (relative gene expression = 1). The two anti-
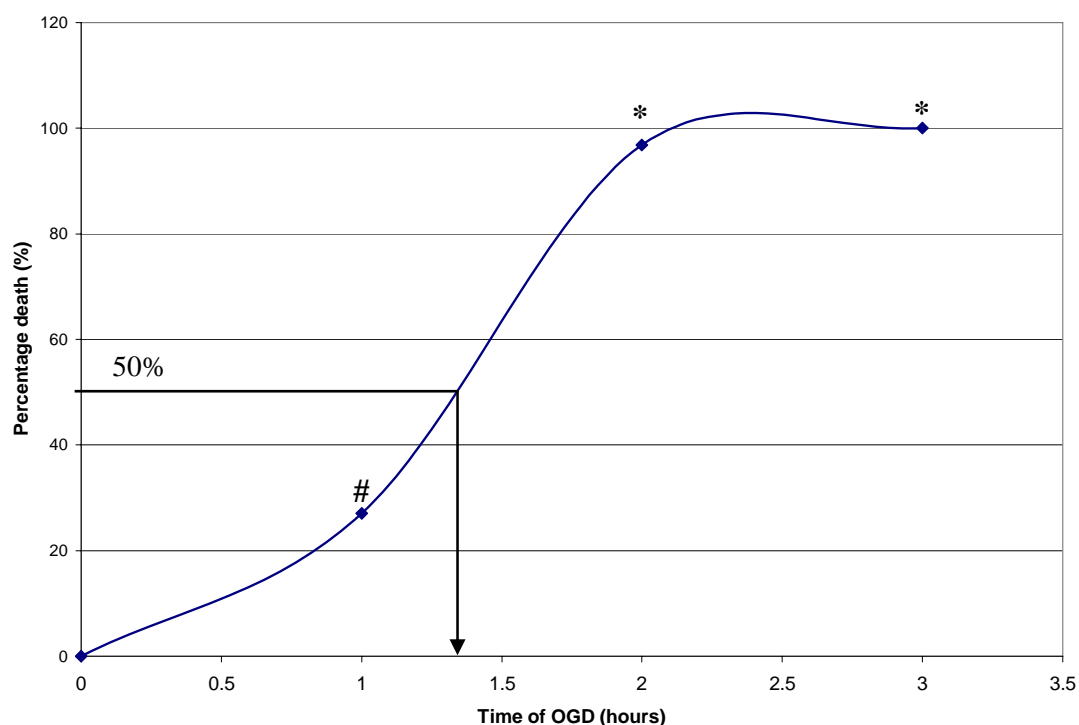
Fig. 5.2: Time-course of oxygen-glucose deprivation (OGD) on hippocampal organotypic cultures. Media from the cultures were collected and assayed for LDH activity. The percentage of death was calculated and the time needed to cause 50% damage was determined. Time dependent manner of cell death of hippocampal organotypic cultures from 1-3 hours was carried out and 1.5h was fixed as 50% cell death. In subsequent experiments, the time of incubation for OGD was kept at 1.5h. Results are a representative of 4 independent experiments and values obtained are expressed as percentage of the maximum percentage of death (3h) $\pm$ SEM. #: p-value < 0.05 and *: p-value < 0.01 by unpaired Student's *t*-test.

A
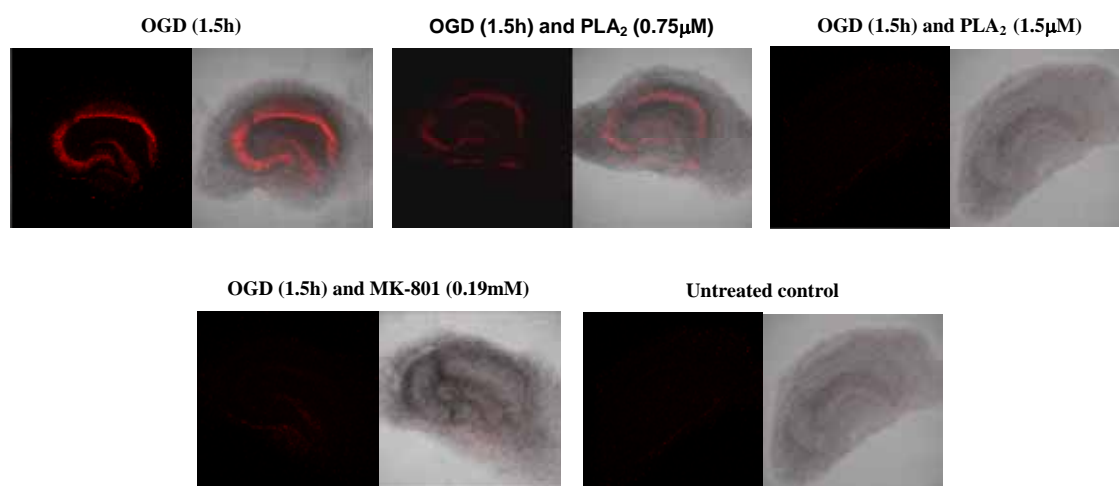
B
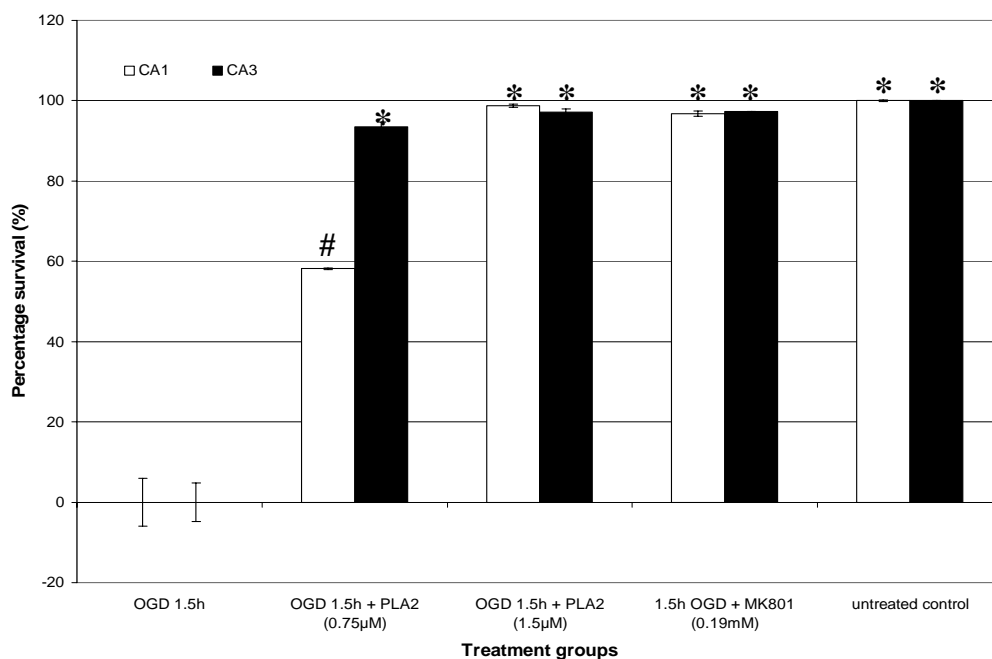
Fig. 5.3: Effect on concurrent treatment of PLA$_2$ on OGD-induced cell death. (A) PI fluorescence of treated groups and **(B)** corresponding percentage survival graphs. The percentage damage to the CA1 and CA3 neuronal cell fields are expressed as a percentage of area expressing fluorescence compared with the untreated control cultures and 1.5h OGD taken as maximum damage. Each point represents the mean ± SEM (n=8). #: p-value < 0.05 and *: p-value < 0.01 versus OGD treatment.
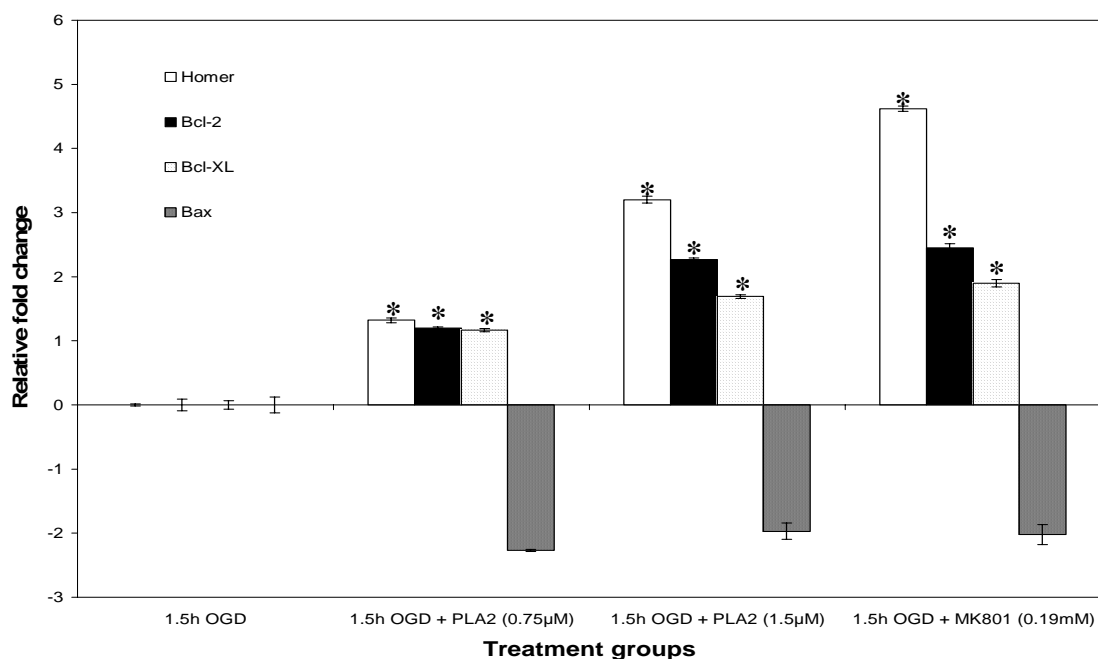
Fig. 5.4: Quantitative gene analysis via SYBR Green assay. The total RNA was isolated from the treated samples and used to study the expression of five genes: NFκB, Homer, Bcl-2, Bcl-$_{XL}$ and Bax. Except for the Bax gene, the rest of the genes were upregulated with PLA$_2$ and MK801 treatments. Each measurement was performed in triplicate and the data is a representative of duplicate experiments. Values are expressed as fold change ± SEM, *: p-value < 0.01 by unpaired Student's *t*-test.

apoptotic genes (Bcl-2 and Bcl-$_{XL}$) were both upregulated in all treatments, while the apoptotic gene (Bax) was downregulated in all treatments. The coupling of Homer with group I glutamate metabotrophic (mGluR) has been implicated in mGluR trafficking and clustering (Ango *et al*., 2000 and 2002). Expression of the Homer gene was upregulated in all treatments; PLA$_2$ (dose-dependent) and MK801. Hence, upon treatment with PLA$_2$ (1.5µM) or MK801 (0.19mM), the pro-survival genes (Bcl-2 and Bcl-$_{XL}$) that also act by promoting cell survival are upregulated, while the pro-apoptotic gene (Bax) is downregulated. These genes, together with upregulation of the Homer gene, suggested that the addition of PLA$_2$ into cultures when exposed to OGD, mediated an overall protective effect, acting via the mGluR pathway.

5.6 Effect of concurrent PLA$_2$ on glutamate-induced neuronal cell death

Fourteen-day organotypic cultures were prepared prior to treatment as described in section 5.3. 5mM glutamate was suggested by Elliott-Hunt *et al.* (2002) to cause significant and consistent levels of neurotoxicity; the survival rate of neurons for both CA1 and CA3 regions was approximately 40 ± 15%. In this study, a similar pattern was observed in with 5mM glutamate 30-50% damage for both CA1 and 3. Addition of 10mM glutamate resulted in total death, and was used as a positive control. No cell death was observed in the cultures using basal MEM alone.

The specificity of this effect was confirmed with a specific inhibitor for the NMDA receptors (MK801) which prevented glutamate-induced neuronal cell death. The concentration was based on 625µg per adult rat; each rat has about 10ml of blood. Hence, for 1ml of basal medium 62.5µg of MK801 was used. In order to study the effect of PLA$_2$ on glutamate-induced neurotoxicity, PLA$_2$ was incubated

concurrently at concentrations of 0.38μM, 0.75μM and 1.5μM for 3h, together with

5mM of glutamate for 3 hours. Figure 5.5 showed that at both concentrations of

PLA_2 (0.75μM and 1.5μM), concurrent treatment of PLA_2 with 5mM glutamate

have shown to protected CA3 dose-dependently, that is similar to protection by

MK801. PLA_2 (0.38μM) offered less protection than both PLA_2 (0.75μM and

1.5μM). PLA_2 is not toxic to the hippocampal cultures. In fact, when PLA_2 was

tested against glutamate-induced (5mM) neuronal cell, results showed (Fig. 5.5) that

PLA_2 (0.75μM and 1.5μM) protected CA3 regions better than MK801 when added

immediately after the 3h insult.

5.7 Effect of post-treatment PLA_2 on glutamate-induced neuronal cell death

Since a concurrent treatment of PLA_2 was able to efficiently reduce the damage by

glutamate (Section 5.6), it was tested further by post-treatment. Cultures were

incubated with 5mM glutamate for 3 hours and post-treated with PLA_2 at 0.38μM,

0.75μM and 1.5μM for additional 24 hours. The cultures were later imaged and

results shown in Figure 5.6. Post treatment with MK801 (0.19mM) and PLA_2

(0.38μM) were unable to protect the cultures from glutamate damage, while PLA_2

(0.75μM and 1.5μM) were still able to significantly protect the CA3 region from

damage. Hence, this results showed that PLA_2 (0.75μM and 1.5μM) were better than

MK801, in reducing damage induced by glutamate.

5.8 PLA_2 and neuronal cell death by AMPA/KA/NMDA

The principal excitatory transmitter in the central nervous system, glutamate, acts

through the following three classes of ionotropic receptors, named after the

A)

Untreated control   MK801 (0.19mM)   PLA$_2$ (0.38µM)

PLA$_2$ (0.75µM)   PLA$_2$ (1.5µM)   Glutamate (10mM)

Glutamate (5mM)   Glutamate (5mM) and MK801 (0.19mM)

Glutamate (5mM) and PLA$_2$(0.38µM)   Glutamate (5mM) and PLA$_2$ (0.75µM)   Glutamate (5mM) and PLA$_2$ (1.5µM)
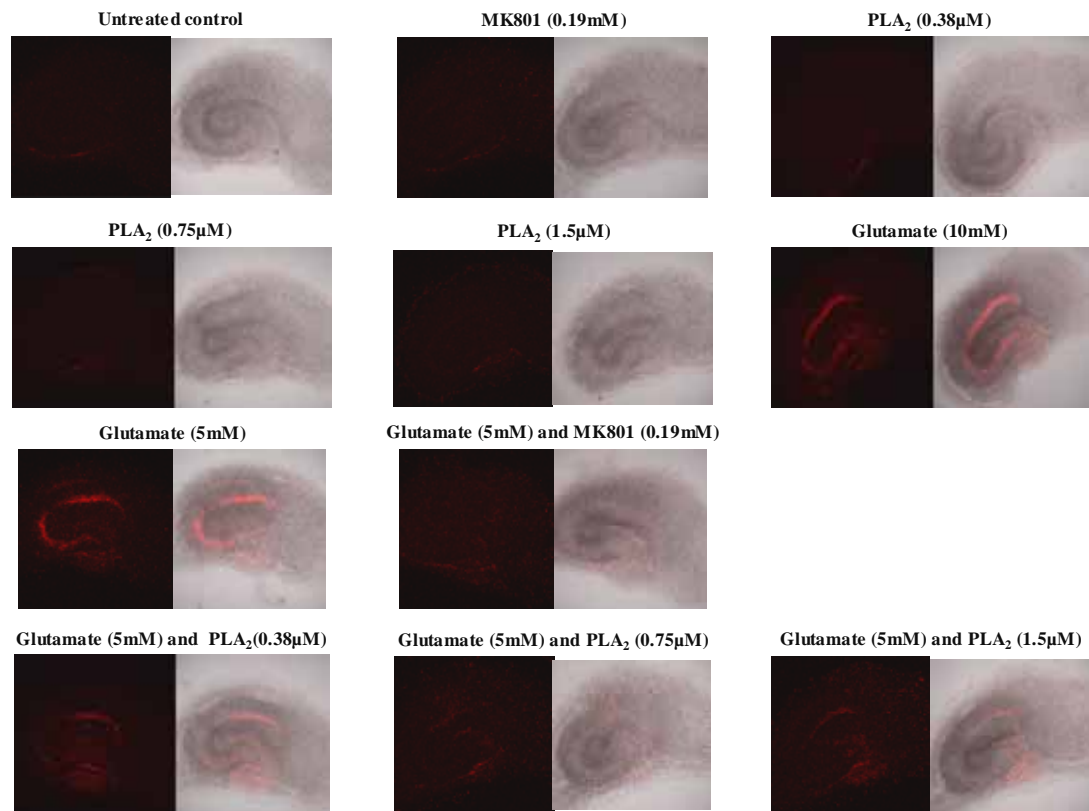
B)
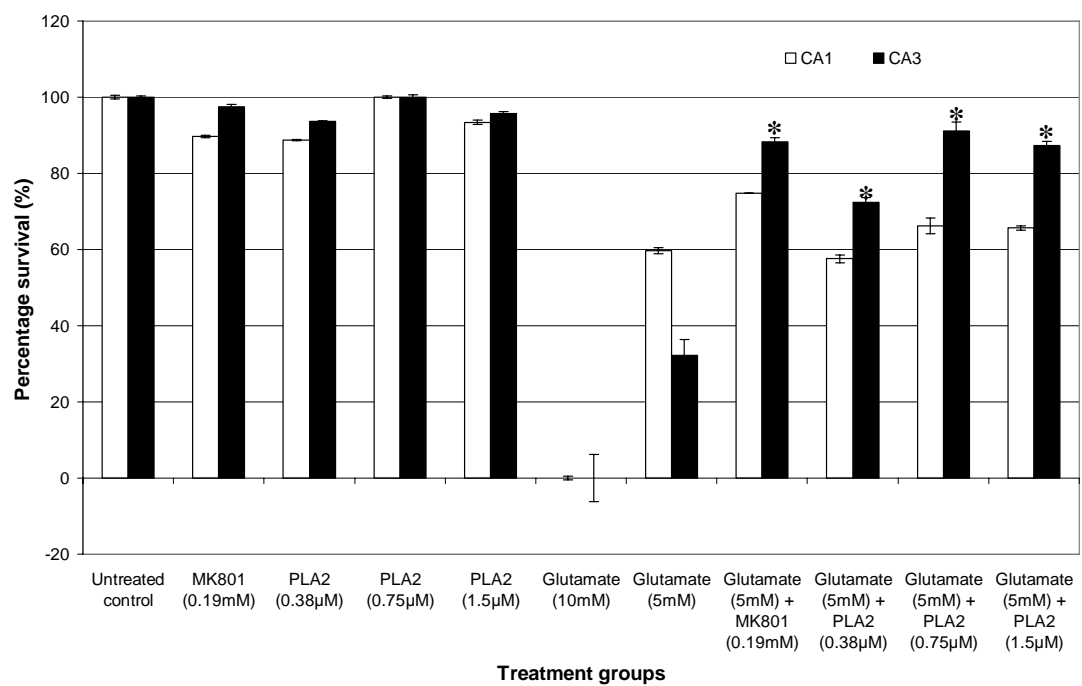
Fig. 5.5: **The effect of concurrent dose-dependent PLA$_2$ on glutamate-induced neuronal cell death. (A)** PI fluorescence of treated groups and **(B)** corresponding percentage survival graphs. Organotypic hippocampal cultures were incubated with MK801 (0.19mM) and various doses of PLA$_2$ (0.38µM, 0.75µM and 1.5µM) separately and found to be non-toxic to the cultures. When treated concurrently with glutamate, PLA$_2$ (0.38µM, 0.75µM and 1.5µM) was able to protect the CA3 region from glutamate damage. The damage of the CA1 and CA3 neuronal cell fields are expressed as a percentage of the area expressing fluorescence as compared with the untreated control cultures and 10mM glutamate was taken as maximum damage. Each point represents the mean ± SEM (n=8). *: p-value < 0.01 versus 5mM glutamate treatment.

A)
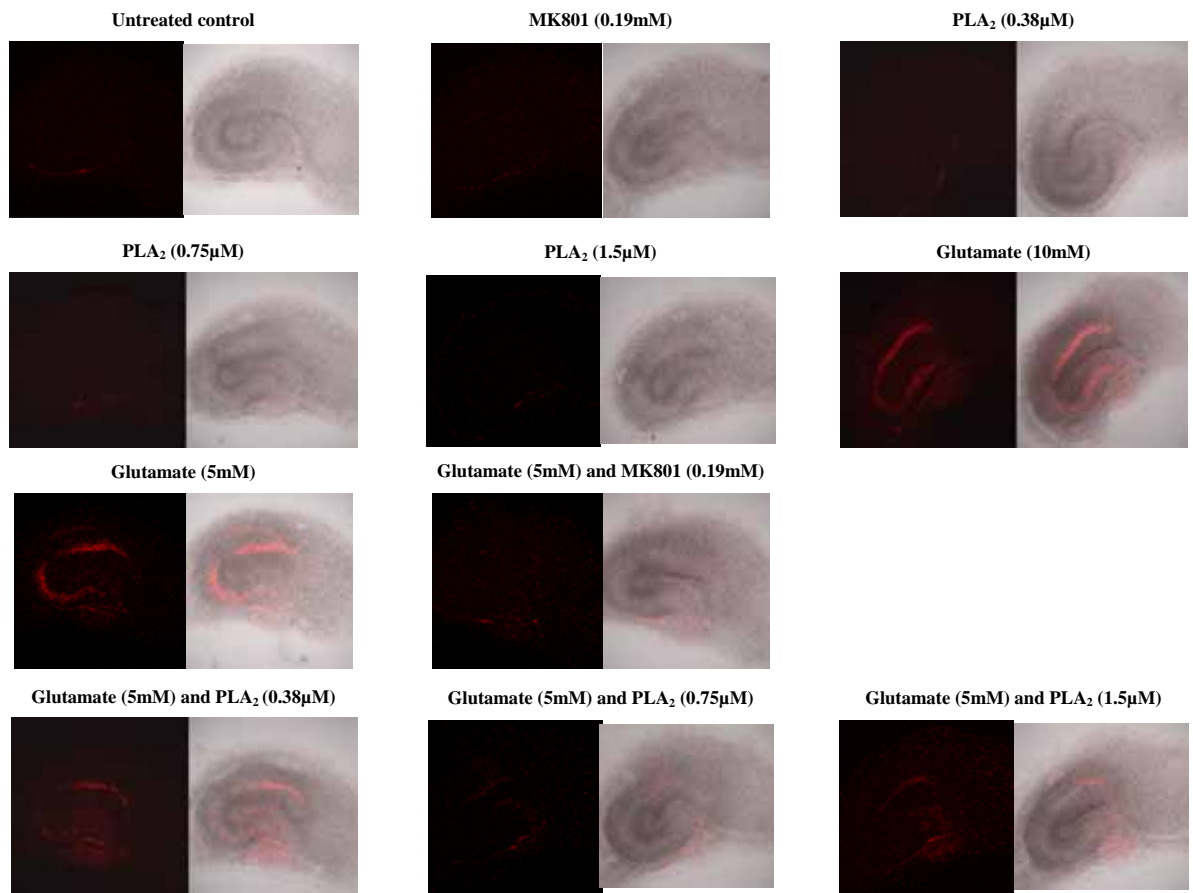
B)
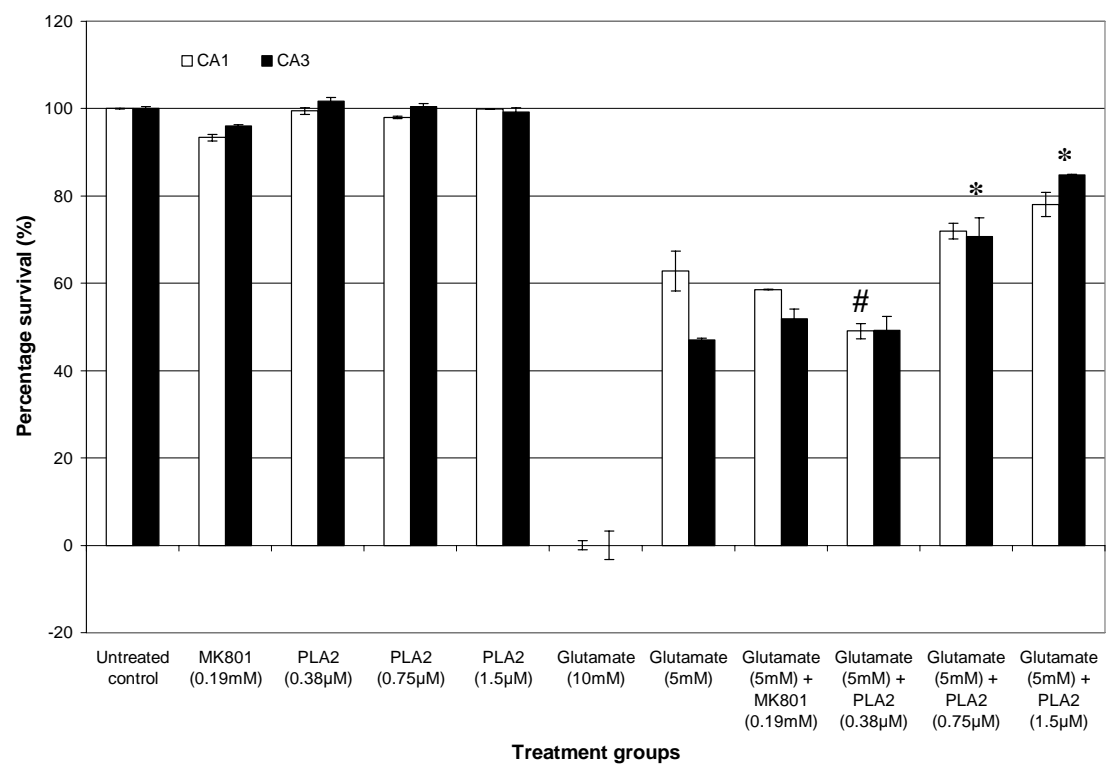
Fig. 5.6: **The effect of post-treatment of dose-dependent PLA$_2$ on glutamate-induced neuronal cell death.** **(A)** PI fluorescence of treated groups and **(B)** corresponding percentage survival graphs. Organotypic hippocampal cultures were incubated with MK801 (0.19mM) and various doses of PLA$_2$ (0.38µm, 0.75µm and 1.5µM) separately and found to be non-toxic to the cultures. When treated after glutamate insult, only PLA$_2$ at 0.75µM and 1.5 µM concentrations were able to protect the CA3 region from glutamate damage. It was better than MK801. In subsequent studies, the concentration of PLA$_2$ of 1.5µM was used. The damage of the CA1 and CA3 neuronal cell fields are expressed as a percentage of the area expressing fluorescence as compared with the untreated control cultures and 10mM glutamate was taken as maximum damage. Each point represents the mean ± SEM (n=8). *: p-value < 0.01 and #: p-value < 0.05 versus 5mM glutamate treatment.

respective classical glutamate receptor agonists: 2-amino-3-hydroxy-5-methyl-4-isoxazole propionic acid (AMPA), kainic acid (KA) and *N*-methyl-D-aspartate (NMDA). The excitotoxic effects of glutamate and its agonists have been studied in various experiments *in vivo* (Nadler *et al.*, 1978; Sheardown *et al.*, 1990; Lees and Leong, 1993) and *in vitro* (Jensen *et al.*, 1998) models. Together with glutamate receptor antagonists, they have provided evidence that activation of glutamate receptors plays a key role in various neurodegenerative diseases and conditions (Choi, 1992 and Dawson *et al.*, 1995). The concentration of agonists (10µM AMPA, 100µM KA and 20µM NMDA) were based on the 50% PI uptake from Kristensten *et al.* (2001). These agonists were concurrently treated with PLA$_2$ (1.5µM) for 3h. Addition of 40µM NMDA has resulted in total death, and as such was used as a positive control. It is known that susceptibility of the different hippocampal subfields (CA1 and CA3) vary for different agonists. AMPA caused damage to both CA1 and CA3 regions, while KA and NMDA caused more damage to the CA3 and CA1, respectively. Figure 5.7 shows the effect of PLA$_2$ (1.5µM) on hippocampal cultures when treated concurrently with the agonists. For the AMPA (10µM) treatment, the addition of PLA$_2$ caused significant protection for both the CA1 and CA3 regions. While with KA (100µM) treatment, the addition of PLA$_2$ provided protection to CA3 but no significant change to the CA1 region. The protection of PLA$_2$ on NMDA-treated cultures was similar to that observed for glutamate-mediated damage, i.e., protection for both CA1 and CA3 regions with PLA$_2$. Hence, the mechanism of action of PLA$_2$ was most likely via the glutamate-NMDA pathway.

A)
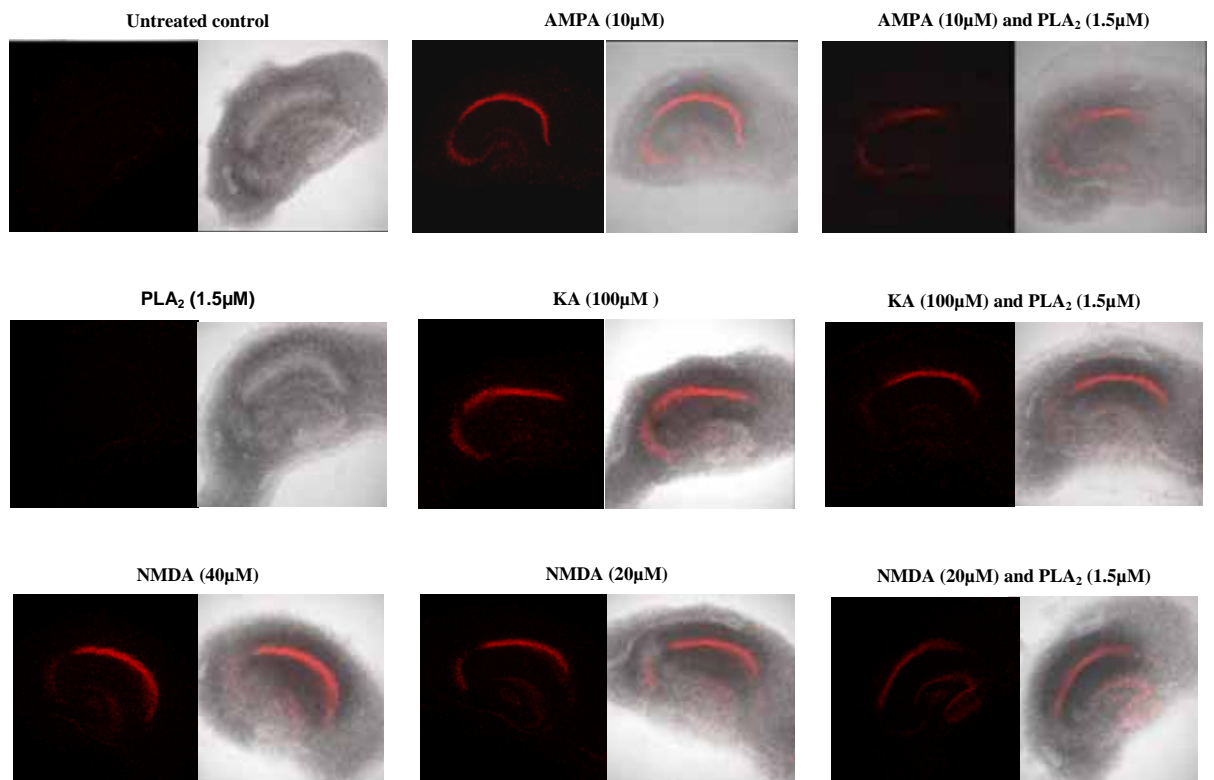
B)
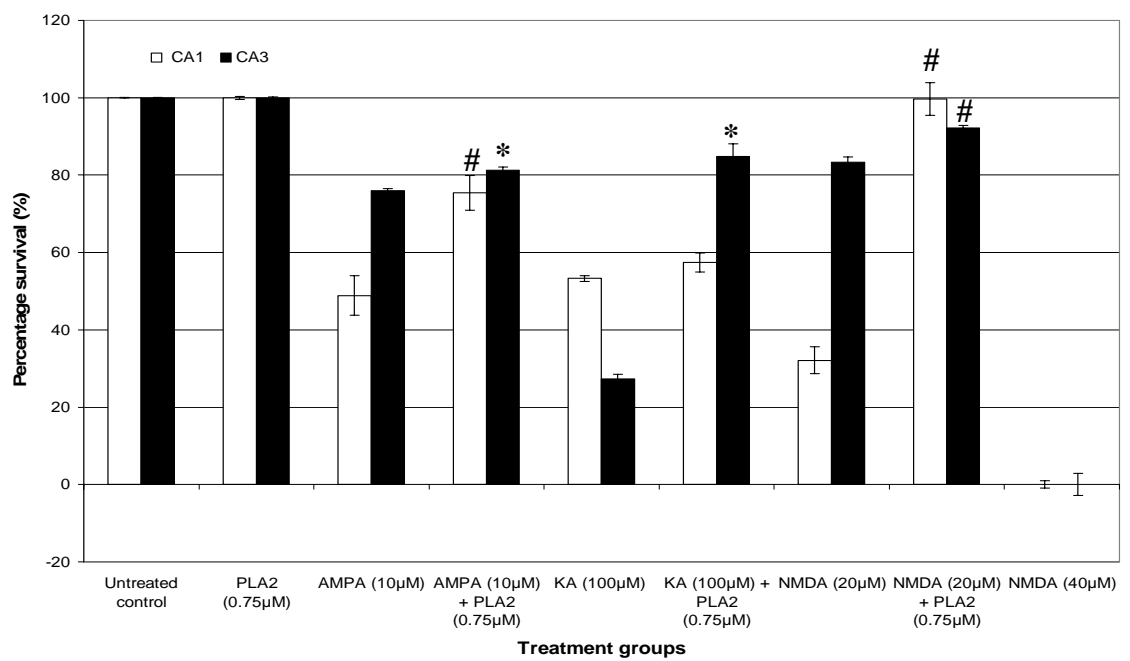
Fig. 5.7: **The effect of PLA$_2$ (1.5µM) and concurrent treatments with AMPA/KA/NMDA on hippocampal cultures.** **(A)** PI fluorescence of treated groups and **(B)** corresponding percentage survival graphs. Organotypic hippocampal cultures were incubated with glutamate agonists (AMPA at 10µM; KA at 100µM and NMDA at 20µM) separately and also concurrently with PLA$_2$ (1.5µM). PLA$_2$ (1.5µM) was able to reduce the damage by AMPA (both CA1 and CA3 region), KA (CA3 region) and NMDA (both CA1 and CA3 regions). The damage of the CA1 and CA3 neuronal cell fields are expressed as a percentage of the area expressing fluorescence as compared with the untreated control cultures and 40µM of NMDA was taken as the maximum damage. Each point represents the mean ± SEM (n=8). *: p-value < 0.01 and #: p-value < 0.05 versus the respective glutamate agonists (AMPA/KA/NMDA) treatments.

5.9 Effects of PLA$_2$ with group I metabotropic glutamate receptors (mGluRs)

Apart from interacting with the above-mentioned ionotropic glutamate receptors, glutamate also interacts with metabotropic glutamate receptors (mGluRs). The role of ionotropic glutamate receptors in neuronal cell death following brain ischemia is well-established (Gill and Logde, 1997; McCulloch, 1991). Recent evidence suggests that mGluRs, which are G-protein coupled receptors, may provide an effective alternative approach for neuroprotection against ischemic nerve cell death (Kalda *et al*., 2000). Since glutamate toxicity is mediated by excessive activation of NMDA receptors, the role of mGluR will be studied in relation to NMDA toxicity.

There are eight mGluR subtypes which have been divided into three major groups on the basis of sequence homology, signal transduction pathways and pharmacological sensitivities. The group I mGluR includes mGluR1 and mGLuR5; activation of these receptors causes the stimulation of phospholipase C, resulting in phosphoinositide (PI) hydrolysis and intracellular calcium mobilization (Pin and Duvoisin, 1995 and Schoepp *et al*., 1999). Since the PLA$_2$ and mGluR are known to mobilize calcium ions for activity, there is a possibility of a cross-talk/relationship between them. To determine the possible involvement of group I mGluR in the protective property of PLA$_2$, selective mGluR1 and mGluR5 agonists/ antagonists were utilized. To investigate the possible role of mGluR5 receptor, the mGluR5 agonist (R, S)-2-chloro-5-hydroxyphenylglycine (CHPG) and antagonist 6-methyl-2-(phenylethylnyl)-pyridine (MPEP) were used. CHPG has been shown to activate only mGluR5, but not mGluR1. MPEP is described as a selective non-competitive mGluR5 antagonist that acts by interacting with the transmembrane domains II and VI of mGluR5 receptor (Pagano *et al*., 2000), making it less sensitive to the

surrounding concentration of glutamate. At present, there is no specific agonist that activates mGluR1, hence a non-specific group I mGluR agonist, (S)-3,5-dihydroxyphenylglycine (DHPG) that activates both mGluR1 and mGluR5 was used. As a comparison, selective antagonist of mGluR1,

7-hydroxyiminocyclopropan[b]chromen-1a-carboxylic acid ethyl ester (CPCCOEt) was used. In this study, CP was used as a term to represent CPCCOEt. Cultures were treated with PLA_2 (1.5µM) for 30min prior to group I mGluR agonist/antagonist (DHPG/CHPG/MPEP/CP; 10µM) application and subsequently together with PLA_2 (1.5µM) for further 2h, followed by a final 30min exposure to 50µM of NMDA. The treated cultures were then transferred to a fresh basal MEM containing 5µg/ml PI for further 24h. Control cultures were subjected to NMDA treatment, followed by a transfer to fresh basal MEM containing PI. Concurrent treatments of PLA_2 (1.5µM) with mGluR agonists (DHPG or CHPG) resulted in protection at the CA1 region, while concurrent treatment of PLA_2 (1.5µM) together with antagonist for mGluR5 (MPEP) resulted in protection of both CA1 and CA3 regions (Fig. 5.8). Hence, the inhibition of mGluR5 did not block the protective effect of PLA_2 (1.5µM). In support of this conclusion, the antagonist for mGluR1, CP, when added together with PLA_2 (1.5µM) was not able to protect the cultures from NMDA damage, thereby, blocking the protective effect of PLA_2.

A)
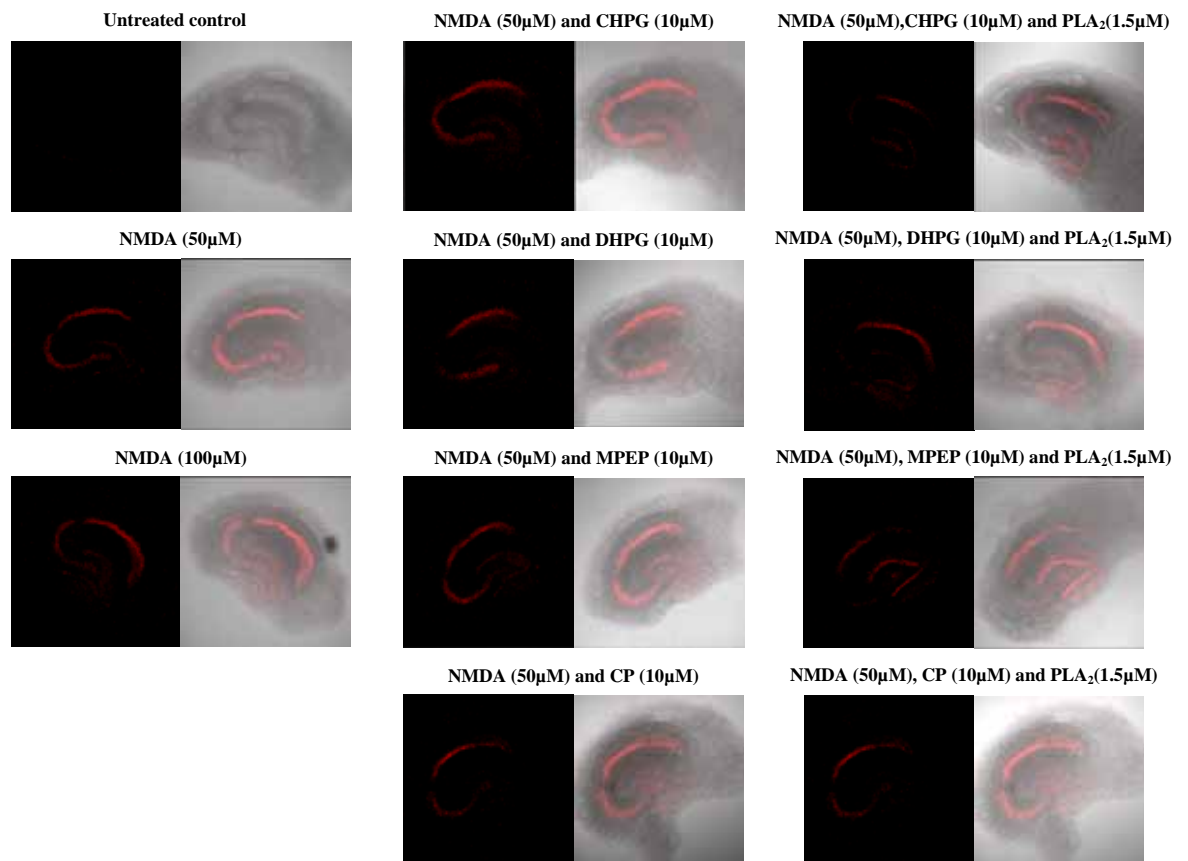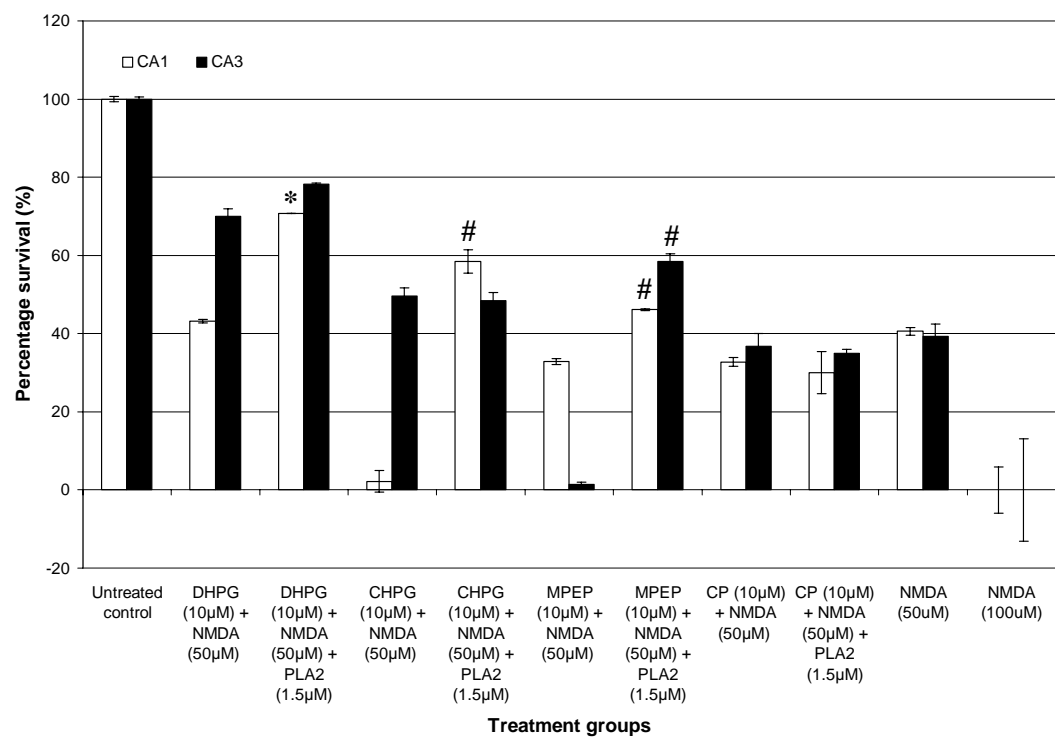
Fig. 5.8: The effect of PLA$_2$ (1.5µM) and concurrent treatments with glutamate metabotrophic agonist/antagonists (DHPG/CHPG/MPEP/CP) on hippocampal cultures. (A) PI fluorescence of treated groups and **(B)** corresponding percentage survival graphs. Cultures were treated with PLA$_2$ (1.5µM) for 30min and later concurrently with the selective metabotrophic agonists/antagonists (DHPG/CHPG/MPEP/CP) at 10µM for 2h and finally a 30min exposure to 50µM NMDA. PLA$_2$ (1.5µM) was able to reduce the damage by DHPG (CA1 region), CHPG (CA1 region) and MPEP (both CA1 and CA3 regions), but no significant improvement for CP. The damage of the CA1 and CA3 neuronal cell fields are expressed as a percentage of the area expressing fluorescence as compared with the untreated control cultures and 100µM of NMDA was taken as the maximum damage. Each point represents the mean ± SEM (n=8). *: p-value < 0.01 and #: p-value < 0.05 versus the respective glutamate metabotrophic agonist/antagonists (DHPG/CHPG/MPEP/CP) treatments.

Chapter 6

Discussion

6.1   **Snake venom and its components**

Snakes and their venoms have fascinated man since time immemorial and the use of venom in the treatment of different pathophysiological conditions has been mentioned in Ayurveda, homeopathy and folk medicine. Snake venom contains a toxic mixture of enzymes, low molecular weight polypeptides, glycoproteins and metal ions that are capable of causing local tissue damage as well as multiple system failure. Hence, the venom serves to immobilize and digest the prey and at the same time, defend against predators. From these complex mixtures of pharmacologically active proteins and polypeptides, several hundreds of toxins have been purified and characterized. Apart from contributing significantly to the understanding of snake venom toxicity and medical management of snake bite, the study of these toxins (e.g NGF and PLA$_2$) have also provided numerous research tools in deciphering the intricate details of various physiological processes at the molecular levels. The medical importance of snake venom components in the treatment of various disease conditions also serves to emphasize the growing interest in and the need for toxin research (Koh *et al*., 2006).

6.2   **Functional studies of mature NGF from *Naja sputatrix***

NGF activity was first described in two sarcoma tissues and in snake venoms, but the physical and biochemical properties have been deduced from the male mouse submaxillary gland (β-NGF). Mouse NGF has been widely studied and is commercially available. Lipps (1998) reported that the NGFs from venomous sources are of the highest potency, especially those from snakes, they approximately 1000-fold more active than the commercially available mouse NGF. The crude venom (250ng/ml) from 4 untested snakes when assayed for neurite outgrowth on

PC12 cells showed that the venom of *Naja sputatrix*, Malayan spitting cobra, exhibited the highest activity. This was followed by the venom from an Australian elapid, *Pseudonaja textiles* (Table 3.1). Thus the NGF from *N. sputatrix* venom was purified and its activity and properties were compared with that of the mouse NGF. The molecular weight of the native sputa NGF was found to be 14kDa, indicating that it is a monomer belonging to β-NGF family as suggested by Inoue *et al.* (1991). The cDNA encoding NGF from *Agkistrodon halys Pallas* has been reported previously (Guo *et al.*, 1999). In this project, the cloning of cDNAs encoding two isoforms of sputa NGF from *N. sputatrix* was done. Each cDNA encoded a signal peptide, pro-domain and the mature protein. The mature protein coding region for *N. sputatrix* was identified from its N-terminal amino acid sequence as well as from the amino acid sequence of *N. atra* NGF (Inoue *et al.*, 1991; Kostiza *et al.*, 1995) Comparison of sequences from the venom-derived NGFs with that of mouse NGF showed distinct variations at their N-terminal ends (Fig. 3.2). The snake NGF shows higher homology (~80%) to the mammalian derived nerve growth factors, suggesting similar function to the mammalian homolog. The venom-derived NGFs showed almost 80-90% homology among them and the two isoforms of *N sputatrix*, NGF (nsNGFI, nsNGFII) showed about 80% homology between them. The nsNGFI and nsNGFII showed 70% and 60% homology to the mammalian NGF, respectively. While the mature protein region for both the nsNGFI and II showed high homology, the pro-region showed considerable variation among them. Based on its higher homology to the mammalian NGF, nsNGFI was selected for the expression as a recombinant protein in *E. coli* and termed 'sputa NGF'. Furthermore, the refolded recombinant protein (sputa NGF) showed a similar CD spectrum to that of the native NGF protein (Fig. 3.4), indicating that sputa NGF

contains the same amount of secondary structure elements as the native NGF protein. Hence, it appears that sputa NGF have 2 pairs of β-sheets that are linked by 3 disulfide bonds. It was refolded in redox solution containing 2mM oxidized glutathione and 4mM reduced glutathione and showed enhanced activity compared to the unfolded NGF (Table 3.1). In addition, this refolded sputa NGF was found to be non-toxic to PC12 cells at 1μg/ml and was able to bring about enhanced neurite outgrowth in a dose dependant manner from 10ng/ml to 100ng/ml (Fig. 3.6B).

6.2.1 Expression of TrkA and p75 receptors

The sputa NGF was found to elicit neurite outgrowth via the TrkA-p75^{NTR} complex. Two protein forms of TrkA that predominate in cell extracts are a) 110-kDa N-glycosylated precursor form, gp110^{TrkA} and b) 140-kDa fully matured form, gp140^{TrkA} (Martin-Zanca *et al*., 1989). PC12 cells are known to respond rapidly to NGF, within minutes with a reproducible burst of tyrosine phosphorylation of many cellular proteins and including the TrkA receptors. We observed that the ratio of gp140^{TrkA} to gp110^{TrkA} decreased upon treatment with both mouse and sputa NGF. This decrease of ratio is attributed to the purpose of replenishing the mature gp140^{TrkA} at the cell surface as reported by Jullien *et al.* (2002). TrkA and p75^{NTR} receptors work in concert to coordinate and modulate responses of neurons to NGF. A competitive study using specific receptor antibodies on the percentage of neurite outgrowth showed that sputa NGF is more sensitive to receptor inhibition compared to that of mouse NGF. Reduced TrkA activation in both PC12 cells and sympathetic neurons has been observed upon addition of p75^{NTR}-specific antibodies (Kimpinski *et al*., 1999). The authors have also shown that any alteration in the optimal TrkA-p75^{NTR} interaction or direct activation of p75^{NTR} at the expense of TrkA will result in

an inhibition of NGF dependent neurite outgrowth in adult sensory neurons. In the present study, inhibition by TrkA and p75^{NTR} receptor-specific antibodies caused a reduction in neurite outgrowth for both mouse and sputa NGF by 34% and 70% for TrkA and 10% and 40% for p75^{NTR}, respectively. Thus, the greater reduction in neurite formation upon sputa NGF treatment implicates that sputa NGF is specific to TrkA and p75^{NTR} and stimulates signaling using the TrkA-p75^{NTR} high affinity complex as in the case of mouse NGF. This antibody based competitive study is in agreement with the quantitative analysis of the receptor (TrkA and p75^{NTR}) genes examined via real-time PCR. The expression of both receptors was higher with sputa NGF than with mouse NGF. Activation of TrkA and p75^{NTR} has been reported to induce the expression of NFκB, which in turn is known to cause neurite extension in PC12 cells (Foehr *et al*., 2000). Real-time PCR (Fig. 3.9) showed a down regulation of the NFκB inhibitor, IκB in both NGF treatments implying that NFκB will be made available to activate and promote neurite extension in PC12 cells and such NGF-induced increase in NFκB is beneficial for the survival of neurons (Maggirwar *et al*., 2000).

Protein profiling and real-time PCR results confirmed that an endogenous NGF synthesis is upregulated upon treatment with sputa NGF. Results from microarray analysis also showed arginine vasopressin receptor 1A (V1a) gene expression to be higher for sputa NGF treatment (20.25-fold change) compared to mouse NGF (5.43-fold change). In addition, arginine vasopressin is known to act mainly through the V1a receptor and to enhance NGF secretion in vascular smooth muscles and rat brain cells (Tuttle *et al*., 1993 and Zhou *et al*., 1997). Hence, sputa NGF could possibly be acting via V1a receptor to enhance the endogenous NGF production, an effect that will prove to be useful in conditions that require neuronal regeneration

and differentiation. Several studies have shown that neurotrophic factors including NGF constitute an important class of endogenous modulators of excitotoxicity, and are known to protect neurons against injury from several causes (Mattson *et al*., 1993). NGF has caused increase in glutathione levels of PC12 cells (Palmer *et al*., 1994) and hence upregulation (endogenous NGF genes) by sputa NGF may have potential neuroprotective roles.

6.2.2 Global gene and protein analysis

Microarray analysis (Table 3.2) showed for the first time the global changes in gene expression upon treatment with either mouse NGF or sputa NGF on PC12 cells. This study also yielded comparable data between the two NGFs. The differentiation pathway upon NGF treatment is characterized by expression of immediate early genes (such as early growth response 1, Egr 1; and serum-inducible kinase, Snk) and delayed response genes (such as Fos-like antigen, fra-1 and prostangladins-endoperoxide synthase 1). It was shown that Egr 1 acts via the ERK pathway to eventually produce neurite outgrowth in PC12 cells (Harada *et al*., 2001). Liby *et al.,* (2001) have shown that Snk has a role in cell proliferation. Expression of transcription factors, Fra-1 may participate in long-term neural responses (Paratcha *et al*., 2000); while over-expression of activating transcription factor 3 (ATF3) inhibited apoptosis (Nakagomi *et al*., 2003). Enhanced expression of transcription factors (Fra-1, ATF3 and Egr 1) may also cause subsequent increase in cathepsin E (CE) expression (Cook *et al*., 2001). This explains the increase in CE observed in this study (Table 3.2). CE is an aspartic proteinase that has been implicated in antigen processing in the class II major histocompatibility complex pathway and is known to be upregulated late in B cell activation (Sealy *et al*., 1996). The concurrent

upregulation of mast cell protease 7 in this study is in agreement with the previously reported effects of NGF on mast-cell development and differentiation (Welker *et al.*, 2000).

Arginine vasopressin receptor 1A (V1a) was observed to be highly expressed by sputa NGF treatment when compared to mouse NGF. V1a receptor is a widely distributed and known to regulate nearly all the physiological actions of the neuropeptide, vasopressin (AVP), except antidiuresis (V2) and corticotrophin secretion (V1b; Hawtin *et al.*, 2001). In addition to these, channel transporter genes (solute carrier family 1, member 3; SLC1A3, voltage-dependent calcium channel and purinergic P2X receptors) were found to be affected by the NGF treatment. Mouse NGF activated both the expression of SLC1A3 and P2X receptor genes, while sputa NGF activated the voltage-dependent calcium channel gene. The SLC1A3 gene encodes the glutamate receptor GLAST that is responsible for removal of glutamate to terminate neurotransmission and prevent neuronal cell death (Takai *et al.*, 1995), while the expression of voltage-dependent calcium channel subunit II is restricted to neuronal tissues for the maintenance of the neuronal physiology (Chemin *et al.*, 2001). Downregulation of P2X receptor was observed in both NGF treatments in this study. This proved to be beneficial as P2X is postulated to be involved in astrocyte-mediated inflammation and neurodegeneration (Gendron *et al.*, 2003). Upregulation of interleukin 12 (IL-12) and prostaglandin-peroxide synthase 1 seen in both cases also supports their beneficial roles. Prostaglandin-peroxide synthase 1 is believed to have a physiological role in neuronal differentiation of PC12 cells (Kaplan *et al.*, 1997). Similarly, IL-12 is known to play an important role in neuronal regeneration (Lin *et al.*, 2000).

Protein profiling results showed that treatment with sputa NGF enhanced the production of growth-associated proteins such as A-kinase anchor protein (Fig. 3.10). The A-kinase anchor protein (AKAP, 11.4kDa) belongs to a family of scaffolding proteins that bind to the regulatory subunits of protein kinase A (PKA), which regulates the phosphorylation of various proteins including those involved in synaptic. AKAP induction is known to stimulate PKA-dependent phosphorylation of the proapoptotic protein BAD (protein at 22.3kDa, thereby inhibiting the release of cytochrome c from mitochondria and protecting the cells from apoptosis (Affaitati *et al*., 2003). Though sputa NGF showed a marginal increase in BAD protein than mouse NGF, with AKAP upregulated about two fold than BAD, the pro-apoptotic property of BAD could be suppressed. This interpretation was confirmed experimentally by measuring for caspase activity on PC12 cells treated with sputa NGF. No caspase activity could be determined in these cells.

The mechanisms by which NGF exerts its neuroprotective effects are presently unknown. However, *in vitro* studies have shown that NGF can stabilize intracellular calcium by preventing accumulation of intracellular calcium and subsequent neuronal damage (Kirschner *et al*., 1996). The protein profiling results (Fig. 3.10) showed a downregulation in neurogranin (Ng; 8kDa). Ng is a neural-specific Ca^{2+}-sensitive calmodulin-binding (CaM) protein. It is believed that phosphorylated Ng has the potential to modulate neuronal free Ca^{2+} and CaM levels (Pak *et al*., 2000). Gene knockout experiments leading to total absence of Ng have resulted in deficiency of hippocampal synaptic plasticity and hippocampus dependent spatial learning (Pak *et al*., 2000). McNamara *et al* (2002) predicted that elevation in Ng expression would perturb Ca^{2+}-CaM signaling that may in turn impair the formation and/or maintenance of synapses. Thus, a reduced level of free Ng detected upon

treatment with sputa NGF indicates that a basal level of intracellular Ca^{2+} is maintained for neuronal differentiation and function.

Protein tyrosine phosphatase (SHP-1; 67.2kDa) was identified as a phosphotyrosine phosphatase that negatively regulates the expression of TrkA. It was shown in sympathetic neurons that expression of SHP-1 induces apoptosis and TrkA dephosphorylation (Marsh *et al.*, 2003). Hence, a downregulation of SHP-1 expression is also in agreement with TrkA activation upon treatment with both NGFs. Microarray and protein profiling analyses showed an increase in the expression of V1a (vasopressin) receptor and AKAP respectively, with sputa NGF treatment. AKAP, apart from regulating the phosphorylation of BAD, also phosphorylates other proteins (e.g. cAMP-specific phosphodiesterase-4D; PDE4D). The increase of V1a expression would indicate a response to vasopressin release. In response to vasopressin, PDE4D is activated through PKA thereby causing a reduction in osmotic water permeability. AKAP co-localized with PKA and PDE4D and therefore has a role in the regulation of water (Stefan *et al.*, 2007). Hence, sputa NGF treatment could possible act via V1a receptor to enhance the endogenous NGF production (protein-profiling) and concurrently reduce the water permeability.

6.3 Functional studies of precursor NGF from *Naja sputatrix*

NGF belongs to the neurotrophin family that regulates neuronal survival and synaptic plasticity (Patapoutian and Reichardt, 2001). They are synthesized as precursors (proneurotrophins) that are proteolytically cleaved to a mature, biologically active neurotrophin (Edwards *et al.*, 1988a). Due to their low expression levels, little is known about their processing and secretion by neurons and non-neuronal cells *in vivo*. However, when expressed in heterologous cells,

proneurotrophins are secreted and cleaved intracellularly by furin or proconvertases at a highly conserved dibasic amino acid cleavage side for secretion as a stable, noncovalent dimer (Heymach and Shooter, 1995; Mowla *et al*., 2001). Until recently, the functions for the neurotrophin prodomains have been limited to promoting the folding of the mature domain (Suter *et al*., 1991; Kolbeck *et al*., 1994; Rattenholl *et al*., 2001) and to sorting neurotrophins to either constitutive or regulated secretory pathway (Farhadi *et al*., 2000). However, sequence comparison of the prodomains revealed regions that are highly conserved across species, suggesting that they may mediate additional biological actions (Heinrich and Lum, 2000). ProNGF has long been postulated to contain biologically active peptide that could induce phosphorylation of the tyrosine residue of the TrkA receptor protein (Dicou *et al*., 1997). On the other hand, secreted proNGF has been reported to activate cell death in brain following an injury via p75^{NTR} and sortilin receptors (Nykjaer *et al*., 2004), thus indicating a pathophysiological role for the proNGF during CNS injury. Similarly, *in vitro* studies showed that proNGF is a high affinity ligand to p75^{NTR} and capable of inducing p75^{NTR}-dependent apoptosis in cultured neurons with minimal activation of TrkA-mediated differentiation or survival (Lee *et al*., 2001). In contrast, Fahnestock *et al* (2004) have shown that the proNGF is abundant in CNS tissues where mature NGF is undetected. The author has demonstrated that this proNGF is responsible for the biological activity normally attributed by mature NGF, in the CNS tissues. The death inducing property, if any, of the proNGF from snakes, in particular, *Naja sputatrix*, was investigated in this case.

6.3.1   Sequence comparison of NGFs from other species

Sequence comparison between *Naja sputatrix* (nsNGF I) and its mammalian counterparts (mouse and human NGFs) shows about 50% homology and the greatest relatedness is in the mature protein sequence (Fig. 4.1F). Differences in the prodomain region may be due to mature human β-NGF forming a complex with its α- and γ- subunits, whereas there is only one report of complex formation for the snake venom NGFs (Perez-Polo *et al*., 1978). Bioinformatics predictions on the NGF sequences from *Naja sputatrix* (nsNGF I), mouse (mNGF) and human (humNGF) revealed the potential differences in post-translational modification. ProNGF is post-translationally processed in the *trans*-Golgi network that may include covalent modification (e.g. phosphorylation, N-glycosylation, O-glycosylation, etc.) and proteolytic cleavage from precursor. Figure 4.1A shows a comparison of possible leucine-rich nuclear export signal (NES) between the three NGFs. Protein NES are hydrophobic-rich sequences with a characteristic spacing of leucine, isoleucine, valine, and/or phenylalanine. Leucine-rich NES consists of four or five hydrophobic residues within a region that is ~10 amino acids in length. The widely accepted NES consensus is LX2,3[LIVFM]X2,3LX[LI] (la Cour *et al*. 2003). At present, there are about 75 experimentally validated protein NES that have been identified and compiled in the NESbase version 1.0 database (la Cour *et al*. 2003). NetNES 1.1 program disclosed a putative NES for nsNGFI and none for mouse and human.

The potential sites for N-glycosylation were based on NetNglyc 1.0 database. Asn23 of the mature protein has been postulated as the glycosylation site in venom NGFs since it forms an *N*-glycosylation consensus sequence (NXS/T) (Kornfield *et al*., 1985; Gavel and von Heijne, 1990) and is absent from the unglycosylated

mammalian and cobra NGFs. Analysis of the elapid NGF amino acid sequences deduced from the cDNAs showed the presence of Asn23 in most snakes (Earl *et al.*, 2006), likewise this sequence was present in nsNGFI (Fig. 4.1F). However, NGF purified from *N. sputatrix* venom migrated at 14kDa by SDS-PAGE despite the presence of Asn23 in the corresponding sequence (Koh *et al.*, 2004), suggests that the glycosylation site is unmodified. Similarly, results obtained from the bioinformatics prediction showed no potential N-glycosylation site for nsNGFI, but mouse and human NGFs had two possible sites (Fig. 4.1C).

ProNGF is also processed by proteases that recognize the dibasic and tetrabasic cleavage sites flanking the sequence for mature NGF (Greene *et al.*, 1968; Edwards *et al.*, 1988a; Seidah *et al.*, 1996). The major furin-cleavage site for the processing of precursor to mature NGF is known to be located at the -1 and -2 positions (Heymach *et al.*, 1996). Most of the recent studies on proNGF had been done on proNGF mutated at this site. Based on the ProP 1.0 database, it disclosed a putative furin-cleavage site for nsNGF I, but two sites for both mouse and human (Fig. 4.1B). In addition, NetPhos 2.0 server also predicted differences in the number of residues phosphorylated between the three NGFs (nsNGF I, human and mouse).

6.3.2 Cloning and expression of mature NGF, pro (R/G) NGF and pro-domain

A cytosine-to-guanine mutation in the nsNGFI cDNA was designed to convert the arginine (R) residue at the -1 position in the proNGF polypeptide to a glycine (G) residue, thereby removing the basic cleavage site required to process proNGF to mature NGF. Recombinant wild-type (cleavable) NGF (mature NGF) or cleavage-resistant proNGF [pro (R/G) NGF] or pro-domain only were used to transfect CHO

cells. Both the mature and pro (R/G) NGFs produced neurites in PC12 cells, but a reduced number of neurites were observed for pro (R/G) treatment (Fig. 4.4). This was also reported by Lee *et al.* (2001). Through specific antibody inhibition of neurite outgrowth and real-time PCR, the presence and specificity of mature, pro (R/G) NGF and pro-domain were determined.

6.3.3 Effects of mature NGF, pro (R/G) NGF and pro-domain on healthy PC12 cells based on morphology and biochemical assays

Prior to treatment with the mature NGF, pro (R/G) NGF or pro-domain individually, PC12 cells were serum starved for 16-18h. There are basically two reasons for serum starvation; 1) NGF activity is due to the conditioned CHO media added and not the serum and 2) to show that NGF is able to act as a surviving factor against cell death. Neurites were observed for both mature and pro (R/G) NGF treatments, but none for pro-domain treatment (Fig. 4.4). Hence, the neurite-promoting activity is most likely from the NGF domain, as only mature and pro (R/G) NGFs contained it, while it is absent in pro-domain. Morphological structures (Fig. 4.4), biochemical analyses (Fig. 4.7A) and DNA laddering (Fig. 4.7B) indicated that pro-domain caused apoptosis. Pro-domain caused a loss of membrane integrity, DNA fragmentation and also an increase in both LDH and caspase activities. Pretreatment with a selective capase inhibitor, Ac-DEVD-CHO, followed by pro-domain treatment caused a decrease in caspase activity (Fig. 4.7C), indicating that pro-domain caused apoptosis via the caspase-mediated cell death pathway.

In normal and serum-deprived PC12 cells, treatment with both mature and pro (R/G) NGFs showed a neuroprotective effect. There were reductions in the loss of membrane integrity and also a decrease in both LDH and caspase activity (Fig.

4.7A). In addition, they [mature and pro (R/G) NGFs] protected the cells against DNA fragmentation (Fig. 4.7B). Taken together, both mature and pro (R/G) NGFs were capable of protecting the cells from the serum-deprived conditions. Hence, the presence of the pro-domain in pro (R/G) NGF did not block the neuroprotective effect of the NGF domain. In both morphological and biochemical studies, staurosporine (STS) was used as a positive control. This leads to a suggestion that when NGF-domain is present, the overall effect is dictated by the NGF-domain [in pro (R/G) NGF], leading to pro-survival and neuroprotection. However, once the NGF-domain is removed (in pro-domain), the overall effect is cell death via apoptosis. This hypothesis was tested in the receptor studies (TrkA, p75^{NTR} and sortilin) in the section 6.3.5.

6.3.4 Effects of mature NGF, pro (R/G) NGF and pro-domain on healthy PC12 cells based gene and protein expression assays

The cellular responses of neurotrophin (mature or precursor) are mediated by three distinct receptor classes (TrkA, p75^{NTR} and sortilin). The various combination of receptors would then dictate and regulate the final fate of the cell (survival or death; Nykjaer *et al*., 2004). P75^{NTR} is the common receptor required for the formation of the high-affinity binding sites and there are two possible outcomes depending on the "partner" receptor it binds to. It could either bind (1) with TrkA that binds to NGF, thereby activating the pro-survival pathway (Roux and Barker, 2002) or (2) with sortilin that binds proNGF and the complex is required for proNGF-mediated apoptosis (Nykjaer *et al*., 2004). The interaction of these three receptors was studied to investigate the possible mechanism of action of mature NGF, pro (R/G) NGF and pro-domain.

The quantitative analysis by real-time PCR (Fig. 4.8A) of the NGF receptor genes (TrkA and p75^{NTR}) is greatly increased for both mature and pro (R/G) NGFs, but higher for the mature NGF. The high expression levels of both receptors indicate the formation of the high-affinity complex with NGF (Roux and Barker, 2002), but since TrkA is present, the pro-survival pathway will most likely predominate. Sortilin is expressed in areas where NGF and proNGF, have well-characterized effects (Sarret *et al*., 2003; Hermans-Borgmeyer *et al*., 1999). While NGF regulates cell survival and cell death via binding to two different receptors TrkA and p75^{NTR} (Chao, 2003), proNGF selectively induces apoptosis through p75^{NTR} but not TrkA (Lee *et al*., 2001). It has been reported that sortilin acts as a co-receptor and molecular switch governing the p75^{NTR}-mediated pro-apoptotic signal induced by proNGF. Hence, the gene regulation of the sortilin gene can give us a clue as to how and which pathway is activated. If sortilin gene is expressed at low levels for all the three treatments [mature NGF, pro (R/G) NGF and pro-domain], thereby indicating no formation of complex with p75^{NTR} and hence no activation of the apoptosis pathway.

Apoptosis can be divided into extrinsic pathway, initiated through death receptors such as Fas, and the cell intrinsic pathway, which is initiated when cells are subjected to DNA damage, growth factor deprivation, etc. (Strasser *et al*., 1995). The cell intrinsic pathway is regulated by the Bcl-2 family of proteins. This family consists of both anti-apoptotic and pro-apoptotic members. One of the major anti-apoptotic members is Bcl-2 that exerts its effect at the mitochondrial outer membrane where they contribute to maintenance of membrane integrity. In the absence of apoptotic stimuli, anti-apoptotic Bcl-2 proteins protect the mitochondrial outer membrane from the pro-apoptotic activity (Lindsten *et al*., 2005). Upon

treatment with mature and pro (R/G) NGFs, the expression of Bcl-2 gene was downregulated, while treatment with pro-domain and staurosporine (positive marker) resulted in an upregulation of Bcl-2 gene. The upregulation of Bcl-2 gene could be a compensatory mechanism of the cell to survive, when faced with death-inducing agents (i.e. pro-domain and staurosporine) the Bcl-2 gene is increased to overcome the cell death signals. Western blot analysis (Fig. 4.8B) showed activation of TrkA for both mature and pro (R/G) NGFs treatments and is in agreement to the real-time results. Treatment of PC12 cells for 16-18h caused an increase in TrkA expression for both mature and pro (R/G) NGFs and none for pro-domain treatment (Fig. 4.8C). The expression of p75^{NTR} was greatly increased for pro (R/G) NGF, much more than mature NGF. This could be attributed to the property of proNGF being a high-affinity ligand for p75^{NTR} as observed by Lee *et al* (2001). In addition, the sortilin protein was upregulated for all treatments. Since p75^{NTR} is a common receptor needed by both TrkA and sortilin, it plays an important for in this balance of cell survival and death. In mature NGF treatment, though sortilin and TrkA are upregulated, TrkA is increased about 3-fold more than sortilin (Fig. 4.8C). The presence of TrkA and together with NGF will cause the pro-survival pathway to predominate. The similar pattern was observed for pro (R/G) NGF, with the expression level of TrkA being much higher than sortilin. However, with pro-domain treatment, there is relatively low expression of TrkA and high expression of p75^{NTR}, thereby causing the formation of the high-affinity complex between p75^{NTR} and sortilin and activating the apoptosis pathway. Apart from the decreased levels of TrkA needed to allow formation of p75-sortilin complex, the availability of p75^{NTR} receptors could be crucial. In the presence of TrkA and NGF, p75^{NTR} would combine with TrkA to form high-affinity binding sites for NGF, reducing the

amount left to bind to sortilin (in mature NGF). Hence, the overall fate of the cell is pro-survival.

To determine the possible complexes formed between the three receptors, specific antibodies to the receptors were used to inhibit their actions. PC12 cells were treated concurrently with specific antibodies to the receptors (TrkA, p75^{NTR} and sortilin) and the percentage of neurites determined (Fig. 4.9A). Treatment with anti-TrkA and anti-p75 antibodies caused a great reduction in neurite for both mature and pro (R/G) NGF. Hence, these two receptors are involved and needed in the neurite formation. Inhibition of sortilin has no effect, as it is not involved in the formation of the high-affinity complex (NGF, TrkA and p75^{NTR}). When both anti-sortilin and anti-p75^{NTR} antibodies were used in both mature and pro (R/G) NGFs treatments, the number of neurites was decreased, leading to an indication that both sortilin and p75^{NTR} may be involved in the neurite formation. Pro-domain did not cause neurite outgrowth, but LDH assay (Fig. 4.9B) showed that inhibition by all the three antibodies increased the cell survival. MTT assay (Fig. 4.9C) showed that inhibition with anti-p75 antibody caused a large decrease in cell survival for both mature and pro (R/G) NGFs. This is most likely due to the lack of p75^{NTR} for the formation of high-affinity complex to bind with TrkA that activate the cell survival pathway.

Taken together, these studies showed that the pro-domain is apoptotic, while the mature and pro (R/G) NGFs are neuroprotective. Differences observed in their function could be attributed to the differences in their structures. Pro-domain of NGF is covalently linked to the mature part to promote oxidative structure formation and to confer a pro-apoptotic activity to the NGF (Lee *et al*., 2001; Rattenholl *et al*., 2001). In addition, spectroscopic analyses revealed that on the NGF domain, a surface area around the tryptophan residue (Trp^{21}) interacted with pro-domain and

also participated in the binding of TrkA and p75^{NTR} receptors (Kliemannel *et al.*, 2007). Hence, the presence of Trp^{21} in both pro (R/G) NGF and mature NGF (contain the NGF domain) allowed them to bind to TrkA and p75^{NTR} and to activate the pro-survival pathway. On the other hand, the absence of Trp^{21} in the pro-domain (without the NGF domain) encouraged the interaction between p75^{NTR} and sortilin that activated the apoptotic pathway.

6.3.5 Oxygen-glucose deprivation- a model for ischemia

A fluorescence staining of the cells with Annexin V and Ethidium Homodimer III, showed that with OGD exposure, a higher percentage of cells undergo necrosis and apoptosis (Fig. 4.10Bii). Koubi *et al* (2005) also reported that PC12 cell death occurs by early necrosis upon exposure to OGD and later by delayed apoptosis during reperfusion. Figure 4.10Bii showed that both mature and the pro (R/G) NGF were able to protect the cells against OGD exposure, but pro (R/G) NGF to a lesser extent, while the pro-domain seemed to enhanced the damage. This observation was also observed in biochemical assays (Fig. 4.10C; LDH and caspase). Both mature and pro (R/G) NGF reduced the level of cytotoxicity for both assays, while pro-domain enhanced the level of cytotoxicity. This is most likely due to the presence of the NGF domain, leading to neuroprotection, whereas the pro-domain caused enhanced cell death. Quantitative gene analysis of the genes showed that NGF receptors (TrkA and p75^{NTR}) were reduced in expression from mature NGF to pro-domain (Fig. 4.10D). The reduction in expression is probably due to the reduction in forming the high-affinity complex and the activation of the pro-survival pathway (Roux and Barker, 2002). Without the NGF domain for pro-domain, the level of both TrkA and p75^{NTR} was very low compared to the rest. Sortilin expression for

mature and pro (R/G) NGFs were relatively low, this is probably due to the lack of binding by both pro (R/G) NGF and p75^{NTR} to activate the apoptotic pathway. It has been reported that sortilin acts as a co-receptor and molecular switch governing the p75^{NTR}-mediated pro-apoptotic signal as induced by proNGF (Nykjaer *et al*., 2004). The expression of sortilin was increased upon treatment with conditioned CHO media containing the pro-domain. This increase, together with p75^{NTR} will most likely activate the apoptotic pathway. This is supported by the increased in expression for NF-κB, IκB, Bcl-2 and Bcl-$_{XL}$ genes. The reason for the increased in these genes could be a compensatory mechanism for the cell to survive. In addition, the Bcl-2 family of proteins (e.g. anti-apoptotic Bcl-2 and Bcl-$_{XL}$; pro-apoptotic Bax and Bcl-$_{XS}$) has been suggested to play a role in ischemic-induced apoptosis. Overexpression of Bcl-2 reduces apoptosis during ischemia *in vivo* (Wang *et al*., 1999; Kitagawa *et al*., 1998). Hence, the expression of anti-apoptotic genes (Bcl-2 and Bcl-$_{XL}$) may help the cells to survive. From the gene expression patterns for the three treatments (mature NGF, pro (R/G) NGF and pro-domain), it gives us a clue about the possible mechanism of action that they exert their effects. Both mature and pro (R/G) NGFs are neuroprotective to OGD-exposure cells, while pro-domain enhanced the OGD damage and hence the cell's compensatory mechanism sets in to rescue.

6.3.6   Staurosporine-induced cell death of PC12 cells

Staurosporine (STS), a microbial alkaloid, has been reported to induce apoptosis in mammalian cells at micromolar concentrations (Jacobson *et al*., 1993; Zhang *et al*., 1996) by inhibiting protein kinases. Treatment of PC12 cells with STS resulted in membrane blebbing, DNA fragmentation and chromatin condensation.

Staurosporine (STS) at 0.5µM was used as a positive marker for apoptosis in this study to study effect of mature NGF, pro (R/G) NGF and pro-domain when treated with STS. However, in this study, there will be no comparison on the ability to cause neurite outgrowth as STS is capable of causing neurite outgrowth in PC12 cells. However, activation of the STS-activated kinase with the induction of neurite outgrowth did not require Ras function, while Ras was required for the activation of ERK pathway and neurite outgrowth by NGF (Yao *et al*., 1997). Morphological studies (Fig. 4.11Aii) with Annexin V and Ethidium Homodimer III showed that with mature NGF, the extent of apoptosis by STS was reduced greatly. There was no change for pro (R/G) NGF, but an increased death with pro-domain treated concurrently with STS. Hoechst staining also showed DNA condensation for all treatments, except for mature NGF (Fig. 4.11Aiii). The LDH assay also showed that mature NGF was able to reduce the cytotoxicity caused by STS treatment (Fig. 4.11B). Taken together, the results showed that mature NGF was capable of protecting the cells from STS, whereas pro (R/G) NGF and pro-domain were not able to protect the cells. This showed that only mature NGF was capable of protecting the cells against STS-mediated apoptosis.

6.4 Two potential neuroprotective agents from snake venom

In ischemic (OGD) condition, two components (NGF and PLA_2) from the venom of *Naja sputatrix* provided protection to PC12 cells and organotypic hippocampal cultures. Post-treatment of PC12 cells with either sputa NGF or PLA_2 individually after hypoxia, resulted in an increase in survival as determined by MTT assay (Fig. 5.1A). Similarly, PC12 cells when subjected to OGD, showed better survival when post-treated with either PLA_2 or sputa NGF individually (Fig. 5.1B). Tabakman *et al*

(2005) reported that pretreatment of PC12 cells with NGF prior to OGD exposure, resulted in 30% neuroprotection. OGD –induced PC12 cell death is largely due to apoptosis (Jiang *et al.*, 2005; Koubi *et al.*, 2005). Hence, it is tempting to suggest that the neuroprotective effect of NGF is related to a reduction in OGD-induced apoptosis. NGF-induced neuroprotection, in the OGD model, supports the role of NGF as a neuroprotective agent in the nervous system as previously documented in a variety of *in vitro* neuronal insults (Rukenstein *et al.*, 1991; Boniece and Wagner, 1995; Pan *et al.*, 1997).

Organotypic hippocampal culture is a good model to study as it maintains the physiological glial-neuronal relationship (Stoppini *et al.*, 1991). The concurrent treatment with NGFs (mouse and sputa), as well as PLA_2, resulted in protection against the OGD exposure, as observed from LDH assay (Fig. 5.1C). The protection by NGF has also been shown in different neurodegenerative disease models. For instance, treatment with neurotrophins (BDNF and NGF) helped to reduce the severity and death of the neurons (Zhang and Pardridge, 2006). Hence, a controlled increase in brain NGF levels may be beneficial in ameliorating certain neurodegenerative diseases such as Alzheimer's disease (Williams *et al.*, 2006). At present, the major obstacle in the therapeutic use of NGF for stroke, Alzheimer's disease and other brain diseases is its inability of the human recombinant NGF to cross the blood-brain barrier. Therefore, the development of novel delivery technologies for proteins such as NGF will provide the way for this important neurotrophin to the clinic. Compared to NGF as a neuroprotective agent for neurodegenerative diseases, PLA_2 is relatively new. Since PLA_2 is able to protect against hypoxia and OGD in PC12 cells, as well as in organotypic hippocampal cultures, its possible mechanism of action was investigated.

6.4.1 Effect of PLA$_2$ on cultures exposed to OGD conditions

PLA$_2$, a component found in *Naja sputatrix* venom has a neuroprotective effect in ischemic injury and a possible underlying mechanism by which this neuroprotection occurs was proposed. The organotypic hippocampal cultures were used to examine its effects in an *in vitro* model of 'ischemic-like' insult' using OGD as they provide good experimental system to mimic the pathophysiological pathways in living tissues (Stoppini *et al*., 1991). In particular, hippocampal slice cultures combined with OGD could provide a surrogate system to investigate cell loss following ischemic injury to the brain. Using this model, it was shown that PLA$_2$ at 0.75μM promoted about 60% and 95% survival at the CA1 and CA3 regions, respectively, whereas PLA$_2$ at 1.5μM showed 95% protection for both regions (Fig. 5.3). The results for PLA$_2$ (1.5μM) was similar to what was observed for MK801, a selective non-competitive antagonist of NMDA receptor channel. MK801 was used as a positive marker for neuroprotection as it has been shown to be highly neuroprotective in both models of ischemia and hypoxia (Wong *et al*., 1986; Pringle *et al*., 1997).

Since apoptosis is implicated in ischemia (Love, 2003), the apoptotic genes were investigated. In addition, the Bcl-2 family of proteins (e.g. anti-apoptotic Bcl-2 and Bcl-$_{XL}$; pro-apoptotic Bcl-$_{XS}$ and Bax) has been suggested to play a role in ischemia-induced apoptosis. Quantitative gene analysis of these apoptotic genes (Fig. 5.4) showed that concurrent treatment with either PLA$_2$ (0.75μM and 1.5μM) or MK801 (0.19mM) on cultures subjected to OGD caused an upregulation of both anti-apoptotic genes (Bcl-2 and Bcl-$_{XL}$), but a downregulation of apoptotic gene (Bax). Bax can homodimerize with itself and heterodimerize with Bcl-2 or Bcl-$_{XL}$. It appears that Bax homodimers activate apoptosis, while heterodimers inhibit the

process (Adams and Cory, 1998). The high expression of both anti-apoptotic genes (Bcl-2 and Bcl-$_{XL}$), could possibly cause heterodimers to form, thereby inhibiting apoptosis and promoting neuroprotection. Moreover, an elevated intracellular ratio of Bax to Bcl-2 occurs during increased apoptotic cell death (Zha and Reed, 1997), while *in vivo* ischemia studies showed that overexpression of Bcl-2 reduces apoptosis (Wang *et al*., 1999; Kitagawa *et al*., 1998). Taken together, the quantitative real-time PCR results showed that apoptosis is reduced upon treatment with PLA$_2$. In addition to genes related to apoptosis, the possible pathway of mGluR was investigated. Homer proteins (Homer 1b, 1c, 2 and 3) induce dendritic localization of group I mGluRs and receptor clustering, either internally or on the plasma membrane (Kammermeier, 2006). The Homer gene (Fig. 5.4) was upregulated for both PLA$_2$ (0.75µM and 1.5µM) or MK801 (0.19mM) treatments on OGD cultures, thereby indicating a possible link between PLA$_2$ and group I mGluRs.

6.4.2 Effect of PLA$_2$ on glutamate-mediated insult

Neurotransmitter such as glutamate has been implicated as potential neurotoxic agents in several neurological disorders including ischemia, epilepsy and neurodegenerative diseases. However, the molecular mechanisms underlying glutamate toxicity in these disorders are not well understood, but it has been shown that accumulation of Ca^{2+} induced cell death by both necrosis and apoptosis. PLA$_2$ was tested for its neuroprotective ability at three different phases of glutamate insult. PLA$_2$ was added either before (pretreatment), during (concurrent) or after (post-treatment) glutamate insult. Pretreatment with PLA$_2$ did not cause any neuroprotection, but MK801 provided protection against glutamate insult (results

not included). Concurrent treatment with PLA_2 caused a protection against glutamate insult in a dose-dependent manner (Fig. 5.5), while post-treatment showed protection with PLA_2 and none for MK801 (Fig. 5.6). The glutamate studies showed that PLA_2 mechanism of action for neuroprotection is possibly through an indirect pathway that blocks the downstream toxic effects of glutamate.

Agonists to the three classes of glutamate ionotrophic receptors; AMPA, NMDA and KA were treated concurrently with PLA_2 (Fig. 5.7). PLA_2 was able to protect the CA3 regions for all the three, but CA1 for only NMDA and AMPA. PLA_2 was able to partially protect against AMPA excitotoxicity. Since AMPA receptors are involved in the neuroprotection by PLA_2, this suggests an involvement of KA receptors. In accordance with this, the activation of KA receptors, which are predominantly expressed in CA3, may account for the selective neuroprotection by PLA_2. During the concurrent treatment with PLA_2 and NMDA (Fig. 5.7), PLA_2 protected both the CA1 and CA3 regions. This may be explained by the general high permeability of NMDA receptors to Ca^{2+} (Moriyoshi *et al*., 1991; Wahl *et al*., 1989) as compared to AMPA (Keinanen *et al*., 1990; Sommer *et al*., 1990; Hollmann *et al*., 1991; Jonas and Burnashev, 1995) and KA (Wisden and Seeburg, 1993; Nakanishi and Masu, 1994; Jorgensen *et al*., 1995; Bernard *et al*., 1999). The neuroprotective role of PLA_2 most likely involved Ca^{2+}, hence a reduction in Ca^{2+} permeability, may restrict its action.

Among the three ionotrophic receptors, NMDA has the most similar pattern of protection to glutamate as both CA1 and CA3 are protected. Unlike ionotrophic glutamate receptors, mGluRs do not activate ion channel directly but instead activate second messenger mechanisms. The group I mGluRs are unique from the other mGluRs, in that certain splice variants (mGluR1a and mGluR5a and b) are directly

connected to the IP_3- and ryanodine receptors on the endoplasmic reticulum by postsynaptic proteins termed Homer (Tu *et al*., 1998; Xiao *et al*., 1998). Coupling of Homer to group I mGluRs have also been implicated in mGluR trafficking and clustering (Ango *et al*., 2000 and 2002). Through the Homer proteins, group I mGluRs can bind directly to NMDA receptors (Tu *et al*., 1998). Apart from their ability to increase intracellular Ca^{2+}, group I mGluRs have also shown to negatively modulate K^+ channels as well as activate cationic channels (Pin and Duvoisin, 1995; Chung *et al*., 2000). Real-time PCR results on the cultures exposed to OGD and concurrently treated with PLA_2 showed a possible involvement of Homer (Fig. 5.3). The activation of group I mGluRs was prior to the NMDA exposure, because no neuroprotection was observed if DHPG was added 2h immediately after the insult (Blaabjerg *et al*., 2003). Co-application of a group I mGluR agonist and NMDA may potentiate NMDA responses through phosphorylation of the NMDA receptors, causing a relief of the Mg^{2+} block and increasing the Ca^{2+} influx through the associated channel to a toxic level (Bruno *et al*., 1995). However, a pretreatment with the group I mGluR agonist would increase intracellular Ca^{2+} causing inhibition of NMDA receptors or result in their internalization (Synder *et al*., 2001), so that subsequent exposure would yield a decreased response. The results showed that activation of group 1 mGluR by both DHPG and CHPG maintained the protection of PLA_2 (Fig. 5.8). Similarly, treatment with group I mGluR antagonists, MPEP that selectively blocked mGluR5, still allowed PLA_2 to be neuroprotective. However, concurrent treatment with an mGluR1-specfic antagonist, CP, blocked totally the neuroprotective effect of PLA_2. Hence, the possible mechanism of action for the neuroprotective effect of PLA_2 is most likely via the mGluR1.

6.5   Conclusion

Since historical days, the inherent toxicity and diversity of snake venoms and its constituents have always fascinated scientists. It is essentially a cocktail of compounds, composed mainly of proteins that the snake uses for attack and defense. At present, there is substantial amount of information available on the composition and distinct toxicities of snake venoms. In addition, the structure, function, molecular biology, chemistry and pharmacology of venom toxins have been well-documented. However, the exact mechanism and targets of many snake venom and its toxins remain ambiguous. This project investigated a potentially useful component from the venom of *Naja sputatrix* – NGF, as well as the functional roles for both mature and precursor NGF. In addition, the possible mechanism of action of another component, PLA$_2$ was deciphered.

Sputa NGF seems to exert potentially life-sustaining and neuroprotective (e.g. NFκB and endogenous NGF genes) effects in a manner similar to that of mouse NGF. The survival-promoting effects have been observed at both gene (microarray) and protein (SELDI-TOF) levels. Sputa NGF was also found to increase the expression of vasopressin 1A receptor and endogenous NGF genes as well as the NGF precursor and the AKAP proteins. However, both neurogranin and SHP-1 proteins have been found to be downregulated upon treatment with sputa NGF. Real-time PCR analysis has revealed additional pro-survival effects of sputa NGF such as enhanced expression of NFκB and the endogenous NGF genes. These effects could have potential neuroprotective roles. In this project, the functional studies of the sputa NGF (mature NGF expressed in *E. coli*) was thoroughly studied at both gene and protein levels and proved to be a preferable substitute to mouse NGF.

Three different physiological conditions were used to study the functional role of the precursor NGF [pro (R/G) NGF]; normal, ischemic (OGD) and apoptotic (STS) conditions. In all these conditions, apart from pro (R/G) NGF, both mature NGF and pro-domain were also tested. In the normal conditions, pro (R/G) NGF behaved in a manner similar to mature NGF as shown by the biochemical assays (LDH and caspase) and cell morphology studies. Under ischemic conditions, pro (R/G) NGF was able to protect the cells from the OGD exposure, but to a lesser extent than mature NGF, while in apoptotic conditions (STS) it could not protect the cells from cell death. A comparison between the three conditions showed that pro (R/G) NGF was able to protect the cells in normal serum-deprived and ischemic conditions, but not for the apoptotic condition. On the contrary, pro-domain caused an increased in cell damage for all three conditions. Real-time studies showed that all three (mature NGF, pro (R/G) NGF and pro-domain) were capable of activating both TrkA and $p75^{NTR}$, in decreasing order. However, western blot protein analysis showed that pro (R/G) NGF caused an upregulation of $p75^{NTR}$ more than the mature NGF and pro-domain treatments, owning possibly to its higher affinity to $p75^{NTR}$. Hence, the possible role of pro (R/G) NGF is to balance cell death or survival depending on the *in vitro* and *in vivo* conditions of the cell, whereby in healthy and ischemic conditions it supports survival while in apoptotic, it triggers the cell-death pathway.

PLA_2 provided protection against glutamate and OGD-mediated cell death in organotypic hippocampal cultures. Real-time PCR results showed that treatment with PLA_2 resulted in an upregulation of anti-apoptotic genes (Bcl-2 and Bcl-$_{XL}$) and a down-regulation of apoptotic gene (Bax), leading to a possible overall reduction in apoptosis-mediated cell death. Using specific agonists and antagonists to the

ionotrophic and metabotrophic glutamate receptors, the possible receptor involved in neuroprotection by PLA_2 was determined to be mGluR1.

The results of this study highlighted the beneficial components from snake venom, in particular NGF and its precursor, in both physiological and pathophysiological states.

6.6   Future studies

This study has just unraveled the "treasure box" of NGF from snake venom as a potential therapeutic agent against ischemia and that the precursor of NGF is not just an innocent bystander. The microarray results of PC12 cells treated with either sputa or mouse NGF (Chapter 3) could be further substantiated with real-time PCR and western blot analysis. In addition, the activation of TrkA receptors could also be proven by immunoprecipitation method to ascertain the identity of the tyrosine phosphorylated protein (TrkA). More studies will be necessary to fully comprehend the delicate balance between the mature and precursor NGF in deciding the overall fate of the cell (survival or death). In the proNGF study (Chapter 4), apart from using bioinformatics tools to predict the glycosylation status of nsNGF and mouse NGF, deglycosylation using N- and O-glycosidases could also show the presence of O- and N-glycosylation in these proteins. The function of the pro (R/G) NGF was found to behave in a similar manner as the mature NGF, but less robust in promoting neuroprotection in apoptotic conditions (STS). Much work is needed to understand the difference between the two [mature and pro (R/G) NGF], possibly by studying the downstream proteins in the pro-survival pathway. In addition, the pro-domain was found to be apoptotic and proteins in the caspase pathway could be investigated.

The interaction between the three receptors (TrkA, p75^{NTR} and sortilin) could be confirmed by silencing the gene individually (siRNA) and observing the overall effect of the cell (neurotrophic or apoptotic).

For the PLA$_2$ (Chapter 5) study, the possible receptor was found to be mGluR1, but more work is needed to validate it, either by western blot or real-time PCR on the pathway. To confirm the interaction of mGluR1 and PLA$_2$, the expression of mGluR1 could be silenced (siRNA). In addition, a neuroarray (DNA microchip with genes from the brain) to determine the genes regulated by NGF and PLA$_2$ treatments separately, will be required to gain a broader understanding of their biological effects. Organotypic hippocampal cultures subjected to OGD/glutamate insult can be treated separately with different forms of NGF [mature NGF, pro (R/G) NGF and pro-domain], as well as with PLA$_2$. The total RNA isolated can be used in microarray studies. These studies will definitely uncover useful and beneficial effects that may be extended for the development of therapeutic agents for disease intervention and treatment.

References

Abu-Raya, S., Trembovler, V., Shohami, E. and Lazarovici, P. (1993) A tissue culture ischemic device to study eicosanoid release by pheochromocytoma PC12 cultures. *J Neurosci Methods*. **50:** 197-203.

Abu-Raya, S., Blaugrund, E. and Trembovler, V., Shohami, E. and Lazarovici, P. (1999) Rasagiline, a monoamine oxidase-B inhibitor, protects NGF-differentiated PC12 cells against oxygen-glucose deprivation. *J Neurosci Res.* **5:** 456-463.

Adams, J.M. and Cory, S. (1998) The Bcl-2 protein family: arbiters of cell survival. *Science* **281:** 1322-1326.

Affaitati, A., Cardone, L., Cristofaro, T., Carlucci, A., Ginsberg, M.D., Varrone, S., Gottesman, M.E., Avvedimento, E.V. and Feliciello, A. (2003) Essential role of A-kinase anchor protein 121 for cAMP signaling to mitochondria. *J Biol Chem.* **278:** 4286-4294.

Agerman, K., Baudet, C., Fundin, B., Willson, C. and Ernfors, P. (2000) Attenuation of a caspase-3 dependent cell death in NT4- and p75- deficient embryonic sensory neurons. *Mol Cell Neurosci.* **16:** 258-268.

Alkin, J.G. and Bradshaw, R.A. (1993) Nerve growth factor and related substances: structure and mechanism of action. In: Neurotrophin factors. Loughlin, S.E and Fallon, J.H. (Eds). San Diego, California, USA: Academic Press Inc. **pp:** 120-180.

Allsopp, T.E., Robinson, M., Wyatt, S. and Davies, A.M. (1994) TrkA mediates an NGF survival response in NGF-independent sensory neurons but not in parasympathetic neurons. *Gene Ther.* **1:** S59.

Aloe, L. (2004) Nerve growth factor, human skin ulcers and vascularization. Our experience. *Prog Brain Res.* **146:** 515-522.

Aloyz, R.S., Bamji, S.X., Pozniak, C.D., Toma, J.G., Atwal, J., Kaplan, D.R. and Miller, F.D. (1998) p53 is essential for developmental neuron death as regulated by the TrkA and p75 neurotrophin receptors. *J Cell Biol.* **143:**1691-1703.

Anand, P. (1992) The skin axon-reflex vasodilation-mechanism, testing and implications in autonomic disorders. In: Bannister, R. and Mathias, C. (Eds). Autonomic failure, 3rd edition. Oxford University Press, Oxford, **pp:** 479-488.

Anand, P. (1997) The role of neurotrophic factors in leprosy and other human peripheral neuropathies. In: Antia, N.H. and Shetty,V.P. (Eds). The peripheral nerve in leprosy and other neuropathies. Oxford University Press Delhi, **pp:** 231-240.

Anand, P., Rudge, P., Mathias, C.J., Springall, D.R., Ghatei, M.A., Naher-Noe, M., Sharief, M., Misra, V.P., Polak, J.M., Bloom, S.R. and Thomas, P.K. (1991) A new autonomic and sensory neuropathy with loss of sympathetic adrenergic function and sensory neuropeptides. *Lancet* **337:** 1253-1254.

Anand, P., Pandya, S., Ladiwala, U., Singhal, B., Sinicropi, D.V. and Williams-Chestnut, R.E. (1994) Depletion of nerve growth factor in leprosy. *Lancet* **344:** 129-130.

Anand, P., Terenghi, G., Warner, G., Kopelman, P., Williams-Chestnut, R., and Sinicropi, D.V. (1996) The role of endogenous nerve growth factor in human diabetic neuropathy. *Nat Med.* **2:** 703-707.

Angeletti, R.A. (1970) Nerve growth factor from cobra venom. *Proc Natl Acad Sci USA* **65:** 668-674.

Ango, F., Pin, J.P., Tu, J.C., Xiao, B., Worley, P.F. and Bockaert, J. and Fagni, L. (2000) Dendritic and axonal targeting of type 5 metabotrophic glutamate receptor is regulated by homer 1 proteins and neuronal excitation. *J Neurosci.* **20:** 8710-8716.

Ango, F., Robbe, D., Tu, J.C., Xiao, B., Worley, P.F., Pin, J.P., Bockaert, J. Fagni, L. (2002) Homer-dependent cell surface expression of metabotrophic glutamate receptor type 5 in neurons. *Mol Cell Neurosci.* **20:** 323-329.

Apfel, S.C., Schwartz, S., Adornato, B.T., Freeman, R., Biton, V., Rendell, M., Vinik, A., Giuliani, M., Stevens, J.C., Barbano, R. and Dyck, P.J. (2000) Efficacy and safety of recombinant human nerve growth factor in patients with diabetic polyneuropathy: A randomized controlled trial. rhNGF Clinical Investigator Group. *JAMA.* **284:** 2215-2221.

Apfel, S.C. (2002) Nerve growth factor for the treatment of diabetic neuropathy: what went wrong, what went right, and what does the future hold? *Int Rev Neurobiol.* **50:** 393-413.

Armugam, A., Earnest, L., Chung, M.C., Gopalakrishnakone, P., Tan C.H., Tan, N.H. and Jeyaseelan, K. (1997) Cloning and characterization of cDNAs encoding three isoforms of phospholipase A2 in Malayan spitting cobra (*Naja naja sputatrix*) venom. *Toxicon* **35:** 27-37.

Ayer-LeLievre, C., Olson, L., Ebendal, T., Seiger, A. and Persson, H. (1988) Expression of the beta-nerve growth factor gene in hippocampal neurons. *Science* **240:** 1339-41.

Bahr, B.A., Kessler, M., Rivera, S., Vanderklish, P.W., Hall, R.A., Mutneja, M.S., Gall, C. and Hoffman, K.B. (1995) Stable maintenance of glutmate receptors and other synaptic components in long-term hippocampal slices. *Hippocampus* **5:** 425-439.

Barrett, G.L. and Bartlett, P.F. (1994) The p75 nerve growth factor receptor mediates survival or death depending on the stage of sensory neuron development. *Proc. Natl. Acad. Sci. USA* **91:** 6501–6505.

Barett, J.C. and Kawasaki, E.S. (2003) Microarrays: the use of oligonucleotides and cDNA for the analysis of gene expression. *Drug Discovery Today* **8:** 134-141.

Beattie, E.C., Howe, C.L., Wilde, A., Brodsky, F.M. and Mobley, W.C. (2000) NGF signals through TrkA to increase clathrin at the plasma membrane and enhance clathrin-mediated membrane trafficking. *J Neurosci.* **20:** 7325-7333.

Beattie M. S., Harrington A. W., Lee R., Kim J. Y., Boyce S. L. and Longo F. M. *et al*. (2002) ProNGF induces p75-mediated death of oligodendrocytes following spinal cord injury. *Neuron* **36:** 375–386.

Benedetti, M., Levi, A. and Chao, M.V. (1994) Differential expression of nerve growth factor receptors leads to altered binding affinity and neurotrophin responsiveness. *Proc Natl Acad Sci USA* **90:** 7859-7863.

Beraud, C., Henzel, W.J. and Baeuerle, P.A. (1999) Involvement of regulatory and catalytic subunits of phosphoinositide-3-kinase in NF-kappaB activation. *Proc Natl Acad Sci USA* **96:** 429-434.

Bernard, A., Fehat, L., Dessi, F., Charton, G., Represa, A., Ben Ari, Y. and Khrestchatisky, M. (1999) Q/R editing of the rat GluR5 and GluR6 kainate receptors in vivo and in vitro: evidence for independent developmental, pathological and cellular regulation. *Eur J Neurosci.* **11:** 604-616.

Bibel M. and Barde, Y.A. (2000) Neurotrophins: key regulators of cell fate and cell shape in the vertebrate nervous system. *Genes Dev.* **14:** 2919-2937.

Birnboim, H.C. and Doly, J. (1979) A rapid alkaline extraction procedure for screening recombinant plasmid DNA. *Nucleic Acids Res*. **7:** 1513-1523.

Bittner, M., Meltzer, P., Chen, Y., Jiang, Y., Seftor, E., Hendrix, M., Radmacher, M., Simon, R., Yakhini, Z., Ben-Dor, A., Sampas, N., Dougherty, E., Wang, E., Marincola, F., Gooden, C., Lueders, J., Glatfelter, A., Pollock, P., Carpten, J., Gillanders, E., Leja, D., Dietrich, K., Beaudry, C., Berens, M., Alberts, D. and Sondak, V. (2000) Molecular classification of cutaneous malignant melanoma by gene expression profiling. *Nature* **406:** 536-540.

Blaabjerg, M., Fang, L., Zimmer, J. and Baskys, A. (2003) Neuroprotection against NMDA excitotoxicity by group I metabotrophic glutamate receptors is associated with reduction of NMDA stimulated currents. *Exp Neurol.* **183:** 573-580.

Boniece, I.R. and Wagner, J.A. (1995) NGF protects PC12 cells against ischemia by a mechanism that requires the N-kinase. *J Neurosci Res.* **40:** 1-9.

Bonni, A., Brunet, A., West, A.E., Datta, S.R., Takasu, M.A. and Greenberg, M.E. (1999) Cell survival promoted by the Ras-MAPK signaling pathway by transcription-dependent and –independent mechanisms. *Science* **286:**1358-1362.

Bothwell, M. (1995) Functional interactions of neurotrophins and neurotrophin receptors. *Annu Rev Neurosci.* **18:** 223-253.

Brunet, A., Bonni, A., Zigmond, M. J., Lin, M. Z., Juo, P., Hu, L. S., Anderson, M.J., Arden, K.C., Blenis, J. and Greenberg, M.E. (1999) Akt promotes cell survival by phosphorylating and inhibiting a Forkhead transcription factor. *Cell* **96:** 857-868.

Bruno, V. Copani, A., Knopfel, T., Kuhn, R., Casabona, G., Dell'Albani, P. Condorelli, D.F. and Nicoletti, F. (1995) Activation of metebotrophic gluatamate receptors coupled to inositol phospholipids hydrolysis amplifies NMDA-induced neuronal degeneration in culture cortical cells. *Neuropharmacology* **34:** 1089-1098.

Bui, N.T., Konig, H.G., Culmsee, C., Bauerbach, E., Poppe, M., Krieglstein, J. and Prehn, J.H. (2002) p75 neurotrophin receptor is required for constitutive and NGF-induced survival signaling in PC12 cells and rat hippocampal neurons. *J Neurochem.* **81:** 594-605.

Bunone, G., Mariotti, A., Compagni, A., Morandi, E. and Della, V.G. (1997) Induction of apoptosis by p75 neurotrophin receptor in human neuroblastoma cells. *Oncogene* **14:** 1463-1470.

Bustin, S.A. (2000) Absolute quantitation of mRNA using real-time reverse transription polymerase chain reaction assays. *J Mol Endocrinol.* **25:** 169-193.

Butte, A. (2002) The use and analysis of microarrays. *Nat Rev.* **1:** 951-960.

Cardone, M. H., Roy, N., Stennicke, H. R., Salvesen, G. S., Franke, T. F., Stanbridge, E. *et al.* (1998) Regulation of cell death protease caspase-9 by phosphorylation. *Science* **282:** 1318-1321.

Casaccia-Bonnefil, P., Carter, B. D., Dobrowsky, R. T. and Chao, M. V. (1996) Death of oligodendrocytes mediated by the interaction of nerve growth factor with its receptor p75. *Nature* **383:** 716-719.

Casaccia-Bonnefil, P., Gu, C. and Chao, M.V. (1999) Neurotrophins in cell survival/death decisions. *Adv Exp Med Biol.* **468:** 275-282.

Chao, M.V. (2003) Neurotrophins and their receptors: a convergence point for many signalling pathways. *Nat Rev Neurosci.* **4:** 299-309.

Chemin, J., Monteil, A., Dubel, S., Nargeot, J. and Lory, P. (2001) The alpha1I T-type calcium channel exhibits faster gating properties when overexpressed in neuroblastoma/glioma NG 108-15 cells. *Eur J Neurosci* **14**: 1678-1686.

Chen, Y., Dicou, E., and Djakiew, D. (1997) Characterization of nerve growth factor precursor expression in rat spermatids and the trophic effects of nerve growth factor in the maintenance of Sertoli cell viability. *Mol Cell Endocrinol.* **127:** 129-136.

Cher, C.D.N. (2005). Molecular mechanisms underlying the pharmacological activities of *Naja Sputatrix* venom. PhD thesis, National University of Singapore. **Pp:** 175-190.

Cheung, A.T., Bavaria, J.E., Weiss, S.J., Patterson, T. and Stecker, M.M. (1998) Neurophysiologic effects of retrograde cerebral perfusion used for aortic reconstruction. *J Cardiothorac Vasc Anesth*. **12:** 252-259.

Choi, D.W. (1988) Glutamate neurotoxicity and diseases of the nervous system. *Neuron* **1:** 623-634. Review.

Choi, D.W. (1992) Excitotoxic cell death. *J Neurobiol.* **23:** 1261-1276. Review.

Chu, S., DeRisi, J., Eisen, M., Mulholland, J., Botstein, D., Brown, P.O. and Herskowitx, I. (1998) The transcriptional program of sporulation in budding yeast. *Science* **282:** 699-705.

Chuang, S.C., Bianchi, R. and Wong, R.K. (2000) Group I mGluR activation turns on a voltage-gated inward current in hippocampal pyramidal cells. *J Neurophysiol.* **83:** 2844-2853.

Cohen, S., Levi-Montalcini, R. and Hamburger, V. (1954) A nerve growth-stimulating factor isolated from sarcomas 37 and 180. *Proc Natl Acad Sci USA* **40:** 1014-1018.

Cohen S. and Levi-Montalcini R. (1956) A nerve growth growth-stimulating factor isolated from snake venom. *Proc Natl Acad Sci U S A* **42:** 571-574.

Cook, M., Caswell, R.C., Richards, R.J., Kay, J. and Tatnell, P.J. (2001) Regulation of human and mouse procathepsin E gene expression. *Eur J Biochem* **268:** 2658-2668.

Corbit, K.C., Foster, D.A. and Rosner, M.R. (1999) Protein kinase Cδ mediates neurogenic but not mitogenic activation of mitogen-activated protein kinase in neuronal cells. *Mol Cell Biol.* **19:** 4209–4218.

Cortazzo, M.H., Kassis, E.S., Sproul, K.A. and Schor, N.F. (1996) Nerve growth factor (NGF)-mediated protection of neural crest cells from antimitotic agent-induced apoptosis and the role of the low-affinity NGF receptor. *J Neurosci.* **16:** 3895-3899.

Cosgaya, J. M., Chan, J. R. and Shooter, E. M. (2002) The neurotrophin receptor p75NTR as a positive modulator of myelination. *Science* **298:** 1245–1248.

Culmsee, C., Gerling, N., Lehmann, M., Nikolova-Karakashian, M., Prehn, J.H., Mattson, M.P. and Krieglstein, J. (2002) Nerve growth factor survival signaling in culture hippocampal neurons is mediated through TrkA and requires the common neurotrophin receptor p75. *Neuroscience* **115:** 1089-1108.

Dahn, M.S. (1998) The role of growth factors in a wound management of diabetic foot ulcers. *Fed Pract.* **7:** 14-19.

Darling, T.L., Petrides, P.E., Beguin, P., Frey, P., Shooter, E.M., Selby, M. and Rutter, W.J. (1983) The biosynthesis and processing of proteins in the mouse 7S nerve growth factor complex. *Cold Spring Harbor Symp Quant Biol.* **48:** 427-434.

Dartsch, D.C., Scharfer, A., Boldt, S., Kolch, W and Marquardt, H. (2002) Comparison of anthracycline-induced death of human leukemia cells: programmed cell death versus necrosis. *Apoptosis* **7:** 537-548.

Datta, S.R., Dudek, H., Tao, X., Masters, S., Fu, H. Gotoh, Y. and Greenberg, M.E. (1997) Akt phosphorylation of BAD couples survival signals to the cell-intrinsic death machinery. *Cell* **91:**1–20.

Datta, S.R., Brunet, A. and Greenberg, M.E. (1999) Cellular survival: a play in three Akts. *Genes Dev.* **13:** 2905–2927.

Dawson, R. Jr., Beal, M.F., Bondy, D.A., Di Monte, D.A. and Isom, G.E. (1995) Excitotoxins, aging and environmental neurotoxins: implications for understanding human neurodegeneration diseases. *Toxicol Appl Pharmacol.* **134:** 1-17.

Dechant, G. and Barde, Y. A. (2002) The neurotrophin receptor p75 (NTR): novel functions and implications for diseases of the nervous system. *Nat Neurosci.* **5:** 1131–1136.

DeFreitas, M.F., McQuillen, P.S. and Shatz, C.J. (2001) A novel p75NTR signaling pathway promotes survival not death of immunopurified neocortical subplate neurons. *J Neurosci.* **21:** 5121-5129.

del Peso, L., Gonzalez-Garcia, M., Page, C., Herrera, R., and Nunez, G. (1997) Interleukin-3-induced phosphorylation of BAD through protein kinase Akt. *Science* **278:** 687-689.

Diaz-Meco, M.T., Dominguez, I. Sanz, L., Dent, P., Lozano, J., Municio, M.M., Bera, E., Hay, R.T., Sturgill, T.W. and Moscat, J. (1994) zeta PKC induces phosphorylation and inactivation of I kappa B-alpha in vitro. *EMBO J.* **13:** 2842-2848.

Dicou, E. (1989) Interaction of antibodies to synthetic peptides of proNGF with in vitro synthesized NGF precursors. *FEBS Lett.* **255:** 215-218.

Dicou, E., Pflug, B., Magazin, M., Lehy, T., Djakiew, D., Ferrara, P., Nerriere, V., and Harvie, D. (1997) Two peptides derived from the nerve growth factor precursor are biologically active. *J Cell Biol.* **136:** 389-398.

Dowling, P., Ming, X., Raval, S., Husar, W., Casaccia-Bonnefil, P., Chao, M., Cook, S. and Blumberg, B. (1999) Up-regulated p75NTR neurotrophin receptor on glial cells in MS plaques. *Neurology* **53:** 1676–1682.

Dubois, C.M., Laprise, M.H., Blanchette, F., Gentry, L.E. and Leduc, R. (1995) Processing of transforming growth factor beta 1 precursor by human furin convertase. *J Biol Chem.* **270:** 10618-10624.

Duggan, D.J., Bittner, M., Chen, Y., Meltzer, P. and Trent, J.M. (1999) Expression profiling using cDNA microarrays. *Nat Genet.* **21:** 10-14.

Earl, S.T., Birrell, G.W., Wallis, T.P., St Pierre, L.D., Masci, P.P., de Jersey, J., Gorman, J.J. and Lavin, M.F. (2006) Post-translational modification accounts for the presence of varied forms of nerve growth factor in Australian elapid snake venoms. *Proteomics* **6:** 6554-6565.

Edstrom, A. (1992) Reptiles. In: Venomous and poisonous animals. Krieger Publishing Company, Malabar, Florida. **Pp:** 125 -152.

Edwards, R.H., Selby, M.J., Garcia, P.D. and Rutter, W.J. (1988a) Processing of the native nerve growth factor precursor to form biologically active nerve growth factor. *J Biol Chem.* **270:** 12297.

Edwards, R.H., Selby, M.J., Mobley, W.C. Weinrich, S.L., Hruby, D.E. and Rutter, W.J. (1988b) Processing and secretion of nerve growth factor: expression in mammalian cells with a vaccinia virus vector. *Mol Cell Biol.* **8:** 2456-2464.

Eisen, M.B., Spellman, P.T., Brown, P.O. and Botstein, D. (1998) Cluster analysis and display of genome-wide expression patterns. *Proc Natl Acad Sci USA* **95:** 14863-14868.

Elliot-Hunt, C.R., Kazlauskaite, J., Wilde, G.J.C., Grammatopoulos, D.K. and Hillhouse, E.W. (2002) Potential signaling pathways underlying corticotrophin-releasing hormone-mediated neuroprotection from excitotoxicity in rat hippocampus. *J Neurochem.* **80:** 416-425.

Facer, P., Mathur, R., Pandya, S., Singhal, B. and Anand, P. (1998) Correlation of quantitative tests of nerve and target organ dysfunction with skin immnuohistology in leprosy. *Brain* **121:** 2239-2247.

Facer, P., Mann, D., Matahur, R., Pandya, S., Ladiwala, U., Singhal, B., Hongo, J.-A., Sinicropi, D.V., Terenghi, G. and Anand, P. (2000) Do NGF-related mechanisms contribute to loss of cutaneous nociception in leprosy? *Pain* **85:** 231-238.

Fahnestock, M., Michalski, B., Xu, B. and Coughlin, M.D. (2001) The precursor pro-nerve growth factor is the predominant form of nerve growth factor in brain and is increased in Alzheimer's disease. *Mol Cell Neurosci.* **18:** 210-220.

Fahnestock, M., Yu, G., Michalski, B., Mathew, S., Colquhoun, A., Ross, G.M., and Coughlin, M.D. (2004) The nerve growth factor precursor proNGF exhibits neurotrophic activity but is less active than mature nerve growth factor. *J Neurochem.* **89**: 581-592.

Farhadi, H.F., Mowla, S.J., Petrecca, K., Morris, S.J., Seidah, N.G. and Murphy, R.A. (2000) Neurotrophin-3 sorts to the constitutive secretory pathway of hippocampal neurons and is diverted to the regulated secretory pathway by coexpression with brain-derived neurotrophic factor. *J Neurosci.* **20:** 4059-4068.

Ferri, C.C., Moore, F.A. and Bisby, M.A. (1998) Effects of facial nerve injury on mouse motoneurons lacking the p75 low-affinity neurotrophin receptor. *J Neurobiol.* **34:** 1-9.

Fischer, W., Wictorin, K., Bjorklund, A., Williams, L.R., Varon, S., and Gage, F.H. (1987) Amerlioration of cholinergic neuron atrophy and spatial memory impairment in aged rats by nerve growth factor. *Nature* **329:** 65-68.

Fletcher, J.E. and Jiang, M.S. (1993) Possible mechanism of action of cobra snake venom cardiotoxin and bee venom mellitin. *Toxicon* **31:** 669-695.

Foehr, E.D., Lin, X., O'Mahony, A., Geleziunas, R., Bradshaw, R.A. and Greene, W.C. (2000) NF-kappa B signaling promotes both cell survival and neurite process formation in nerve growth factor-stimulated PC12 cells. *J Neurosci* **20:** 7556-7563.

Frade, J.M. and Barde, Y.-A. (1999) Genetic evidence for cell death mediated by nerve growth factor and the neurotrophin receptor p75 in the developing mouse retina and spinal cord. *Development* **126:** 683-690.

Friedman, W.J. (2000) Neurotrophins induce death of hippocampal neurons via the p75 receptor. *J Neurosci.* **20:** 6340–6346.

Gahwiler, B.H. (1984) Development of the hippocampus *in vitro*: cell types, synapses and receptors. *Neuroscience* **11:** 751-760.

Gahwiler, B.H., Capogna, M., Debanne, D., McKinney, R.A. and Thompson, S.M. (1997) Organotypic slice cultures: a technique has come of age. *Trends Neurosci.* **20:** 471-477. Review.

Gavel, Y. and von Heijne, G. (1990) Sequence differences between glycosylated and non-glycosylated Asn-X-Thr/Ser acceptor sites: implications for protein engineering. *Protein Eng.* **3:** 433–442.

Geetha, T. and Wooten, M.W. (2003) Association of the atypical protein kinase C-interacting protein p62/ZIP with nerve growth factor receptor TrkA regulates receptor trafficking and Erk5 signaling. *J Biol Chem.* **278:** 4730-4739.

Gendron, F.P., Neary, J.T., Theiss, P.M., Sun, G.Y., Gonzalez, F.A. and Weisman, G.A. (2003) Mechanisms of P2X7 receptor-mediated ERK1/2

phosphorylation in human astrocytoma cells. *Am J Physiol Cell Physiol* **284:** C571- C581.

Gentry, J.J., Casaccia-Bonnefil, P. and Carter, B.D. (2000) Nerve growth factor activation of nuclear factor kappa B through its p75 receptor is an anti-apoptotic signal in RN22 schwannoma cells. *J Biol Chem.* **275:** 7558-7565.

Gentry, J.J., Barker, P.A. and Carter, B.D. (2004) The p75 neurotrophin receptor: multiple interactors and numerous functions. *Prog Brain Res.* **146:** 25-39.

Giehl, K.M., Rohrig, S., Bonatz, H., Gutjahr, M., Leiner, B., Bartke, I., Yan, Q., Reichardt, L.F., Backus, C., Welcher, A.A., Dethleffsen, K., Mestres, P. and Meyer, M. (2001) Endogenous brain-derived neurotrophic factor and neurotrophin-3 antagonistically regulate survival of axotomized corticospinal neurons in vivo. *J Neurosci.* **21:** 3492–3502.

Gill, R. and Logde, D. (1997) Pharmacology of AMPA antagonists and their role in neuroprotection. *Int Rev Neurobiol.* **40:** 197-232.

Goldberg, M.P., Weiss, J.H., Pham, P.-C. and Choi, D.W. (1987). Methyl-D-aspartate receptors mediate hypoxic neuronal injury in cortical cultures. *J Pharm Exp Ther.* **243:** 784-791.

Goldstein, L.D., Reynolds, C.P. and Perez-Polo, J.R. (1978) Isolation of human nerve growth factor from placental tissue. *Neurochem Res.* **3:** 175-183.

Gopalakrishnakone, P., Chou, L.M., Aye, M.M., Lim, F.L.K., Chao, T.C., Lim, S. K. and Anantharaman, S. (1990) Clinical features and treatment of specific snake bites. In: Snake bites and their treatment. Singapore University Press, Singapore. **Pp:** 34-40.

Greene, L.A. and Rukenstein, A. (1989) The quantitative bioassay of nerve growth factor with PC12 cells. In: Nerve Growth Factors. Rush, R.A. (Ed.) IBRO Handbook series: Methods in the neurosciences. Chichester, U.K. John Wiley & Sons. Vol (12). **Pp:** 139-147.

Greene, L.A., Shooter, E.M. and Varon, S. (1968) Enzymatic activities of mouse nerve growth factor and its subunits. *Proc Natl Acad Sci USA* **60:** 1383-1388.

Greene, L.A. and Tishler, A.S. (1976) Establishment of a noradrenergic clonal line of rat adrenal pheochromocytoma cells which respond to nerve growth factor. *Proc Natl Acad Sci USA* **73:** 2424-2428.

Grewal, S.S., York, R.D. and Stork, P.J.S. (1999) Extracellular signal-regulated kinase signalling in neurons. *Curr. Opin. Neurobiol.* **9:**544–553.

Grob, P. M, Ross, A. H., Koprowski, H. and Bothwell, M. (1985) Characterization of the human melanoma nerve growth factor receptor. *J Biol Chem.* **260**: 8044.

Gu, C., Casaccia-Bonnefil P., Srinivasan, A. and Chao M. V. (1999) Oligodendrocyte apoptosis mediated by caspase activation. *J Neurosci.* **19:** 3043-3049.

Guo, L.Y., Zhu, J.F., Wu, X.F. and Zhou, Y.C. (1999) Cloning of a cDNA encoding a nerve growth factor precursor from the *Agkistrodon halys Pallas. Toxicon* **37:** 465-470.

Hamanoue, M., Middeton, G., Wyatt, S., Jaffray, E., Hay, R.T. and Davies, A.M. (1999) p75-mediated NF-kappa B activation enhances the survival response of developing sensory neurons to nerve growth factor. *Mol Cell Neurosci.* **14:** 28-40.

Haniu, M., Montestruque, S., Bures, E. J., Talvenheimo, J., Toso, R., Lewis-Sandy, S. Welcher, A.A. and Rohde, M.F. (1997) Interactions between brain-derived neurotrophic factor and the TRKB receptor: identification of two ligand-binding domains in soluble TRKB by affinity separation and chemical crosslinking. *J Biol Chem.* **272:** 25296–25303.

Harada, T., Morooka, T., Ogawa, S. and Nishida, E. (2001) ERK induces p35, a neuron-specific activator of Cdk5, through induction of Egr1. *Nat Cell Biol.* **3**: 453-459.

Harrington, A.W., Leiner, B., Blechschmitt, C., Arevalo, J.C., Lee, R., Morl, K., Meyer, M., Hempstead, B.L., Yoon, S.O., and Giehl, K.M. (2004) Secreted proNGF is a pathophysiological death-inducing ligand after adult CNS injury. *Proc Natl Acad Sci USA* **101:** 6226-6230.

Harvey, A.L. (1991) Cardiotoxins from cobra venoms. In: Reptile venoms and toxinx. Tu, A.T. (Ed). Marcel Dekker, New York. **Pp:** 85-106.

Hawtin, S.R., Davies, A.R., Matthews, G. and Wheatley, M. (2001) Identification of the glycosylation sites utilized on the V1a vasopressin receptor and assessment of their role in receptor signalling and expression. *Biochem J.* **357:** 73-81.

He, X-L. and Garcia, C. (2004) Structure of nerve growth factor complexed with the shared neurotrophin receptor p75. *Science* **304:** 870-875.

Hefti, F. (1986) Nerve growth factor (NGF) promotes survival of septal cholinergic neurons after fimbrial transaction. *J Neurosci.* **6:** 2155-2162.

Heid, C.A., Stevens, J., Livak, K.J. and Williams, P.M. (1996) Real-time PCR quantitative PCR. *Genome Res*. **6:** 986-994.

Heinrich, G. and Lum, T. (2000) Fish neurotrophins and Trk receptors. *Int J Dev Neurosci.* **18:** 1-27.

Hempstead, B.L., Martin-Zanca, D., Kaplan, D.R., Parada, L.F. and Chao, M.V. (1991) High-affinity NGF binding requires co expression of the *trk* proto-oncogene and the low affinity NGF receptor. *Nature* **350:** 678–683.

Hempstead, B. L. (2002) The many faces of p75[NTR]. *Curr Opin Neurobiol.* **12:** 260–267.

Hermans-Borgmeyer, I., Hermey, G., Nykjaer, A. and Schaller,C. (1999) Expression of the 100-kDa neurotensin receptor sortilin during mouse embryonal development. *Brain Res Mol Brain Res.* **65:** 216-219.

Heymach, J.V., Jr., Kruttgen, A., Suter, U. and Shooter, E.M. (1996) The regulated secretion and vectorial targeting of neurotrophins in neuroendocrine and epithelial cells. *J Biol Chem.* **271:** 25430-25437.

Heymach, J.V. Jr and Shooter, E.M. (1995) The biosynthesis of neurotrophin heterodimers by transfected mammalian cells. *J Biol Chem.* **270:** 12297-12304.

Hogue-Angeletti, R.A. and Bradshaw, R.A. (1979) Nerve growth factors in snake venoms. In: Snake Venoms. (Lee, C.Y., Ed.) Berlin: Springer. **Pp:** 276-294.

Holden, P. H., Asopa, V., Robertson, A. G., Clarke, A. R., Tyler, S., Bennett, G. S. *et al.* (1997) Immunoglobulin-like domains define the nerve growth factor binding site of the TrkA receptor. *Nat Biotechnol.* **15:** 668–672.

Holgado-Madruga, M., Moscatello, D.K., Emlet, D.R., Dieterich, R., Wong, A.J. (1997) Grb2-associated binder-1 mediates phosphatidylinositol- 3-OH kinase activation and the promotion of cell survival by nerve growth factor. *Proc Natl Acad Sci USA* **94:** 12419–12424.

Hollmann, M., Hartley, M. and Heinemann, S. (1991) Ca^{2+} permeability of KA-AMPA-gated glutamate receptor channels depends on subunit composition. *Science* **252:** 851-853.

Hosaka, M., Nagahama, M., Kim, W.-S., Watanabe, T., Hatsuzawa, K., Ikemizu, J., Murakami, K. and Nakayama, K. (1991) Arg-X-Lys/Arg-Arg motif as a signal for precursor cleavage catalyzed by furin within the constitutive secretory pathway. *J Biol Chem.* **266:** 12127-12130.

Howard-Jones, N.A. (1995) A CIOMS ethical code for animal experimentation. *WHO Chronicle* **39:** 51-56.

Hsu, C.Y., An, G., Liu, J.S., Xue, J.J., He, Y.Y. and Lin, T.N. (1993).Expression of immediate early gene and growth factor mRNAs in a focal cerebral ischemia model in rat. *Stroke* **24:** I78-I81.

Huang, E.J. and Reichardt, L.F. (2001) Neurotrophins: roles in neuronal development and function. *Annu Rev Neurosci.* **24:** 677-736.

Huang, E.J. and Reichardt, L.F. (2003) Trk receptors: roles in neuronal signal transduction. *Annu Rev Biochem.* **72:** 609-642. Review.

Inagaki, N., Thoenen, H. and Lindholm, D. (1995) TrkA tyrosine residues involved in NGF induced neurite outgrowth of PC12 cells. *Eur J Neurosci.* **7:**1125–1133.

Indo, Y., Tsuruta, M., Hayashida, Y., Karim, M.A., Ohta, K., Kawano, T., Mitsubuchi, H., Tonki, H., Awaya, Y. and Matsuda, I. (1996) Mutations in the TrkA/NGF receptor gene in patients with congenital insensitivity to pain with anhidrosis. *Nat Genet.* **13:** 485-488.

Inoue, S., Oda, T., Koyama, J., Ikeda, K. and Hayashi, K. (1991) Amino acid sequences of nerve growth factors derived from cobra venoms. *FEBS Lett.* **279:** 38-40.

Issaq, H.J., Veenstra, T.D., Conrads, T.P. and Felschow, D. (2002) The SELDI-TOF MS approach to proteomics: protein profiling and biomarker identification. *Biochem Biophys Res Commun.* **292:** 587-592.

Jacobson, M.D., Burne, J.F., King, M.P., Miyashita, T., Reed, J.C. and Raff, M.C. (1993) Bcl-2 blocks apoptosis in cells lacking mitochondrial DNA. *Nature* **361:** 365-369.

Jensen, J.B., Pickering, D.S. and Schousboe, A. (1998) AMPA receptor mediated excitotoxicity in neocortical neurons is developmentally regulated and dependent upon receptor desensitization. *Neurochem Int.* **32:** 505-513.

Jiang, H., Koubi, D., Zhang, L., Kuo, J., Rodriguez, A.I., Hunter, Gautam, S.C. and Levine, R.A. (2005) Inhibitors of iNOS protects PC12 cells against apoptosis induced by oxygen and glucose deprivation. *Neurosci Lett.* **375:** 59-63.

Jing S., Tapley, P. and Barbacid, M. (1992) Nerve growth factor mediates signal transduction through trk homodimer receptors. *Neuron* **9**: 1067-1079.

Jonas, P. and Burnashev, N. (1995) Molecular mechanisms controlling calcium entry through AMPA-type glutamate receptor channels. *Neuron* **15:** 987-990.

Jorgensen, M., Tygesen, C.K., Andersen, P.H. (1995) Ionotrophic glutatmate receptors-focus on non-NMDA receptors. *Pharmacol Toxicol.* **76:** 312-319.

Jullien, J., Guili, V., Reichardt, L.F. and Rudkin, B.B. (2002) Trafficking of TrkA-green fluorescent protein chimerae during nerve growth factor-induced differentiation. *J Biol Chem.* **277:** 38700-38708.

Kalda, A., Kaasik, A., Vassiljev, V., Pokk, P. and Zharkovsky, A. (2000) Neuroprotective action of group I metabotropic glutamate receptor agonists against oxygen-glucose deprivation-induced neuronal death. *Brain Res.* **853:** 370-373.

Kammermeier, P.J. (2006) Surface clustering of metabotropic glutamate receptor 1 induced by long Homer proteins. *BMC Neurosci.* **7:** 1.

Kaplan, D.R., Hempstead, B.L., Martin, Z.D., Chao, M.V., Parada, L.F. (1991) The Trk proto-oncogene product: a signal transducing receptor for nerve growth factor. *Science* **252:** 554-558.

Kaplan, D.R and Miller, F.D. (1997) Signal transduction by the neurotrophin receptors. *Curr Opin Cell Biol.* **9:** 213–221.

Kaplan, D.R. and Miller, F.D. (2000) Neurotrophin signal transduction in the nervous system. *Curr Opin Neurobiol.* **10:** 381-391.

Kaplan, D.R. and Miller, F.D. (2004) A move to sort life from death. *Nature* **427:** 798-799.

Karin, M. and Lin, A. (2002) NF-kappa B at the crossroads of life and death. *Nat Immunol.* **3:** 221-227.

Kashima, S., Soares, A.M., Roberto, P.G., Pereira, J.O., Astolfi-Filho, S., Cintra, A.O., Fontes, M.R., Giglio, J.R., de-Castro Franca, S. (2002) cDNA sequence and molecular modeling of a nerve growth factor from *Bothrops jararacussu* venomous gland. *Biochimie* **84:** 675-680.

Keinanen, K., Wisden, W., Sommer, B., Werner, P., Herb, A., Verdoorn, T.A. Sakmann, B., Seeburg, P.H. (1990) A family of AMPA-selective glutamate receptors. *Science* **249:** 556-560.

Khursigara, G., Bertin, J., Yano H., Moffett, H., DiStefano, P. S. and Chao, M. V. (2001) A prosurvival function for the p75 receptor death domain mediated via the caspase recruitment domain receptor-interacting protein 2. *J Neurosci.* **21:** 5854– 5863.

Kim, A.H., Yano, H., Cho, H., Meyer, D., Monks, B., Margolis, B., Birnbaum, M.J. and Chao, M.V. (2002) Akt1 regulates a JNK scaffold during excitotoxic apoptosis. *Neuron* **35:** 697-609.

Kimpinski, K., Jelinski, S. and Mearow, K. (1999) The anti-p75 antibody, MC192, and brain-derived neurotrophic factor inhibit nerve growth factor-dependent neurite growth from adult sensory neurons. *Neuroscience* **93:** 253-263.

Kini, R.M. (1997) Phospholipase A2- a complex multifunctional protein puzzle. In: Venom phospholipase A_2 enzymes: Structure, function and mechanism. Kini, R.M. (Ed) John Wiley and Sons Ltd., U.K. **pp:** 1-28.

Kirschner, P.B., Jenkins, B.G., Schulz, J.B., Finkelstein, S.P., Matthews, R.T., Rosen, B.R. and Beal, M.F. (1996) NGF, BDNF and NT-5, but not NT-3 protect against MPP+ toxicity and oxidative stress in neonatal animals. *Brain Res.* **713:** 178-185.

Kitagawa, K., Matsumoto, M., Tsulimoto, Y., Ohtsuki, T., Kuwabara, K., Matsushita, K., Yang, G., Tanabe, H., Martinou, J.C., Hori, M. and Yanagihara, T. (1998) Amelioration of hippocampal neuronal damage after global ischemia by neuronal overexpression of Bcl-2 in transgenic mice. *Stroke* **29:** 2616-2621.

Klein, D. (2002) Quantification using real-time PCR technology: applications and limitations. *Trends Mol Med.* **8:** 257-260.

Kliemannel, M., Golbik, R., Rudolph, R., Schwarz, E. and Lilie, H. (2007) The pro-peptide of proNGF: structure formation and intramolecular association with NGF. *Protein Sci.* **16:** 411-419.

Koh, D.C., Armugam, A., Jeyaseelan, K. (2004) Sputa nerve growth factor forms a preferable substitute to mouse 7S-beta nerve growth factor. *Biochem J.* **383:** 149-158.

Koh, D.C., Armugam, A., Jeyaseelan, K. (2006) Snake venom components and their applications in biomedicine. *Cell Mol Life Sci.* **63:** 3030-3041.

Koike, T., Uno, S., Ishizawa, M., Takahashi, H., Ikeda, K., Yokota, S. and Makishima, M. (2006) The heat shock protein inhibitor KNK437 induces neurite outgrowth in PC12 cells. *Neurosci Lett.* **410:** 212-217.

Kolbeck, R., Jungbluth, S. and Barde, Y.A. (1994) Characterization of neurotrophin dimers and monomers. *Eur J Biochem.* **225:** 995-1003.

Kong, H., Boulter, J., Weber, J.L., Lai, C. and Chao, M.V. (2001) An evolutionarily conserved transmembrane protein that is a novel downstream target of neurotrophin and ephrin receptors. *J Neurosci.* **21:**176-185.

Kornfeld, R. and Kornfeld, S. (1985) Assembly of asparagine-linked oligosaccharides. *Annu. Rev Biochem.* **54:** 631-664.

Korsching, S., Auburger, G., Heumann, R., Scott, J. and Thoenen, H. (1985) Levels of nerve growth factor and its mRNA in the central nervous system of the rat correlate with cholinergic innervation. *EMBO J.* **4:** 1389-1393.

Kostiza, T., Dahinden, C.A., Rihs, S., Otten, U. and Meier, J. (1995) Nerve growth factor from the venom of the Chinese cobra *Naja naja atra*: purification and description of non-neuronal activities. *Toxicon* **33**: 1249-1261.

Kostiza, T. and Meier, J. (1996) Nerve growth factors from snake venoms: chemical properties, mode of action and biological significance. *Toxicon* **34:** 787-806.

Koubi, D., Jiang, H., Zhang, L., Tang, W., Kuo, J., Rodriguez, A.I., Hunter, T.J., Seidman, M.D., Corcoran, G.B and Levine, R.A. (2005) Role of Bcl-2 family of proteins in mediating apoptotic death of PC12 cells exposed to oxygen and glucose deprivation. *Neurochem Int*. **46:** 73-81.

Kristensten, B.W., Noraberg, J. and Zimmer, J. (2001) Comparison of excitotoxic profiles of ATPA, AMPA, KA and NMDA in organotypic hippocampal slice cultures. *Brain Res*. **917:** 21-44.

Kristian, T. and Siesjo, B.K. (1998) Calcium in ischemic cell death. *Stroke* **29:** 705-718. Review.

Krohn, A.J., Preis, E. and Prehn, J.H. (1998) Staurosporine-induced apoptosis of cultured rat hippocampal neurons involves caspase-1-like proteases as upstream initiators and increased production of superoxide as a main downstream effector. *J Neurosci*. **18:** 8186-8197.

Krohn, A.J., Wahlbrink, T. and Prehn, J.H. (1999) Mitochondrial depolarization is not required for neuronal apoptosis. *J Neurosci.* **19:**7394-7404.

la Cour, T., Gupta, R., Rapacki, K., Skriver, K. Poulsen, F.M. and Brunak, S. (2003) NESbase version 1.0 : a database of nuclear export signals. *Nucleic Acids Res.* **31:** 393-396.

Lahtinen, H., Autere, A.M., Paalasmaa, P., Lauri, S.E. and Kaila, K. (2001) Post-insult activity is a major cause of delayed neuronal death in organotypic hippocampal slices exposed to glutamate. *Neuroscience* **105:** 131-137.

Lamballe, F., Klein, R. and Barbacid, M. (1991) TrkC, a new member of the trk family of tyrosine protein kinases, is a receptor for neurotrophin-3. *Cell* **66:** 967–979.

Lee, R., Kermani, P., Teng, K.K. and Hempstead, B.L. (2001) Regulation of cell survival by secreted proneurotrophins. *Science* **294:** 1945-1948.

Lees, G.J. and Leong, W. (1993) Differential effects of NBQX on the distal and local toxicity of glutamate agonists administered intra-hippocampally. *Brain Res*. **628:** 1-7.

Lewin, G.R. and Barde, Y.A. (1996) Physiology of neurotrophins. *Annu Rev Neurosci.* **19:** 514-520.

Li, Y., Li. X., Hussain, M. and Sarkar, F.H. (2004) Regulation of microtubule, apoptosis, and cell cycle-related genes by taxotere in prostate cancer cells analyzed by microarray. *Neoplasia* **6:**158-167.

Liby, K., Wu, H., Ouyang, B., Wu, S., Chen, J. and Dai, W. (2001) Identification of the human homologue of the early-growth response gene Snk, encoding a serum-inducible kinase. *DNA Seq.* **11:** 527-533.

Lin, H., Hikawa, N., Takenaka, T. and Ishikawa, Y. (2000) Interleukin-12 promotes neurite outgrowth in mouse sympathetic superior cervical ganglion neurons. *Neurosci Lett.* **278:** 129-132.

Lindsten, T., Zong, W.X. and Thompson, C.B. (2005) Defining the role of the Bcl-2 family of proteins in the nervous system. *Neuroscientist* **11:**10-15.

Lipps, B.V. (1998) Biological and immunological properties of nerve growth factor from snake venoms. *J Nat Toxins* **7:** 121-130.

Lipps, B.V. (2000) Isolation of nerve growth factor (NGF) from human body fluids; saliva, serum and urine: comparison between cobra venom and cobra serum NGF. *J Nat Toxins* **9:** 349-356.

Lipshutz, R. J., Fodor, S. P., Gingeras, T.R. and Lockhart, D.J. (1999). High density synthetic oligonucleotide arrays. *Nat Genet.* **21:** 20-24.

Lipton, P. (1999) Ischemic cell death in brain neurons. *Physiol Rev.* **79:** 1431-1568.

Lockhart, D.J. and Winzeler, E.A. (2000) Genomics, gene expression and DNA arrays. *Nature* **405:** 827-836.

Longo, F.M., Manthorpe, M., Xie, Y.M. and Varon, S. (1997) Synthetic NGF peptide deriviatives prevent neuronal death via a p75 receptor-dependent mechanism. *J Neurosci Res.* **48:** 1-17.

Longo, F.M., Woo, J.E. and Mobley, W.C. (1989) Purification of nerve growth factor. In: Nerve growth factor. Rush, R.A. (Ed). IBRO Handbook series: Methods in neurosciences. Chichester, U.K.: John Wiley and Sons. Vol (12). **Pp:** 3-30.

Love, S. (2003) Apoptosis and brain ischemia. *Prog Neuropsychopharmacol Biol Psychiatry.* **27:** 267-282.

MacDonald, J. I. and Meakin, S. O. (1996) Deletions in the extracellular domain of rat trkA lead to an altered differentiative phenotype in neurotrophin responsive cells. *Mol Cell Neurosci.* **7:** 371–390.

Maggirwar, S.B., Samiere, P.D., Dewhurst, S. and Freeman, R.S. (1998) Nerve growth factor-dependent activation of NF-kappaB contributes to the survival of sympathetic neurons. *J Neurosci.* **18:**10356–10365.

Maggirwar, S.B., Ramirez, S., Tong, N., Gelbard, H.A. and Dewhurst, S. (2000) Functional interplay between nuclear factor-kappaB and c-Jun integrated by coactivator p300 determines the survival of nerve growth factor-dependent PC12 cells. *J Neurochem.* **74**: 527-539.

Mahadeo, D., Kaplan, L., Chao, M.V. and Hempstead, B.L. (1994) High affinity nerve growth factor binding displays a faster rate of association than p140trk binding. Implications for multi-subunit polypeptide receptors. *J Biol Chem.* **269:** 6884-6991.

Mahoney, M. J. and Saltzman, W. M. (1999) Millimeter-scale positioning of a nerve growth factor source and biological activity in the brain. *Proc Natl Acad Sci USA* **96:** 4536-4539.

Margarita, G.-C., Erin, P. P., Barbara, L., Rejean, R., Donald W. N. and Nancy, A. T. (1998) Inhibition of human caspases by peptide-based and macromolecular inhibitors. *J Biol Chem.* **273:** 32608-32613.

Marsh, H.N., Dubreuil, C.I., Quevedo, C., Lee, A., Majdan, M., Walsh, G.S., Hausdirff, S., Said, F.A., Zoueva, O., Kozlowski, M., Siminovitch, K., Neel, B.G., Miller, F.D. and Kaplan, D.R. (2003) SHP-1 negatively regulates neuronal survival by functioning as a TrkA phosphatase. *J Cell Biol.* **163:** 999-1010.

Martin-Zanca, D., Oskam, R., Mitra, G., Copeland, T. and Barbacid, M. (1989) Molecular and biochemical characterization of the human trk proto-oncogene. *Mol Cell Biol.* **9:** 24-33.

Marton, M.J., DeRisi, J.L., Bennett, H.A., Iyer, V.R., Meyer, M.R., Roberts, C.J., Stoughton, R., Burchard, J., Slade, D., Bassett, D.J., Hartwell, L.H., Brown, P.O. and Friend, S.H. (1998) Drug target validation and identification of secondary drug targets effects using DNA microarrays. *Nat Med.* **4:** 1293-1301.

Massie, B., Couture, F., Lamoureux, L., Mosser, D.D., Guilbault, C., Jolicoeur, P., Belanger, F. and Langelier, Y. (1998) Inducible overexpression of a toxic protein by an adenovirus with a tetracycline-regulatable expression cassette. *J Virol.* **72:** 2289-2296.

Mattson, M.P., Cheng, B. and Smith-Swintosky, V.L. (1993) Mechanisms of neurotrophic factor protection against calcium- and free radical-mediated excitotoxic injury: implications for treating neurodegenerative disorders. *Exp Neurol.* **124:** 89-95.

McArthur, J.C., Yiannoutsos, C., Simpson, D.M., Adornato, B.T., Singer, E.J., Hollander, H., Marra, C., Rubin, M., Cohen, B.A., Tucker, T., Navia, B.A., Schifitto, G., Katzenstein, D., Rask, C., Zaborski, L., Smith, M.E., Shriver, S., Millar, L., Clifford, D.B and the AIDS Clinical Trials Group Team 291 (2000) A phase II trial of nerve growth factor for sensory neuropathy associated with HIV infection. *Neurology* **54:**1080-1088.

Mcbean, G.J. and Roberts, P.J. (1985). Neurotoxicity of L-glutamate and DL-threo-3-hydroxyaspartate in the rat striatum. *J Neurochem.* **44:** 247-254.

McCulloch, J. (1991) Ischaemic brain damage--prevention with competitive and non-competitive antagonists of N-methyl-D-aspartate receptors. *Arzneimittelforschung* **41:** 319-324.

McDonald, N.Q., Lapatto, R., Murray-Rust, J., Gunning, J., Wlodawer, A. and Blundell, T.L. (1991) New protein fold revealed by a 2.3-Å resolution crystal structure of nerve growth factor. *Nature* **354:** 411-414.

257

McDonald, N.Q. and Hendrickson, W.A. (1993). A structural superfamily of growth factors containing a cystine knot motif. *Cell* **73:** 421-424.

McNamara, R.K., Huot, R.L., Lenox, R.H. and Plotsky, P.M. (2002) Postnatal maternal separation elevates the expression of the postsynaptic protein kinase C substrate RC3, but not presynaptic GAP-43, in the developing rat hippocampus. *Dev Neurosci.* **24:** 485-494.

Meakin, S.O., MacDonald, J.I.S., Gryz, E.A., Kubu, C.J. and Verdi, J.M. (1999) The signaling adapter FRS-2 competes with Shc for binding to the nerve growth factor receptor TrkA. *J Biol Chem.* **274:**9861-9870.

Micera, A., Lambiase, A., Puxeddu, I., Aloe, L., Stampachiacchiere, B., Levi-Schaffer, F. and Bonini, S. (2006) Nerve growth factor effect on human primary fibroblastic-keratocytes: Possible mechanism during corneal healing. *Exp Eye Res.* **83:** 747-757.

Middleton, G., Hamanoue, M., Enokido, Y., Wyatt, S., Pennica, D., Jaffray, E., Hay, R.T. and Davies, A.M. (2000). Cytokine-induced nuclear factor kappa B activation promotes the survival of developing neurons. *J Cell Biol.* **148:** 325-332.

Minton, S.A. (1990). Neurotoxic snake envenoming. *Semin Neurol*. **10:** 52-61.

Mohamed, A.H., Saleh, A.M. and Ahmed, F. (1970) Nerve growth factor from Egyptian snake venoms. *Toxicon*. **9:** 201-205.

Monyer, H., Goldberg, M.P.,and Choi, D.W. (1989). Glucose deprivation neuronal injury in cortical culture. *Brain Res*. **483:** 347-354.

Morcellin, S., Rossi, C.R., Pilati, P., Nitti, D. and Marincola, F.M. (2003) Quantitative real-time PCR: a powerful ally in cancer research. *Trend in Mol Med.* **9:** 189-195.

Moriyoshi, K., Masu, M., Ishii, T., Shigemoto, R., Mizuno, N. and Nakanishi, S. (1991) Molecular cloning and characterization of the rat NMDA receptor. *Nature* **354:** 31-37.

Morrison, T.B., Weis, J.J. and Wittwer, C.T. (1998) Quantification of low-copy transcripts by continuous SYBR Green I monitoring during amplification. *BioTechniques* **24:** 954-958.

Mowla, S.J., Farhadi, H.F., Pareek, S., Atwal, J.K., Morris, S.J., Seidah, N.G. and Murphy, R.A. (2001) Biosynthesis and post-translational processing of the precursor to brain-derived neurotrophic factor. *J Biol Chem.* **276:** 12660-12666.

Nadler, J.V., Perry, B.W. and Cotman, C.W. (1978) Intraventricular kainic acid preferentially destroys hippocampal pyramidal cells. *Nature* **271:** 676-677.

Nagasawa, H. and Kogure, K. (1989) Correlation between cerebral blood flow and histologic changes in a new rat model of middle cerebral artery occlusion. *Stroke* **20:**1037-43.

Nakagomi, S., Suzuki, Y., Namikawa, K., Kiryu-Seo, S. and Kiyama, H. (2003) Expression of the activating transcription factor 3 prevents c-Jun N-terminal kinase-induced neuronal death by promoting heat shock protein 27 expression and Akt activation. *J Neurosci.* **23:** 5187-5196.

Nakagawa, I., Nakata, M., Kawabata, S. and Hamada, S. (1999) Regulated expression of the Shiga toxin B gene induces apoptosis in mammalian fibroblastic cells. *Mol Microbiol.* **33:** 1190-1199.

Nakanishi, S. and Masu, M. (1994) Molecular diversity and functions of glutamate receptors. *Ann Rev Biophys Biomol Struct.* **23:** 319-348.

Nosaka, Y., Arai, A., Miyasaka, N. and Miura, O. (1999) CrkL mediates ras-dependent activation of the Raf/ERK pathway through the guanine nucleotide exchange factor C3G in hematopoietic cells stimulated with erythropoietin or interleukin-3. *J Biol Chem.* **274:** 30154-30162.

Nykjaer, A., Lee, R., Teng, K.K., Jansen, P., Madsen, P., Nielsen, M.S., Jacobsen, C., Kliemannel, M., Schwarz, E., Willnow, T.E., Hempstead, B.L. and Petersen, C.M. (2004) Sortilin is essential for proNGF-induced neuronal cell death. *Nature* **427:** 843-848.

Oh, J., Zhong, L.T., Yang, J., Bitler, C.M., Butcher, L.L., Bredsen, D.E. and Rabizadeh, S. (1993) Induction of apoptosis of the low-affinity NGF receptor. *Science* **261:** 345-348.

Ownby, C.L., Fletcher, J.E. and Colberg, T.R. (1993) Cardiotoxin I from cobra (*Naja naja atra*) venom causes necrosis of skeletal muscle *in vivo*. *Toxicon* **31:** 697-709.

Pagano, A., Ruegg, D., Litschig, S., Stoehr, N., Stierlin, C., Heinrich, M., Floersheim, P., Prezeau, L., Carroll, F., Pin, J.P., Cambria, A., Vranesic, I., Flor, P.J., Gasparini, F. and Kuhn, R. (2000) The non-competitive antagonists 2-methyl-6-(phenylethynyl)pyridine and 7 hydroxyiminocyclopropan[b]chromen-1a-carboxylic acid ethyl ester interact with overlapping binding pockets in the transmembrane region of group I metabotropic glutamate receptors. *J Biol Chem*. **275:** 33750-33758.

Pak, J.H., Huang, F.L., Li, J., Balschun, D., Reymann, K.G., Chiang, C., Westphal, H. and Huang, K.P. (2000) Involvement of neurogranin in the modulation of calcium/calmodulin-dependent protein kinase II, synaptic plasticity, and spatial learning: a study with knockout mice. *Proc Natl Acad Sci USA* **97:** 11232-11237.

Palmada M., Kanwal S., Rutkoski N. J., Gufstafson-Brown C., Johnson R. S., Wisdom R. *et al*. (2002) c-jun is essential for sympathetic neuronal death

induced by NGF withdrawal but not by p75 activation. *J Cell Biol.* **158:** 453–461.

Palmer, C., Roberts, R.L. and Bero, C. (1994) Deferoxamine posttreatment reduces ischemic brain injury in neonatal rats. *Stroke* **25**: 1039-1045.

Pan, Z., Sampath, D. and Jackson, G. (1997) Nerve growth factor and oxidative stress in the nervous system. In Brain Plasticity. Plenum. New York. **Pp** 173-193

Paratcha, G., de Stein, M.L., Szapiro, G., Lopez, M., Bevilaqua, L., Cammarota, M., de Iraldi, A.P., Izquierdo, I. and Medina, J.H. (2000) Experience-dependent decrease in synaptically localized Fra-1. *Brain Res Mol Brain Res.* **78:** 120-130.
Parkhouse, N. and Le Quesne, P.M. (1988) Impaired neurogenic vascular response in patients with diabetes and neuropathic foot lesions. *N Engl J Med.* **318:** 1306-1309.

Patapoutian, A. and Reichardt, L.F. (2001) Trk receptors: mediators of neurotrophin action. *Curr Opin Neurobiol.* **11:** 272-280.

Pawson, T and Nash, P. (2000) Protein-protein interactions define specificity in signal transduction. *Genes Dev.* **14:**1027–1047.

Pérez, P., Coll, P. M., Hempstead, B. L., Martin-Zanca, D. and Chao, M. V. (1995) NGF binding to the trk tyrosine kinase receptor requires the extracellular immunoglobulin-like domains. *Mol Cell Neurosci.* **6:** 97–105

Perez-Polo, J. R., Bomar, H., Beck, C., Hall, K., (1978) Nerve growth factor from *Crotalus adamenteus* snake venom. *J Biol Chem.* **253:** 6140–6148.

Perry, V.H., Anthony, D.C., Bolton, S.J. and Brown, H.C. (1997) The blood–brain barrier and the inflammatory response. *Mol Med Today* **3:** 335–341.

Pin, J.P. and Duvoisin, R. (1995) The metabotrophic glutamate receptors: structure and functions. *Neuropharmacology* **34:** 1-26.

Pollock, R., Issner, R., Zoller, K., Natesan, S., Rivera, V.M. and Clackson, T. (2000) Delivery of a stringent dimerizer-regulated gene expression system in a single retroviral vector. *Proc Natl Acad Sci USA* **97:** 13221-13226.

Powell, E. M., Sobarzo, M. R. and Saltzman, W. M. (1990) Controlled release of nerve growth factor from a polymeric implant. *Brain Res.* **515:** 309-311.

Pringle, A.K., Iannotti, F., Wilde, G.J.C., Chad, J.E., Seeley, P.J. and Sundstrom, L.E. (1997) Neuroprotection by both NMDA and non-NMDA receptor antagonists *in vitro* ischemia. *Brain Res.* **755:** 36-46.

Rabizadeh, S. and Bredesen, D.E. (2003) Ten years on: mediation of cell death by the common neurotrophin receptor p75 (NTR). *Cytokine Growth Factor Rev.* **14:** 225- 239. Review.

Racke, M.M., Mason, P.J., Johnson, M.P., Brankamp, R.G. and Linnik, M.D. (1996) Demonstration of a second pharmacologically active promoter region in the NGF gene that induces transcription at the exon 3. *Mol Brain Res*. **41:** 192-199.

Rattenholl, A., Ruoppolo, M., Flagiello, A., Monti, M., Vinci, F., Marino, G., Lilie, H., Schwarz, E. and Rudolph, R. (2001) Pro-sequence assisted folding and disulfide bond formation of human nerve growth factor. *J Mol Biol*. **305:** 523-533.

Reid, A.H. (1964) Cobra-bites. *Brit Med J*. **2:** 540-545.

Reichardt, L.F. and Fariñas, I. (1997) Neurotrophic factors and their receptors. Roles in neuronal development and function. In *Molecular and Cellular Approaches to Neural Development*, (Ed. Cowan W.M., Jessell T.M., Zipursky, S.L.) New York: Oxford Univ. Press **pp:** 220–63.

Riccio, A., Ahn, S., Davenport, C.M., Blendy, J.A. and Ginty, D.D. (1999) Mediation by a CREB family transcription factor of NGF-dependent survival of sympathetic neurons. *Science* **286:** 2358–2361.

Rodriguez-Tebar, A., Dechant, G. and Barde, Y.-A. (1990) Binding of brain-derived neurotrophic factor to the nerve growth factor receptor. *Neuron* **4:** 487–492.

Rodriguez-Tebar, A., Dechant, G., Gotz, R. and Barde, Y. A. (1992) Binding of neurotrophin-3 to its neuronal receptors and interactions with nerve growth-factor and brain-derived neurotrophic factor. *EMBO J*. **11:** 917–922.

Rothman, S. (1988) Non-competitive N-methyl-D-aspartate antagonists affect multiple ionic currents. *J Pharmac Exp Ther*. **246:** 137-142.

Roux, P.P., Colicos, M.A., Barker, P.A. and Kennedy, T.E. (1999) p75 neurotrophin receptor expression is induced in apoptotic neurons after seizure. *J Neurosci*. **19:** 6887–6896.

Roux P. P., Bhakar A. L., Kennedy T. E. and Barker P. A. (2001) The p75 neurotrophin receptor activates Akt (protein kinase B) through a phosphatidylinositol 3-kinase-dependent pathway. *J Biol Chem*. **276:** 23097–23104.

Roux, P. P. and Barker, P. A. (2002) Neurotrophin signaling through the p75 neurotrophin receptor. *Prog Neurobiol*. **67:** 203-233

Rukenstein, A., Rydel, R.E., Greene, L.A. (1991) Multiple agents rescue PC12 cells from serum-free cell death by translation- and transcription-independent mechanisms. *J Neurosci.* **11:** 2552-2563.

Salehi, A.H., Roux, P.P., Kubu, C.J., Zeindler, C., Bhakar, A., Tannis, L.L., Verdi, J.M. and Barker, P.A. (2000) NRAGE, a novel MAGE protein, interacts

with the p75 neurotrophin receptor and facilitates nerve growth factor-dependent apoptosis. *Neuron* **27:** 279–288.

Sambrook, J., Fritsch, F.F. and Maniatis, T. (1989) Molecular cloning: a laboratory manual. 2nd Ed. Cold Spring Harbor Laboratory, Cold Spring Harbor, N.Y.

Samuels, I.S., Seibenhener, M.L., Neidigh, K.B. and Wooten, M.W. (2001) Nerve growth factor stimulates the interaction of ZIP/p62 with atypical protein kinase C and targets endosomal localization: evidence for regulation of nerve growth factor-induced differentiation. *J Cell Biochem.* **82:** 452-466.

Sanger, F., Nicklen, S. and Coulson, A.R. (1977) DNA sequencing with chain-terminating inhibitors. *Proc Natl Acad Sci USA* **74:** 5463-5467.

Sarret, P., Krzywkowski, P., Segal, L., Nielsen, M.S., Petersen, C.M., Mazella, J., Stroh, T. and Beaudet, A. (2003) Distribution of NTS3 receptor/sortilin mRNA and protein in the rat central nervous system. *J Comp Neurol.* **461:** 483-505.

Saunders, J.J.W. (1966) Death in embryonic systems. *Science* **154:** 604-612.

Schabitz, W.R., Schwab, S. Spranger, M. and Hacke, W. (1997) Intraventricular brain-derived neurotrophic factor reduces infarct size after focal cerebral ischemia in rats. *J Cereb Blood Flow Metab*. **17:** 500-506

Schagger, H. and von Jagow, G. (1987) Tricine-sodium dodecyl sulfate-polyacrylamide gel electrophoresis for the separation of proteins in the range from 1-100kDa. *Anal Biochem.* **166:** 368-379.

Schneider, R. and Schweiger, M. (1991) A novel modular mosaic of cell adhesion motifs in the extracellular domains of the neurogenic trk and trkB tyrosine kinase receptors. *Oncogene* **6:** 1807–1811.

Schoepp, D.D., Jane, D.E. and Monn, J.A. (1999) Pharmacological agents acting at subtypes of metabotropic glutamate receptors. *Neuropharmacology* **38:**1431-1476. Review.

Schulze, A. and Downward, J. (2001) Navigating gene expression using microarrays- a technology review. *Nat Cell Biol.* **3:** E190-195.

Schwab, M., Otten, U., Agid, Y and Thoenen, H. (1979) Nerve growth factor (NGF) in the rat CNS: absence of specific retrograde axonal transport and tyrosine hydroxylase induction in locus coeruleus and substantia nigra. *Brain Res.* **168:** 473-483.

Sealy, L., Mota, F., Rayment, N., Tatnell, P., Kay, J., Chain, B. (1996) Regulation of cathepsin E expression during human B cell differentiation in vitro. *Eur J Immunol.* **26:** 1838-1843.

Seidah, N.G., Benjannet, S., Pareek, S., Savaria, D., Hamelin, J., Goulet, B., Laliberte, J., Lazure, C., Chretien, M. and Murphy, R.A. (1996) Cellular processing of the nerve growth factor precursor by the mammalian pro-protein convertase. *Biochem J*. **314:** 951-960.

Selby, M.J., Edwards, R., Sharp, F. and Rutter, W.J. (1987) Mouse nerve growth factor gene: structure and expression. *Mol Cell Biol*. **7:** 3057-3064.

Server, A.C., Herrup, K., Shooter, E.M., Hogue-Angeletti, R.A., Frazier, W.A. and Bradshaw, R.A. (1976) Comparison of the nerve growth factor proteins from cobra venom (*Naja naja*) and mouse submaxillary gland. *Biochemistry* **15:** 35-39.

Sheardown, M.J., Nielsen, E. ∅., Hansen, A.J., Jacobsen, P. and Honore, T. (1990). 2, 3-Dihydroxy-6-nitro-7-sulfamoyl-benzo (F)quinoxaline: a neuroprotectant for cerebral ischemia. *Science* **247:** 571-574.

Shetty, V.P., Anita, N.H. and Jacobs, J.M. (1988) The pathology of early leprosy. *J Neurol Sci*. **88:** 115-131.

Siigur, J., Arumae, U., Neumann, T. and Saarma, M. (1987) Monoclonal antibody immunoaffinity chromatography of the nerve growth factor from snake venoms. *Comp Biochem Physiol*. **87B:** 329-334.

Siigur, J., Arumae, U., Siigur, E., Paalme, V., Neumann, T. and Saarma, M. (1992) Nerve growth factor from snake venoms. Comparative aspects. In: Recent Advances in Toxinology Research. Gopalakrishnakone, P. and Tan, C.K (Eds). **1:** 154-191.

Smith, P.J., Brandt, W.F., Stickells, B.J. and von Holt, C. (1992) *Bitis arierans* nerve growth factor is a disulphide-linked homodimer. *Comp Biochem Physiol*. **103B:** 975-980.

Sommer, B., Keinanen, K., Verdoorn, T.A., Wisden, W., Burnashev, N., Herb, A., Kohler, M., Takagi, T., and Sakmann, B. (1990) Flip and flop: a cell-specific functional switch in glutamate-operated channels of the CNS. *Science* **249:** 1580-1585.

Stefan, E., Wiesner, B., Baillie, G.S., Mollajew, R., Henn, V., Lorenz, D., Furkert, J., Santamaria, K., Nedvetsky, P., Hundsrucker, C., Beyermann, M., Krause, E., Pohl, P., Gall, I., MacIntyre, A.N., Bachmann, S., Houslay, M.D., Rosenthal. W. and Klussmann, E. (2007) Compartmentalization of cAMP-dependent signaling by phosphodiesterase-4D is involved in the regulation of vasopressin-mediated water reabsorption in renal principal cells. *J Am Soc Nephrol*. **18:**199-212.

Stephens, R.M., Loeb, D.M., Copeland, T.D., Pawson, T., Greene, L.A. and Kaplan, D.R. (1994) Trk receptors use redundant signal transduction pathways involving SHC and PLC-gamma 1 to mediate NGF responses. *Neuron* **12:**691–705.

Stoppini, L., Buchs, P.A. and Muller, D. (1991) A simple method for organotypic cultures for nervous tissue. *J Neurosci Methods.* **37:** 173-182.

Strasser, U. and Fisher, G. (1995) Protection from neuronal damage induced by combined oxygen and glucose deprivation in organotypic hippocampal cultures by glutamate receptor antagonists. *Brain Res.* **687:**167-174.

Suter, U., Heymach, J.V. Jr and Shooter, E.M. (1991) Two conserved domains in the NGF propeptide are necessary and sufficient for the biosynthesis of correctly processed and biologically active NGF. *EMBO J.* **10:** 2395-2400.

Sutter, A., Riopelle, R.J., Harris Warrick, R.M. and Shooter, E.M. (1979) Nerve growth factor receptors. Characterization of two distinct classes of binding sites on chick embryo sensory ganglia cells. *J Biol Chem.* **254:** 5972-5982.

Swanson, R.A. and Choi, D.W. (1993). Glial glycogen stores affect neuronal survival during glucose deprivation *in vitro*. *J Cereb Blood Flow Metab*. **13:** 162-169.

Synder, E.M., Philpot, B.D., Huber, K.M., Dong, X., Fallon, J.R., Bear, M.F. (2001) Internalization of ionotrophic glutamate receptors in response to mGluR activation. *Nat Neurosci.* **4:** 1079-1085.

Syroid, D. E., Maycox, P. J., Soilu-Hanninen, M., Petratos, S., Bucci, T., Burrola, P., Murray, S., Cheema, S., Lee, K.F., Lemke, G. and Kilpatrick, T.J. (2000) Induction of postnatal schwann cell death by the low-affinity neurotrophin receptor in vitro and after axotomy. *J Neurosci*. **20:** 5741–5747.

Tabakman, R., Lazarovici, P. and Kohen, R. (2002) Neuroprotective effects of carnosine and homocarnosine on pheochromocytoma PC12 cells exposed to ischemia. *J Neurosci Res.* **68:** 463-469.

Tabakman, R., Jiang, H., Shahar, I., Arien-Zakay, H., Levine, R.A. and Lazarovici. (2005) Neuroprotection by NGF in the PC12 *in vitro* OGD model. Involvement of mitogen-activated protein kinases and gene expression. *Ann N Y Acad Sci.* **1053:** 84-96.

Taglialatela, G., Robinson, R. and Perez-Polo, J.R. (1997) Inhibition of nuclear factor kappa B (NFkappaB) activity induces nerve growth factor-resistant apoptosis in PC12 cells. *J Neurosci Res.* **47:**155–162.

Takai, S., Yamada, K., Kawakami, H., Tanaka, K. and Nakamura, S. (1995) Localization of the gene (SLC1A3) encoding human glutamate transporter (GluT-1) to 5p13 by fluorescence in situ hybridization. *Cytogenet Cell Genet.* **69:** 209-210.

Tan, N.H. (1982) Cardiotoxins from the venom of Malayan cobra (*Naja naja sputatrix*). *Arch Biochem Biophy.* **218:** 51-58.

Tan, N.H. (1983) Improvement of Malayan cobra antivenom. *Toxicon* **21:** 75-79.

Tan, N.H. and Armugam, A. (1989a) Isolation and characterization of a lethal acidic phospholipase A_2 from Malayan cobra (*Naja naja sputatrix*). *Biochem Int.* **18:** 785-792.

Tan, N.H. and Armugam, A. (1989b) The anticoagulant activity of Malayan cobra (*Naja naja sputatrix*) venom and venom phospholipase A_2 enzymes. *Biochem Int.* **19:** 803-810.

Tan, N.H. and Armugam, A. (1990) *In vivo* interactions between neurotoxin, cardiotoxin and phospholipase A2 isolated from Malayan cobra (*Naja sputatrix*) venom. *Toxicon* **28:** 1193-1198.

Thiagarajan, P. and Tait, J.F. (1990) Binding of annexin V/ placental anticoagulant protein I to platelets. Evidence for phosphatidylserine exposure in the procoagulant response to activated platelets. *J Biol Chem.* **265:** 17420-17423.

Thomas, P.K. and Tomlinson, D.R. (1993) Diabetic and hypoglycemic neuropathy. In: Dyck, P.J., Thomas, J.W., Griffin, J.W., P.A Low and Poduslo, J.F. (Eds), Peripheral neuropathy, 3rd edition. WB Saunder & Co, Philadelphia/London, **pp:** 1219-1250.

Thompson, J.D., Higgins, D.G. and Gibson, T.J. (1994) CLUSTAL W: improving the sensitivity of progressive multiple sequence alignment through sequence weighting, position-specific gap penalties and weight matrix choice. *Nucleic Acids Res.* **22:** 4673-4680.

Troy, C.M., Friedman, J.E. and Friedman, W.J. (2002) Mechanisms of p75-mediated death of hippocampal neurons. Role of caspases. *J Biol Chem.* **277:** 34295-34302.

Tu, J.C., Xiao, B., Yuan, J.P., Lanahan, A.A., Leoffert, K., Li, M., Linden, D.J. and Worley, P.F. (1998) Homer binds to a novel proline-rich motif and links group I metabotrophic glutmate receptors with IP3 receptors. *Neuron* **21:** 717-726.

Tuszynski, M.H. ,Thal, L., Pay, M., Slamon, D.P., U, H.S., Bakay, R., Patel, P., Blesch, A., Vahlsing, H.L., Ho, G., Tong, G., Potkin, S.G., Fallon, J., Hansen, L., Mufson, E.J., Kordower, J.H., Gall, C. and Conner, J. (2005) A phase 1 clinical trial of nerve growth factor gene therapy for Alzheimer disease. *Nat Med.* **11:** 551-555.

Tuttle, J.B., Etheridge, R. and Creedon, D.J. (1993) Receptor-mediated stimulation and inhibition of nerve growth factor secretion by vascular smooth muscle. *Exp Cell Res.* **208:** 350-361.

Tuveri, M.A., Generini, S., Matucci-Cerinic, M. and Aloe, L. (2000) NGF, a useful tool in the treatment of chronic vasculitic ulcers in rheumatoid arthritis. *Lancet* **356:** 1739-1740.

Tuveri, M.A., Triaca, V. and Aloe, L. (2006) The nerve growth factor induces cutaneous ulcer healing in "non-responder" tranplanted skin. *Ann Ist Super Sanita.* **42:** 94-96.

Tweedie, M.W.F. (1983) The snakes of Malaya. Singapore National Printers, Singapore.

Ullrich, A., Gray, A., Berman, C. and Dull, T.J. (1983) Human beta-nerve growth factor gene sequence highly homologous to that of mouse. *Nature* **303:** 821-825.

Ultsch, M.H., Wiesmann, C., Simmons, L.C., Henrich, J., Yang, M., Reilly, D., Bass, S.H. and de Vos, A.M. (1999) Crystal structures of the neurotrophin-binding domain of TrkA, TrkB and TrkC. *J Mol Biol.* **290:**149-159.

Urfer, R., Tsoulfas, P., O'Connell, L., Hongo, J.A., Zhao, W. and Presta, L.G. (1998). High resolution mapping of the binding site of TrkA for nerve growth factor andTrkC for neurotrophin-3 on the second immunoglobulin-like domain of the Trk receptors. *J Biol Chem.* **273:** 5829- 5840.

Vaillant, A.R., Mazzoni, I., Tudan, C., Boudreau, M., Kaplan, D.R. and Miller, F.D. (1999) Depolarization and neurotrophins converge on the phosphatidylinositol 3-kinase-Akt pathway to synergistically regulate neuronal survival. *J Cell Biol.* **146:** 955–966.

Vanden Heuvel, J.P., Tyson, F.L. and Bell, D.A. (1993) Construction of recombinant RNA templates for use in internal standards in quantitative RT-PCR. *BioTechniques* **14:** 395-398.

Vaudry, D., Stork, P.J., Lazarovici, P. and Eiden, L.E. (2002) Signaling pathways for PC12 differentiation: making the right connections. *Science* **296:** 1648-1649.

Viravan, C., Veeravat, U., Warrell, M.J., Theakston, R.D.G. and Warrell, D.A. (1986) ELISA confirmation of acute and past envenoming by the monocellate Thai cobra (*Naja kaouthia*). *Am J Trop Med Hyg.* **35:** 173-181.

Vornov, J.J., Tasker, R.C. and Coyle, J.T. (1994). Direct observation of the agonist specific regional vulnerability to glutamate, NMDA and kainite neurotoxicity in organotypic hippocampal cultures. *Exp Neurol.* **114:** 11-22.

Vornov, J.J., Tasker, R.C. and Park, J. (1995). Neurotoxicity of acute glutamate transport blockade depends on coactivation of both NMDA and AMPA/Kainate receptors in organotypic hippocampal cultures. *Exp Neurol.* **133:** 7-17.

Wahl, P., Schousboe, A., Honore, T. and Drejer, J. (1989) Glutamate-induced increase in intracellular Ca^{2+} in cerebral cortex neurons is transient in immature cells but permanent in mature cells. *J Neurochem.* **53:** 1316-1319.

Wang, H.D., Fukuda, T., Suzuki, T., Hashimoto, K., Liou, S.Y., Momoi, T., Kosaka, T., Yamamoto, K., Nakanishi, H. (1999) Differential effects of Bcl-2 overexpression on hipppocampal CA1 neurons and dentate granule cells following hypoxic ischemia in adult mice. *J Neurosci Res.* **57:** 1-12.

Wang, S., Bray, P., McCaffrey, T., March, K., Hempstead, B.L. and Kraemer, R., (2000) p75NTR mediates neurotrophin-induced apoptosis of vascular smooth muscle cells. *Am J Pathol.* **157:** 1247–1258.

Weeraratna, A.T., Nagel, J.E., Mello-Coelho, V.D. and Taub, D.D. (2004) Gene-expression profiling: From microarrays to medicine. *J Clin Immunol.* **24:** 213-224.

Welker, P., Grabbe, J., Gibbs, B., Zuberbier, T. and Henz, B.M. (2000) Nerve growth factor-beta induces mast-cell marker expression during in vitro culture of human umbilical cord blood cells. *Immunology* **99:** 418-426.

Whitehouse, P.J., Price, D.L., Struble, R.G., Clark, A.W., Coyle, J.T. and Delon, M.R. (1982) Alzheimer's disease and senile dementia: loss of neurons in basal forebrain. *Science* **215:** 1237–1239.

Whittemore, S.R., Ebendal, T., Larkfors, L., Olson, L., Seigerm A., Stromberg, I. and Persson, H. (1986) Developmental and regional expression of β-nerve growth factor messenger RNA and protein in the rat central nervous system. *Proc Natl Acad Sci USA* **83:** 817-821.

Whittemore, S.R., Friedman, P.L., Larmammar, D., Persson, H., Gonzalez-Carvajal, M. and Holets, V.R. (1988) Rat β-nerve growth factor sequence and the site of synthesis in the adult rat hippocampus. *J Neurosci Res.* **20:** 403-410.

Wiesmann, C., Ultsch, M.H., Bass, S.H. and de Vos, A.M. (1999) Crystal structure of nerve growth factor in complex with the ligand-binding domain of TrkA receptor. *Nature* **401:** 184-188.

Wiesmann, C. and de Vos, A.M. (2001) Nerve growth factor: Structure and function. *Cell Mol Life Sci.* **58:** 748-759.

Wilde, A., Beattie, E.C., Lem, L., Riethof, D.A., Liu, S.H., Mobley, W.C., Soriano, P. and Brodsky, F.M. (1999) EGF receptor signaling stimulates SRC kinase phosphorylation of clathrin, influencing clathrin redistribution and EGF uptake. *Cell 96***:** 677-687.

Wilhelm, J. and Pingoud, A. (2003) Real-time Polymerase Chain Reaction. *ChemBioChem.* **4:** 1120-1128.

Williams, B.J., Eriksdotter-Jonhagen, M. and Granholm, A.C. (2006) Nerve growth factor in treatment and pathogenesis of Alzheimer's disease. *Prog Neurobiol.* **80:** 114-128.

Williams, L., Varon, R. S., Peterson, G., Wictorin, K., Fischer, W., Bjorklund, A. and Gage, F.H. (1986) Continuous infusion of nerve growth factor prevents basal forebrain neuronal cell death after fimbria–fornix transaction. *Proc Natl Acad Sci USA* **83:** 9231–9236.

Winzeler, E., Shoemaker, D.D., Astromoff, A., Liang, H., Anderson, K., Andre, B., Bangham, R., Benito, R., Boeke, J.D., Bussey, H., Chu, A.M. Connelly, C., Davis, K., Dietrich, F., Dow, S.W., El Bakkoury, M., Foury, F., Friend, S.H., Gentalen, E., Giaever, G., Hegemann, J.H., Jones, T., Laub, M., Liao, H., Liebundguth, N., Lockhart, D.J., Lucau-Danila, A., Lussier, M., M'Rabet, N., Menard, P., Mittmann, M., Pai, C., Rebischung, C., Revuelta, J.L., Riles, L., Roberts, C.J., Ross-MacDonald, P., Scherens, B., Snyder, M., Sookhai-Mahadeo, S., Storms, R.K., Veronneau, S., Voet, M., Volckaert, G., Ward, T.R., Wysocki, R., Yen, G.S., Yu, K., Zimmermann, K., Philippsen, P., Johnston, M. and Davis, R.W. (1999) Functional characterization of the *Saccharomyces cerevisiae* genome by precise deletion and parallel analysis. *Science* **287:** 873-880.

Wisden, W. and Seeburg, P.H. (1993) Mammalian ionotrophic glutamate receptors. *Curr Opin Neurobiol.* **3:** 291-298.

Wolfsberg, T.G. (1999) Candidate regulatory sequence elements for cell cycle-dependent transcription in *Saccharomyces cerevisiae*. *Genome Res.* **9:** 775-792.

Wong E.H.F., Kemp, J.A., Priestly, T., Knight, A.R., Woodruff, G.N. and Iversen, L.L. (1986) The anticonvulsant MK-801 is a potent N-methyl-D-aspartate antagonist. *Proc Natl Acad Sci USA* **83:** 7104-7108.

Wooten, M.W., Seibenhener, M.L., Mamidipudi, V., Diaz-Meco, M.T., Barker, P.A. and Moscat, J. (2001) The atypical protein kinase C-interacting protein p62 is a scaffold for NF-kappaB activation by nerve growth factor. *J Biol Chem.* **276:** 7709-7712.

Wright, J.H., Drueckes, P., Bartoe, J., Zhao, Z., Shen, S.H. and Krebs, E.G. (1997) A role for the SHP-2 tyrosine phosphatase in nerve growth-induced PC12 cell differentiation. *Mol Biol Cell* **8:**1575-1585.

Wyllie, A.H. (1980) Glucocorticoid-induced thymocyte apoptosis is associated with endogenous endonuclease activation. *Nature* **284:** 555-556.

Xiao, B., Tu, J.C., Petralia, R.S., Yuan, J.P., Doan, A., Breder, C.D. Ruggiero, A., Lanahan, A.A., Wenthold, R.J. and Worley, P.F. (1998) Homer regulates the association of group I metabotrophic glutamate receptors with multivalent complexes of homer-related, synaptic proteins. *Neuron* **21:** 707-716.

Xing, J., Ginty, D.D. and Greenberg. M.E. (1996) Coupling of the RAS-MAPK pathway to gene activation of RSK2, a growth factor-regulated CREB kinase. *Science* **273:**959-963.

Xing, J., Kornhauser, J.M., Xia, Z., Thiele, E.A. and Greenberg, M.E. (1998) Nerve growth factor activates extracellular signal-regulated kinase and p38 mitogen-activated protein kinase pathways to stimulate CREB serine 133 phosphorylation. *Mol Cell Biol.* **18:**1946-1955.

Yamada, M., Ohnishi, H., Sano, S.I., Nakatami, A., Ikeuchi, T. and Hatanaka, H. (1997) Insulin receptor substrate (IRS)-2 and IRS-2 are tyrosine-phosphorylated and associated with phosphatidylinositol 3-kinase in response to brain-derived neurotrophic factor in cultured cerebral cortical neurons. *J Biol Chem.* **48:** 30334–30339.

Yamamoto, S., Yoshimine, T., Fujita, T., Kuroda, R., Irie, T., Fujioka, K. and Hayakawa, T. (1992) Protective effect of NGF atelocollagen mini-pellet on the hippocampal delayed neuronal death in gerbils. *Neurosci Lett.* **141:** 161-165.

Yamashita, T., Tucker, K. L. and Barde, Y.-A. (1999) Neurotrophin binding to the p75 receptor modulates Rho activity and axonal outgrowth. *Neuron* **24:** 585–593.

Yao, F., Svensjo, T., Winkler, T., Lu, M., Eriksson, C. and Eriksson, E. (1998) Tetracycline repressor, tetR, rather than the tetR-mammalian cell transcription factor fusion deriviatives, regulates inducible gene expression in mammalian cells. *Hum Gene Ther.* **9:** 1939-1950.

Yao, R., Osada, H. and Yoshihara, M. (1997) Specific activation of a c-Jun NH2-terminal kinase isoform and induction of neurite outgrowth in PC-12 cells by staurosporine. *J Biol Chem.* **272:** 18261-18266.

Yoon S. O., Casaccia-Bonnefil P., Carter B. and Chao M. V. (1998) Competitive signaling between TrkA and p75 nerve growth factor receptors determine cell survival. *J Neurosci.* **18:** 3273–3281.

York, R.D., Yao, H., Dillon, T., Ellig, C.L., Eckert, S.P., McCleskey, E.W. and Stork P.J. (1998) Rap1 mediates sustained MAP kinase activation induced by nerve growth factor. *Nature* **393:** 622–626.

York, R.D., Mollivar, D.C., Grewal, S.S., Steinberg, P.E., McCleskey, E.W. and Stork, P.J.S. (2000) Role of phosphoinositide 3-kinase and endocytosis in NGF induced extracellular signalregulated kinase activation via Ras and Rap1. *Mol Cell Biol.* **20:**18069–18083.

Yuan, J. and Yankner, B.A. (2000) Apoptosis in the nervous system. *Nature* **407:** 802–809.

Zha, H. and Reed, J.C. (1997) Heterodimerization-independent functions of cell death regulatory proteins Bax and Bcl-2 in yeast and mammalian cells. *J Biol Chem.* **272:** 31482-31488.

Zhang, H., Hoang, T., Saeed, B. and Ng, S.C. (1996) Induction of apoptosis in prostatic tumor cell line DU14S by staurosporine, a potent inhibitor of protein kinases. *Prostate* **26:** 69-76.

Zhang, Y. and Pardridge, W.M. (2006) Blood-brain barrier targeting of BDNF improves motor function in rats with middle cerebral artery occlusion. *Brain Res.* **1111:** 227-229.

Zhao, Q., Pahlmark, K., Smith, M.L. and Siesjo, B.K. (1994) Delayed treatment with the spin trap alpha-phenyl-N-tert-butyl nitrone (PBN) reduces infarct size following transient middle cerebral artery occlusion in rats. *Acta Physiol Scand.* **152:** 349-350.

Zhou, A.W., Li, W.X., Guo, J. and Du, Y.C. (1997) Facilitation of AVP (4-8) on gene expression of BDNF and NGF in rat brain. *Peptides* **18:** 1179-1187.

Zou, L. L., Huang, L., Hayes, R.L., Black, C., Qiu, Y. H., Perez-Polo, J. R., Le, W., Clifton, G. L. and Yang, K. (1999) Liposome-mediated NGF gene transfection following neuronal injury: potential therapeutic applications. *Gene Ther.* **6:** 994-1005.

Appendices

Publications

Sputa nerve growth factor forms a preferable substitute to mouse 7S-β nerve growth factor

Dawn C.-I. KOH, A. ARMUGAM and K. JEYASEELAN[1]

Department of Biochemistry, Faculty of Medicine, National University of Singapore, 8 Medical Drive, Singapore 117597, Singapore

The NGF (nerve growth factor) from *Naja sputatrix* has been purified by gel filtration followed by reversed-phase HPLC. The protein showed a very high ability to induce neurite formation in PC12 cells relative to the mouse NGF. Two cDNAs encoding isoforms of NGF have been cloned and an active recombinant NGF, sputa NGF, has been produced in *Escherichia coli* as a His-tagged fusion protein. Sputa NGF has been found to be non-toxic under both *in vivo* and *in vitro* conditions. The induction of neurite outgrowth by this NGF has been found to involve the high-affinity trkA–p75$^{\mathrm{NTR}}$ complex of receptors. The pro-survival mechanism of p75$^{\mathrm{NTR}}$ has been mediated by the activation of nuclear factor κB gene by a corresponding down-regulation of inhibitory κB gene.

Real-time PCR and protein profiling (by surface-enhanced laser-desorption–ionization time-of-flight) have confirmed that sputa NGF up-regulates the expression of the endogenous NGF in PC12 cells. Preliminary microarray analysis has also shown that sputa NGF is capable of promoting additional beneficial effects such as the up-regulation of arginine vasopressin receptor 1A, voltage-dependent T-type calcium channel. Hence, sputa NGF forms a new and useful NGF.

Key words: *Naja sputatrix*, nerve growth factor (NGF), neurite outgrowth, PC12 cells, sputa NGF.

INTRODUCTION

In the past decade, the neurotrophin family has gathered much interest as potentially useful therapeutic agents against neurological disorders. The neurotrophin family is made up of NGF (nerve growth factor), BNDF (brain-derived growth factor), NT-3 (neurotrophin-3), NT-4 and a newly discovered NT-6. Neurotrophins are made up of small, homodimeric proteins and they use two different receptors (i) Trk (tropomyosin-related kinase) receptor tyrosine kinase and (ii) p75 neurotrophin receptor [a member of the TNF (tumour necrosis factor) receptor superfamily]. The binding of neurotrophin to its receptors has been shown to mediate the survival, differentiation, growth or apoptosis of neurons. Both receptors have been found in the same cell and are known to act synergistically to bring about the targeted response of neurotrophins from the neurons during the development of the nervous system [1]. NGF is required for the survival of the differentiated cells. Both p75$^{\mathrm{NTR}}$ and TrkA receptors act synergistically to mediate the trophic effects of NGF in cells that produce them (e.g. PC12 cells). Co-expression of p75$^{\mathrm{NTR}}$ has also been found to enhance the biological response of cells expressing TrkA [2]. Interestingly, the TrkA receptor activates positive signals such as increased survival and growth, whereas the p75$^{\mathrm{NTR}}$ receptor is known to activate both positive and negative signals. Complexes of p75$^{\mathrm{NTR}}$ with TrkA have been found to enhance the neurotrophin-binding affinity and TrkA-associated signalling pathway [3]. Neuroprotection by NGF and activation of NF-κB (nuclear factor κB, a pro-survival transcription factor) have also been shown to be dependent on the expression of p75$^{\mathrm{NTR}}$ in PC12 cells [4].

NGF has been detected in various animals including snakes [5–7]. NGFs from human placental tissues and body fluids have been documented by Goldstein et al. [8] and Lipps [7]. However, the most extensively studied NGF has been obtained from the male mouse submaxillary glands (mouse NGF; [9]). NGF from snakes, particularly from cobras, has been reported to be superior in inducing neurite outgrowth on PC12 cells when compared with NGFs derived from other types of snakes [9]. Server et al. [10] reported that NGFs from cobra, *Naja naja*, and mouse submaxillary glands could also elicit neurite outgrowth from chick embryonic dorsal root ganglion.

NGF is normally produced as a pre-pro-precursor, which is then processed to a mature protein by endopeptidases [11]. The NGF from snakes has also been produced as a pre-pro-NGF molecule with 241 amino acids, which is later processed to form a mature NGF comprising 119 amino acids. Approx. 60 % homology has been seen between the NGF from snakes and rodents. cDNAs encoding mouse, human, bovine, chick and snake NGFs have also been cloned and sequenced [5,6]. In the present study, we describe the cloning and sequencing of two new cDNAs encoding the NGF in the venom glands of a spitting cobra, *Naja sputatrix*. The expressed and refolded recombinant protein, sputa NGF, has been found to be equally active as the mouse NGF in forming neurites in PC12 cells. Functional studies have shown that the sputa NGF promotes neurite outgrowth via the TrkA and p75$^{\mathrm{NTR}}$ receptors. Activation of NF-κB gene showed that the pro-survival mechanism of p75$^{\mathrm{NTR}}$-mediated signalling is initiated after the addition of sputa NGF. Furthermore, the endogenous NGF in the PC12 cells has been found to be up-regulated only after treatment with sputa NGF. Oligoprobe microarray analysis also showed that the sputa NGF, although acting through similar mechanisms to mouse NGF, may be capable of bringing about additional beneficial effects.

MATERIALS AND METHODS

Venom, venom glands and PC12 cells

An adult snake (*N. sputatrix*) obtained from Singapore Zoological Gardens (Singapore), kept undisturbed, was milked and the venom was freeze-dried and stored at −20 °C. The venom glands from the same snake were frozen in liquid nitrogen immediately after killing the animal and stored at −85 °C. PC12 cells were obtained from A.T.C.C. (Manassas, VA, U.S.A.) and maintained in Dulbecco's modified Eagle's medium supplemented with 10 % (v/v) fetal bovine serum and 1 % antibiotics (penicillin and streptomycin; [12]) at 37 °C in 5 % CO_2. The ability of the sputa NGF to elicit neurite outgrowth on PC12 cells was determined as described by Greene and Tishler [13].

Purification of native cobra NGF

Freeze-dried crude venom (50 mg) was reconstituted in 1 ml of water and subjected to gel filtration followed by reversed-phase HPLC (Vision system; Applied Biosystems, Foster City, CA, U.S.A.) using a Sephasil C18 column as described by Armugam et al. [14]. Fractions showing neurite outgrowth on PC12 cells were used for further studies.

Cloning and sequencing of cDNAs

Total RNA was isolated from the venom glands using the guanidine isothiocyanate method [15], and the integrity of the total RNA was analysed by denaturing formaldehyde agarose electrophoresis. Oligonucleotide primers were synthesized by Oswel DNA Services (Southampton, U.K.) based on the sequence at the 5′- and 3′-untranslated regions of cDNA encoding NGF in *Agkistrodon halys* Pallas [6]. Total RNA (3 μg) was reverse-transcribed and amplified by PCR as described by Armugam et al. [14].

The PCR products were cloned into pT7Blue (R) vector (Novagen, Madison, WI, U.S.A.) and transformed into *Escherichia coli* DH5α: *sup*E44 Δ*lac*U169 (Φ80*lac*ZΔm15) *hsd*R17 *rec*A1 *end*A1 *gyr*A96 *thi*-1 *rel*A1 [16]. The recombinant plasmids from the transformants were subjected to Sanger dideoxy DNA sequencing using M13/pUC forward and reverse primers [14,17] on an automated DNA sequencer (Model 3100; Applied Biosystems).

Expression and purification of recombinant sputa NGF

The cDNA-encoding NGF was amplified using sense and antisense primers, 5′-cctggatccgaagatcatcctgtg-3′ and 5′-ctcaagctttcagtttccagtt-3′ respectively, and subcloned into pQE-30 expression vector (Qiagen, Chatsworth, CA, U.S.A.) between *Bam*HI and *Hin*dIII sites.

The expression of the sputa NGF was induced by isopropyl β-D-thiogalactoside (1 mM) at 37 °C for 3 h and the protein was purified under denaturing conditions (8 M urea) on a Ni^{2+}-nitrilotriacetate Sepharose resin (Qiagen) column. The purified fractions were analysed by Tris/Tricine SDS/10 %-(w/v)-PAGE [18]. *In vitro* renaturation [19] of the denatured proteins was performed overnight at room temperature (25 °C) in 1 × PBS (pH 8.0), containing 4 mM GSH and 2 mM GSSG.

CD spectral analysis

CD spectra for both the native NGF and recombinant sputa NGF were recorded on a Jasco spectropolarimeter (J715) equipped with an interfaced personal computer. It was calibrated with ammonium *d*-10-camphorsulphonate. Data collected and averaged from at least five recordings were considered acceptable. Spectral measurements were performed at appropriate concentrations using cells of 0.1 cm path-length [19].

Western-blot analysis

Western blotting was performed as described by Cher et al. [20], using either monoclonal anti-phosphotyrosine (AG10; Upstate Biological, Lake Placid, NY, U.S.A.) or polyclonal anti-TrkA and affinity-purified polyclonal anti-p75^NTR (Advanced Targeting Systems, San Diego, CA, U.S.A.) at 1 μg/ml or monoclonal anti-β-actin (Sigma Chemicals, St. Louis, MO, U.S.A.) at a dilution of 1:2500. Anti-β-actin was used as a reference for quantification.

Real-time quantitative PCR

Total RNA from PC12 cells was extracted by a single-step method using TRIzol® reagent (Invitrogen, Carlsbad, CA, U.S.A.). Gene-specific primers for TrkA, p75^NTR, endogenous NGF, NF-κB and IκB (inhibitory κB) were designed using the PrimerExpress 2.0 software (Applied Biosystems) and their corresponding mRNA sequences. The primers were designed to yield amplicons of < 100 bp and synthesized by Alpha-DNA (Montreal, Quebec, Canada). β-Actin was used as an internal calibrator. The primer sequences were as follows: TrkA, 5′-catggagaacccacagtacttcag-3′ (sense) and 5′-ctagctcccacttgagaatgatgtc-3′ (antisense); p75^NTR, 5′-gtggtcgtgggccttgtg-3′ (sense) and 5′-gcgccttgtttattttgtttgc-3′ (antisense); rat endogenous NGF, 5′-catggtacaatccctttcaac-3′ (sense) and 5′-ccaacccacacactgacactg-3′ (antisense); NF-κB, 5′-gaagagtcctttcaatggaccaa-3′ (sense) and 5′-tcgggaaggcacagc-aata-3′ (antisense); IκB, 5′-gctgcccgagagtgcggat-3′ (sense) and 5′-cagtcatcgtagggcaactcatc-3′ (antisense); β-actin 5′-agggaaatc-gtgcgtgaca-3′ (sense) and 5′-gccatctcctgctcgaagtc-3′ (antisense).

In the present study, a two-step RT (reverse transcription)–PCR was used. RT was performed as described in [20]. PCR mixtures contained RT products, forward and reverse primers each at 125 nM and SYBR® Green master mixture (Applied Biosystems). The PCR amplification was then performed for 1 cycle at 50 °C for 2 min and 95 °C for 10 min followed by 40 cycles with each cycle at 94 °C for 15 s and 60 °C for 1 min. All reactions were performed in triplicate using the ABI Prism 7000 SDS (Applied Biosystems).

Protein profiling [SELDI-TOF (surface-enhanced laser-desorption–ionization time-of-flight)]

PC12 cells showing neurite outgrowth were rinsed with 0.9 % NaCl and lysed with lysis buffer (50 mM Tris/HCl, pH 7.4, 0.4 mM NaCl, 0.25 M sucrose and 1 mM EDTA, containing 8 M urea). The supernatant was fractionated on hydrophobic reverse-phase chip (H4 Protein Chip TM) using SELDI-TOF MS (Protein Biology System II) both from Ciphergen (Palo Alto, CA, U.S.A.) according to the manufacturer's instructions.

Microarray GeneChip™ analysis

Microarray analysis was performed as described by Cher et al. [20] with the following modifications. Total RNA isolated from control and treated (mouse NGF or sputa NGF) PC12 cells were processed and hybridized to each array of the rat expression 230A GeneChip™ Array set according to the methods described in the GeneChip™ expression analysis package (Affymetrix, Santa Clara, CA, U.S.A.). Relative mRNA expression levels were expressed as positive or negative fold changes when compared with untreated controls based on the Microarray Suite software 5.0 (Affymetrix). All genes showing a change of 2-fold or more were included in subsequent analysis. Members in each cluster were classified according to their biological functions as described in the NetAffix database (Affymetrix).

Table 1 Neurite outgrowth in PC12 cells

Protein concentrations at 100 ng/ml were used unless otherwise stated. '+' denotes neurite outgrowth observed.

Sample	Neurite outgrowth
Mouse NGF (positive control; 100 ng/ml)	+++
B. candidus (250 ng/ml)	++
N. sputatrix (250 ng/ml)	++++
A. superbus (250 ng/ml)	++
P. textilis (250 ng/ml)	+++
Chinese scorpion (250 ng/ml)	++
Indian scorpion (250 ng/ml)	+
Bee venom (250 ng/ml)	++
Biogel P10 gel fractions of *N. sputatrix* (Figure 1A)	
Fraction 27	++
Fraction 28	+++
Fraction 29	++
Fraction 30	+++
Fraction 31 (1 ng/ml)	+++++
Fraction 33	++
Fraction 34	Lysis
Fraction 35	Lysis
Fraction 36	Lysis
HPLC fractions (Figure 1B)	
Fraction 3	–
Fraction 4	–
Fraction 5	+
Fraction 6	++
Fraction 7	+++++
Fraction 8 (1 ng/ml)	++++++
Fraction 9	+++
Fraction 10	+
Denatured and refolded recombinant NGF	
Denatured recombinant NGF (100 ng/ml)	++
Refolded recombinant NGF (100 ng/ml)	++++

RESULTS

Bioassay of NGF on PC12 cells

Venoms from several elapids, *N. sputatrix*, *Bungarus candidus*, *Pseudonaja textilis* and *Austrelaps superbus*, as well as venoms from Chinese and Indian scorpions (*Buthus martensi* Karsch and *Mesobuthus tumulus*) and honey bee (*Apis mellifera*) were tested for neurite outgrowth in PC12 cells. β-NGF (7Sβ-NGF) from the mouse submaxillary gland was used as a positive control. The highest neurite outgrowth was observed for *N. sputatrix* crude venom at 250 ng/ml. Mouse NGF (7S) showed a comparable activity at 100 ng/ml (Table 1).

Identification of a NGF in *N. sputatrix* venom

The *N. sputatrix* venom was chromatographed on Biogel P10 (Figure 1A). The first peak, Peak I, consisted of high-molecular-mass proteins (14–50 kDa), whereas Peak II contained the low-molecular-mass proteins (4–10 kDa). Each fraction (100 ng/ml) was tested for its ability to promote neurite growth (Table 1). The corresponding fraction was also subjected to SDS/PAGE analysis to verify their homogeneity and to determine the molecular mass. The fraction showing the highest neurite outgrowth was purified further on HPLC (Figure 1B). One homogeneous protein peak was obtained, which showed neurite outgrowth at 1 ng/ml (Table 1). This active protein was 14 kDa in mass (Figure 1B, inset). The N-terminal amino acid sequence of this protein was found to be -ETHPVHNRGEYSV- and the protein was found to be non-lethal up to 1 μg/g in mouse.
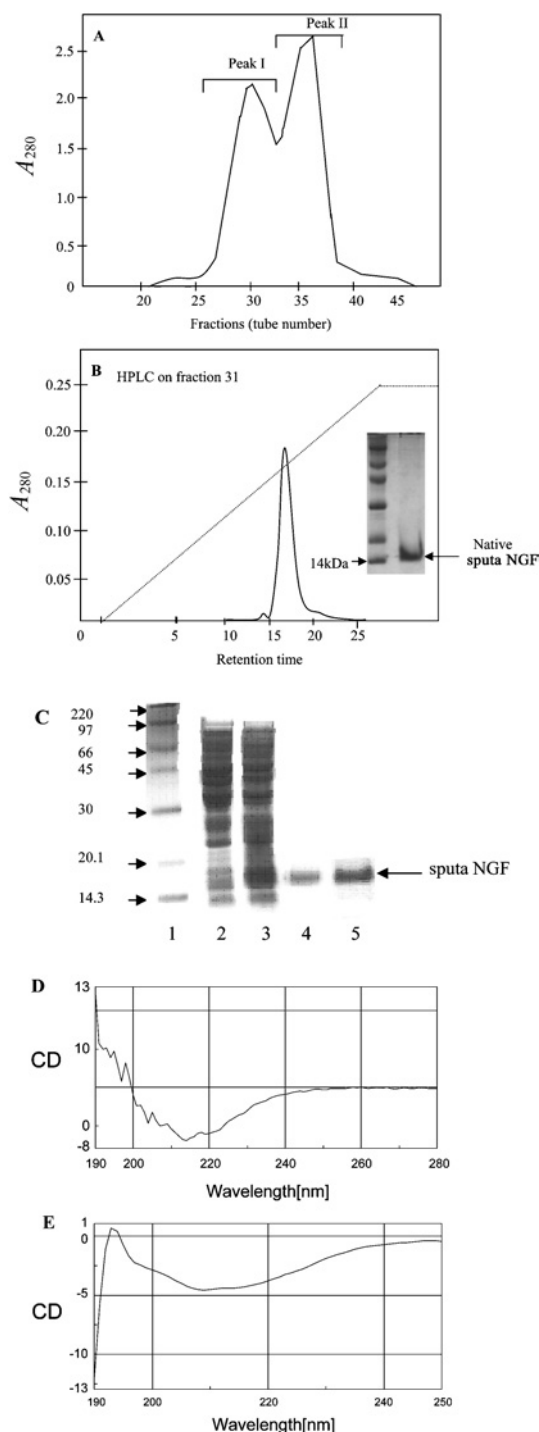
Figure 1 Purification of NGF

(**A**) Gel-filtration chromatography of crude *N. sputatrix* venom. (**B**) Reversed-phase chromatography of the active fraction obtained from gel filtration. Inset shows the protein (native sputa NGF fraction) analysed by SDS/PAGE. (**C**) Purification and refolding of recombinant NGF (sputa NGF). Lane 1, protein molecular mass standards (sizes indicated in kDa); lane 2, *E. coli* cell lysate before induction; lane 3, *E. coli* cell lysate (inclusion bodies) after 3 h induction; lane 4, purified sputa NGF; lane 5, refolded sputa NGF. (**D**) CD spectrum obtained from refolded recombinant sputa NGF and (**E**) CD spectrum of native NGF protein.

Cloning and expression of the NGF from *N. sputatrix*

The cDNA encoded for a 22-amino-acid signal peptide, a 112-amino-acid pre-pro-domain of NGF and a mature NGF protein

```
nsngfII    MSMLCYTLITAFLIGIWAAPKSEDNVPLGSPATSDLSDTSCAQTHEGLKTSRNTDQRHPA
bmngf      MSMLCYTLIIAFLIGIWAAPKSEDNVPLGSPAKSDFSDTNCAQTHEGLKTSRNTDQHHPT
nsngfI     MSMLCYTLIIAFLIGIWAVPKSEDNAPLGSPATSDLSDTSCAQTHEGLKTSRNTDQRHPA
agpngf     MSMLCYTLIIAFLIGVWAAPKSEDNVPLGSPATSDLSDTSCAKTHEALKTSRNTDQHYPA
mousengf   MSMLFYTLITAFLIGVQAEPYTDSNVPEGDSVPEAHWTKLQHSLDTALRRARSAPTAPIA
humNGF     MSMLFYTLITAFLIGIQAEPHSESNVPAGHTIPQVHWTKLQHSLDTALRRARSAPAAAIA
           **** **** ***** * *       * * *               *     *
           ++++++++++ +
nsngfII    PQKAEDQELRTAANIIVDPKLFQKRQFQSPRVLFSTQPPLLSRDEESVEFLDNEDS-LNR
bmngf      PKKSEDQELGSAANIIVDPKLFQKRRFQSPRVLFSTQPPPLSRDEQSVKFLDTEDT-LNR
nsngfI     PRSQRIKQFGSASNIIVDPKLFQKRRFQSPRVLFSTQPPPLSRDEQSVEFLDNEDA-LNR
agpngf     PKKAEDQEFGSAANIIVDPKLFQKRRFQSPRVLFSTQPPPLSRDEQ---SVDNVNS-LNR
mousengf   AR-----VTGQTRNITVDPRLFKKRRLHSPRVLFSTQPPPTSSDTLDLDFQAHGTIPFNR
humNGF     AR-----VAGQTRNITVDPRLFKKRRLRSPRVLFSTQPPREAADTQDLDFEVGGAAPFNR
                      ** *** ** **    ** ********* *            **
             +        +   +      + +  ++          ++      ++    + +
nsngfII    NIRAKRED-HPVHNLGEHSVCDSVSAWVT-KTTATDIKGNTVTVMENVNLDNKVYKQYFF
bmngf      NIWANNEN-HPVHNQGEHSVCDSISVWVTNKTKATDIKGNTVTVMVDVNLNNEVYKQYFF
nsngfI     NIRAKRET-HPVHNRGEYSVCDSISVWVANKTTATDIKGKPVTVMVDVNLNNHVYKQYFF
agpngf     NIRAKRED-HPVHNRGEYSVCDSVSVWVGNKTTATDIRGNLVTVMVDVNLNNNVYKQYFF
mousengf   THRSKRSSTHPVFHMGEFSVCDSVSVWVGDKTTATDIKGKEVTVLAEVNINNSVFRQYFF
humNGF     THRSKRSSSHPIFHRGEFSVCDSVSVWVGDKTTATDIKGKEVMVLGEVNINNSVFKQYFF
           ^^      **      ** ***** * **   ** **** *   * *   ** * * ****
             +        +   +        +        +       +            +       ++
nsngfII    ETKCKNPNPVPSGCRGIDSSHWNSYCTETDTFIKALTMEGNQASWRFIRIDTACVCVITK
bmngf      ETKCRNPNPVPSGCRGIDSRHWNSYCTTTDTFVKALTMEGNRASWRFIRIDTACVCVISR
nsngfI     ETKCRNPNPVPSGCRGIDSRHWNSYCTTTHTFVKALTMEGNRASWRFIRIDTACVCVISR
agpngf     ETKCRNPNPVPTTCGGIDARHWNSYCTTTHTFVKALTMEDNQASWRFIRIDTACVCVISR
mousengf   ETKCRASNPVESGCRGIDSKHWNSYCTTTHTFVKALTTDEKQAAWRFIRIDTACVCVLSR
humNGF     ETKCRDPNPVDSGCRGIDSKHWNSYCTTTHTFVKALTMDGKQAAWRFIRIDTACVCVLSR
           ****   ***   * ***   ******* * **  ****     * ************
             + +
nsngfII    KTGNN--
bmngf      KTENFPP
nsngfI     KTENF--
agpngf     KNENFG-
mousengf   KATRRG-
humNGF     KAVRRA-
           *
```

Figure 2   Comparison of amino acid sequences of various NGF

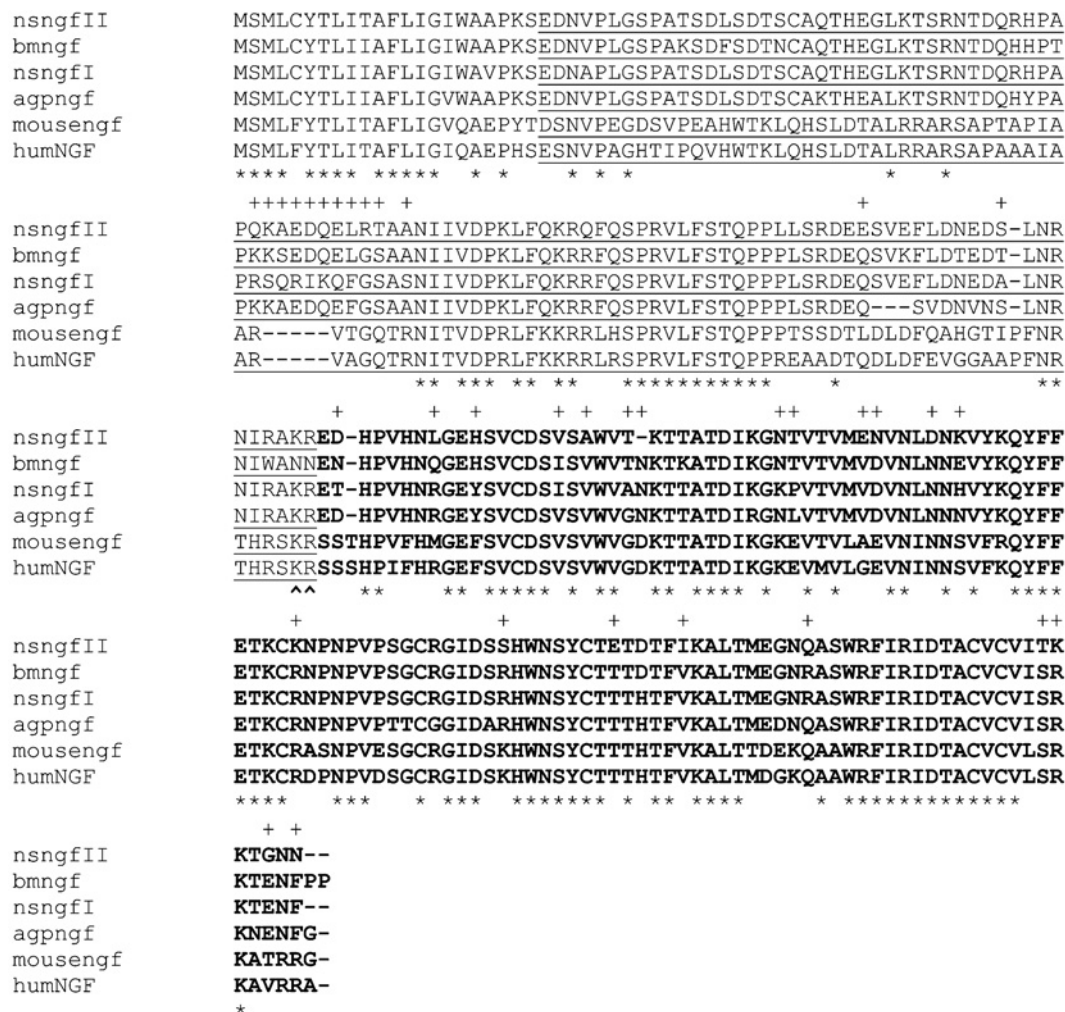Sputa nsngfI and nsngfII refer to the two isoforms of NGF from *N. sputatrix*; bmNGF is from *Bungarus multicinctus* (S56212); agpngf is from *Agkistrodon halys* Pallas [6]; mousengf (K01759) and human ngf (humNGF, X52599). The pro-NGF region is underlined and the mature peptides are shown in boldface letters. Identical amino acids are shown by (*) and the proteolytic cleavage site (KR) for the mature peptide is indicated by ^^. The variant residues between nsngfI and nsngfII are shown by +.

consisting of 117 amino acid residues. Analysis of the sequences indicated the presence of two isoforms (nsNGFI and nsNGFII) of venom NGF (Figure 2). The cDNA encoding the mature protein of nsNGFI (identical with the NGF isolated from the venom, Figure 1B) was expressed as a His$_6$-tagged fusion protein (sputa NGF) and analysed on an SDS/12% (w/v) polyacrylamide gel (Figure 1C, lane 3). The sputa NGF protein was purified by affinity chromatography using a Ni^{2+}-nitrilotriacetate column (Figure 1C, lane 4) and was renatured in the presence of GSSG and GSH (Figure 1C, lane 5). The yield of the refolded protein was found to be approx. 3 mg/l. Both the denatured and refolded recombinant NGFs varied in their potency to induce neurite outgrowth on PC12 cells (Table 1). Both the mouse and sputa NGF were found to exhibit comparable levels of biological activity (Figures 3A–3D). The CD spectrum of the refolded recombinant sputa NGF has been found to correlate well with that of the native NGF protein (Figures 1D and 1E). Quantification of neurite outgrowth in the presence of either mouse or sputa NGF (i) with increasing concentration (Figure 3E) and (ii) with increasing duration of NGF treatment (Figure 3G) has shown that the refolded sputa NGF exhibits a comparable activity with that of

mouse NGF. The native NsNGF has also been found to induce neurite outgrowth in a dose-dependent manner but at relatively lower protein concentrations (1–10 ng/ml; Figure 3F).

Expression of TrkA and p75 receptors

Western-blot analysis of the PC12 cells treated separately with the mouse and sputa NGF for 15 min showed that the sputa NGF increased the production of the precursor gp110^{trkA} receptors when compared with the mouse NGF. However, the mature gp140^{trkA} receptor was found in equal amounts for both treatments (Figures 3H and 3I). Neurite extensions can be observed only after 12 h of treatment (optimal at 16–18 h). Under this condition, the cells showed higher concentrations of TrkA and p75^{NTR} receptors than the untreated control. These results were also confirmed by real-time PCR (Figure 3J). Figure 3(J) also shows the expression patterns of endogenous NGF, NF-κB and IκB. The expression of IκB (inhibitor of NF-κB gene) has been found to be negatively regulated. Interestingly, an increased expression of the endogenous NGF gene has been observed only after treatment with the sputa NGF (Figure 3J).
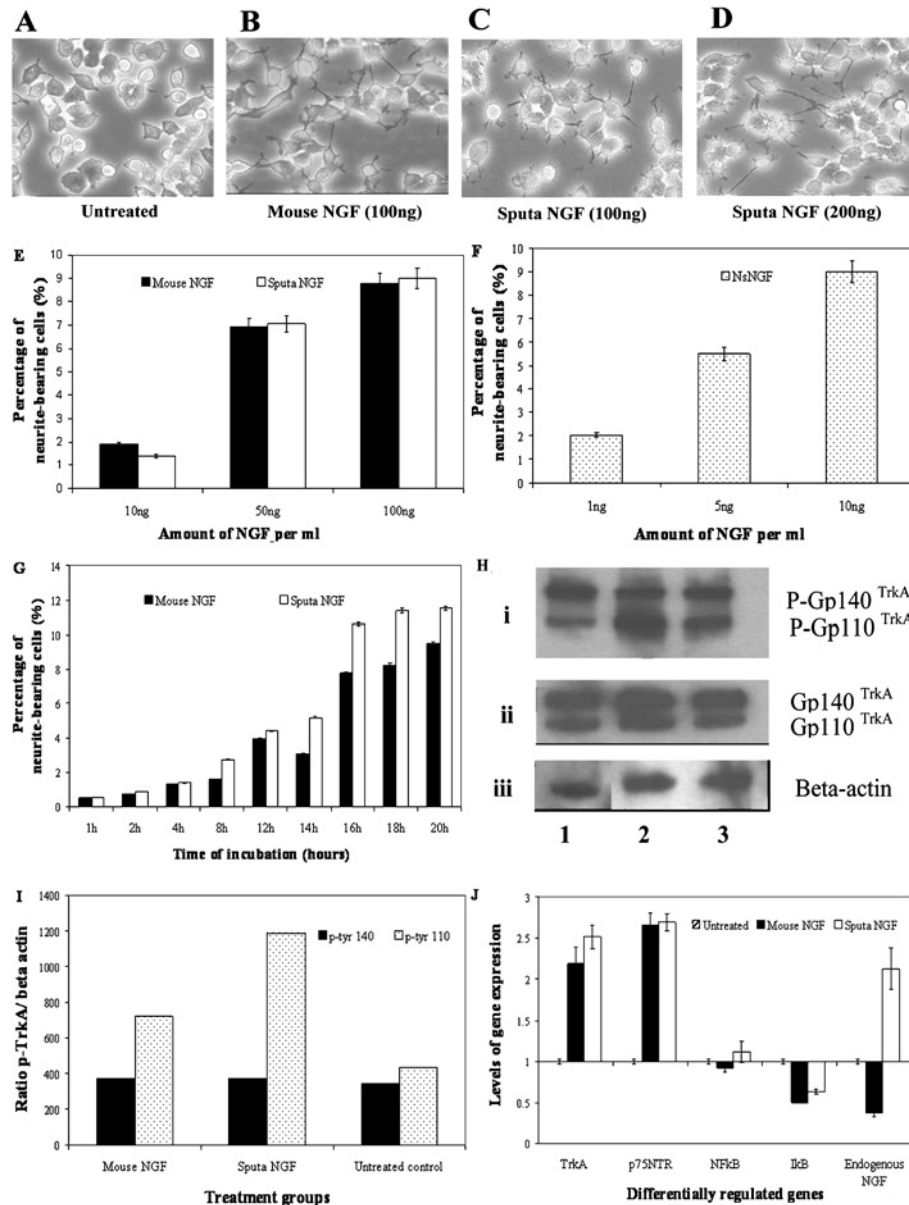
Figure 3   Neurite extension and receptor protein expression after treatment with mouse and sputa NGF

PC12 cells at 1×10^6 were plated and grown overnight. On the following day, cells were treated with either mouse or sputa NGF, at 200 ng for 16–18 h unless otherwise stated. (**A**, **B**) Neurite extensions observed after treatment with mouse NGF. (**C**, **D**) Neurites induced by sputa NGF. (**E**) Neurite extensions quantified for mouse (black bars) and sputa (white bars) NGF (10, 50 and 100 ng). (**F**) Neurite outgrowth observed for native nsNGF (stippled bars) at 1, 5 and 10 ng. (**G**) Time-course induction of neurite outgrowth by mouse (black bars) and sputa (white bars) NGF. (**H**) Activation of TrkA receptor determined by Western-blot analysis. Cells were treated for 15 min and total protein was extracted. Equal amounts of protein were separated on a SDS/7.5 % polyacrylamide gel and subsequently blotted on to nitrocellulose membrane. (i) Phosphorylated TrkA receptors (gp110 and gp140) were detected using monoclonal anti-phosphotyrosine antibody. The same membrane was stripped and probed with (ii) anti-TrkA and (iii) β-actin antibodies. Lane 1, mouse NGF-treated cells; lane 2, sputa NGF-treated cells and lane 3, untreated control cells. (**I**) Ratios of the phosphorylated TrkA and β-actin (internal control) levels measured by densitometry. (**J**) Quantitative gene analysis via SYBR Green assay. The RNAs from treated and untreated samples were used to study the expression of five genes: TrkA, p75[NTR], NF-κB and IκB.

Protein profiling (SELDI-TOF) analysis

Protein profiling identified five proteins that showed significant changes after NGF treatment (Figure 4). The analysis showed changes in expression of both growth-related (NGF precursor and neurogranin) and an apoptotic protein (BAD, **B**cl-2/Bcl-X$_L$-**a**ntagonist, causing cell **d**eath). Cells treated with sputa NGF (Figure 4A) showed a decrease (approx. 6-fold) in an 8 kDa protein and an increase (approx. 2-fold) in an 11.4 kDa protein.

Cells treated with mouse NGF (Figure 4B) showed a down-regulation (approx. 10-fold) of a 13.9 kDa protein. Comparison between sputa NGF and mouse NGF treatments (Figure 4C) showed that sputa NGF caused an increase in the growth-associated proteins similar to AKAP (A-kinase anchoring protein, 11.4 kDa) and the endogenous NGF precursor (13.9 kDa) when compared with pro-apoptotic protein (BAD). Expression of protein at 8 kDa (possibly neurogranin) was greatly decreased (approx. 5-fold), whereas proteins at 22.3 kDa (BAD) and
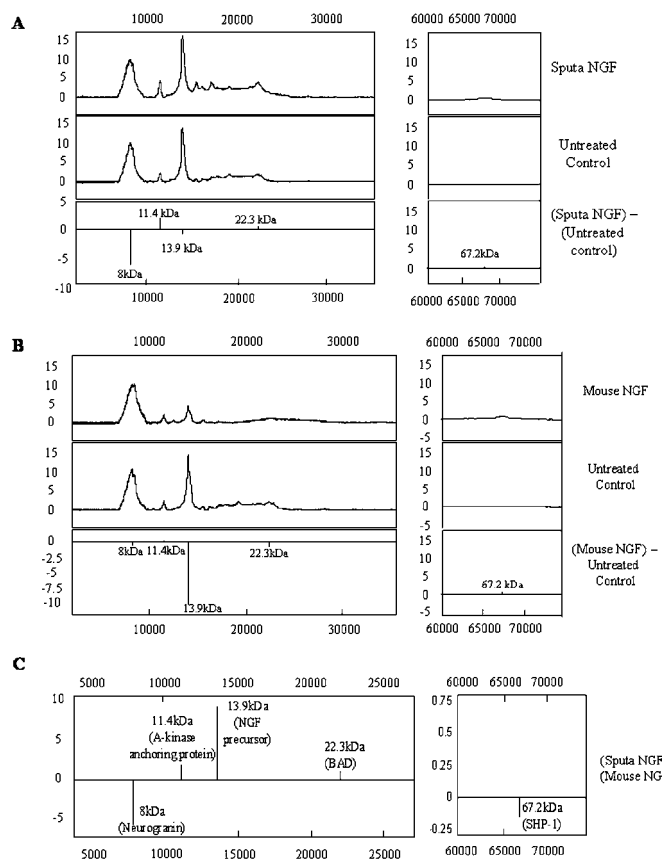
Figure 4   Protein profiling analysis

Total protein extracts from cells treated with either mouse NGF or sputa NGF for 16–18 h were used. (**A**) Protein profiles obtained from cells treated with sputa NGF versus untreated control. (**B**) Protein profiles obtained from cells treated with mouse NGF versus untreated control. (**C**) Protein profiles obtained for sputa NGF versus mouse NGF.

67.2 kDa [SHP-1 (Src homology 2 domain-containing tyrosine phosphatase-1)] showed a marginal up and down-regulation respectively (Figure 4C).

Microarray analysis of NGF-treated PC12 cells

The global gene expression after treatment with both NGFs was studied using oligoprobe microarrays. The genes whose expression is altered by 2-fold or more were taken as significant from approx. 730 genes examined in our study. These probe sets were subjected to a self-organizing map (Data Mining Tool; Affymetrix) clustering and were grouped according to their expression patterns. The genes were also further assigned to categories according to their biological functions. Some of them are shown in Table 2. Most of these genes were found to be involved in the cell cycle and growth pathways.

DISCUSSION

Cloning and expression of a new recombinant NGF protein

A widely studied and commercially available NGF, β-NGF, is from the mouse submaxillary gland. Lipps [9] reported that the NGFs from venomous sources are of the highest potency and particularly the NGF from snakes is approx. 1000-fold more active than the commercially available mouse NGF. The crude venom (250 ng/ml) from four untested snakes when assayed for neurite

outgrowth on PC12 cells showed that the venom of *N. sputatrix*, Malayan spitting cobra, exhibited the highest activity. This was followed by the venom from an Australian elapid, *P. textilis*. Thus the NGF from *N. sputatrix* venom was purified, and its activity and properties were compared with those of mouse NGF. The molecular mass of the native sputa NGF was found to be 14 kDa, thus indicating that it is a monomer belonging to β-NGF family as suggested by Inoue et al. [21].

The cDNA encoding NGF from *Agkistrodon halys* Pallas has been reported previously [6]. In the present study, we report the cloning of cDNAs encoding two isoforms of sputa NGF from *N. sputatrix*. Each cDNA encoded a signal peptide, pre-pro-domain and the mature protein. The mature protein-coding region for *N. sputatrix* was identified from its N-terminal amino acid sequence as well as from the amino acid sequence of *Naja atra* NGF [21,22]. Comparison of sequences from the venom-derived NGFs with those of mouse NGF showed distinct variations at their N-terminal ends. The snake NGF shows higher homology (approx. 80%) with the mammalian-derived NGFs, thus suggesting similar function to the mammalian homologue. The pro-region of the cobra NGF however shows approx. 50% homology to the mammalian counterpart. Pro-NGF has long been postulated to contain a biologically active peptide that could induce phosphorylation of the tyrosine residue of the TrkA receptor protein [23]. On the other hand, secreted pro-NGF has been reported to activate cell death in brain following an injury via p75 and sortilin receptors [24], thus indicating a pathophysiological role for the pro-NGF during CNS (central nervous system) injury. In contrast, Fahnestock et al. [25] have shown that the pro-NGF is in abundance in CNS tissues where mature NGF is not detected. The researchers have demonstrated that this pro-NGF is responsible for the biological activity normally attributed by mature NGF, in the CNS tissues. The pro-NGF in snakes shows approx. 50% homology to the mammalian pro-NGF. Furthermore, a deletion of five amino acids can be observed in the mammalian pro-NGF sequence. Hence, their functions may be different. The snake pro-NGF could possibly be involved in the positioning of NGF moiety for proper proteolytic processing and activation of proper *in vitro* folding of the mature peptide [26]. The death-inducing property, if any, of the pro-NGF from snakes remains to be elucidated.

The venom-derived NGFs showed approx. 80–90% homology among them, and the two isoforms of *N. sputatrix* NGF (nsNGFI and nsNGFII) showed approx. 80% homology between them. nsNGFI and nsNGFII showed 70 and 60% homology to the mammalian NGF respectively. Whereas the mature protein region for both nsNGFI and nsNGFII showed high homology, the pro-region showed considerable variation among them. Owing to its higher homology to the mammalian homologue, nsNGFI was selected for the expression of recombinant protein in *E. coli* and termed sputa NGF. This recombinant molecule appears to have two pairs of β-sheets that are linked by three disulphide bonds. We were able to refold it in redox solution containing 2 mM GSSG and 4 mM GSH. The refolded recombinant protein showed a CD spectrum similar to that of the native protein, and it showed enhanced activity when compared with the unfolded NGF (Table 1). This refolded sputa NGF was also found to be non-toxic to PC12 cells at 1 μg/ml. It was able to bring about enhanced neurite outgrowth in a dose-dependent manner from 100 to 500 ng/ml.

Expression of TrkA and p75 receptors

The sputa NGF has been found to elicit neurite outgrowth via the TrkA–p75^{NTR} complex. Two protein forms of TrkA that predominate in cell extracts are: (i) the 110 kDa N-glycosylated precursor form, gp110^{TrkA} and (ii) the 140 kDa fully matured form, gp140^{TrkA}

Table 2 Classification of genes from microarray

Genes were grouped based on their biological functions. Notable changes in gene expression are shown in boldface.

Category of genes	Description	Mouse NGF (fold change)	Sputa NGF (fold change)
Cell cycle	Growth arrest and DNA-damage-inducible 45α	3.63	3.18
	Proliferating cell nuclear antigen	−2.07	−1.74
	ret proto-oncogene	2.87	2.91
	ret proto-oncogene	4.06	4.41
	Cyclin-dependent kinase inhibitor 1A	4.99	4.26
	Growth-associated protein 43	2.27	2.10
Apoptosis	Apoptotic death agonist BID	3.36	2.85
	Bcl-2-like-1	2.22	1.77
Eicosanoid synthesis	Prostaglandins endoperoxide synthase 1	**4.59**	**2.36**
	IL-12 p35 subunit	**6.19**	**4.72**
Transcription factors	Core promoter element-binding protein	2.53	1.57
	fos-like antigen 1	**8.57**	**3.51**
	Nuclear transcriptional factor-Y-β	2.01	1.14
	ISL1 transcriptional factor, LIM/homeodomain 1	2.75	1.74
	Global ischaemia-induced protein GIIG15B	−2.38	−2.07
	DNA polymerase β	2.20	1.88
	GATA-binding protein 4	1.39	2.17
	Myelin transcription factor 1-like	−2.20	−1.33
	Signal transducer and activator of transcription 3	2.04	1.66
	ATF3	**2.2**	**−1.54**
	Egr 1	**15.14**	**12.91**
Translational factors	Eukaryotic initiation factor-5	2.03	1.60
	Eukaryotic initiation factor-2B, subunit 3	2.04	1.82
Others	Meprin 1α	2.55	2.10
	CE	**11.08**	**8.22**
	Mast cell protease 7	**88.65**	**71.51**
	Plysia ras-related homologue A2	2.69	2.33
	Small GTP-binding protein rab5	2.20	1.79
	GTP cyclohydrolase 1	3.20	2.10
	Phospholipase D	2.41	2.55
	Kinesin family member 1B	1.45	2.01
	Procollagen, type XII, α1	2.30	1.41
	Integrin β1	2.31	2.39
	Insulin receptor substrate 1	2.06	1.27
	Double cortin and calcium/CaM-dependent protein kinase-like 1	2.69	1.84
	Gap junction membrane channel protein β5	2.79	2.04
	Jun-B oncogene	2.28	2.39
	Opioid receptor-like	2.13	2.73
	Arginine V1a	**5.43**	**20.25**
	Purinergic receptor P2X, ligand-gated ion channel 2	**−2.91**	**−1.59**
	Purinergic receptor P2X, G-protein coupled 2	2.06	2.11
	Adenosine monophosphate deaminase 3	2.48	1.85
	Myelin basic protein	1.04	2.35
	Prolactin receptor	2.17	1.54
	Serum-inducible kinase	**7.26**	**3.12**
	Syntaxin	2.71	1.45
	Dynamin 1	−2.07	−1.39
	Guanosine diphosphate dissociation inhibitor 3	2.17	2.39
	Annexin 5	3.03	2.77
	Neural receptor protein-tyrosine kinase	9.19	3.16
	Moesin	2.97	2.48
	Vesicle-associated membrane protein, associated proteins B and C	1.71	2.10
	ADP-ribosylation-like 4	2.71	2.28
	Solute carrier family 1, member 3	**6.28**	**4.99**
	Solute carrier family 9, member 4	−1.44	2.23
	Syndecan 1	2.95	2.39
	Myosin IXA	2.22	1.99
	Potassium inwardly rectifying channel, subfamily J, member 6	2.20	1.95
	Protein kinase, cAMP-dependent regulatory, type I, α	2.53	2.08
	Coated vesicle membrane protein	2.00	1.89
	Regulator of G-protein signalling protein 2	2.25	1.38
	Cold-inducible RNA-binding protein	1.97	2.30
	Microtubule-associated protein 1b	2.31	1.29
	Acid phosphatase 5	2.01	1.91
	Profilin II	2.38	2.06
	Glutamate receptor, ionotrophic, NMDA2C	−2.50	−1.91
	Lysosomal membrane glycoprotein 2	−1.97	−2.20
	NGF receptor-associated protein	−2.03	−1.55

Table 2   **(contd.)**

Category of genes	Description	Mouse NGF (fold change)	Sputa NGF (fold change)
Calcium-related pathway	Very-low-density lipoprotein receptor	2.16	1.83
	Very-low-density lipoprotein receptor	2.57	2.00
	Very-low-density lipoprotein receptor	2.22	2.10
	Calcium-binding protein p22	3.66	2.19
	S-100-related protein, clone 42C	3.36	2.71
	S-100-related protein A4	2.06	1.95
	Cadherin	− 3.14	− 2.33
	Calcium channel, voltage-dependent, T-type, αII subunit	**5.54**	**7.21**
	Protein phosphatase 3, regulatory subunit B, α isoform, type 1	2.23	1.78

[27]. PC12 cells are known to respond rapidly to NGF within minutes, with a reproducible burst of tyrosine phosphorylation of many cellular proteins and include the TrkA receptors. We observed that the ratio of gp140^{TrkA} to gp110^{TrkA} decreased on both mouse and sputa NGF treatments for the purpose of replenishing the mature gp140^{TrkA} at the cell surface as described by Jullien et al. [28]. TrkA and p75^{NTR} receptors work in concert to co-ordinate and modulate responses of neurons to NGF. A competitive study using specific receptor antibodies on the percentage of neurite outgrowth showed that sputa NGF is more sensitive to receptor inhibition compared with that of mouse NGF. Reduced TrkA activation in both PC12 cells and sympathetic neurons has been observed after the addition of p75^{NTR}-specific antibodies [29]. The researchers have also shown that any alteration in the optimal TrkA–p75^{NTR} interaction or direct activation of p75^{NTR} at the expense of TrkA, will result in an inhibition of NGF-dependent neurite outgrowth in adult sensory neurons. In the present study, inhibition by TrkA and p75^{NTR} receptor-specific antibodies caused a reduction in neurite outgrowth for both mouse and sputa NGF by 34 and 70% for TrkA and 10 and 40% for p75^{NTR} respectively. Thus the greater reduction in neurite formation on sputa NGF treatment implicates that the sputa NGF is more specific to TrkA and p75^{NTR}, and stimulates signalling using the TrkA–p75^{NTR} high-affinity complex as for mouse NGF. This antibody-based competitive study is in agreement with the quantitative analysis of the receptor (TrkA and p75^{NTR}) genes examined via real-time PCR. The expression of both receptors was higher with sputa NGF when compared with mouse NGF. Activation of TrkA and p75^{NTR} has been reported to induce the expression of NF-κB, which in turn is known to cause neurite extension in PC12 cells [30]. Real-time PCR (Figure 3C) showed a down-regulation of the NF-κB inhibitor, IκB, in both NGF treatments, implying that NF-κB will be made available to activate and promote neurite extension in PC12 cells. However, an increase in NF-κB expression is observed for sputa NGF treatment compared with mouse NGF treatment and such an NGF-induced increase in NF-κB is beneficial for the survival of neurons [31]. Similarly, the endogenous NGF level was up-regulated after treatment with sputa NGF in contrast with mouse NGF. Several studies have shown that neurotrophic factors, including NGF, constitute an important class of endogenous modulators of excitotoxicity, and are known to protect neurons against injury from several causes [32]. NGF has caused increase in glutathione levels of PC12 cells [33], and hence up-regulation (of NF-κB and endogenous NGF genes) by sputa NGF may have potential neuroprotective roles.

Global gene and protein analysis

Microarray analysis (Table 2) showed for the first time the global changes in gene expression after treatment with either mouse NGF

or sputa NGF on PC12 cells. This study also yielded comparable data between the two NGFs. The differentiation pathway after NGF treatment is characterized by expression of immediate early genes [such as Egr 1 (early growth response 1) and serum-inducible kinase] and delayed response genes (such as Fos-like antigen, Fra-1 and prostaglandin-endoperoxide synthase 1). It was shown that Egr 1 acts via the extracellular-signal-regulated kinase pathway to produce eventually neurite outgrowth in PC12 cells [34]. Liby et al. [35] have shown that serum-inducible kinase has a role in cell proliferation. Expression of transcription factors, e.g. Fra-1, may participate in long-term neural responses [36], whereas overexpression of ATF3 (activating transcription factor 3) inhibited apoptosis [37]. Enhanced expression of transcription factors (Fra-1, ATF3 and Egr 1) may also cause subsequent increase in CE (cathepsin E) expression [38]. This explains the increase in CE observed in the present study (Table 2). CE is an aspartic protease, which has been implicated in antigen processing in the class II MHC pathway and is known to be up-regulated late in B-cell activation [39]. The concurrent up-regulation of mast cell protease 7 in the present study is in agreement with the previously reported effects of NGF on mast-cell development and differentiation [40].

Arginine V1a (vasopressin receptor 1A) was observed to be highly expressed by sputa NGF treatment when compared with mouse NGF. V1a is widely distributed and known to regulate nearly all the physiological actions of the neuropeptide, vasopressin (AVP), except antidiuresis (V2) and corticotrophin secretion (V1b; [41]). In addition to these, channel transporter genes (solute carrier family 1, member 3; SLC1A3, voltage-dependent calcium channel and purinergic P2X receptors) were found to be affected by the NGF treatment. Mouse NGF activated both the expression of SLC1A3 and P2X receptor genes, whereas sputa NGF activated the voltage-dependent calcium channel gene. The SLC1A3 gene encodes the glutamate receptor GLAST (glutamate/aspartate transporter) responsible for the removal of glutamate to terminate neurotransmission and prevent neuronal cell death [42], whereas the expression of voltage-dependent calcium channel subunit II is restricted to neuronal tissues for the maintenance of the neuronal physiology [43]. In the present study, the down-regulation of P2X receptor was observed in both NGF treatments. This proved to be beneficial as P2X is postulated to be involved in astrocyte-mediated inflammation and neurodegeneration [44]. Up-regulation of IL-12 (interleukin-12) and prostaglandin-endoperoxide synthase 1 seen in both cases also supports their beneficial roles. Prostaglandin-endoperoxide synthase 1 is believed to have a physiological role in neuronal differentiation of PC12 cells [45]. Similarly, IL-12 is known to play an important role in neuronal regeneration [46]. Hence, both NGFs showed similar activities, except for V1a expression. Arginine vasopressin that acts mainly through the V1a receptor

is known to enhance NGF secretion in vascular smooth muscles and rat brain cells [47,48].

Protein profiling and real-time PCR results confirmed that an endogenous NGF synthesis is up-regulated after treatment with sputa NGF. Hence, sputa NGF could possibly be acting through V1a receptor to enhance the endogenous NGF production, an effect that will prove to be useful under conditions that require neuronal regeneration and differentiation.

The sputa NGF is also found to enhance the production of growth-associated proteins such as AKAP. The AKAP (11.4 kDa) belongs to a family of scaffolding proteins that bind to the regulatory subunits of protein kinase A, which regulates the phosphorylation of various proteins including those involved in synaptic plasticity. AKAP induction is known to stimulate protein kinase A-dependent phosphorylation of the pro-apoptotic protein BAD (protein at 22.3 kDa), thereby inhibiting the release of cytochrome *c* from mitochondria and protecting the cells from apoptosis [49]. Although sputa NGF showed a marginal increase in BAD protein when compared with mouse NGF, with AKAP up-regulated approx. 2-fold more than BAD, the pro-apoptotic property of BAD could be suppressed. This interpretation was confirmed experimentally by measuring for caspase activity on PC12 cells treated with sputa NGF. No caspase activity could be determined in these cells.

The mechanisms by which NGF exerts its neuroprotective effects are currently unknown. However, *in vitro* studies have shown that NGF can stabilize intracellular calcium by preventing accumulation of intracellular calcium and subsequent neuronal damage [50]. The protein profiling results showed a down-regulation in neurogranin (8 kDa). Neurogranin is a neural-specific Ca^{2+}-sensitive CaM (calmodulin)-binding protein. It is believed that phosphorylated neurogranin has the potential to modulate neuronal free-Ca^{2+} and CaM levels [51]. Gene knock-out experiments leading to a total absence of neurogranin have resulted in deficiency of hippocampal synaptic plasticity and hippocampus-dependent spatial learning [51]. McNamara et al. [52] predicted that an increase in neurogranin expression would perturb Ca^{2+}-CaM signalling that may in turn impair the formation and/or maintenance of synapses. Thus a decreased level of free neurogranin detected after treatment with sputa NGF indicates that a basal level of intracellular Ca^{2+} is maintained for neuronal differentiation and function.

Protein tyrosine phosphatase (SHP-1; 67.2 kDa) was identified as a phosphotyrosine phosphatase, which negatively regulates the expression of TrkA. It was shown in sympathetic neurons that expression of SHP-1 induces apoptosis and TrkA dephosphorylation [53]. Hence, a down-regulation of SHP-1 expression is also in agreement with TrkA activation after treatment with both NGFs.

In conclusion, sputa NGF seems to exert potentially life-sustaining and neuroprotective (NF-κB and endogenous NGF genes) effects in a manner similar to that of mouse NGF. The life-sustaining effects have been observed at both gene (microarray) and protein (SELDI-TOF) levels. Sputa NGF has also been found to increase the expression of V1a and endogenous NGF genes as well as the NGF precursor and the AKAPs. However, both neurogranin and SHP-1 proteins have been found to be down-regulated after treatment with sputa NGF. Real-time PCR analysis has revealed additional pro-survival effects of sputa NGF such as enhanced expression of NF-κB and the endogenous NGF genes. These effects could have potential neuroprotective roles.

REFERENCES

1   Eide, F. F., Lowenstein, D. H. and Reichardt, L. F. (1993) Neurotrophins and their receptors – current concepts and implications for neurologic disease. Exp. Neurol. **121**, 200–214

2   Culmsee, C., Gerling, N., Lehmann, M., Nikolova-Karakashian, M., Prehn, J. H., Mattson, M. P. and Krieglstein, J. (2002) Nerve growth factor survival signaling in cultured hippocampal neurons is mediated through TrkA and requires the common neurotrophin receptor P75. Neuroscience **115**, 1089–1108

3   Casaccia-Bonnefil, P., Gu, C. and Chao, M. V. (1999) Neurotrophins in cell survival/death decisions. Adv. Exp. Med. Biol. **468**, 275–282

4   Bui, N. T., Konig, H. G., Culmsee, C., Bauerbach, E., Poppe, M., Krieglstein, J. and Prehn, J. H. (2002) p75 neurotrophin receptor is required for constitutive and NGF-induced survival signalling in PC12 cells and rat hippocampal neurones. J. Neurochem. **81**, 594–605

5   Kashima, S., Soares, A. M., Roberto, P. G., Pereira, J. O., Astolfi-Filho, S., Cintra, A. O., Fontes, M. R., Giglio, J. R. and de Castro Franca, S. (2002) cDNA sequence and molecular modeling of a nerve growth factor from *Bothrops jararacussu* venomous gland. Biochimie **84**, 675–680

6   Guo, L. Y., Zhu, J. F., Wu, X. F. and Zhou, Y. C. (1999) Cloning of a cDNA encoding a nerve growth factor precursor from the *Agkistrodon halys* Pallas. Toxicon **37**, 465–470

7   Lipps, B. V. (2000) Isolation of nerve growth factor (NGF) from human body fluids; saliva, serum and urine: comparison between cobra venom and cobra serum NGF. J. Nat. Toxins **9**, 349–356

8   Goldstein, L. D., Reynolds, C. P. and Perez-Polo, J. R. (1978) Isolation of human nerve growth factor from placental tissue. Neurochem. Res. **3**, 175–183

9   Lipps, B. V. (1998) Biological and immunological properties of nerve growth factor from snake venoms. J. Nat. Toxins **7**, 121–130

10 Server, A. C., Herrup, K., Shooter, E. M., Hogue-Angeletti, R. A., Frazier, W. A. and Bradshaw, R. A. (1976) Comparison of the nerve growth factor proteins from cobra venom (*Naja naja*) and mouse submaxillary gland. Biochemistry **15**, 35–39

11 Kostiza, T. and Meier, J. (1996) Nerve growth factors from snake venoms: chemical properties, mode of action and biological significance. Toxicon **34**, 787–806

12 Koike, T. (1983) Nerve growth factor-induced neurite outgrowth of rat pheochromocytoma PC 12 cells: dependence on extracellular Mg^{2+} and Ca^{2+}. Brain Res. **289**, 293–303

13 Greene, L. A. and Tishler, A. S. (1976) Establishment of a noradrenergic clonal line of rat adrenal pheochromocytoma cells which respond to nerve growth factor. Proc. Natl. Acad. Sci. U.S.A. **73**, 2424–2428

14 Armugam, A., Earnest, L., Chung, M. C. M., Gopalakrishnakone, P., Tan, C. H., Tan, N. H. and Jeyaseelan, K. (1997) Cloning and characterization of cDNAs encoding three isoforms of phospholipase A2 in Malayan spitting cobra (*Naja naja sputatrix*) venom. Toxicon **35**, 27–37

15 Chomczynski, P. and Sacchi, N. (1987) Single-step method of RNA isolation by acid guanidinium thiocyanate–phenol–chloroform extraction. Anal. Biochem. **162**, 156–159

16 Sambrook, J., Fritsch, E. F. and Maniatis, T. (1989) Molecular Cloning: A Laboratory Manual, 2nd edn, Cold Spring Harbor Laboratory, Plainview, NY

17 Sanger, F., Nicklen, S. and Coulson, A. R. (1977) DNA sequencing with chain-terminating inhibitors. Proc. Natl. Acad. Sci. U.S.A. **74**, 5463–5467

18 Schagger, H. and Von-Jagow, G. (1987) Tricine-sodium dodecyl sulfate-polyacrylamide gel electrophoresis for the separation of proteins in the range from 1 to 100 kDa. Anal. Biochem. **166**, 368–379

19 Ma, D., Armugam, A. and Jeyaseelan, K. (2002) Cytotoxic potency of cardiotoxin from *Naja sputatrix*: development of a new cytolytic assay. Biochem. J. **366**, 35–43

20 Cher, C. D. N., Armugam, A., Lachumanan, R., Coghlan, M.-W. and Jeyaseelan, K. (2003) Pulmonary inflammation and edema induced by phospholipase A2: global gene analysis and effects on aquaporins and Na$^+$/K$^+$-ATPase. J. Biol. Chem. **278**, 31352–31360

21 Inoue, S., Oda, T., Koyama, J., Ikeda, K. and Hayashi, K. (1991) Amino acid sequences of nerve growth factors derived from cobra venoms. FEBS Lett. **279**, 38–40

22 Kostiza, T., Dahinden, C. A., Rihs, S., Otten, U. and Meier, J. (1995) Nerve growth factor from the venom of the Chinese cobra *Naja naja atra*: purification and description of non-neuronal activities. Toxicon **33**, 1249–1261

23 Dicou, E., Pflug, B., Magazin, M., Lehy, T., Djakiew, D., Ferrara, P., Nerriere, V. and Harvie, D. (1997) Two peptides derived from the nerve growth factor precursor are biologically active. J. Cell Biol. **136**, 389–398

24 Nykjaer, A., Lee, R., Teng, K. K., Jansen, P., Madsen, P., Nielsen, M. S., Jacobsen, C., Kliemannel, M., Schwarz, E., Willnow, T. E. et al. (2004) Sortilin is essential for proNGF-induced neuronal cell death. Nature (London) **427**, 843–848

25 Fahnestock, M., Yu, G., Michalski, B., Mathew, S., Colquhoun, A., Ross, G. M. and Coughlin, M. D. (2004) The nerve growth factor precursor proNGF exhibits neurotrophic activity but is less active than mature nerve growth factor. J. Neurochem. **89**, 581–592

26   Suter, U., Heymach, Jr, J. V. and Shooter, E. M. (1991) Two conserved domains in the NGF propeptide are necessary and sufficient for the biosynthesis of correctly processed and biologically active NGF. EMBO J. **10**, 2395–2400

27   Martin-Zanca, D., Oskam, R., Mitra, G., Copeland, T. and Barbacid, M. (1989) Molecular and biochemical characterization of the human trk proto-oncogene. Mol. Cell. Biol. **9**, 24–33

28   Jullien, J., Guili, V., Reichardt, L. F. and Rudkin, B. B. (2002) Trafficking of TrkA-green fluorescent protein chimerae during nerve growth factor-induced differentiation. J. Biol. Chem. **277**, 38700–38708

29   Kimpinski, K., Jelinski, S. and Mearow, K. (1999) The anti-p75 antibody, MC192, and brain-derived neurotrophic factor inhibit nerve growth factor-dependent neurite growth from adult sensory neurons. Neuroscience **93**, 253–263

30   Foehr, E. D., Lin, X., O'Mahony, A., Geleziunas, R., Bradshaw, R. A. and Greene, W. C. (2000) NF-κ B signaling promotes both cell survival and neurite process formation in nerve growth factor-stimulated PC12 cells. J. Neurosci. **20**, 7556–7563

31   Maggirwar, S. B., Ramirez, S., Tong, N., Gelbard, H. A. and Dewhurst, S. (2000) Functional interplay between nuclear factor-κB and c-Jun integrated by coactivator p300 determines the survival of nerve growth factor-dependent PC12 cells. J. Neurochem. **74**, 527–539

32   Mattson, M. P., Cheng, B. and Smith-Swintosky, V. L. (1993) Mechanisms of neurotrophic factor protection against calcium- and free radical-mediated excitotoxic injury: implications for treating neurodegenerative disorders. Exp. Neurol. **124**, 89–95

33   Palmer, C., Roberts, R. L. and Bero, C. (1994) Deferoxamine posttreatment reduces ischemic brain injury in neonatal rats. Stroke **25**, 1039–1045

34   Harada, T., Morooka, T., Ogawa, S. and Nishida, E. (2001) ERK induces p35, a neuron-specific activator of Cdk5, through induction of Egr1. Nat. Cell Biol. **3**, 453–459

35   Liby, K., Wu, H., Ouyang, B., Wu, S., Chen, J. and Dai, W. (2001) Identification of the human homologue of the early-growth response gene Snk, encoding a serum-inducible kinase. DNA Seq. **11**, 527–533

36   Paratcha, G., de Stein, M. L., Szapiro, G., Lopez, M., Bevilaqua, L., Cammarota, M., de Iraldi, A. P., Izquierdo, I. and Medina, J. H. (2000) Experience-dependent decrease in synaptically localized Fra-1. Mol. Brain Res. **78**, 120–130

37   Nakagomi, S., Suzuki, Y., Namikawa, K., Kiryu-Seo, S. and Kiyama, H. (2003) Expression of the activating transcription factor 3 prevents c-Jun N-terminal kinase-induced neuronal death by promoting heat shock protein 27 expression and Akt activation. J. Neurosci. **23**, 5187–5196

38   Cook, M., Caswell, R. C., Richards, R. J., Kay, J. and Tatnell, P. J. (2001) Regulation of human and mouse procathepsin E gene expression. Eur. J. Biochem. **268**, 2658–2668

39   Sealy, L., Mota, F., Rayment, N., Tatnell, P., Kay, J. and Chain, B. (1996) Regulation of cathepsin E expression during human B cell differentiation *in vitro*. Eur. J. Immunol. **26**, 1838–1843

40   Welker, P., Grabbe, J., Gibbs, B., Zuberbier, T. and Henz, B. M. (2000) Nerve growth factor-β induces mast-cell marker expression during *in vitro* culture of human umbilical cord blood cells. Immunology **99**, 418–426

41   Hawtin, S. R., Davies, A. R., Matthews, G. and Wheatley, M. (2001) Identification of the glycosylation sites utilized on the V1a vasopressin receptor and assessment of their role in receptor signalling and expression. Biochem. J. **357**, 73–81

42   Takai, S., Yamada, K., Kawakami, H., Tanaka, K. and Nakamura, S. (1995) Localization of the gene (SLC1A3) encoding human glutamate transporter (GluT-1) to 5p13 by fluorescence *in situ* hybridization. Cytogenet. Cell Genet. **69**, 209–210

43   Chemin, J., Monteil, A., Dubel, S., Nargeot, J. and Lory, P. (2001) The α1I T-type calcium channel exhibits faster gating properties when overexpressed in neuroblastoma/glioma NG 108-15 cells. Eur. J. Neurosci. **14**, 1678–1686

44   Gendron, F. P., Neary, J. T., Theiss, P. M., Sun, G. Y., Gonzalez, F. A. and Weisman, G. A. (2003) Mechanisms of P2$\times$7 receptor-mediated ERK1/2 phosphorylation in human astrocytoma cells. Am. J. Physiol. Cell Physiol. **284**, C571–C581

45   Kaplan, M. D., Olschowka, J. A. and O'Banion, M. K. (1997) Cyclooxygenase-1 behaves as a delayed response gene in PC12 cells differentiated by nerve growth factor. J. Biol. Chem. **272**, 18534–18537

46   Lin, H., Hikawa, N., Takenaka, T. and Ishikawa, Y. (2000) Interleukin-12 promotes neurite outgrowth in mouse sympathetic superior cervical ganglion neurons. Neurosci. Lett. **278**, 129–132

47   Tuttle, J. B., Etheridge, R. and Creedon, D. J. (1993) Receptor-mediated stimulation and inhibition of nerve growth factor secretion by vascular smooth muscle. Exp. Cell Res. **208**, 350–361

48   Zhou, A. W., Li, W. X., Guo, J. and Du, Y. C. (1997) Facilitation of AVP (4–8) on gene expression of BDNF and NGF in rat brain. Peptides **18**, 1179–1187

49   Affaitati, A., Cardone, L., Cristofaro, T., Carlucci, A., Ginsberg, M. D., Varrone, S., Gottesman, M. E., Avvedimento, E. V. and Feliciello, A. (2003) Essential role of A-kinase anchor protein 121 for cAMP signaling to mitochondria. J. Biol. Chem. **278**, 4286–4294

50   Kirschner, P. B., Jenkins, B. G., Schulz, J. B., Finkelstein, S. P., Matthews, R. T., Rosen, B. R. and Beal, M. F. (1996) NGF, BDNF and NT-5, but not NT-3 protect against MPP$^+$ toxicity and oxidative stress in neonatal animals. Brain Res. **713**, 178–185

51   Pak, J. H., Huang, F. L., Li, J., Balschun, D., Reymann, K. G., Chiang, C., Westphal, H. and Huang, K. P. (2000) Involvement of neurogranin in the modulation of calcium/calmodulin-dependent protein kinase II, synaptic plasticity, and spatial learning: a study with knockout mice. Proc. Natl. Acad. Sci. U.S.A. **97**, 11232–11237

52   McNamara, R. K., Huot, R. L., Lenox, R. H. and Plotsky, P. M. (2002) Postnatal maternal separation elevates the expression of the postsynaptic protein kinase C substrate RC3, but not presynaptic GAP-43, in the developing rat hippocampus. Dev. Neurosci. **24**, 485–494

53   Marsh, H. N., Dubreuil, C. I., Quevedo, C., Lee, A., Majdan, M., Walsh, G. S., Hausdirff, S., Said, F. A., Zoueva, O., Kozlowski, M. et al. (2003) SHP-1 negatively regulates neuronal survival by functioning as a TrkA phosphatase. J. Cell Biol. **163**, 999–1010

Review

Snake venom components and their applications in biomedicine

D. C. I. Koh., A. Armugam and K. Jeyaseelan*

Department of Biochemistry, Yong Loo Lin School of Medicine, National University of Singapore, 8 Medical Drive, Singapore 117597 (Singapore), Fax: +65 67791453, e-mail: bchjeya@nus.edu.sg

Abstract. Snake envenomation is a socio-medical problem of considerable magnitude. About 2.5 million people are bitten by snakes annually, more than 100,000 fatally. However, although bites can be deadly, snake venom is a natural biological resource that contains several components of potential therapeutic value. Venom has been used in the treatment of a variety of pathophysiological conditions in Ayurveda, homeopathy and folk medicine. With the advent of biotechnology, the efficacy of such treatments has been substantiated by purifying components of venom and delineating their therapeutic properties. This review will focus on certain snake venom components and their applications in health and disease.

Introduction

Snakes have been a subject of fascination, fear and myths throughout history. In ancient Egypt, the cobra was worshipped and its replica was used to decorate the crowns of Roman emperors, while in the ancient Greek world, the god of medicine was depicted with a stick entwined with a snake, the symbol that is still used to represent the guilds of medicine and pharmacy. Snake venoms are complex mixtures of proteins, nucleotides and inorganic ions. These combinations confer a formidable array of toxic properties on the venom, the peptides and polypeptides being responsible for a variety of toxic properties. Annually, about 2.5 million people around the world are the victims to snake bites, of whom about 100,000 lose their lives. Most morbidity and mortality occurs in rural areas in the tropics [1, 2]. The populations of temperate western countries are not spared from wild snake bites, but they occur at a lower frequency. In addition, there are substantial incidents of envenomation by exotic captive

snakes. The clinical manifestations of snakebite are dependent on two factors, the intrinsic toxicity and amount of venom injected. There are many signs and symptoms following envenomation by snakes, but the major ones with clinical significance can be divided into a few broad categories: (a) flaccid paralysis; (b) systemic myolysis; (c) coagulopathy and haemorrhage; (d) renal damage and failure; (e) cardiotoxicity and (f) local tissue injury at the bite site. The symptoms suggest that snake venoms affect various systems, particularly the central nervous system (CNS), cardiovascular system, muscular and vascular system. The aim of this review is to highlight some of the snake venom components that can be used as molecular probes in human health and disease.

Toxins affecting the CNS

The main toxins from snake venom that affect the CNS are neurotoxins (Table 1) and dendrotoxins. The general observation from neurotoxin envenomation is the development of cranial nerve palsies, which are characterized

---

* Corresponding author.

Table 1. Snake venom neurotoxins and their targets in the CNS.

Type of neurotoxin	Functional target	Source
Short-chain neurotoxins	post-synaptic toxin; high affinity to skeletal and Torpedo nAChR; bind to neuronal α7 nAChR with lower affinity or none.	elapids and hydrophids (cobras, sea snakes, kraits, Australian elapids)
Long-chain neurotoxins	post-synaptic toxin; comparatively higher affinity towards neuronal α7 nAChR than the skeletal receptors.	elapids and hydrophids (cobras, sea snakes, kraits, Australian elapids)
Weak neurotoxins	post-synaptic toxin; weak affinity to both the skeletal and neuronal nAChRs	elapids (cobras, kraits, Australian elapids)
Taipoxin	presynaptic toxin; binds specifically to neuronal plasma membranes especially at the neuromuscular junction.	Australian elapid (taipan)
β-Bungarotoxins	presynaptic toxin; presynaptic voltage dependent K$^+$ channel	elapids (kraits)
Muscarinic toxins	specific to mAChR subtype and bind with high affinity	elapids (mamba, kraits and cobras)

nAChR, nicotinic acetylcholine receptor; mAChR, muscarinic acetylcholine receptor.

by ptosis, blurred vision, difficulty in swallowing, slurred speech and weakness in facial muscle. Similarly, dendrotoxins have been demonstrated to block particular subtypes of voltage-dependent potassium channels in neurons.

Neurotoxins
Neurotoxins form one of the largest families of proteins with established primary structures. Among the best studied snake neurotoxins are the α-neurotoxins that bind to nicotinic acetylcholine receptors (nAChRs). They are capable of reversibly blocking nerve transmission by competitively binding to the nAChR located at the post-synaptic membranes of skeletal muscles and neurons, preventing neuromuscular transmission and thereby leading to death by asphyxiation [3]. The post-synaptic (α) neurotoxins are classified into four major groups: (a) short neurotoxin, (b) long neurotoxin, (c) κ-neurotoxins and (d) other unconventional neurotoxins called the weak neurotoxins.
The high specificity of neurotoxins for nAChRs has been utilized as a tool in understanding the structure and function of the nervous system. In particular, α-neurotoxins have been crucial for the isolation and characterization of the nAChR at the motor end plate [4]. Figure 1 shows the structure of α-neurotoxins binding to their molecular target nAChR. Figure 1a shows the binding between 5 α-neurotoxin to the acetylcholine receptor subunit while its interaction with a specific peptide of the nAChR isolated from *Torpedo californica* is shown in Figure 1b. The function of the neurotoxins of some elapids can be compared with curare or with the auto-antibodies detected in myasthenia gravis. A comprehensive review of neurotoxins can be found in Siew et al. [5] and Tsetlin and Hucho [3].

Activation of central cholinergic pathways by nicotine and nicotinic agonists has been shown to elicit anti-nociceptive effects in a variety of species and pain tests [6, 7]. Neurotoxins isolated from cobra venoms have shown significant analgesia in animal models. Cobrotoxin, a short-chain post-synaptic α-neurotoxin and α-cobratoxin, a long-chain α-neurotoxin isolated from *Naja atra*, have been reported to show analgesic activity. Cobrotoxin is a specific ligand for the muscle-based α1 nAChR and it produces strong, centrally mediated analgesic effects through an opiate-independent mechanism while the α-cobratoxin shows high affinity for the neuronal α7 nAChR and elicits an opiate-independent, anti-nociceptive effect [8]. Additionally, evidence is emerging that cobrotoxin can substitute for morphine and suppress the effects of morphine withdrawal [8]. Similarly, an α-neurotoxin from the king cobra, *Ophiophagus hannah*, has also been reported to exhibit potent analgesic activity [9].
Neurotoxins that recognize the muscarinic acetylcholine receptors (mAChRs) have been isolated from green mamba venom [10]. Due to their potency and selectivity, the muscarinic toxins (MT1–7) can be useful pharmacological tools for investigating the physiological roles of the muscarinic receptor subtypes [11–13]. These muscarinic receptors are of great interest in the treatment of neurodegenerative diseases, such as Alzheimer's and Parkinsons, and it is hoped that selective blocking of these receptors will greatly aid in restoring normal movement. In fact, the involvement of muscarinic receptors in Azheimer's disease was elucidated using these subtype-specific mamba toxins [14]. Potential sources of nicotinic and muscarinic neurotoxins are summarized in Table 1.
The β-neurotoxins, on the other hand, act presynaptically by affecting the release of acetylcholine via mechanisms
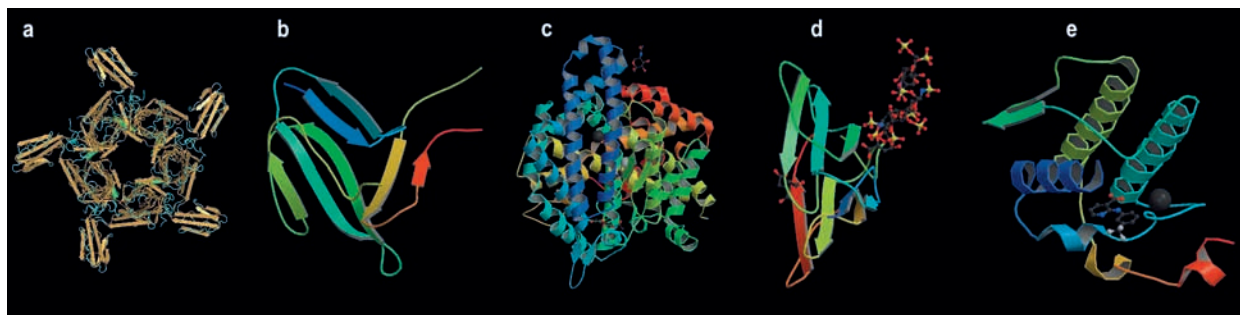
Figure 1. (*a*) Structure of the α-cobratoxin-AChBP complex (1YI5) [from ref. 88]. (*b*) Nuclear magnetic resonance structure of an AChR-peptide (*Torpedo californica*, alpha subunit residues 182–202) in complex with α-bungarotoxin (1L4W) [from ref. 89]. (*c*) Complex of the anti-hypertensive drug captopril and the human testicular angiotensin I-converting enzyme (1UZF) [from ref. 90]. (*d*) Structural Basis of venom citrate-dependent heparan sulphate-mediated cell surface retention of cobra cardiotoxin A3 (1XT3) [from ref. 91]. (*e*) Interactions of a specific non-steroidal anti-inflammatory drug with group I phospholipase A2 (PLA2): crystal structure of the complex formed between PLA$_2$ and niflumic acid at 2.5Å resolution (1TD7) [from ref. 92].

that differ for different *β*-neurotoxins. They are responsible for high toxicity and ultimately respiratory paralysis. They act by causing the disappearance of acetylcholine-containing vesicles, preventing the controlled release of acetylcholine and blocking impulse transmission. The pre-synaptic neurotoxins that have been thoroughly investigated to date are crotoxin (from *Crotalus durissus terrificus*), *β*-bungarotoxin (from *Bungarus multicinctus*), notexin (from *Notechis scutatus*) and taipoxin from the Australian taipan (*Oxyuranus scutellatus*) [15]. Crotoxin, a pre-synaptic neurotoxin with cytotoxic activity, is currently being used in phase 1 clinical trials. This toxin has been tried on advanced cancer patients, as an anti-cancer agent and is believed to act through a novel mechanism of action [16].

Dendrotoxins

Apart from the classical *α*-neurotoxins, another type of neurotoxin that has been identified in other snake venoms are the dendrotoxins isolated from the African mamba, *Dendroaspis* sp. The best-characterized dendrotoxins are highly potent blockers of $K_V1.1$, $K_V1.2$ and $K_V1.6$ potassium channels and are derived from the venom of the green mamba (*Dendroaspis angusticeps*). Mambas belong to the elapid family and have venom that contains toxins to potentiate acetylcholine release and subsequent synaptic transmission at the neuromuscular junction, leading to excessive muscular activity, trembling and fasciculation of the prey. This action has been ascribed to a small protein, dendrotoxin, that selectively blocked voltage-dependent potassium channels in neurons [17]. In the past 20 years, structural analogues of dendrotoxins have aided in defining the molecular recognition properties of different types of potassium channels, and radiolabelled dendrotoxins have been used to identify other toxins binding to potassium channels. They are also important markers for subtypes of potassium channels *in vivo*, and have been widely used

as probes for studying the function of potassium channels both in physiological and pathophysiological conditions [17], and hence have been implicated in the development of new drugs for the treatment of neurodegenerative disorders, such as Alzheimer's disease (www.chemsoc.org/chembytes/ezine/1999/berressem-apr99.htm).

Toxins affecting the cardiovascular system

The first venom-based drug captopril discovered in 1975 also formed the first oral angiotensin-converting enzyme (ACE) inhibitor. This success story started with the observation of the toxic effect of venom from a Brazilian viper (*Bothrops jararaca*) that caused a sudden, massive drop in blood pressure. This piqued the interest of Nobel Prize winner Sir John Vane, who found that the viper venom was a potent inhibitor of ACE. Vane took this discovery to the pharmaceutical company Squibb where two scientists, David Cushman and Miguel Ondetti, created captopril, the first oral ACE inhibitor [18]. With the success of captopril, snake venoms have been explored for potential applications pertaining to the cardiovascular system. The binding of the anti-hypertensive drug captopril to its substrate ACE is shown in Figure 1c.

A toxin isolated from Indian cobra venom in the late 1940s was named cardiotoxin because it caused cardiac arrest when injected into experimental animals. Cardiotoxins, also known as cytotoxins are found exclusively in the venom of cobras and ringhals [19, 20], and are direct lytic factors and membrane-active polypeptides. They are single-chain, highly hydrophobic, basic, short polypeptides closely related to the *α*-neurotoxin that binds to nAChR, but cardiotoxins do not show any significant affinity for the receptors [21]. The main targets of cardiotoxins are on excitable cells. They cause depolarization and contracture of cardiac, skeletal and smooth muscles, and depolarization and loss of excitability of nerves.

These toxins are pore-forming agents [22] that lead to the depolarization and degradation of the plasma membrane of skeletal muscle cells. The mechanism of action of degeneration is most probably calcium dependent, involving the direct activation of calcium-dependent proteases and the eventual failure of mitochondrial respiration due to a calcium overload [23]. Cobra cardiotoxins may be useful probes in a number of cellular processes, including lipid metabolism and calcium ion regulation in skeletal as well as cardiac muscle [24]. Cardiotoxins have also been shown to be membrane-active proteins that recognize the proteoglycans of the membrane. Their cardiotoxicity is attributed to specific binding to the glycosaminoglycans, the sulphated carbohydrate moieties that occur abundantly in cells of cardiovascular tissues [25]. Figure 1d shows the binding of cardiotoxin to the heparan sulphate moiety. Cardiotoxin is currently being used in a phase 1 clinical trial for cancer treatment along with crotoxin (a pre-synaptic neurotoxin) in a combined therapy [26]. Cardiotoxin expression at higher levels (60% of the venom dry weigh) has been attributed to the difference in promoter activity [27]. The promoter activity of α-neurotoxin from *Naja sputatrix* was down-regulated by the presence of a 24 nucleotide (nt -678 to -655) silencer at the 5′-flanking region. These findings indicated that snakes produce venoms that contain highly lethal and specific toxins at lower levels than the multi-functional toxins like cardiotoxins. A study by Cher et al. [28] has revealed that the changes at the molecular level and physiological states in a victim upon cobra envenomation are initially due to cardiotoxins followed by the synergistic effects of all the other components including neurotoxins and phospholipase A_2 (PLA_2) and the spreading factor, hyaluronidase.

Toxins affecting the muscular system

There are three main classes of venom components that initiate cycles of degeneration and regeneration of skeletal muscle: (a) myotoxins, which are small polypeptides that can be isolated from the venoms of the New World viper subfamily Crotalinae, and which specifically act on skeletal muscles [29]; (b) cardiotoxins, polypeptides of 60–65 amino acids that can be isolated from venoms of cobras and which act on smooth muscles (see above) and (c) PLA_2, which can be isolated from venoms of a number of snake families, including Viperidae, Elapidae and Hydrophiidae. The PLA_2s can have either myotoxic, cardiotoxic or neurotoxic actions [30, 31].

Myotoxins

Myotoxins are also called myonecrotic toxins and are found in venoms from rattlesnakes and other pit vipers. One of the best-known myotoxins is myotoxin-a, isolated

from the venom of the Prairie rattlesnake *C. viridis viridis* [29]. It is a small (4600 Da), basic protein devoid of enzymatic activity. Mytotoxin-a binds specifically to the sarcoplasmic reticulum of muscles, causing a change in ion permeability of the sarcoplasmic reticulum (an important calcium regulatory system) leading to swelling and disintegration of both the sarcoplasmic reticulum and muscle fibrils. Hence antibody to myotoxin-a has been used to treat myonecrosis resulting from Prairie rattlesnake venom poisoning [32].

Phospholipase A_2

PLA_2 enzymes may be single-chain polypeptides of around 120 amino acid residues or mixtures of two to five complementary polypeptides, and are Ca^{2+} enzymes. The structure of the complex formed between PLA_2 and the non-steroidal anti-inflammatory drug, niflumic acid, is shown in Figure 1e.

These enzymes catalyze the hydrolysis of phospholipids at the *sn-2* position of the glycerol backbone to release fatty acid and corresponding *1-acyl* lysophospholipid [33]. PLA_2s from snake venoms exhibit a wide variety of pharmacological effects by interfering in normal physiological processes [34].

PLA_2 triggers a cascade of inflammatory events characterized by increased microvascular permeability and oedema formation, leukocyte recruitment into tissues, nociception and release of inflammatory mediators which mimic a number of systemic and local inflammatory disorders in humans. These studies have helped to clarify the pathophysiological roles of these proteins in diverse inflammatory processes. In addition, knowledge of the mechanism of action of myotoxic PLA_2s has provided important clues for understanding snakebite envenomation and has formed a template for the design of new alternatives to conventional anti-venoms.

Anti-inflammatory and anti-neoplastic activities of PLA_2. Naturally occurring anti-toxic factors that neutralize PLA_2 from the blood of both venomous and non-venomous animals have been isolated and studied [35–37]. Snake PLA_2 inhibitors (PLIs) are large multimeric, serum proteins that form soluble complexes with PLA_2 enzymes, thereby inhibiting their actions. The first PLIs were isolated from the serum of Habu snake, *Trimeresurus flavoviridis* (*Protobothrops flavoviridis*; EMBL Reptile Database) [38]. PLIs show specific affinities for various PLA_2 enzymes and some have been shown to have anti-enzymatic, anti-myotoxic, anti-oedema-inducing, anti-cytotoxic and anti-bacterial activities [39]. In addition to its role in various extra-neuronal (extra-cerebral) inflammatory processes, PLA_2 is also thought to be crucial in inflammatory processes present in numerous acute and chronic neurological disorders as-

sociated with neurodegenerative diseases, such as neural trauma, Alzheimer's disease and Parkinson's disease, and in some brain tumours [40]. Treatment of these disorders with non-specific inhibitors has met with limited success. Hence specific PLIs derived from animal sources might provide potentially more specific pharmacological tools. PLA$_2$ isolated from *Bothrops neweidii* venom and Indian cobra, *Naja naja* venom, was found to be cytotoxic towards B16 F10 melanoma and Ehrlich ascites tumour cells, respectively, suggesting its employment as an anti-cancer drug [41].

Toxins affecting the haemostatic system

The major symptoms from snakebite affecting the hae-mostatic system are (a) reduced coagulability of blood, resulting in an increased tendency to bleed, (b) bleeding

due to the damage to blood vessels, (c) secondary effects of increased bleeding, ranging from hypovolaemic shock to secondary-organ damage, such as intracerebral haem-orrhage, anterior pituitary haemorrhage or renal damage and (d) direct pathologic thrombosis and its sequelae, par-ticularly pulmonary embolism [42]. More recently, snake venoms have been used in the development of platelet aggregation and blood-clotting inhibitors.

Venoms from vipers and some Australian snakes are rich sources of proteases that strongly affect the haemostatic mechanism [43]. Coagulant enzymes include activators of the blood coagulation factors II (prothrombin), V and X, while anti-coagulants include protein C activa-tors, inhibitors of prothrombin complex formation and fibrinogenases (based on their specificity for the alpha, beta and gamma chains of fibrinogen). Intermediates between the true coagulants and true anti-coagulants are the thrombin-like enzymes which bring about clotting *in*
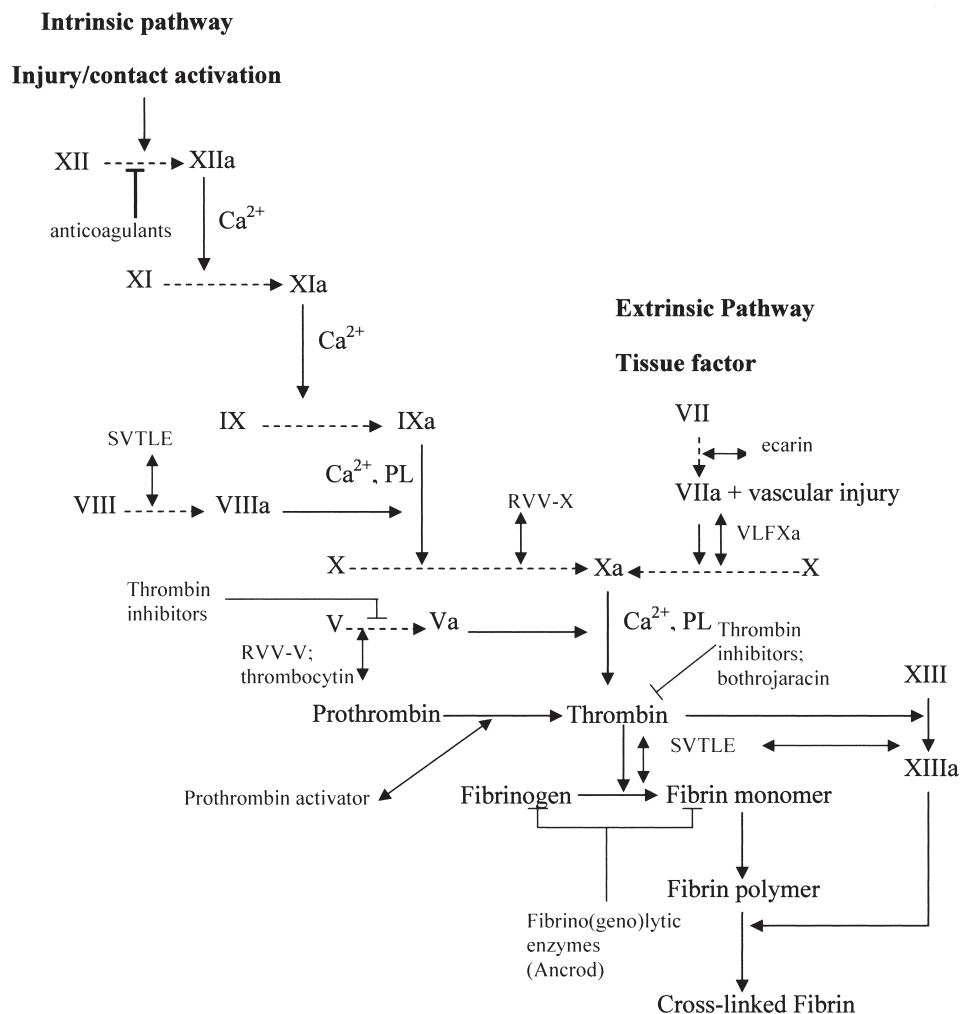

Figure 2. Blood coagulation pathways and the steps in which snake venom proteins interfere. SVTLE, snake venom thrombin-like en-zymes; RVV-V, Russell's viper venom factor V activator; RVV-X, Russell's viper venom factor X activator; VLFXa, *Vipera lebetina* factor X activator. Activation by venom protein is denoted by ◄━━►; inhibition by ┝━━━.

vitro but defibrination (anti-coagulation) *in vivo*. Snake venoms (including the disintegrins, a group of RGD-containing proteins) also affect platelets by inducing or inhibiting platelet aggregation, fibrinolytic activators and haemorrhagins (alpha-fibrinogenases) to cause haemorrhage by acting via platelets or proteolysis of the blood vessel wall [44]. Snake venom proteins that affect the blood coagulation cascade are summarized in Figure 2. It appears that for every factor involved in the blood coagulation cascade, there is a counterpart among the snake venom compounds that could either activate or inactivate the factors. These activators or inhibitors usually belong to various families such as serine proteases, metalloproteinases, C-type lectins, disintegrins and phospholipases. The structure of a protein C activator from *Agkistrodon contortrix contortrix*, Protac, is shown in Figure 3a.

Thrombin-like enzymes and fibrinogen studies
Approximately 100 snake venom toxins have been identified as 'thrombin-like' enzymes [45]. Thrombin is able to cleave both fibrinopeptide A (FPA) and fibrinopeptide B (FPB) from fibrinogen and activating factor XIII (fibrin-stabilizing factor). While some actions of these snake venom thrombin-like enzymes (SVTLEs) mimic the effects of thrombin, they usually cleave FPA alone; only a few cleave FPB. Thus, without cleavage of both FPA and FPB, they are unable to activate factor XIII and the clots produced can easily be broken down. The failure of the clots to be cross-linked leads to a breakdown in the fibrinolytic system and effective removal of fibrinogen from the plasma. The most widely used SVTLEs are those from *Bothrops atrox* venom (Batroxobin, Reptilase) (Pentapharm, Basel, Switzerland) and from *Callosellasma rhodostoma* venom (Ancrod). Ancrod has been shown to be effective in limiting infarct volume [46]. The fibrinogenase family from snake venom that is able to cleave specifically one or more fibrinogen chains has received more attention in the last few years. The fibrin(ogen)olytic enzymes are either serine proteases or metalloproteinases. Though targeting a different factor (fibrin or fibrinogen), these proteins break down the fibrin-rich clots and prevent progression of clot formation. Fibrolase from southern copperhead (*A. contortrix*) snake venom can degrade both the α and β chains of fibrin and shows potential as a thrombolytic agent [47]. Other enzymes that dissolve blood clots both *in vitro* and *in vivo* include afaacytin from horned viper (*Cerastes cerastes*) venom [48], atroxase from western diamondback rattlesnake venom [49] and fibrinogenase from *Vipera lebetina* (*Microvipera lebetina*, EMBL Reptile Database) venom [50]. In 2001, alfimeprase, produced as a truncated recombinant form of fibrolase, was produced and introduced into clinical trials [51]. It is presently in a phase II clinical trial for two indications: (a) treatment of peripheral arterial occlusions and (b) clearance of occluded vascular excess catheters, in direct competition with plasminogen activators [52].

Prothrombin
Snake venoms are rich sources of prothrombin activators and hence are utilized in prothrombin assays, especially for studying dysprothrombinaemias and for preparing meizothrombin and non-enzymatic forms of prothrombin. Russell's viper (*Daboia russelli*) venom (RVV) contains toxins which have been used to assay blood clotting factors V, VII, X, platelet factor 3 and, importantly, lupus anti-coagulants (LAs). Other prothrombin activators (from the taipan, Australian brown snake and saw-scaled viper) have also been used to assay for LA. Protein C and activated protein C resistance can be measured by RVV and Protac, a fast-acting inhibitor from southern copperhead snake venom. A C-type lectin-like protein, botrocetin, isolated from *B. jararaca* venom can be used to study the von Willebrand factor [53]. These proteins are useful tools for elucidating the mechanisms involved in clotting and platelet activation as well as the structure-function relationships of both blood-clotting factors and platelet glycoproteins.

Platelet aggregation inhibitors
Many snake venom toxins affect platelet function [54]. They can be grouped into a few major families, such as enzymes like serine proteinases, zinc-dependent PI-PIV metalloproteinases of the reprolysin family and group II PLA$_2$ isoenzymes as well as proteins with no enzymatic activity, such as C-type lectins, CRISP and disintegrins [55]. Of these, disintegrins and C-type lectins [54, 56] have been considered as useful modulators of platelet function.

Disintegrins. Snake venom disintegrins are natural products that have been investigated as potent inhibitors of
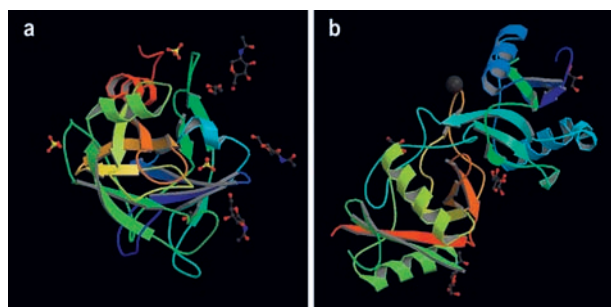

Figure 3. (*a*) Structure of native protein C activator from the venom of the copperhead snake *Agkistrodon contortrix contortrix* (2AIP) [from ref. 93]. (*b*) Structure of EMS16, an Antagonist of collagen receptor integrin α2β1 (GPIa/IIa; 1UKM) [from ref. 94].

various integrins, and major progress has been made in the functional characterization of disintegrins. Functionally, disintegrins can be divided into three groups according to their integrin selectivity and the presence of specific and active motifs. The specific adhesion molecule recognition motifs, their respective sequences and the specific targets are listed in Table 2. They are (a) those interacting with RGD motif-dependent integrins, (b) leukocyte integrin-binding disintegrins and (c) the $\alpha1\beta1$ integrin-binding disintegrins. The first group includes most of the monomeric disintegrins that contain the RGD motif, as well as disintegrins without the RGD motif but with inhibitory activity against RGD-dependent integrins such as KGD, MVD, MGD and WGD disintegrins. The second group is represented by MLD motif – containing disintegrins which interact with $\alpha4\beta1$, $\alpha4\beta7$ and $\alpha9\beta1$ integrins. The last group consists of the recently discovered, KTS motif-containing disintegrins, obtustatin and viperistatin. These disintegrins are potent and selective inhibitors of $\alpha1\beta1$, characterized as specific receptors for collagen IV [57]. Targeting and inhibiting RGD-dependent integrins is a major goal of the pharmacological research for many diseases. In thromboembolic disorders, the main aim is to block the fibrinogen receptor $\alpha II\beta3$ integrin on the platelet. The structure of disintegrins has been used as a template to design compounds that bind to endogenous fibrinogen with higher affinity. This resulted in the introduction of two drugs, eptifibatide and tirofiban. Eptifibatide (integrelin) was modelled on the active site of barbuorin, (*Sistrurus m. barbouri*) and is, in fact, a KGD-containing protein [58], while tirofiban (Aggra-

stat) which was designed from echistatin (a disintegrin) is a synthetic compound that mimics RGD [59, 60]. Both drugs have been approved for the therapy of acute coronary ischaemic syndrome and the prevention of thrombotic complications in patients undergoing percutaneous coronary intervention such as balloon angioplasty and stenting [61, 62].

Blockers of platelet integrins and especially $\alpha II\beta3$ could have applications in certain types of cancer treatment. It is well known that platelets contribute to tumor growth, angiogenesis and metastasis [63]. The calcium-dependent glycoprotein IIb/IIIa complex is the most prevalent platelet cell surface receptor and may combine with one of the four adhesive proteins, fibrinogen, fibronectin, von Willebrand factor and vitronectin, all containing the RGD-motif. The RGD-containing snake venom proteins interfere with platelet aggregation by reversibly blocking the GPIIb/IIIa receptor. The most studied disintegrins include trigramin [*Trimeresurus gramineus*; 64], rhodostomin [*C. rhodostoma*; 65] and triflavin [*T. flavoviridis (P. flavoviridis* (EMBL Reptile Database); 66].

Snake venom RGD-disintegrins have been the target for investigation of $\alpha v\beta3$ integrin as a potential target for the suppression of cancer. These disintegrins are useful tools to decipher the mechanisms that occur during $\alpha v\beta3$-dependent angiogenesis. Monomeric RGD-disintegrins, accutin [67], triflavin [68], salmosin [69], rhodostomin [70, 71], and the homodimeric RGD-disintegrin, contortrostatin [72], inhibit angiogenesis by binding to endothelial cells via $\alpha v\beta3$. It has been suggested that the binding of disintegrins to endothelial cells inhibits

Table 2. Adhesion molecule recognition motifs in snake venom disintergins.

Motifs recognized by adhesion molecules	Amino acid sequence	Physiological target	Examples/source
RGD	arginine-glycine-aspartate	blocks the GPIIb/IIIa receptor and binds to integrins $\alpha IIb\beta3$, $\alpha8\beta1$, $\alpha v\beta3$, $\alpha v\beta5$ and/or $\alpha5\beta1$	trigramin (*Trimeresurus gramineus*); contortrostatin (*Agkistrodon contortrix contortrix*)
KGD	lysine-glycine-aspartate	binds specifically to integrin $\alpha IIb\beta3$	barbuorin (*Sistrurus m. barbouri*)
MVD	methionine-valine-aspartate	potent inhibitor of both collagen- and ADP-stimulated platelet aggregation	atrolysin-E/D (*Crotalus atrox*)
MGD	methionine-glycine-aspartate	potent and selective inhibitor of $\alpha5\beta1$	EMF10 (*Eristocophis macmahoni*)
WGD	tryptophan-glycine-aspartate	potent inhibitor of the RGD-dependent integrins $\alpha5\beta1$, $\alpha v\beta3$, and $\alpha IIb\beta3$.	CC8 (*Cerastes cerastes*)
MLD	methionine-leucine-aspartate	binds $\alpha4\beta1$, $\alpha4\beta7$, $\alpha9\beta1$, $\alpha5\beta1$ and $\alpha IIb\beta3$ integrins	EC5 (*Echis carinatus sochureki*), VLO5 (*Vipera lebetina obtusa*)
KTS	lysine-tryptophan-serine	selective integrin $\alpha1\beta1$ inhibitors	obtustatin (*Vipera lebetina obtusa*)
RTS	arginine-tryptophan-serine	selectively blocks integrin $\alpha1\beta1$	jerdostatin (*Trimeresurus jerdonii*)

their motility and proliferation, possibly by induction of apoptosis in endothelial cells. Snake venom RGD-disintegrins showed direct interaction in several tumor cell lines. The blocking of $\alpha v \beta 3$ integrin in tumor cells inhibited their adhesion to the extracellular matrix and significantly reduced their motility, subsequently inhibiting metastasis. This effect was noted for monomeric medium-sized disintegrins, such as salmosin [69] and triflavin [68] and the homodimeric disintegrin, contortrostatin [73]. These drugs may be considered as alternatives to the humanized monoclonal antibodies used in cancer therapy.

Another RGD-dependent integrin that is targeted by certain snake venom disintegrins is fibronectin receptor, $\alpha 5 \beta 1$ integrin. This cell surface receptor has been studied in the pathology of several diseases such as Alzheimer's disease [74], vascular diseases [75] and cancer [76]. This integrin is the target for regulation of angiogenesis [77, 78]. Most of the monomeric RGD-disintegrins are inhibitors of $\alpha 5 \beta 1$ integrin. MLD- and KTS-disintegrins are specific for leukocyte integrins and collagen receptors, respectively, and are also being investigated as new areas in pharmaceutical research [57].

C-type lectin-like proteins. C-type lectins such as the mannose-binding proteins bind a sugar moiety in the presence of Ca^{2+} and contain the carbohydrate recognition domain (CRD). C-type lectins are a class of proteins widely distributed in nature that display various functions in important physiological processes. The C-type lectin-like proteins are an important group of proteins among the haemorrhagic components in snake venom. Most C-type lectin-like proteins in snake venom do not contain the classic calcium/sugar-binding loop and they

have evolved to bind a wide range of physiologically important proteins and receptors [79]. Based on their structural and functional entities, these proteins in snake venom have been classified into the true C-type lectins (contains the CRD domain) that bind a sugar molecule and the C-type lectin-like proteins with CRD-related non-carbohydrate-binding C-type lectin-like domains (CTLDs) that do not bind a sugar moiety [80]. They are further divided into CRD-containing proteins, factor IX/X-binding proteins and those that bind to the platelet receptors [81].

Snake C-type lectin-like proteins bind to a wide range of coagulation factors that are important in haemostasis and to platelet receptors and display both anti-coagulant- and platelet-modulating activities. They activate platelets by binding to von Willebrand factor or specific receptors such as GPIb, $\alpha 2 \beta 1$ and GPVI. Heterodimeric GPIb-binding molecules mainly inhibit platelet functions, while the multimeric binding molecules activate platelets. Some tetrameric snake venom C-type lectin-like proteins activate platelets by binding to GPVI, while others affect platelet function via integrin $\alpha 2 \beta 1$. Some act by inducing von Willebrand factor to bind to GPIb as well, or activate platelets via $\alpha 2 \beta 1$ and GPIb [81].

While the earliest described C-type lectin, botrocetin, clearly activates platelets by inducing interactions between GPIb and von Willebrand factor, many GPIb-binding C-type lectins are described as inhibitory [82]. In the last decade, numerous C-type lectin-like proteins, including IX/X-binding protein, CA-1, RVV-X, Convulxin, EMS16, botocetin and flavocetin-A, have been isolated from various snake venoms, sequenced and characterized. Echicetin, isolated from the *Echis carinatus*, spe-

Table 3. Drugs/clinical diagnostic kits from snake venoms.

Drug/trade name®	Target and function/treatment	Source
Captopril; enalapril	ACE inhibitor/high blood pressure	*Bothrops jaracusa* (Brazilian arrowhead viper)
Integrilin (eptifibatide)	platelet aggregation inhibitor/acute coronary syndrome	*Sisturus miliarus barbouri* (south-eastern pigmy rattlesnake)
Aggrastat (tirofiban)	GPIIb-IIIa inhibitor/myocardial infarct, refractory ischaemia	*Echis carinatus* (African saw-scaled viper)
Ancrod (Viprinex)	Fibrinogen inhibitor/stroke	*Agkistrodon rhodostoma* (Malayan pit viper)
Defibrase	thrombin and protrhombin inhibitor/acute cerebral infarction, unspecific angina pectoris	*Bothrops moojeni*
Hemocoagulase	thrombin-like effect and thromboplastin activity/ prevention and treatment of haemorrhage	*Bothrops atrox*
Protac/protein C activator	protein C activator/clinical diagnosis of haemostatic disorder	*Agkistrodon contortix contortix* (American copperhead)
Reptilase	diagnosis of blood coagulation disorder	*Bothrops jaraca* (South American lance adder)
Ecarin	prothrombin activator/diagnostic	*E. carinatus*
Exanta; ximelagatran	blood thinner/anti-coagulant, thrombin inhibitor	Cobra

cifically binds platelet GPIb and blocks platelet binding with von Willebrand factor and thrombin [83], while convulxin, isolated from *C. durissus terrificus*, activates platelets through interaction with GPVI [84]. The inhibitor protein isolated from *Echis multisquamatus*, EMS16, is a potent and selective inhibitor of integrin $\alpha 2\beta 1$ [85] while aggretin (*C. rhodostoma* [86] activates platelets by binding to $\alpha 2\beta 1$ and GPIb. The structure of EMS16 is shown in Figure 3b. Therefore, the C-type lectin-like proteins could be useful tools for elucidating the mechanisms involved in clotting and platelet activation as well as providing new possibilities in diagnosis and treatment through their interaction with platelets, plasma and the vascular wall [81, 87].

Conclusion

Nature has been a source of medicinal products for thousands of years, among which snake venoms form a rich source of bioactive molecules, such as peptides, proteins and enzymes with important pharmacological activities. Moreover, blood and bile duct from snakes have been widely used in Chinese traditional medicine. With the advent of protein fold structures, a rich source of peptides that interact specifically and with high affinity with human protein can be developed. This will help not only in understanding the implications of each interaction but will also lead to the development of effective drugs targeted to particular protein functions. Examples of drugs that have been derived from snake venom proteins and have progressed the clinic are listed in Table 3. From the initial discovery of captopril, the first oral ACE inhibitor to the recent application of disintegrins for the potential treatment of cancer, the various components of snake venoms have never failed to reveal amazing new properties. Snake venoms have been used in the coagulation laboratory for the routine assay of coagulation factors and as reagents to study both coagulopathy and haemostasis. A number of useful compounds have been identified; most notably, the disintegrins (eptifibatide and tirofiban) have been shown both *in vitro* and *in vivo* to be powerful anti-platelet aggregates. While the original native snake venom compounds are usually unsuitable as therapeutics, interventions by medicinal chemists as well as scientists and clinicians in pharmaceutical R & D have made it possible to use the snake venom proteins as therapeutics for multiple disorders based on the available structural and functional information. Snake venoms, with their cocktail of individual components, have great potential as therapeutic agents for human diseases.

1 Lalloo, D., Trevett, A. J., Saweri, A., Naraqui, S., Theakston R. D. G. and Warrell, D. A. (1995) The epidemiology of snake bite in Central Province and National Capitol District. Papau New Guinea. Trans. R. Soc. Trop. Med. Hyg. 89, 178–182.

2 Warrell, D. A., Bhetwal, B. B., Chugh, K. S., Lallo, D. G., Looareesuwan, S., Win, M. M., Sjostrom, L., Theakston R. D. G., Watt, G. and White, J. (1999) Asian snakes and snakebite. Southeast Asian J. Trop. Med. Public Health 30, 1–85.

3 Tsetlin, V. I. and Hucho, F. (2004) Snake and snail toxins acting on nicotinic acetylcholine receptors: fundamental aspects and medical applications. FEBS Lett. 557, 9–13.

4 Silverira, R. and Dajas, F. (1994) Neurotoxins in neurobiology. In: Neurotoxins in Neurobiology: Their Actions and Applications, pp. 3–26, K. S. Tipton, F. Dajas (eds), Horwood, New York.

5 Siew, J. P., Khan, A. M., Tan, P. T., Koh, J. L., Seah, S. H., Koo, C. Y., Chai, S. C., Armugam, A., Brusic, V. and Jeyaseelan, K. (2004) Systematic analysis of snake neurotoxins' functional classification using a data warehousing approach. Bioinformatics 20, 3466–3480.

6 Damaj, M. I., Meyer, E. M. and Martin, B. R. (2000) The antinociceptive effects of alpha7 nicotinic agonists in an acute pain model. Neuropharmacology 39, 2785–2791.

7 Decker, M. W., Meyer, M. D. and Sullivan, J. P. (2001) The therapeutic potential of nicotinic acetylcholine receptor agonists for pain control. Expert Opin. Investig. Drugs 10, 1819–1830.

8 Chen, Z. X., Zhang, H. L., Gu, Z. L., Chen, B. W., Han, R., Reid, P. F., Raymond, L. N. and Qin, Z. H. (2006) A long-form alpha-neurotoxin from cobra venom produces potent opioid-independent analgesia. Acta Pharmacol. Sin. 27, 402–408.

9 Pu, X. C., Wong, P. T. and Gopalakrishnakone, P. (1995) A novel analgesic toxin (hannalgesin) from the venom of king cobra (*Ophiophagus hannah*). Toxicon 33, 1425–1431.

10 Harvey, A. L., Kornisiuk, E., Bradley, K. N., Cervenansky, C., Duran, R., Adrover, M., Sanchez, G. and Jerusalinsky, D. (2002) Effects of muscarinic toxins MT1 and MT2 from green mamba on different muscarinic cholinoceptors. Neurochem. Res. 11, 1543–1554.

11 Bradley K. N. (2000) Muscarinic toxins from the green mamba. Pharmacol. Ther. 85, 87–109.

12 Potter, L. T. (2001) Snake toxins that bind specifically to individual subtypes of muscarinic receptors. Life Sci. 68, 2541–2547.

13 Jerusalinsky, D., Alfaro, P., Kornisiuk, E., Quillfeldt, J., Alonso, M., Rial Verde, E., Durán, R. and Cerveñansky, C. (2000) Muscarinic toxins: novel pharmacological tools for the muscarinic cholinergic system. Toxicon 38, 747–761.

14 Mulugeta, E., Karlsson, E., Islam, A., Kalaria, R., Mangat, H., Winblad, B. and Adem, A. (2003) Loss of muscarinic M4 receptors in hippocampus of Alzheimer patients. Brain Res. 960, 259–262.

15 Rossetto, O., Rigoni, M. and Montecucco, C. (2004) Different mechanism of blockade of neuroexocytosis by presynaptic neurotoxins. Toxicol. Lett. 149, 91–101.

16 Cura, J. E., Blanzaco, D. P., Brisson, C., Cura, M. A., Cabrol, R., Larrateguy, L., Mendez, C., Sechi, J. C., Silveira, J. S., Theiller, E., de Roodt, A. R. and Vidal, J. C. (2002) Phase I and pharmacokinetics study of crotoxin (cytotoxic PLA(2), NSC-624244) in patients with advanced cancer. Clin. Cancer Res. 8, 1033–1041.

17 Harvey, A. L. and Robertson, B. (2004) Dendrotoxins: structure-activity relationships and effects on potassium ion channels. Curr. Med. Chem. 11, 3065–3072.

18 Patlak, M. (2003) From viper's venom to drug design: treating hypertension. FASEB J. 18, 421.

19 Jeyaseelan, K., Armugam, A., Lachumanan, R., Tan, C. H. and Tan, N. H. (1998) Six isoforms of cardiotoxin in malayan spit-

ting cobra (*Naja naja sputatrix*) venom: cloning and characterization of cDNAs. Biochim. Biophys. Acta 1380, 209–222.

20 Chang, L. S., Huang, H. B. and Lin, S. R. (2000) The multiplicity of cardiotoxins from *Naja naja atra* (Taiwan cobra) venom. Toxicon 38, 1065–1076.

21 Dufton, M. J. and Hider, R. C. (1991) The structure and pharmacology of elapid cytotoxins. In: Snake Toxins, pp. 259–302, A. L. Harvey (ed.), Pergamon, New York.

22 Forouhar, F., Huang, W. N., Liu, J. H., Chien, K. Y., Wu, W. G. and Hsiao, C. D. (2003) Structural basis of membrane-induced cardiotoxin A3 oligomerization. J. Biol. Chem. 278, 21980–21988.

23 Harris, J. B. (2003) Myotoxic phospholipases A2 and the regeneration of skeletal muscles. Toxicon 42, 933–945.

24 Fletcher, J. E. and Jiang, M. S. (1993) Possible mechanism of action of snake venom cardiotoxins and bee venom melittin. Toxicon 31, 669–695.

25 Wang, C. H., Liu, J. H., Lee, S. C., Hsiao, C. D. and Wu, W. G. (2006) Glycosphingolipid-facilitated membrane insertion and internalization of cobra cardiotoxin: the sulfatide.cardiotoxin complex structure in a membrane-like environment suggests a lipid-dependent cell-penetrating mechanism for membrane binding polypeptides. J. Biol. Chem. 281, 656–667.

26 Costa, L. A., Miles, H., Araujo, C. E., Gonzalez, S. and Villarrubia, V. G. (1998) Cardiotoxin in therapy: immunopharmacology Immunotoxicology 20, 15–25.

27 Ma, D., Armugam, A. and Jeyaseelan, K. (2001) Expression of cardiotoxin-2 gene: cloning, characterization and deletion analysis of the promoter. Eur. J. Biochem. 268, 1844–1850.

28 Cher, C. D., Armugam, A., Zhu, Y. Z. and Jeyaseelan, K. (2005) Molecular basis of cardiotoxicity upon cobra envenomation. Cell. Mol. Life Sci. 62, 105–118.

29 Ownby, C. L., Cameron, D. and Ju, A. T. (1976) Isolation of mytotoxic component from rattlesnake (*Crotalus viridis viridis*) venom. electron microscopic analysis of muscle damage. Am. J. Pathol. 85, 149–166.

30 Harris, J. B., Johnson, M. A. and Karlsson, E. (1975) Pathological responses of rat skeletal muscle to a single subcutaneous injection of a toxin isolated from the venom of Australian tiger snake, *Notechis scutatus scutatus*. Clin. Exp. Pharmacol. Physiol 2, 383–404.

31 Gutiérrez, J. M., Ownby, C. L. and Odell, G. V. (1984) Skeletal muscle regeneration after myonecrosis induced by crude venom and a myotoxin from the snake *Bothrops asper* (Fer-De-Lance). Toxicon 22, 719–731.

32 Ownby, C. L., Colberg, T. R. and Odell, G. V. (1986) *In vivo* ability of antimyotoxin a serum plus polyvalent (Crotalidae) antivenom to neutralize Prairie rattlesnake (*Crotalus viridus viridus*) venom. Toxicon 24, 197–200.

33 Verheij, H. M., Boffa, M. C., Rothen, C., Bryckert, M. C., Verger, R. and de Hass, G. H. (1980) Correlation of enzymatic activity and anticoagulant properties of phospholipase A2. Eur. J. Biochem. 112, 25–32.

34 Valentin, E. and Lambeau, G. (2000) Increasing molecular diversity of secreted phospholipases A(2) and their receptors and binding proteins. Biochim. Biophys. Acta 1488, 59–70.

35 Thwin, M. M., Gopalakrishnakone, P., Kini, R. M., Armugam, A. and Jeyaseelan, K. (2000) Recombinant antitoxic and anti-inflammatory factor from the non-venomous snake *Python reticulatus*: phospholipase A2 inhibition and venom neutralizing potential. Biochemistry 39, 9604–9611.

36 Dunn, R. D. and Broady, K. W. (2001) Snake inhibitors of phospholipase A2 enzymes. Biochim. Biophys. Acta 1533, 29–37.

37 Faure G (2000) Natural inhibitors of toxic phospholipases A(2). Biochimie 82, 833–840.

38 Kihara, H. (1976) Studies on phospholipase A in *Trimeresurus flaoviridis* venom. III. Purification and some properties of phospholipase A inhibitor in Habu serum. J. Biochem. (Tokyo) 80, 341–349.

39 Soares, A. M., Marcussi, S., Stabeli, R. G., Franca, S. C., Giglio, J. R., Ward, R. J. and Arantes, E. C. (2003) Structural and functional analysis of BmjMIP, a phospholipase A2 myotoxin inhibitor protein from *Bothrops moojeni* snake plasma. Biochem. Biophys. Res. Commun. 302, 193–200.

40 Farooqui, A. A., Litsky, M. L., Farooqui, T. and Horrocks, L. A. (1999) Inhibitors of intracellular phospholipase A2 activity: their neurochemical effects and therapeutical importance for neurological disorders. Brain Res. Bull. 49, 139–153.

41 Basavarajappa, B. S. and Gowda, T. V. (1992) Comparative characterization of two toxic phospholipases A2 from Indian cobra (*Naja naja naja*) venom. Toxicon 30, 1227–1238.

42 Numeric, P., Moravie, V., Didier, M., Chatot-Henrey, D., Cirille, S., Bucher, B. and Thomas, L. (2002) Multiple cerebral infarctions following snakebite by *Bothrops carribbaeus*. Am. J. Trop. Med. Hyg. 67, 287–288.

43 White, J. (2005) Snake venom and coagulopathy. Toxicon 45, 951–967.

44 Marsh, N. A. (1994) Inventory of haemorrhagic factors from the snake venoms. Thromb. Haemost. 71, 793–797.

45 Pirkle, H. (1998) Thrombin-like enzymes from snake venoms: an updated inventory. Thromb. Haemost. 79, 675–683.

46 Samsa, G. P., Matchar, D. B., Williams, G. R. and Levy, D. E. (2002) Cost effectiveness of ancrod treatment of acute ischaemic stroke: results from the Stroke Treatment with Ancrod Trial (STAT). J. Eval. Clin. Prac. 8, 61–70.

47 Markland, F. S. (1998) Snake venom fibrinogenolytic and fibrinolytic enzymes: a updated inventory. Thromb. Haemost. 79, 668–674.

48 Laraba-Djebari, F., Martin-Eauclaire, M. F., Mauco, G. and Marchot, P. (1995) Afaacytin, an alpha beta-fibrinogenase from *Cerastes cerastes* (horned viper) venom, activates purified factor X and induces serotonin release from human blood platelets. Eur. J. Biochem. 233, 756–765.

49 Baker, B. J. and Tu, A. T. (1996) Atroxase: a fibrinolytic enzyme isolated from the venom of Western diamondback rattlesnake: isolation, characterization and cloning. Adv. Exp. Med. Biol. 391, 203–211.

50 Gasmi, A., Chabchoub, A., Guermazi, S., Karoui, H., Elayeb, M. and Dellagi, K. (1997) Further characterization and thrombolytic activity of a rat model of a fibrinogenase from *Vipera lebetina* venom. Thromb. Haemost. 86, 233–242.

51 Toombs, C. F. (2001) Alfimeprase: pharmacology of a novel fibrinolytic metalloproteinase for thrombolysis. Haemostasis 31, 141–147.

52 Swenson, S., Toombs, C. F., Pena, L., Johansson J. and Markland, F. S. Jr. (2004) Alpha-fibrinogenases. Curr. Drug Targets Cardiovasc. Haematol. Disord. 4, 417–435.

53 Marsh, N. and Williams, V. (2005) Practical applications of snake venom toxins in haemostasis. Toxicon 45, 1171–1181.

54 Andrews, R. K. and Berndt, M. C. (2000) Snake venom modulators of platelet adhesion receptors and their ligands. Toxicon 38, 775–791.

55 Juárez, P., Sanz, L. and Calvete, J. J. (2004) Snake venomics: characterization of protein families in *Sistrurus barbouri* venom by cysteine mapping, N-terminal sequencing, and MS/MS analysis. Proteomics 4, 327–338.

56 Wisner, A., Leduc, M. and Bon, C. (2002) C-type lectins from snake venoms: new tools for research in thrombosis and haemostasis. In: Perspectives In Molecular Toxinology, pp. 357–375, Ménez, A. (ed.) Wiley, Chichester, UK.

57 Marcinkiewicz, C. (2005) Functional characterization of snake venom disintegrins: potential therapeutic implication. Curr. Pharm. Des. 11, 815–827.

58 Scarborough, R. M., Naughton, M. A., Teng, W., Rose, J. W., Philips, D. R. and Nannizzi, L. (1991) Design of potent and specific integrin antagonists. peptide antagonists with high specificity for glycoprotein IIb-IIIa. J. Biol. Chem. 268, 1066–1073.

59 Marwick, C. (1998) Nature's agents help heal humans – some now take steps to reciprocate. JAMA 279, 1679–1681.

60 Hantgan, R. R., Stahle, M. C., Connor, J. H, Lyles, D. S., Horita, D. A., Rocco, M., Nagaswami, C., Weisel, J. W. and McLane, M. A. (2004) The disintegrin echistatin stabilizes integrin alphaIIbbeta3's open conformation and promotes its oligomerization. J. Mol. Biol. 342, 1625–1636.

61 Pang, J. T., Fort, S., Della Siega, A. and Cohen, E. A. (2002) Emergency coronary artery bypasses surgery in the era of glycoprotein IIb/IIIa receptor antagonist use. J. Card. Surg. 17, 425–431.

62 Gilchrist, I. C. (2003) Platelet glycoprotein IIb/IIIa inhibitors in percutaneous coronary intervention: focus on the pharmacokinetic-pharmacodynamic relationship of eptifibatide. Clin. Pharmacokinet. 42, 703–720.

63 Trikha, M. and Nakada, M. T. (2002) Platelets and cancer: implications for antiangiogenic therapy. Semin. Thromb. Hemost. 28, 39–44.

64 Huang, T. F., Holt, J. C., Lukasiewicz, H. and Niewiarowski, S. (1987) Trigramin: a low molecular weight peptide inhibiting fibrinogen interaction with platelet receptors expressed on glycoprotein IIb/IIIa complex. J. Biol. Chem. 262, 16157–16163.

65 Huang, T. F., Wu, Y. J. and Ouyang, C. (1987) Characterization of a potent platelet aggregation inhibitor from *Agkistrodon rhodostoma* snake venom. Biochim. Biophys. Acta 925, 248–257.

66 Huang, T. F., Sheu, J. R. and Teng, C. M. (1991) A potent antiplatelet peptide, triflavin from *Trimeresurus flavoviridis* snake venom. Biochem. J. 277, 351–357.

67 Yeh, C. H., Peng, H. C. and Huang, T. F. (1998) Accutin, a new disintegrin inhibits angiogenesis *in vitro* and *in vivo* by acting as integrin alphabeta3 antagonist and inducing apoptosis. Blood 92, 3268–3276.

68 Sheu, J. R., Yen, M. H., Kan, Y. C., Hung, W. C., Chang, P. T. and Luk, H. N. (1997) Inhibition of angiogenesis *in vitro* and *in vivo*: comparison of the relative activities of triflavin, an Arg-Gly-Asp- containing peptide and anti-alpha(v)beta3 integrin monoclonal antibody. Biochim. Biophys. Acta 1336, 445–454.

69 Kim, S. I., Kim, K. S., Kim, H. S., Choi, M. M., Kim, D. S. and Chung, K. H. (2004) Inhibition of angiogenesis by salmosin expressed *in vitro*. Oncol. Res. 14, 227–233.

70 Yeh, C. H., Peng, H. C., Yang, R. S. and Huang, T. F. (2001) Rhodostomin, a snake venom disintegrin, inhibits angiogenesis elicited by basic fibroblast growth factor and suppresses tumor growth by a selective alpha(v)beta(3) blockade of endothelial cells. Mol. Pharmacol. 59, 1333–1342.

71 Huang, T. F., Yeh, C. H. and Wu, W. B. (2001) Viper venom components affecting angiogenesis. Haemostasis 31, 192–206.

72 Markland, F. S., Shieh, K., Zhou, Q., Golubkov, V., Sherwin, R. P. and Richters, V. (2001) A novel snake venom disintegrin that inhibits human ovarian cancer dissemination and angiogenesis in an orthotopic nude mouse model. Haemostasis 31, 183–191.

73 Zhou, Q., Sherwin, R. P., Parrish, C., Richters, V., Groshen, S. G. and Tsao-Wei, D. (2000) Contortrostatin, a dimeric disintegrin from *Agkistrodon contortrix contortrix*, inhibits breast cancer progression. Breast Cancer Res. Treat. 61, 249–260.

74 Matter, M. L., Zhang, A., Nordstedt, C. and Ruoslahti, E. (1998) The alpha5beta1 integrin mediates elimination of amyloid-beta peptide and protects against apoptosis. J. Cell. Biol. 141, 1019–1030.

75 Hein, T. W., Platts, S. H., Waitkus-Edwards, K. R., Kuo, L., Mousa, S. A. and Meininger, G. A. (2001) Integrin-binding peptides containing RGD produce coronary arteriolar dilation via cyclooxygenase activation. Am. J. Physiol. Heart Circ. Physiol. 281, H2378–H2384.

76 Adachi, M., Taki, T., Higashiyama, M., Kohno, N., Inufusa, H. and Miyake, M. (2000) Significance of integrin alpha5 gene expression as a prognostic factor in node-negative non-small cell lung cancer. Clin. Cancer Res. 6, 96–101.

77 Kim, S., Bell, K., Mousa, S. A. and Varner, J. A. (2000) Regulation of angiogenesis *in vivo* by ligation of integrin alpha5beta1 with the central cell-binding domain of fibronectin. Am. J. Pathol. 156, 1345–1362.

78 Wickstrom, S. A., Alitalo, K. and Keski-Oja, J. (2002) Endostatin associates with integrin alpha5beta1 and caveolin-1 and activates Src via tyrosyl phosphatase-dependent pathway in human endothelial cells. Cancer Res. 62, 5580–5589.

79 Lu, Q., Navdaev, A., Clemetson, J. M. and Clemetson, K. J. (2005) Snake venom C-type lectins interacting with platelet receptors: structure-function relationships and effects on haemostasis. Toxicon 45, 1089–1098.

80 Drickamer, K. (1999) C-type lectin-like domains. Curr. Opin. Struct. Biol. 9, 585–590.

81 Clemetson, K. J., Lu, Q. and Clemetson J. M. (2005) Snake C-type lectin-like proteins and platelet receptors. Pathophysiol. Hemost. Thromb. 34, 150–155.

82 Fukuda, K., Doggett, T. A., Bankston, L. A., Cruz, M. A., Diacovo, T. G. and Liddington, R. C. (2002) Structural basis of von Willebrand factor activation by the snake toxin botrocetin. Structure 10, 943–950.

83 Navdaev, A., Dormann, D., Clemetson, J. M. and Clemetson, K. J. (2001) Echicetin, a GPIb-binding snake C-type lectin from *Echis carinatus*, also contains a binding site for IgMκ responsible for platelet agglutination in plasma and inducing signal transduction. Blood 97, 2333–2341.

84 Polgar, J., Clemetson, J. M., Kehrel, B. E., Wiedemann, M., Magnenat, E. M., Wells, T. N. and Clemetson, K. J. (1997) Platelet activation and signal transduction by convulxin, a C-type lectin from *Crotalus durissus terrificus* (tropical rattlesnake) venom via the p62/GPVI collagen receptor. J. Biol. Chem. 272, 13576–13583.

85 Horii, K., Okuda, D., Morita, T. and Mizuno, H. (2004) Crystal structure of EMS16 in complex with the integrin α_2-I domain. J. Mol. Biol. 341, 519–527.

86 Chung, C. H., Peng, H. C. and Huang, T. F. (2001) Aggretin, a C-type lectin protein, induces platelet aggregation via integrin alpha(2)beta(1) and GPIb in a phosphatidylinositol 3-kinase independent pathway. Biochem. Biophys. Res. Commun. 285, 689–695.

87 Morita, T. (2005) Structures and functions of snake venom CLPs (C-type lectin-like proteins) with anticoagulant-, procoagulant-, and platelet-modulating activities. Toxicon 45, 1099–1114.

88 Bourne, Y., Talley, T. T., Hansen, S. B., Taylor, P. and Marchot, P. (2005) Crystal structure of a Cbtx-AChBP complex reveals essential interactions between snake alpha-neurotoxins and nicotinic receptors. EMBO J. 24, 1512–1522.

89 Samson, A., Scherf, T., Eisenstein, M., Chill, J. and Anglister, J. (2002) The mechanism for acetylcholine receptor inhibition by alpha-neurotoxins and species-specific resistance to α-bungarotoxin revealed by NMR. Neuron 35, 319–332.

90 Natesh, R., Schwager, S. L. U., Evans, H. R., Sturrock, E. D. and Acharya, K. R. (2004) Structural details on the binding of antihypertensive drugs captopril and enalaprilat to human testicular angiotensin I-converting enzyme. Biochemistry 43, 8718.

91 Lee, S.-C., Guan, H.-H., Wang, C.-H., Huang, W.-N., Tjong, S.-C., Chen, C.-J. and Wu, W.-G. (2005) Structural basis of citrate-dependent and heparan sulfate-mediated cell surface retention of cobra cardiotoxin A3. J. Biol. Chem. 280, 9567–9577.

92 Jabeen, T., Singh, N., Singh, R. K., Sharma, S., Somvanshi, R. K., Dey, S. and Singh, T. P. (2005) Non-steroidal anti-inflammatory drugs as potent inhibitors of phospholipase A(2): structure of the complex of phospholipase A(2) with niflumic

acid at 2.5 Å resolution. Acta Crystallogr. Sect. D. 61, 1579–1586.

93 Murakami, M. T. and Arni, R. K. (2005) Thrombomodulin-independent activation of protein C and specificity of hemostatically active snake venom serine proteinases: crystal structures of native and inhibited A*gkistrodon contortrix*

contortrix protein C activator. J. Biol. Chem. 280, 39309–39315.

94 Horii, K., Okuda, D., Morita, T. and Mizuno, H. (2003) Structural characterization of EMS16, an Antagonist of collagen receptor (GPIa/IIa) from the venom of *Echis multisquamatus*. Biochemistry 42, 12497–12502.

To access this journal online:
http://www.birkhauser.ch

Cellular Fate: Proliferation, Survival, Differentiation Processes

P17-01

Influence of prenatal irradiation by 131-I on the heparin-binding activity of newborn rat brain proteins

T. V. Belousova and G. A. Ushakova

Dniepropetrovsk National University, Ukraine; Dniepropetrovsk Division of the International Center of Molecular Physiology, National Academy of Science of Ukraine

Prenatal low-dose irradiation leads to decrease of brain cell number, breach of cell migration and neuronal net formation but in most cases some compensatory mechanisms prevent rude changes of brain structure and functions during further ontogenesis. The possible participators of compensatory reconstruction are HSPGs, which as known take part in control of brain development process due to interactions with numerous heparin-binding proteins. We investigated heparin-binding site localisation and total heparin-binding activity of proteins (HBAP) in the brains of newborn rats under the influence of 131I (150 μCu) on different stage of embryogenesis. Results of histochemical analysis revealed that the nucleus of progenitor cells are the main heparin-positive compounds of newborn rat brain as under the normal so under the experimental conditions. Less intensive specific staining was noted on the levels of internal granular layer in cerebellum, layer of pyramidal neurons in CA1–CA3 fields and granular neurons of dentate gyrus in hyppocampus. Moreover our data suggest that heparin-positivity of nucleus connects with presence of heparin-binding sites in the structure of some nucleus cytoskeletal proteins. Consequences of 131I influence – decrease of progenitor-cell number as a result of the irradiation and reduction of cell proliferation level as result of hypothyroidism – lead to strong increase of heparin-positivity, with maximal changes after 131I-injection on 16 e.d. Obtained data allow suggest that influence of HSPGs to cell proliferation depend on their concentration and compartmentalization.

Keywords: brain development, glycosaminoglycans.

P17-02

Cannabinoid inhibition of neuronal differentiation

I. Galve-Roperh, D. Rueda, A. Martínez-Serrano and M. Guzmán

Department of Biochemistry and Molecular Biology I, Complutense University, Madrid, Spain

Cannabinoids, the active components of Cannabis sativa, exert their effects by mimicking a family of endogenous lipid ligands such as anandamide and 2-arachidonoylglycerol. In the brain cannabinoids act through their seven transmembrane receptor CB1, and exert an important neuromodulatory role inhibiting the release of several neurotransmitters. In addition, cannabinoids can regulate the cell fate decision of different neural cell types. Thus, cannabinoids induce apoptosis of transformed glial cells whereas they are effective neuroprotective mediators against different brain insults. Therefore we investigated the potential regulation of neurogenesis by the endocannabinoid system. Anandamide treatment of cortical neuron precursors inhibited neuronal generation. Thus anandamide, via CB1 receptor, decreased the number of neurite-bearing cells and diminished and delayed the appearance of the neuronal markers β-tubulin III and Neu N. Signal transduction studies using PC12 cells show that cannabinoid-mediated inhibition of neuronal differentiation relies on their ability to inhibit NGF-induced sustained extracellular signal-regulated kinase (ERK) activation. Cannabinoids attenuate NGF-evoked Rap-1 and B-Raf activation, crucial upstream mediators of sustained ERK activation. In addition, neurogenesis was determined *in vivo* in the dentate gyrus of adult rats treated with cannabinoids. Cannabinoid administration decreased the number of newly generated cells (BrdU+) that acquire and differentiate into a neuronal phenotype (Neu N+), whereas the CB1 antagonist enhanced neurogenesis. In summary, our results suggest that endocannabinoids constitute a new endogenous system involved in the regulation of neurogenesis.

Keywords: Cannabis, MAP kinase, neural progenitors, NGF, PC12 cells.

P17-03

Molecular cloning and characterization of a novel glial cell line-derived neurotrophic factor family receptor α-like gene

Z. Li, Z. Li, B. Wang and J. Zhou

Institute of Biochemistry and Cell biology, Shanghai Institutes for Biological Sciences, Chinese Academy of Sciences, 320 Yueyang Road, Shanghai, China

Members of the glial cell line-derived neurotrophic factor (GDNF) family comprising GDNF, neurturin, persephin, and enovin/artemin, are crucial for the development and maintenance of distinct sets of central and peripheral neurons. All ligands signal through the oncogene c-RET which is activated only if the ligand is first bound to GDNF family receptor-α (GFRα) receptors, which are linked to the plasma membrane by a GPI anchor. Four different GFRα receptors have been identified (GFRα 1–4), which determine the ligand specificity of the GFRα–RET complex. Here we described the cloning of a novel gene that may be related to the GFRα receptor family. Using bioinformatics tools and rapid amplification of cDNA ends (RACE), a full-length cDNA (2013 bp) was cloned from mouse brain that shows moderate homology to members of GFRα receptor family. The gene contains a putative signal peptide at its N terminal and shares conserved spacing of cystine residues which were also present in other GFRα receptors. At least two splice variants of the gene existed in mouse brain, differing at their respective COOH termini. One of the splice variants encoded a transmembrane form of the gene, while the other encoded a secreted one. RT-PCR analysis suggested that the mRNA is expressed primarily in the central nervous system, although at low levels, but not in peripheral organs. The putative transmembrane variant was localized on plasma membrane, determined by fluorescence immunohistochemistry. Further investigations on its biological function and potential signaling cascades are currently under way.

Keywords: GDNF, receptor α.

P17-04

Evaluation of neuronal maturation following sustained exposure to static magnetic field in cultured rat hippocampal neurons

T. Hirai and Y. Yoneda

Laboratory of Molecular Pharmacology, Kanazawa University Graduate School of Natural Science and Technology, Kanazawa, Ishikawa, Japan

In the present study, we have investigated the influence of sustained exposure to static magnetic field on mechanisms underlying cellular maturation and differentiation in cultured rat hippocampal neurons and astrocytes as a guidepost for possible functional alterations induced by magnetism in the brain. Hippocampal neurons and astrocytes were cultured for different days *in vitro* (DIV) under sustained exposure to static magnetic field at 100 mT generated by permanent magnets equipped at both sides of culture dishes. Sustained exposure to static magnetic field significantly decreased the expression of microtubule-associated protein 2 and neuronal nuclei in hippocampal neurons cultured for 1–9 DIV, without markedly affecting that of growth associated protein-43. Although sustained exposure led to a significant increase in the expression of glial fibrillary acidic protein (GFAP) in hippocampal neuronal preparations cultured for 6–9 DIV under sustained exposure to magnetism, sustained exposure did not markedly affect the expression of both GFAP and proliferating cell nuclear antigen in cultured astrocytes irrespective of cellular maturity. No significant alteration was seen with the cell survivability quantified by 3-[4,5-dimethylthiazol-2-yl]-2,5-diphenyltetrazolium bromide reduction assay in cultured hippocampal neurons and astrocytes. These results suggest that cultured rat hippocampal neurons may be more sensitive to sustained exposure to static magnetic field than cultured rat hippocampal astrocytes in terms of modulation of mechanisms associated with cellular maturation and development, but not survivability.

Keywords: hippocampus, MAP2, maturation.

P17-05

Riluzole enhances expression of BDNF with consequent proliferation of granule precursor cells in the rat hippocampus

R. Katoh-Semba, T. Asano, H. Ueda, R. Morishita, R. Kaneko, I. K. Takeuchi and K. Kato

Institute for Developmental Research, Aichi Human Service Center, Kasugai, Aichi, Japan

The dentate gyrus of the hippocampus, generating new cells throughout life, is essential for normal recognition memory performance. Reduction of brain-derived neurotrophic factor (BDNF) in this structure impairs its functions. To elucidate the association between BDNF levels and hippocampal neurogenesis, first, we have conducted a search for compounds that stimulate endogenous BDNF production in the hippocampal granule neurons. Among ion channel modulators tested, an intraperitoneal injection of riluzole, a neuroprotective agent with anticonvulsant properties that is approved for treatment of amyotrophic lateral sclerosis, was highly effective as a single dose, causing a rise in BDNF localized in dentate granule neurons, the hilus and the stratum radiatum of the CA3 region. Repeated, but not single, injections resulted in prolonged elevation of hippocampal BDNF and, moreover, was associated with increased numbers of newly generated cells in the granule cell layer. This appeared due to promoted proliferation, rather than survival, of precursor cells, a large amount of which differentiated into neurons. Intraventricular administration of BDNF-specific antibodies blocked such riluzole effects, suggesting that BDNF increase is necessary for the promotion of precursor proliferation. We also report on mechanisms of riluzole-induced BDNF production.

Keywords: BDNF, granule cells, hippocampus, neurotrophins, stem cells.

P17-06

Secretoneurin promotes pertussis toxin-sensitive neurite outgrowth in cerebellar granule cells

A. Saria,* M. C. Gasser,* I. Berti,* K. F. Hauser† and R. Fischer-Colbrie‡

**Department of Psychiatry, Division of Neurochemistry, Innsbruck, Austria; †Department of Anatomy and Neurobiology, University of Kentucky College of Medicine, Lexington, KY, USA; ‡Department of Pharmacology, University of Innsbruck, Innsbruck, Austria*

The neuropeptide secretoneurin (SN) is an endoproteolytic product of the chromogranin secretogranin II. We investigated the possibility that SN, like other structurally similar neuropeptides, might influence the differentiation of immature cerebellar granule cells derived from the external granular layer. SN caused concentration-dependent increases in neurite outgrowth, which was taken as a parameter of differentiation. The maximum effect was reached at a concentration of 100 nM SN. SN immunoneutralization using selective antiserum significantly decreased neurite outgrowth; however, neurite morphology was altered, presumably due to extraneous growth factors in the rabbit serum. An affinity chromatography purified antibody inhibited the outgrowth response to SN significantly ($p < 0.001$) without altering the morphology. Binding studies suggest the existence of specific G-protein coupled receptors on the surface of monocytes that recognize SN. Assuming SN promotes neurite outgrowth in EGL cells by acting through a similar G-protein coupled mechanism, we treated SN-stimulated EGL cultures with pertussis toxin (PTx). Exposure to PTx (0.1 μg/mL) showed a significant inhibition of the SN-induced outgrowth. To establish a second messenger pathway we used the protein kinase C inhibitor staurosporine. These data indicate that SN is a novel trophic substance that can affect cerebellar maturation, primarily by accelerating granule cell differentiation through a signaling mechanism that is coupled to pertussis toxin-sensitive G-proteins.

Keywords: cerebellum, G protein-coupled receptors, neuropeptides, receptor.

P17-07

Effect of retinoic acid differentiation of c6 glioma cells on free radical scavengers and NCAM expression

J. Singh and G. Kaur

Neurochemistry and Neuroendocrinology Laboratory, Department of Biotechnology, Guru Nanak Dev University, Amritsar, India

Glial cells are the most abundant cell type in the central nervous system and provide structural and metabolic support to the neurons and modulate synaptic activity. Accordingly impairment of glial functions during various metabolic insults can critically influence neuron survival. Cells exposed to oxidants develop multiple ultrastructural alterations. These alterations are more pronounced in differentiated in comparison with the undifferentiated cells. Recent evidence however, in both neuronal and non-neuronal cells, suggests that reactive oxygen molecules also function as messenger molecules in processes such as synaptic plasticity. Accordingly we studied the oxidant defense system and changes in neural cell adhesion molecule (NCAM) expression in undifferentiated and retinoic acid (RA) induced differentiated C6 glioma cells. The strong inhibitory effects of RA on proliferation and clear changes in morphological features such as shrinkage in cell size and elongation of cell processes confirmed differentiation. A significant increase was observed in the activity of catalase and CuZn superoxide dismutase (CuZn-SOD), while there was a decrease in the activity of GPx in differentiated as compared to undifferentiated C6 cells. Total glutathione content (GSH) increased marginally under same set of conditions.The neural cell adhesion molecule expression was studied in undifferentiated and in RA induced differentiated cultures. Results suggest an increase in the expression of NCAM120 and NCAM 140 isoforms. RA induced differentiation of C6 glioma cell line in the present study is associated with the upregulation of both oxidative stress scavenger profile and NCAM expression.

Keywords: antioxidant, free radicals, glioma, NCAM, retinoic acid.

P17-08

Involvement of multiple signaling pathways in insulin-like growth factor-I-mediated survival of oligodendrocyte progenitor

Q.-L. Cui and G. Almazan

Department of Pharmacology and Therapeutics, McGill University, Montreal, Quebec, Canada

Insulin-like growth factor-I (IGF-I) protects oligodendrocyte progenitors (OGP) from apoptosis induced by a variety of pathologic stimuli. The underlying mechanisms are not fully understood. We have investigated involvement of phosphatidylinositol 3-kinase (PI3K), mitogen-activated protein kinase (MEK1) and Src family tyrosine kinases (SFTK) in IGF-I signaling in OGP. We cultured rat primary OGP in medium deprived of growth factors to induce apoptosis. MTT and TUNEL assays were used to detect cell survival and apoptosis. Changes in levels of PI3K/Akt (a downstream target of PI3K) cascade and caspase3 were detected by Western blotting. We observed that (1) IGF-I promoted a twofold increase in cell survival and reduced apoptotic cells by 60% of control; (2) IGF-I sustained Akt activation, and inhibited caspase3 activation induced by growth-factor withdrawal. LY294002 or Wortmannin, specific inhibitors of PI3K, inhibited cell survival and anti-apoptotic effects of IGF-I, and reversed IGF-I-induced Akt activation and caspase3 inhibition; (3) MEK1 specific inhibitors, PD98059 or U0126, had no significant effects on IGF-I-mediated changes; (4) a SFTK inhibitor, PP2, reduced cell survival and inhibited Akt activation produced by IGF-I, but did not reverse the anti-apoptotic effect of IGF-I. These data indicate that (1) PI3K/Akt cascade is implicated in IGF-I-mediated survival and anti-apoptotic effects; (2) SFTK is involved in IGF-I-mediated survival effect by regulating Akt activation.

Keywords: IGF-I, oligodendrocyte progenitor, PI3K, Src family tyrosine kinases, survival.

P17-09

Upregulation of GFAP in astrocytes is associated with decreased expression of EPO, proliferation and survival of the cells

C. Schneider, S. Harsch, S. Kugi, H. Wiesinger, M. Weller, M. Morgalla, G. H. Buniatian, C. H. Gleiter and L. Danielyan

Department of Clinical Pharmacology, University Hospital, Tuebingen, Germany

Erythropoietin (EPO) exerts neurotrophic and neuroprotective activities in different *in vivo* and *in vitro* models of brain damage. In the present study, we used double immunofluorescence technique and real-time RT-PCR to examine the correlation between the expression of GFAP and the synthesis of EPO and proliferative cell nuclear antigen (PCNA) in early (day 7) and late (day 21) astroglial primary cultures. In order to examine the influence of EPO on the survival of GFAP-positive cells, the human astrocytic cell line SV-40 FHAS was studied. The number of the cells grown under hypoxic and normoxic conditions in EPO-free and EPO-supplemented medium was determined. There was an inverse correlation of the dynamics of EPO synthesis and the expression of GFAP. These results were confirmed by real-time RT-PCR studies which showed decreased EPO-mRNA levels in late astroglial primary cultures. As judged from the expression of PCNA, proliferation decreased during the differentiation of astrocytes. Down-regulation of EPO in astrocytes which lost their capacity to proliferate and strongly expressed GFAP, a protein that supports the cytoskeleton of the cells during pathological situations, suggested a role for EPO in the survival of astrocytes. To address this question, human astrocytes were cultured under hypoxic conditions in the presence and as control in the absence of EPO. Addition of EPO blocked the massive disappearance of the cells under hypoxic conditions. In conclusion, EPO may be involved in the mechanisms regulating the survival and the proliferation of astrocytes, that might play an important role in diseases of the central nervous system.

Keywords: astrocytes, cell proliferation, differentiation, glial fibrillary acidic protein, hypoxia.

P17-10

Transferrin (Tf) mRNA is inversely correlated with MBP and P0 in the sciatic nerve of the rat

C. P. Setton-Avruj, C. Salis, E. F. Soto and J. M. Pasquini

Department of Biochemical Chemistry, School of Pharmacy and Biochemistry, University of Buenos Aires, Buenos Aires, Argentina

Tf is an iron carrier protein playing a key role in cell metabolic activity that is regarded as a growth, survival and differentiation factor. Previous studies have demonstrated the presence of Tf mRNA in oligodendrocytes (1). The mRNA levels were highly correlated with the myelination peak in the central nervous system (CNS) (2). The aim of the present study was to evaluate the presence of the mRNA of Tf in embryonic and mature sciatic nerves of the rat and its possible correlation with the mRNA of MBP and P0, the major proteins of peripheral myelin. Sciatic nerves from 15 embryonic day old rats (E15) and from 4-day-old rats (P4) were dissected out and their total RNA was isolated.The presence of the mRNA for Tf, MBP and P0 was detected by Northern blot, using specific probes for each protein. We have been able to demonstrate for the first time that the mRNA of Tf is present in sciatic nerve at E15 when the nerve is still immature, while it is absent when total RNA was isolated from rats of 4 days of age. In contrast the mRNA of MBP and P0 appeared only in the postnatal period, when the most of the Schwann cell (SC) population of the sciatic nerve function as myelin forming cells. Taking into consideration the absence of Tf mRNA in neuron cells, these results appear to suggest that Tf may play an important role in the maturation of SC, as in the rat these cells are completely mature at the time of birth. At variance with what occurs in the CNS, the mRNA of Tf decreases with the appearance of the mRNA of two important peripheral myelin markers such as MBP and P0.

Keywords: mRNA, myelin proteins, myelination, peripheral nerve, transferrin.

References
1. Bloch B, Popovici T, Levin MJ, Tuil D, Kahn A. *Proc Natl Acad Sci USA* 1985 **82**, 6706–6710.
2. Espinosa de los Monteros A, Pena LA, de Vellis J. *J Neurosci Res*. 1989 **24**, 125–136.

P17-11

Pctaire1 regulates the neurite outgrowth and dendritic development in primary cortical neurons

W.-Y. Fu, K. Cheng, A. K. Fu and N. Y. Ip

Department of Biochemistry, Molecular Neuroscience Center and Biotechnology Research Institute, Hong Kong University of Science and Technology, Clear Water Bay, Hong Kong, China

Pctaire1, a Cdk-related protein kinase, is prominently expressed in terminal differentiated tissues such as brain and testis. Based on a yeast two-hybrid screen, we have demonstrated that Pctaire1 interacts with p35, a specific Cdk5 activator. Serine 95 (S95) of Pctaire1 is the major phosphorylation site for Cdk5. More importantly, Pctaire1 activity is enhanced by S95 phosphorylation. Similar to Cdk5 and p35, Pctaire1 is expressed along the neurites and at the growth cones of developing cortical neurons. The kinase activity and S95 phosphorylation of Pctaire1 increase in primary cortical neurons during the process of neuronal differentiation in culture. The temporal profile of changes in Pctaire1 activity correlates with that observed for Cdk5 kinase activity. To further explore the functional roles of Pctaire1 kinase in neuronal development, various Pctaire1 constructs (including wild type, dominant negative and S95A mutant) are transfected into cortical cultures. Expression of dominant negative and S95A mutants of Pctaire1 inhibits neurite outgrowth as well as the formation of dendritic arborization. On the other hand, wild type Pctaire1 increases neurite branching and dendritic arborization in cortical neurons. Taken together, our findings demonstrate that the activity of Pctaire1 is regulated by Cdk5 and suggest that Pctaire1 is involved in the regulation of neuronal development.

Keywords: dendrite, neurite outgrowth, neuronal differentiation, protein kinase.

P17-12

Leukemia inhibitory factor receptor signaling negatively modulates NGF-induced neurite outgrowth

Y. P. Ng, W. He and N. Y. Ip

Department of Biochemistry, Biotechnology Research Institute and Molecular Neuroscience Center, Hong Kong University of Science and Technology, Clear Water Bay, Hong Kong, China

Nerve growth factor (NGF) is required for the development of sympathetic neurons and subsets of sensory neurons. Our current knowledge on the molecular mechanisms underlying the biological functions of NGF is in part based on the studies with PC12 rat pheochromocytoma cells, which differentiate into sympathetic neuron-like cells upon NGF treatment. Here we report that the expression of leukemia inhibitory factor receptor (LIFR), one of the signaling molecules shared by several neuropoietic cytokines of the IL-6 family, is upregulated in PC12 cells following treatment with NGF. Attenuation of LIFR signaling through stable transfection of antisense or dominant negative LIFR constructs enhances NGF-induced neurite extension in PC12 cells. On the contrary, overexpression of LIFR retards the growth of neurites. More importantly, while NGF-induced Rac1 activity is enhanced in AS-LIFR and DN-LIFR expressing PC12 cells, it is reduced in LIFR expressing PC12 cells. In sympathetic neurons lacking LIFR, both neurite length and branching are enhanced when compared with control neurons. Taken together, our findings suggest that LIFR signaling, besides its known function in cell survival and phenotype development, can be specifically induced by NGF and exert negative regulatory effect on neurite extension and branching of sympathetic neurons.

Keywords: CNTF, LIFR, nerve growth factor, neuronal differentiation, sympathetic nerves.

P17-13

EGF and FGF cooperate with estradiol to promote neuroglia differentiation

R. Wong, A. Chen, E. Thung, G. Chinn, H. Ra and P. S. Timiras

Department of Molecular and Cell Biology, University of California, Berkeley, CA, USA

Administration of epidermal growth factor (EGF) and fibroblast growth factor (FGF) stimulates cell proliferation. Increased cell proliferation may be associated with increased responsiveness to steroid hormones. In this study, we investigated whether simultaneous administration of EGF or FGF with estradiol would enhance neuroglia response to the hormone. We used C-6 rat glioma 2B-clone cells, a mixture of astrocytes and oligodendrocytes. They were cultured for 8 days with EGF (50 ng/mL) or FGF (80 ng/mL), the lowest doses effective in promoting cell proliferation. Both growth factors alone stimulated cell proliferation, with FGF being more active. When estradiol was added to the culture containing EGF or FGF, even small concentrations of estradiol (0.05 mM) were capable of inhibiting cell proliferation and promoting cell differentiation. Cell differentiation was measured by increased activity of glutamine synthetase, GS (the marker for astrocytes) and 2′,3′-cyclic nucleotide 3′-phosphohydrolase, CNP (the marker for oligodendrocytes). In all cases, there was a dose-dependent response in promoting GS and CNP activity, even with very low doses of estradiol. These data show that maintaining neuroglia cells in a highly proliferative state makes them more responsive to low doses of estradiol. The data also suggests possible interventive therapies, whereby the dose of a hormone, potentially carcinogenic as estradiol, may be significantly lowered by the administration of growth factors, without affecting its desired action of promoting neuroglia cell differentiation.

Keywords: epidermal growth factor, estradiol, fibroblast growth factor, glial cells.

P17-14

Early and late patterns of caveolins expression in differentiating C6 astroglia

W. Silva,* J. Miranda,* G. Velázquez,* F. Valentín,* M. Quiñones,* N. Mayol† and H. Maldonado†

*Physiology Department, University of Puerto Rico School of Medicine, San Juan, Puerto Rico; †Department of Pharmacology, Universidad Central del Caribe, School of Medicine, Bayamón, Puerto Rico

The discovery of caveolae (CAV) and caveolins (caveolin-1, -2 and -3) in the brain has led to increased interest to elucidate their neurobiological role(s). Here we evaluated the temporal and spatial patterns of caveolins expression in C6 differentiation from an 'oligodendrocyte-like' to an 'astrocyte-like' phenotype. Time course analysis of the expression of caveolin-1 and -2 using semi-quantitative RT-PCR and Western blots, shows that both isoforms are gradually up-regulated late (12–48 h postinduction) in the differentiation process. In contrast, caveolin-3 displays an early pattern of up-regulation (∼4–12 h postinduction). Indirect immunofluorescence analysis reveals that caveolin-l and -2, display similar perinuclear and punctuate distribution patterns in the 'oligodendrocyte-like' phenotype. After induction of differentiation these are more evident as plasmalemma micropatches in the cellular processes, suggestive of the expression of caveolae. In contrast, caveolin-3 is restricted in distribution in both glial phenotypes, to the soma of C6 cells. Therefore, the C6 astroglia model system permits the assessment of the role of CAV and caveolins in glial cell maturation and differentiation. The C6 differentiation process is akin to developmental events of gliogenesis, and to the astrogliosis, seen in neurological insults, therefore the value of this model system to further the understanding of the relevance of CAV and caveolins in these physiological and pathophysiological events.

Keywords: astrocytes, caveolins, cell culture, glial cells, plasma membrane.

P17-15

Neurotrophins facilitate neuronal differentiation of cultured neural stem cells via induction of basic HLH transcription factors

S. Furukawa, H. Ito, A. Nakajima and H. Nomoto

Laboratory of Molecular Biology, Gifu Pharmaceutical University, Mitahora-higashi 5-6-1, Gifu, Japan

Neurogenesis is promoted by basic helix-loop-helix (bHLH) transcription factors Mash1, Math1 and/or NeuroD but suppressed by another set, Hes1 and Hes5. It is still unknown what kinds of extracellular signals are involved in their regulation. Therefore, the effects of neurotrophins on the expression of bHLH factors and neuronal differentiation were investigated by the use of cultured mouse neural stem cells. Each neurotrophin increased Mash1 and Math1 mRNAs of the stem cells growing in the presence of fibroblast growth factor-2 (FGF-2), but did not alter Hes1, Hes5 or NeuroD mRNA levels. Simultaneously, most of the cells expressed nestin, but not microtubule-associated protein 2 (MAP2), and still remained undifferentiated. FGF-2 removal from the medium reduced the levels of Hes1 and Hes5 mRNAs and increased those of Mash1, Math1, and NeuroD mRNAs, resulting in substantial neuronal differentiation. However, when the cells were pretreated with a neurotrophin, brain-derived neurotrophic factor, FGF-2 removal enhanced earlier NeuroD expression and generated many more MAP2-positive cells. The high level of Mash1 and Math1 that had been elevated at FGF-2 withdrawal accelerated NeuroD expression in cooperation with the reduced Hes1 and Hes5 expression. Our present results suggest that neurotrophins stimulate neuronal differentiation via altering the balance of expression of various bHLH transcription factors.

Keywords: BDNF, neural stem cells, neurotrophins, transcription factors.

P17-16

NGF form cobra venom, promotes the expression of the endogenous NGF in PC12 cells

K.-C. I. Dawn, P. N. Ramkishen, A. Armugam and K. Jeyaseelan

Department of Biochemistry, Faculty of Medicine, National University of Singapore, Singapore 117597

The nerve growth factor (NGF) from the cobra, *Naja sputatrix*, has been purified by gel filtration followed by reverse-phase HPLC. The protein showed about 1000-fold higher activity than the mouse NGF in forming neurite outgrowths on PC12 cells. Two cDNAs (NsNGFI & II; 700 bp) encoding isoforms of NGF have been cloned from the venom gland mRNA. These cDNAs show ∼60–70% homology to the 7S-beta NGF. The mature protein coding region NsNGFII has been produced as a his-tagged fusion protein in *Escherichia coli*. The inclusion bodies formed were solubilised in 8 M urea, purified by affinity chromatography and then refolded to yield an active protein. The functional analysis of the recombinant NGF showed similar results to that of the native protein. SELDI-TOF (surface-enhanced laser desorption/ionization-time of flight), protein-profiling confirmed that cobra NGF promotes endogenous expression of NGF in PC12 cells a beneficial effect, which could not be seen with mouse beta-NGF in.

Keywords: cobra venom, neurite outgrowth, NGF, PC12 cells.

P17-17

The roles of the chondroitin sulfate proteoglycan versican V1 isoform in neuronal differentiation and neurite outgrowth

Y. Wu,*,† L. Chen,*,† W. Sheng,*,† H. Dong,*,‡ V. Lee,*,†
F. Lu,*,§ S. Wong,*,§ W.-Y. Lu*,‡ and B. B. Yang*,†
*Sunnybrook & Women's College Health Sciences Centre;
†Department of Laboratory Medicine and Pathobiology, University of Toronto; ‡Department of Anaesthesia, University of Toronto;
§Department of Radiation Oncology, University of Toronto

The chondroitin sulfate proteoglycan versican is one of the major extracellular components in the developing and developed brain, but little is known of its functions in the neuronal system. We have previously demonstrated that the C-terminal domain of versican interacts with b1-integrin and this interaction modulates cell adhesion (1). Here we show that different isoforms of versican play different roles in neuronal differentiation and neurite outgrowth. In PC12 cells, the versican V1 isoform induced complete differentiation, while V2 induced an incomplete differentiation accompanied by early apoptosis. V1 promoted neurite outgrowth of primary hippocampal neurons, while V2 inhibited this process. V1 up-regulated expression of epidermal growth factor receptor and integrins and facilitated sustained-ERK/MAPK phosphorylation. Blockade of the epidermal growth factor receptor, integrin b1, or Src significantly inhibited neuronal differentiation. V1 expression altered NGF-induced expression and current patterns of nicotinic acetylcholine receptor (nAChR) in PC12 cells. Finally, we demonstrated that versican V1 isoform also induced neuronal stem cell differentiation and neurite outgrowth. Our results have implications for understanding how versican regulates neuron development and repair.

Keywords: PC12 cell, Neurons, proteoglycams, neuronal differentiation, neurite outgrowth.

Reference

1. Wu Y, Chen L, Zheng P-S, Yang BB. *J. Biol. Chem.* 2002, **277**, 12294–12301.

P17-18

The neural NPDC-1 protein interacts with several regulatory proteins

C. Evrard and P. Rouget
Unité de Génétique Oncologique, Institut Gustave Roussy, Villejuif, France

We identified a gene expressed in neural cells, which is involved in the control of proliferation and differentiation. The strategy was to clone cDNAs that both hybridized with HLH probes and corresponded to RNAs expressed preferentially when neural precursor cells stopped dividing. This led to the isolation of NPDC-1 cDNA and then of the genomic sequence (1). The stable introduction of NPDC-1 cDNA into dividing neural precursor cells resulted in the inhibition of cell proliferation and in the induction of differentiation (2). We observed that the protein was able to interact directly with the E2F-1 transcription factor and with D-cyclins (3). This interaction reduced the binding of E2F-1 to DNA and its transcriptional activity. Taken together, the data suggest that NPDC-1 may play a role in the regulation of neural cell proliferation and differentiation, through interactions with E2F-1. Recent results showed that NPDC-1 was also able to interact with Rab3-GDP/GTP Exchange Protein (Rab3-GEP) which is involved in presynaptic vesicles trafficking and release of neurotransmitters. With the aim to elucidate the biological function of NPDC-1, we are studying the phenotype of transgenic mice carrying the npdc-1 gene inactivated by homologous recombination.

Keywords: cell proliferation, differentiation, gene expression, transgenic mouse.

References

1. Galiana E, Vernier P, Dupont E, Evrard C, Rouget P. *Proc. Natl. Acad. Sci. USA* 1995, **92**, 1560–1564.
2. Dupont E, Sansal I, Evrard C, Rouget P. *J. Neurosci. Res.* 1998, **51**, 257–267.
3. Sansal I, Dupont E, Toru D, Evrard C, Rouget P. *Oncogene* 2000, **19**, 5000–5009.

P17-19

Role of ciliary neurotrophic factor (CNTF) family growth factors in the survival and neurite outgrowth of retinal ganglion cells

S. C. Yeung, R. C. C. Chang and H. K. Yip
Department of Anatomy, Faculty of Medicine, University of Hong Kong, 5 Sassoon Rd, Hong Kong, China

Although mature mammalian retinal ganglion cells (RGCs) normally fail to regrow injured axons, exposure to the molecular environment of the peripheral nervous system stimulates regenerative growth. The present study uses dissociated RGCs to examine the role of ciliary neurotropic factor (CNTF) and its related cytokines in promoting RGC survival and neurite outgrowth. Postnatal 1-day-old SD rats are anesthetized and their RGCs are retrogradely labeled from superior colliculi by fluorescent dye, DiASP. The pups are killed after 3–4 days for retinal cell culture. Cytokines (IL-1, etc.) are added to the retinal cell culture in 96-well plate for appropriate time periods. The number of RGCs will be counted by using a fluorescent inverted microscope using a FITC filter. The effect of cytokines, alone or in combination with neurotrophic factors (BDNF, NGF) on the survival of RGCs is examined. In addition, we investigate whether the survival effect of those factors is mediated through the JAK-STAT and/or PI-3 pathway. To evaluate the importance of the JAK-STAT pathway in the effect of CNTF-related cytokines, the JAK inhibitor AG490 at 25 mM is used. To analyze the participation of PI-3 on signal transduction of those factors a specific inhibitor of PI-3, LY294002 at 25 μM is also tested.

Keywords: cell culture, CNTF, JAK/stat, retinal ganglion cell.

P17-20

PEDF expression and promoter activity is regulated by retinoic acid

J. Tombran-Tink and C. J. Barnstable
University Missouri-Kansas City, MO, USA and Yale University, New Haven, CT, USA

Retinoic acid (RA) controls differentiation and apoptosis in the developing nervous system. RA effects are mediated through a group of cytoplasmic receptors (RAR) that regulate transcription of genes containing RAR-binding motifs. An RAR motif is present in the PEDF promoter. This study determined the effects of all trans RA (ATRA) on PEDF promoter activity and tested the effects of PEDF on the expression of RARs in PEDF-producing and PEDF-target cells. Two human cell lines expressing PEDF, ARPE19 and Y79, and primary mouse Müller glial cells, were treated for 5 days with 1–10 nM of ATRA in serum-free medium and PEDF expression analyzed. Cells were also treated with PEDF for 48 h, harvested, and RNA extracted for transcriptional profiling. To test the effect of RA on the PEDF promoter, the 5′ flanking region of the PEDF gene, −869/+59, was cloned into pGL3 vector upstream of a luciferase genev and used to transfect cells. PEDF mRNA levels in treated cells and PEDF levels in conditioned-medium of treated cells were elevated about 3X. ATRA increased luciferase activity in cell lines treated following transfection with the PEDF promoter pGL3 plasmid. Array data indicated that PEDF induces expression of the RAR gamma and RAR orphan C by fivefold and twofold, respectively, but downregulates the RAR alpha by twofold. Both ATRA and PEDF can regulate cell differentiation and cell death. By regulating the activity of each other, they may have complementary effects in these processes.

Keywords: apoptosis, neurodegeneration, retina, retinoic acid.